

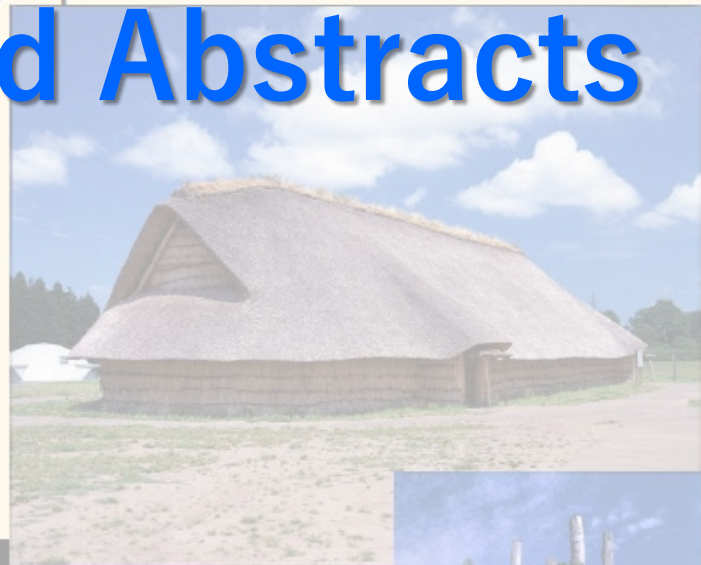
The foundation of human civilization:  
Fire in Jomon period, and Plasma in modern time

# Global Plasma Forum in **AOMORI** October 15 sun – 18 wed, 2023

<https://plasma-aomori.jp/>

Venue:  
Nebuta Museum **WA RASSE**, and World Heritage **Sannai Maruyama Site**,  
Aomori, Japan

## Program and Abstracts



©Aomori Tourism and  
Convention Association

あおもり市民ふるた実行委員会/制作者 北村麻子

### Topics

SOL/divertor plasmas and PW,  
Data-driven & DX plasma,  
Green DX plasma,  
Plasma catalysis,  
Plasma agriculture,  
Plasma bio-applications,  
Plasma nano-processes,  
Advanced semiconductor,  
Industrial consortium, etc.

### Program

Oct 15, evening public lecture  
Oct 16–18, Scientific Program  
(networking at Sannai Maruyama Site on Oct 17, afternoon)

### Chairs of Committees

Organizing: Noriyasu OHNO (Nagoya Univ.)  
Program: Kenji ISHIKAWA (Nagoya Univ.)  
Local: Masayuki YOKOYAMA (NIFS Rokkasho)

Supported by

“Demonstration of post-corona convention programs”, Japan Tourism Agency

Oct.15 (Sun)

Oct.16 (Mon)

Oct.17 (Tue)

Oct.18 (Wed)

9:00
9:05
9:10
9:15
9:20
9:25
9:30
9:35
9:40
9:45
9:50
9:55
10:00
10:05
10:10
10:15
10:20
10:25
10:30
10:35
10:40
10:45
10:50
10:55
11:00
11:05
11:10
11:15
11:20
11:25
11:30
11:35
11:40
11:45
11:50
11:55
12:00
12:05
12:10
12:15
12:20
12:25
12:30
12:35
12:40
12:45
12:50
12:55
13:00
13:05
13:10
13:15
13:20
13:25
13:30
13:35
13:40
13:45
13:50
13:55
14:00
14:05
14:10
14:15
14:20
14:25
14:30
14:35
14:40
14:45
14:50
14:55
15:00
15:05
15:10
15:15
15:20
15:25
15:30
15:35
15:40
15:45
15:50
15:55
16:00
16:05
16:10
16:15
16:20
16:25
16:30
16:35
16:40
16:45
16:50
16:55
17:00
17:05
17:10
17:15
17:20
17:25
17:30
17:35
17:40
17:45
17:50
17:55
18:00
18:05
18:10
18:15
18:20
18:25
18:30
18:35
18:40
18:45
18:50
18:55
19:00
19:05
19:10
19:15
19:20
19:25
19:30
19:35
19:40
19:45
19:50
19:55
20:00

Table for Oct.16 (Mon) with columns Room A, Room B, Room C, Room D. Includes sessions like 'Opening 15 min', 'PL-1 Plenary 30 min', 'PSLO-KN-1 25 min', etc.

Table for Oct.17 (Tue) with columns Room A, Room B, Room C, Room D. Includes sessions like 'Poster 150 min', 'PL-5 Plenary (30 min)', 'PSLO-I-3 20 min', etc.

Table for Oct.18 (Wed) with columns Room A, Room B, Room C, Room D. Includes sessions like 'PL-5 Plenary (30 min)', 'PL-6 Plenary (30 min)', 'PSLO-I-3 20 min', etc.

Wa Rasse 2F Public lecture (in Japanese)
Plasma Exhibition (up to ~17:30)
Pre-registration Wa Rasse 2F

PSLO: PWI/SOL/Laser/Optics
DX: Data-driven
B: Bio
S: Semiconductor
GN: Green & nano
WFPP: Workshop on Fine Particles Physics (jointly held)

Chairs in red

## GPF-Aomori Program

In the order of Day, Room, Time      Poster List from p.10

### Oct. 16 (Mon)

#### Room A

9:15-9:30 Opening Ceremony

#### Room A

9:30-10:00 **PL-1 Jyh-Wei Lee (Ming Chi University of Technology, Taiwan)**

Current research of cold atmospheric plasma and plasma-based thin film technologies in CPTFT, MCUT, Taiwan

10:00-10:30 **PL-2 Eun Ha Choi (Kwangwoon University, Republic of Korea)**

Plasma Agriculture Works with Plasma Treated Nitric Oxide Water (PTNOW) in Korea

**Group Photo (Place will be announced)**

**Coffee Break (2F)**

#### Room A

11:00-11:25 **PSLO-KN-1 Minyou Ye (University of Science and Technology of China, China)**

Hydrogen isotope behavior in tungsten and RAFM steels

11:25-11:50 **PSLO-KN-2 Guang-Hong Lu (Beihang University, China)**

Beneficial Effects of Helium in Tungsten in Context of Fusion Plasma and Wall Interactions

11:50-12:15 **PSLO-KN-3 Shin Kajita (The University of Tokyo, Japan)**

Effect of co-deposition on helium plasma irradiation to tungsten

12:15-12:35 **PSLO-I-1 Yue Yuan (Beihang University, China)**

Performance of tungsten materials under sequential high heat flux loading and deuterium plasma exposure

#### Room B

11:00-11:25 **B-KN-1 Shinaya Toyokuni (Nagoya University, Japan)**

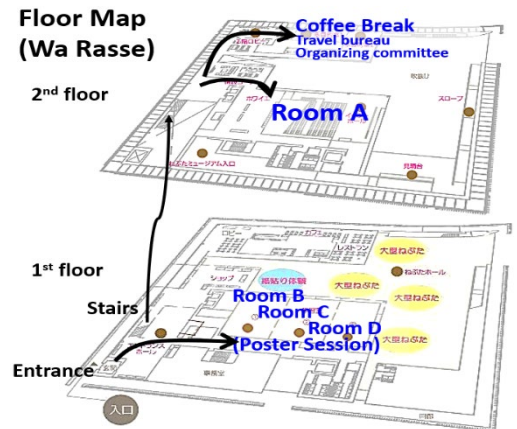
Low-temperature plasma as a ferroptosis inducer in cancer cells

11:25-11:45 **B-I-1 Ihn Han (Kwangwoon University, Republic of Korea)**

Assessment of probability estimation on human tissue-derived fibroblast/stromal cells response to non-thermal biocompatible plasma

11:45-12:05 **B-I-2 Bih-Show Lou (Chang Gung University, Taiwan)**

Cold atmospheric plasma facilitates wound healing for type 2 diabetes and skin flap treatments



12:05-12:25 **B-I-3 Ying-Hung Chen (Feng Chia University, Taiwan)**

In vivo toxicity test of DBD plasma activated water by using Zebrafish

12:25-12:40 **B-O-1 Camelia Miron (Nagoya University, Japan)**

Chemically active compounds formed in low-temperature plasma treated liquids for cancer treatment

### **Room C**

11:00-11:20 **S-I-1 Jaeho Kim (Samsung Electronics, Republic of Korea)**

Recent trends of plasma deposition technologies for the development of next-generation electronic devices

11:20-11:45 **S-KN-1 Shinjae You (Chungnam National University, Republic of Korea)**

On the mechanism of Arcing phenomenon in low temperature plasma

11:45-12:10 **S-KN-2 Shu-Kai S. Fan (National Taipei University of Technology, Taiwan)**

Enterprise intelligentization of semiconductor manufacturing in Taiwan

12:10-12:35 **S-KN-3 Hisashi Yamada (National Institute of Advanced Industrial Science and Technology, Japan)** Ammonia-free plasma-enhanced MOCVD for nitride semiconductors

### **Room D - Workshop on Fine Particle Plasma -**

10:00-10:20 **WFPP-I-1 Giichiro Uchida (Meijo University, Japan)**

Property control of Ge and Si nanostructured films by high-pressure He sputtering process for next-generation Li ion battery

10:20-10:40 **WFPP-I-2 Munaswamy Murugesu (Hokkaido University, Japan)**

A process for synthesizing melted tin-carbon core-shell nanoparticles using dusty plasma

10:40-11:00 **WFPP-I-3 Shinjiro Ono (Kyushu University)**

Controlling the synthesis, transport, and surface coverage of carbon nanoparticles using plasma CVD

11:00-11:40 **WFPP-KN-1 Takeshi Kitajima (National Defense Academy of Japan, Japan)**

Plasmonic plasma process using nanoparticles on substrate

### **Lunch Break**

### **Room A**

14:00-14:30 **PL-3 Jenq-Gong Duh (National Tsing-Hua University, Taiwan)**

Exploration of atmospheric pressure plasma technique in the surface modification on anode material for high-rate lithium-ion battery and rapid organic fertilizer manufacturing for sustainable farming

14:30-15:00 **PL-4 Heeyeop Chae (Sungkyunkwan University, Republic of Korea)**

Plasma-enhanced atomic layer etching for metals and dielectric materials

### **Room A**

15:10-15:35 **PSLO-KN-4 Ivo Classen (Dutch Institute For Fundamental Energy Research, The Netherlands)** Overview of plasma heat exhaust studies in the DIFFER linear devices

15:35-16:00 **PSLO-KN 5 Kyu-Sun Chung (Hanyang University, Republic of Korea)**  
Review on DiPS-2 as a linear plasma device: source, diagnostics, physics and PMI

### **Room B**

15:10-15:30 **DX-I-1 Mi-Young Song (Korea Institute of Fusion Energy, Republic of Korea)**  
Plasma fundamental research activities based on atomic and molecular data in Korea institute of fusion energy

15:30-15:50 **DX-I-2 Ryohtaro T. Ishikawa (National Institute for Fusion Science, Japan)**  
Multi-scale deep learning for estimating horizontal velocity fields on the solar surface

15:50-16:10 **DX-I-3 Yoh-ichi Mototake (Hitotsubashi University, Japan)**  
Interpretable AI supporting scientists' insight into large-scale dynamics

### **Room C**

15:10-15:30 **GN-I-1 Hideaki Yamada (National Institute of Advance Industrial Science and Technology, Japan)** Plasma processing for diamond wafers

15:30-15:50 **GN-I-2 Adnan Ali (Jeju National University, Republic of Korea)**  
Nitrogen doped and undoped  $Ti_3C_2Tx/Co_3O_4$  hybrid composites synthesis for application as anode materials in flexible Supercapacitor

15:50-16:10 **GN-I-3 Moo Been Chang (National Central University, Taiwan)**  
Development of plasma catalysis system for reducing the emissions of GHGs and air pollutants

### **Room D - Workshop on Fine Particle Plasma -**

15:10-15:30 **WFPP-I-4 Yasuaki Hayashi (Yamato University, Japan)**  
Gradient-descent-method analysis of Mie-scattering ellipsometry during fine-particle growth in plasma

15:30-15:50 **WFPP-I-5 Kazuo Takahashi (Kyoto Institute of Technology, Japan)**  
Analyses of Coulomb crystals in dusty plasmas under gravity and microgravity

15:50-16:10 **WFPP-I-6 Masaharu Shiratani (Kyushu University, Japan)**  
Highly sensitive electric field vector measurements using an optically trapped fine particle

**Coffee Break (2F)**

## **Room A**

16:40-17:05 **PSLO-KN-6 Hongbin Ding (Dalian University of Technology, China)**

Laser-induced breakdown spectroscopy for wall diagnosis in nuclear fusion devices

17:05-17:25 **PSLO-I-2 Yong Sup Choi (Korea Institute of Fusion Energy, Korea)**

Development of plasma application technology in IPT-KFE

17:25-17:40 **PSLO-O-1 Jia-Guan Peng (Beihang University, China)**

Surface morphology and grain structure changes induced by helium ion implantation and subsequent thermal annealing

17:40-17:55 **PSLO-O-2 Ze Chen (University of Science and Technology of China, China)**

MD simulation of the interaction between hydrogen and helium bubble in bcc iron

## **Room B**

16:40-17:00 **DX-I-4 Akira Kusaba (Kyushu University, Japan)**

Data assimilation in semiconductor crystal growth: chemical reaction network modeling

17:00-17:20 **DX-I-5 Keisuke Yano (The Institute of Statistical Mathematics, Japan)**

A new approach to mixed-domain and higher-order dependence modeling

17:20-17:40 **DX-I-6 Pierre Vinchon (Osaka University, Japan)**

Monolayer Graphene, an ideal material for exploring out-of-equilibrium phenomena involved in plasma-surface interactions

17:40-18:00 **DX-I-7 Nikolay Britun (Nagoya University, Japan)**

Poly-diagnostics of a nanosecond He-based atmospheric plasma

## **Room C**

16:40-17:00 **GN-I-4 Avik Denra (Jeju National University, Republic of Korea)**

Application of gliding arc plasma in nitrogen fixation: conversion of atmospheric nitrogen into nitro compounds

17:00-17:20 **GN-I-5 Sosiawati Teke (Jeju National University, Republic of Korea)**

The potential of a simple microplasma reactor in cobalt oxide nanoparticle synthesis

17:20-17:40 **GN-I-6 Masahiro Shibuta (Osaka Metropolitan University, Japan)**

Sputter-grown size-selected nanocluster synthesis: deposition and characterization for material science

17:40-18:00 **GN-I-7 Takashi Tsuji (National Institute of Advanced Industrial Science and Technology, Japan)** A microplasma-based approach for the growth of highly crystalline carbon nanotubes

## **Room D - Workshop on Fine Particle Plasma -**

16:40-17:00 **WFPP-I-7 JongYoon Park (Seoul National University, Republic of Korea)**

Discharge mode transition triggered by three-wave coupling in partially magnetized cross-field plasma

17:00-17:20 **WFPP-I-8 Massimiliano Romé (University of Milano, and INFN-Milano, Italy)**

Non-neutral plasmas in Penning-Malmberg traps: fundamental studies and applications

17:20-17:40 **WFPP-I-9 Kosuke Takenaka (Osaka University, Japan)**

Plasma-assisted mist CVD for formation of 3D nanostructured zinc oxide thin films

17:40-18:00 **WFPP-I-10 Kazunori Koga (Kyushu University)**

Evaluation of carbon nanoparticle adhesion on substrate surface deposited by plasma CVD

18:00-18:20 **WFPP-I-11 Yasunori Tanaka (Kanazawa University)**

Contribution of Condensation and Coagulation for Nanoparticle Growth in Modulated Induction Thermal Plasmas

## **Light Meal (Coffee Break Place)**

## **Room A**

18:20-18:35 **PSLO-O-3 Hao Yin (Beihang University, China)**

Surface blistering and deuterium retention in chemical vapor deposition tungsten exposed to deuterium plasma

18:35-18:50 **PSLO-O-4 Yuto Toda (SOKENDAI, Japan)**

Time-dependent density functional theory simulation for neutralization process of hydrogen ion injected onto graphene

## **Room B**

18:20-18:40 **DX-I-8 Micheal Mo (Nagoya University, Japan)**

Simultaneous measurements of F, O and H ground state atom density in an industry-grade etching plasma

18:40-18:55 **DX-O-1 Fatima Jenina Arellano (Osaka University, Japan)**

Machine learning prediction of plasma parameters from optical emission spectra in argon plasma

18:55-19:10 **DX-O-2 Sarah S. N. Alamri (Osaka University, Japan)**

Numerical simulation of RF-driven capacitively coupled argon plasmas and comparison with experimental observations

19:10-19:25 **DX-O-3 Pierre Mathieu (University of Mons, Belgium)**

Preliminary investigation of methane plasmalysis in an atmospheric pressure gliding arc plasma

## **Room C**

18:20-18:45 **GN-KN-1 Ju-Liang He (Feng Chia University, Taiwan)**

Broadening plasma polymerization process for functional coatings

18:45-19:05 **GN-I-8 Magdaleno R Vasquez Jr. (University of the Philippines Diliman, Philippines)**

Development of atmospheric pressure plasma sources for material modification

19:05-19:25 **GN-I-9 Jinjing Luo (Xiamen University, China)**

Surface modification by non-thermal plasma for gaseous mercury removal

19:25-19:40 **GN-O-1 Mark D. Iasin (University of the Philippines Diliman, Philippines)**

Amorphous carbon film deposition using low-energy ions

19:40-19:55 **GN-O-2 Liugang Hu (Nagoya University, Japan)**

Selective removal of graphene by irradiation of remote oxygen plasma

19:55-20:10 **GN-O-3 Ngo Quang Minh (Nagoya University, Japan)**

Synthesis and characteristics of carbon nanowalls using two-step growth combining different plasma chemical vapor deposition methods

## **Oct. 17 (Tue)**

**9:10~11:40 Poster Session (Room B+C+D), “poster list” at the end of this program**

**13:00 Assembly at Coffee Break Place**

**13:10 Bus departure for Sannai-Maruyama Site**

**16:45 Assembly at Sannai-Maruyama Site Entrance**

**17:00 Bus departure for Wa Rasse**

**17:30 “Feel and Enjoy Aomori” Banquet at Wa Rasse**

## **Oct. 18 (Wed)**

### **Room A**

9:15-9:45 **PL-5 Cristian Petrica Lungu (National Institute for Laser, Plasma and Radiation Physics, Romania)** Beryllium dust preparation to mimic particle formation in fusion devices

9:45-10:15 **PL-6 Juergen F. Kolb (Leibniz Institute for Plasma Science and Technology, Germany)**



Plasma treatment of water for agricultural production

## **Coffee Break (2F)**

### **Room A**

10:45-11:05 **PSLO-I-3 Long Cheng (Beihang University, China)**

Mechanism of blistering and retention in recrystallized tungsten exposed to deuterium plasma in the linear plasma device STEP

11:05-11:25 **PSLO-I-4 Dogyun Hwangbo (University of Tsukuba, Japan)**

Spectroscopic measurement of deuterium recycling at molybdenum surfaces

11:25-11:45 **PSLO-I-5 Yuki Hayashi (National Institute for Fusion Science, Japan)**

Study on effects of neutral particle behavior on detached plasma formation using linear plasma device and modeling

11:45-12:05 **PSLO-I-6 Hirohiko Tanaka (Nagoya University, Japan)**

Newly developed integrated transport code for detached plasma simulation

12:05-12:25 **PSLO-I-7 Satoshi Togo (The University of Tsukuba, Japan)**

Development of a plasma fluid model covering a range of coulomb collisionality by comparison with a particle-in-cell model

### **Room B**

10:45-11:10 **B-KN-2 Yuzuru Ikehara (Chiba University, Japan)**

The feasibility of using ions and charges in the medical field

11:10-11:35 **B-KN-3 Mudtorlep Nisoa (Walailak University, Thailand)**

Low-temperature and thermal plasma research at PEwave, Walailak University

11:35-11:55 **B-I-4 Yun-Chien Cheng (National Yang Ming Chiao Tung University, Taiwan)**

Atmospheric-pressure plasma effects on cancer cells and RONS generation for medical applications

11:55-12:15 **B-I-5 Jun Sup Lim (Kwangwoon University, Republic of Korea)**

Effect of accumulated charge on the dynamics of plasma bullet propagation

### **Room C**

10:45-11:10 **DX-KN-1 Young-Chul Ghim (Korea Advanced Institute of Science and Technology,**

**Republic of Korea)** Ion flux reduction factor at the sheath edge as a function of ion-neutral collisions in low temperature Ar or He DC plasmas

11:10-11:30 **DX-I-9 Fumikazu Miwakeichi (The Institute of Statistical Mathematics, Japan)**

Quantification of causality among frequency modes in linear plasma using vector autoregressive models

11:30-11:50 **DX-I-10 Kotaro Yamasaki (Hiroshima University, Japan)**

Basis function analysis technique for the two-dimensional structure of fluctuation in magnetized plasma

11:50-12:10 **DX-I-11 Yuichi Kawachi (Kyoto Institute of Technology, Japan)**

Applications of conditional sampling technique to time series of experimental plasma data

12:10-12:30 **DX-I-12 Takuma Yamada (Kyushu University, Japan)**

Multiple correlation analysis of nonlinear dynamics in plasma turbulence

## **Room D**

10:45-11:10 **S-KN-4 Geun Young Yeom (Sungkyunkwan University, Republic of Korea)**

Beam-assisted atomic layer etching

11:10-11:35 **S-KN-5 Sang Hoon Ahn (Samsung Electronics Co. Ltd., Republic of Korea)**

Past, present, and future plasma solutions to semiconductor challenges

11:35-11:55 **S-I-2 Satoshi Hamaguchi (Osaka University, Japan)**

Plasma-enhanced atomic layer processing for semiconductor processing

11:55-12:15 **GN-I-10 Ghayas Uddin Siddiqui (Jeju National University, Republic of Korea)**

Adsorptive removal of cationic and anionic dyes using nanocomposite of graphene oxide/zinc oxide from aquatic environment

12:15-12:35 **GN-I-11 Mineo Hiramatsu (Meijo University, Japan)**

3D-graphene networks: synthesis and applications

## **Lunch Break**

## **Room A**

13:25-13:55 **PL-7 Masahiro Horibe (National Institute of Advanced Industrial Science and Technology, Japan)** Near-future industrial innovation Digital transformation (DX) to Quantum transformation (QX)

13:55-14:25 **PL-8 Detlev Reiter (Heinrich-Heine-Universität Düsseldorf, Germany)**

Divertor detachment: Fusion plasma physics meets plasma chemistry

## **Room A**

14:30-14:50 **PSLO-I-8 Hiroaki Nakamura (National Institute for Fusion Science, Japan)**

Verification of birth process of primordial organic molecules in the solar system from molecular clouds using molecular dynamics simulations

14:50-15:10 **PSLO-I-9 Yoshihisa Fujita (Nihon University, Japan)**

Angular momentum coupling of tilted gaussian beam with waveguide mode

15:10-15:30 **PSLO-I-10 Quan Shi (The University of Tokyo, Japan)**

A simple method for modifying the surface morphology of various semiconductors and its application in random lasing

### **Room B**

14:30-14:50 **B-I-6 Roopesh Mohandas Syamaladevi (M. S. Roopesh) (University of Alberta, Canada)**

Applications of cold plasma technology in the agri-food industry

14:50-15:10 **B-I-7 Hiromasa Yamada (National Institute Technology, Nagano College, Japan)**

Behavior of gas flow and characteristics of atmospheric pressure plasma jet for bio-applications

15:10-15:30 **B-I-8 Katsuyuki Takahashi (Iwate University, Japan)**

Environmental control for plant growth and preservation using high-voltage pulsed discharges

### **Room C**

14:30-14:50 **DX-I-13 Takashi Nishizawa (Kyushu University, Japan)**

Simultaneous inference of multiple plasma parameter profiles by utilizing transport properties

14:50-15:10 **DX-I-14 Eiichirou Kawamori (National Cheng Kung University, Taiwan)**

Information thermodynamics of plasma wave turbulence

15:10-15:30 **DX-I-15 Shih-Nan Hsiao (Nagoya University, Japan)**

On the mechanism of high-speed SiO<sub>2</sub> etching using hydrogen fluoride-contained plasmas at cryogenic temperature

### **Room D**

14:30-14:50 **GN-I-12 Wei-Cheng Lin (Ming Chi University of Technology, Taiwan)**

Feasibility of applying non-thermal plasma to the degradation of pharmaceuticals in real medical wastewater

14:50-15:10 **GN-I-13 ChinWook Chung (Hanyang University, Republic of Korea)**

Novel plasma source for atomic scale processing

15:10-15:30 **GN-I-14 Ping-Yen Hsieh (Feng Chia University, Taiwan)**

Yttrium-based plasma etching resistant coating obtained by gas flow sputter deposition

### **Room A**

15:30-16:00 Closing, Award Ceremony

Adjourn

## **Poster Presentation List**

**Oct. 17 (Tue) 9:10~11:40 Room B+C+D**

**P-1 Young-Gi Kim (Korea Institute of Fusion Energy, Republic of Korea)**

Design of a Thomson scattering system for atmospheric plasma sources

**P-2 Masayuki Tokitani (National Institute for Fusion Science, Japan)**

Irradiation experiment of new type of divertor heat removal component fabricated by AMSB to LHD divertor plasma

**P-3 Yuki Goto (National Institute for Fusion Science, Japan)**

Theoretical issue of the electron cyclotron emission with decay process in a waveguide

**P-4 Mamoru Shoji (National Institute for Fusion Science, Japan)**

Simulation analysis of lithium transport in the peripheral plasma during impurity powder injection in the Large Helical Device

**P-5 Sotaro Tsuru (Nagoya University, Japan)**

Molecular dynamics simulation for elucidation of vacancy coalescence in tungsten crystal

**P-6 Zhe Liu (University of Science and Technology of China, China)**

Nanopatterning of Si by low-energy He plasma irradiation

**P-7 Rongshi Zhang (Nagoya University, Japan)**

Growth of micro-pillars on tungsten by helium plasma exposure with impurity gases

**P-8 Long Li (University of Science and Technology of China, China)**

Surface modification of ZrC dispersion-strengthened W under low energy He plasma irradiation

**P-9 Ryutaro Kanno (National Institute for Fusion Science, Japan)**

Probabilistic modeling of impurity transport based on the drift-kinetic equation

**P-10 Naonori Okada (Tokai University, Japan)**

2-D spectroscopic measurement of Balmer series in detached plasma with ICR heating

**P-11 Keigo Yoshimura (Tohoku University, Japan)**

Analysis of molecular activated recombination in hydrogen plasma produced in radio-frequency plasma

source DT-ALPHA

**P-12 Arimichi Takayama (National Institute for Fusion Science, Japan)**

Diffusion Behavior of Adatom on Tungsten Surface Evaluated by Density Functional Theory Calculation

**P-13 Gakushi Kawamura (National Institute for Fusion Science, Japan)**

Weighted sum estimation of radiation power and toroidal asymmetry in LHD

**P-14 Hiroyuki Takahashi (Tohoku University, Japan)**

Evaluation of proton density ratio in a bucket-type ion source based on kinetic code plasma simulation and rate equation for hydrogen ions

**P-15 Mitsuo Tajima (University of Hyogo, Japan)**

Formation of fiber-form nanostructures and He bubbles/holes on tungsten surfaces by collisional helium arc plasma irradiation

**P-16 Atsushi Ito (National Institute for Fusion Science, Japan)**

Simulation development for the next stage of plasma-material interaction

**P-17 Ryusei Koyama (Nihon University, Japan)**

Visualization of metastable helium distribution using ghost imaging absorption spectroscopy

**P-18 Hideki Kawaguchi (Muroran Institute of Technology, Japan)**

Analysis of scattering of UV vortex from helix conductor using MoM

**P-19 Wang Chenxu (Muroran Institute of Technology, Japan)**

Evaluation of propagation of millimeter wave vortex using FDTD method

**P-20 Yuta Uematsu (Nagoya University, Japan)**

Observation of global structural changes in two-dimensional emission profiles associated with attached and detached plasma transitions

**P-21 Masanori Yamamoto (Nagoya University, Japan)**

Formation of helium-tungsten co-deposition layers and spectroscopic measurements during sputtering

**P-22 Kazuma Emoto (University of Tsukuba, Japan)**

A preliminary kinetic study on plasma flow in open magnetic systems using a quasi-one-dimensional particle-in-cell model

**P-23 Kiho Tabata (Nagoya University, Japan)**

Porous silicon produced with helium plasma for lithium-ion battery anode

**P-24 Masahiro Katoh (Hiroshima University, Japan)**

Phase structure and angular momentum of cyclotron radiation

**P-25 Kazutaka Onoda (University of Tsukuba, Japan)**

Spectroscopic measurement of microwave atmospheric pressure nitrogen plasma and the effect of vapor addition on the hydrophilicity of polystyrene surface

**P-26 Kaito Miura (Tokai University, Japan)**

Effect of argon additive in Cs-free negative hydrogen ion source

**P-27 Ryo Sasaki (University of Tsukuba, Japan)**

Correlation of tungsten surface morphology changes and deuterium absorption properties by deuterium plasma exposure with pulsed heat load

**P-28 Kota Saito (University of Tsukuba, Japan)**

The appearance of deuterium low temperature desorption at modified tungsten surfaces under helium pre-exposure conditions

**P-29 Takuma Okamoto (University of Tsukuba, Japan)**

Investigation of reaction process during combined seeding of nitrogen and hydrogen in divertor simulated plasma

**P-30 Toseo Moritaka (National Institute for Fusion Science, Japan)**

Electrostatic field calculation on a curved surface for gyrokinetic modeling of stellarator edge plasmas

**P-31 Joseph Xinze Li (SOKENDAI, Japan)**

Development of a kinetic transport model in broken flux surfaces

**P-32 Yoshihide Shibata (National Institute of Technology, Gifu College, Japan)**

Example of medical and engineering collaboration in data analysis in the field of the nuclear fusion

**P-33 Kouta Ishigure (Meijo University, Japan)**

Synthesis of graphitic carbon nitride on carbon nanowalls

**P-34 Kodai Ishikawa (Meijo University, Japan)**

Nitrogen addition to diamond using radical injection-CVD

**P-35 Zhe-Wei Gong (Ming Chi University of Technology, Taiwan)**

Defluorinated degradation of per/poly fluoro alkyl substances (PFAS) in water using non-thermal plasma

**P-36 Jumma Kagami (Meijo University, Japan)**

Immobilization of glucose oxidase on carbon nanowalls

**P-37 Yukei Ishihara (University of Tsukuba, Japan)**

Protein aggregation driven by atmospheric pressure plasma between needle electrode and surface of albumin solution

**P-38 Mitsutaka Isobe (National Institute for Fusion Science, Japan)**

Advances in development of quasi-axisymmetric stellarator at National Institute for Fusion Science

**P-39 Yuto Yanagihara (National Institute for Fusion Science, Japan)**

Low-temperature sintering of activated carbon using spark plasma sintering

**P-40 Kazuki Nagahara (National Institute for Fusion Science, Japan)**

Enhancement to gas puffing control system in LHD

**P-41 Sho Nakagawa (National Institute for Fusion Science, Japan)**

Surface observation on heat-treated activated carbon derived from unutilized biomass

**P-42 Yang Ming (Nagoya University, Japan)**

Ferroptosis induced by plasma-activated Ringer's lactate solution prevents oral cancer progression

**P-43 Kae Nakamura (Nagoya University, Japan)**

Plasma-activated solutions invigorate anti-tumor immune response in the intraperitoneal environments of ovarian cancer

**P-44 Chih-Yu Ma (Louis Pasteur Center for Medical Research, Taiwan)**

Prevalence of antibiotic-resistant E. coli in wastewater treatment plant effluent and the southern watershed of Lake Biwa

**P-45 Dhammanoon Srinoum (Walailak University, Thailand)**

Production of large volume plasma-activated water (PAW) for food and agricultural applications

**P-46 Suttirak Kaewpawong (Walailak University, Thailand)**

Development of 10 kW helicon plasma source for material-plasma interaction studies

**P-47 Ridvee Taleh (Walailak University, Thailand)**

Characteristics of high-power DC thermal plasmas for treatment of medical wastes

**P-48 Akihiro Kajino (Meijo University, Japan)**

Atmospheric pressure hybrid plasma jet for oxygen atom generation

**P-49 In Je Kang (Korea Institute of Fusion Energy, Republic of Korea)**

Analysis of plasma flow velocity in highly collisional plasma jet by using Mach probe for plasma aerosol

deposition

**P-50 Hyunyeong Lee (Korea Institute of Fusion Energy, Republic of Korea)**

Design on versatile large area PECVD system for the assessment of plasma property

**P-51 Jong Woo Hong (Sungkyunkwan University, Republic of Korea)**

Etch characteristics of ITO using various hydrofluorocarbon gases

**P-52 Hyun Woo Tak (Sungkyunkwan University, Republic of Korea)**

Etching characteristics of SiON films with a low global warming potential gas replacing CF<sub>4</sub>

**P-53 Hiroharu Kawasaki (National Institute of Technology, Sasebo College, Japan)**

Dependence of the film qualities on the solid densities of the targets prepared by sputtering deposition with mixture powder targets

**P-54 Masayuki Yokoyama (National Institute for Fusion Science, Japan)**

Introduction to IAEA coordinated research program (CRP): AI for Fusion (AI4F)

**“Meet the Aomori” (in Japanese)**

青森県産業技術センター様からのポスター展示：5件予定

(内訳：予定) 本部企画経営室＋工業、農林、水産、食品加工の4部門

(募集中)



October 16  
(Monday)

## Current research of cold atmospheric plasma and plasma-based thin film technologies in CPTFT, MCUT, Taiwan

Jyh-Wei Lee<sup>1,2,3\*</sup>, Chi-Lung Chang<sup>1,2</sup>, Li-Chun Chang<sup>1,2</sup>, Jang-Hsing Hsieh<sup>1,2</sup>

<sup>1</sup>Department of Materials Engineering, Ming Chi University of Technology, New Taipei, Taiwan,

<sup>2</sup>Center for Plasma and Thin Film Technologies, Ming Chi University of Technology, New Taipei, Taiwan

<sup>3</sup>Department of Mechanical Engineering, Chang Gung University, Taoyuan, Taiwan

E-mail: jefflee@mail.mcut.edu.tw

The Center for Plasma and Thin Film Technologies (CPTFT) at Ming Chi University of Technology (MCUT), Taiwan, was established in December 2010. CPTFT is designed to develop and promote advanced plasma and thin film technologies. In CPTFT, there are five research groups: biomedical thin films, energy-related thin films, HiPIMS technologies, optoelectronic and semiconductor thin films, and plasma technologies. Currently, we focus on the research and application of cold atmospheric plasma techniques and plasma-based thin film fabrications. In the research of cold atmospheric plasma, the biomedical applications in the antimicrobial, wound healing, and skin flap treatment have been studied extensively. The sewage treatment by cold atmospheric plasma technique became an important cooperation project with Prof. Wen-Hui Kuan in MCUT. Recently, we started to promote the unique power supply for cold atmospheric plasma systems, pet animal wound healing treatment systems, and the plasma-activated water machine.

Plasma-based thin film fabrication methods have been widely used in academia and industries due to their flexibility and enabling the growth of many functional coatings. Among many plasma-based thin film deposition methods, the high power impulse magnetron sputtering (HiPIMS) technique is characterized by its ability to fabricate functional thin films with dense microstructure and better film quality. Currently, CPTFT has the largest research group and facilities in the research and development of HiPIMS technology. Some successful HiPIMS research results have been transferred to industries, including anti-sticking coatings on microdrills, embossing dies, and plastic injection molds. The design and manufacturing of the HiPIMS-Arc hybrid deposition system was also a successful product in CPTFT. The research of thin film metallic glasses and high entropy alloy thin films applied in the biomedical fields is highlighted in CPTFT. Researching semiconductor thin films fabricated by atomic layer deposition systems is also an important topic. In this presentation, we will present some We are willing to collaborate with academia and industries worldwide in every aspect of plasma technology and thin film technology.

[1] B.-S. Lou, W.-T. Chen, W. Diyatmika, J.-H. Lu, C.-T. Chang, P.-W. Chen, J.-W. Lee, *Curr. Opin. Chem. Eng.*, **36** 100782 (2022).

[2] S. K. Bachani, C.-J. Wang, B.-S.. Lou, L.-C. Chang, J.-W.. Lee, *J. Alloys Compd.*, **873** 159605 (2021)

## Plasma Agriculture Works with Plasma Treated Nitric Oxide Water (PTNOW) in Korea

Eun Ha Choi<sup>1</sup>, Ihn Han<sup>1</sup>, Youn June Hong<sup>1</sup>, Jinsung Choi<sup>1</sup>, Gyu Sung Cho<sup>1</sup>

<sup>1</sup>*Plasma Bioscience Research Center, Kwangwoon University, Seoul, Korea  
ehchoi@kw.ac.kr*

Plasma treated NO water (PTNOW) irrigation induced NO and H<sub>2</sub>O<sub>2</sub> levels increase in the extracellular space. From the extracellular space NO and H<sub>2</sub>O<sub>2</sub> levels either directly transport into cell cytoplasm through aquaporin or induce the production of H<sub>2</sub>O<sub>2</sub> from NADH oxidase, chloroplasts, peroxisome, and NO from mitochondria. NO and H<sub>2</sub>O<sub>2</sub> both activate the production of other RONS, such as superoxide ion, peroxyxynitrite, and hydroxyl radicals in the cytoplasm, which causes lipid oxidation at higher concentrations. NO and H<sub>2</sub>O<sub>2</sub> both induce the expression of PR proteins, antioxidant enzyme activity, SA and JA pathway enzymes via MAPK signaling pathways. All these defense proteins and phytohormones strengthen the plant pathogen defense pathway [1].

Demonstration project for plasma agriculture with PNTNOW in Korea will be introduced for translation to field site from laboratory. For this project the multicylinder dielectric barrier plasma source has been developed for the major production of NO, from which some of other ROS could be controlled and adjusted for the respective their applications under low power consumption less than 150 W. The plasma characteristics of multicylinder dielectric barrier plasma source as well as its electrical properties will also be described for mutual understandings.

Especially the plasma agriculture demonstration is being performed at Yeon-Chon Agricultural Technical Center (ATC), Kyunggi Province, and other region's ATC for lettuce, strawberry, radish, and basil. Also we will discuss the many other applications to odor removal from piggery or animal farms based on the nonthermal atmospheric pressure plasma.

[1] B. Ahikari, M. Adhikari, B. Ghimire, G. Park, E. H. Choi, Sci. Rep. 9,16080 (2019)

## Hydrogen Isotope Behavior in Tungsten and RAFM Steels

Minyou Ye, Ze Chen

*School of Nuclear Science and Technology, University of Science and Technology of China  
Anhui, Hefei 230026, China  
yemy@ustc.edu.cn*

The transport and retention of hydrogen isotopes is of vital importance for the realization of future commercial fusion reactors, because it is closely related to plasma operation, fuel recycling and safety. However, the hydrogen isotope behavior in fusion reactor materials is not well understood. Reduced activation ferritic-martensitic (RAFM) steel and tungsten (W) are promising candidate structural materials and first wall materials, respectively. In this presentation, we reported the deuterium permeation and retention behaviors of seven kind of RAFM steels and two kind of W. Gas-driven permeation (GDP) method was used to investigate the deuterium permeability, diffusivity, and solubility of the studied materials, with loading pressure up to  $1 \times 10^5$  Pa. For RAFM steels, the results indicates that the deuterium permeability has little materials dependence. In contrast, the deuterium diffusivity of seven studied RAFMs showed significant variation. And W show lower permeability and diffusivity than RAFMs in the working temperature range. The influence of low-energy high-flux plasma irradiation on deuterium permeation in W has also been studied. Besides, thermal desorption spectroscopy (TDS) was performed to assess the retention behaviors of RAFMs and W with a temperature ramping rate of 0.5 K/s following a static thermal gas charging. Dominant desorption peak of  $\sim 1000$  K was observed for W while  $\sim 500$  K for RAFMs. And the retention of deuterium in RAFMs is about 1 to 2 order of magnitude higher than W. Finally, microstructural features contributing to the desorption and retention properties was discussed.

## Beneficial Effects of Helium in Tungsten in Context of Fusion Plasma and Wall Interactions

Guang-Hong Lu<sup>1,\*</sup>, Yue Yuan<sup>1</sup>, Hong-Bo Zhou<sup>1</sup>, Yu-Hao Li<sup>1</sup>, Long Cheng<sup>1</sup>, Wei-Zhong Han<sup>2</sup>, and Si-Mian Liu<sup>2</sup>

<sup>1</sup> School of Physics, Beihang University,  
Beijing 100191, China  
LCheng@buaa.edu.cn

<sup>2</sup> Center for Advancing Materials Performance from the Nanoscale, State Key Laboratory for Mechanical Behavior of Materials, Xi'an Jiaotong University,  
Xi'an, 710049, China

Helium is a typical impurity in nuclear materials. Its closed-shell electronic structure leads to a significant "electrophobic" property [1], which makes helium atoms easy to form clusters or bubbles in metals. Helium in fusion reactor materials is mainly derived from the product of deuterium-tritium fusion reaction and the transmutation during neutron irradiation, of which the former is mainly a surface effect and the latter is a body effect. Helium is generally considered to be hazardous that can lead to degradation of material properties. Interestingly, a series of recent works have shown that helium, regardless of its source, exhibits "beneficial" effects, especially in tungsten as a plasma-facing material, in terms of the microstructural evolution, hydrogen isotope retention and mechanical properties of materials. These studies have deepened the understanding and knowledge of helium effects in metals.

**Helium could effectively retard recrystallization and displacement damage in tungsten** due to the effect of helium on microstructure evolution, including the effect on grain boundary migrations, self-interstitials migrations, and the recombination between self-interstitials and vacancies. These microstructural changes could potentially slow down the degradation of tungsten exposed to fusion edge plasma and neutrons. **Hydrogen isotopes retention in tungsten could be greatly reduced by helium.** The formation of helium-rich layer could enhance hydrogen trapping but reduce hydrogen diffusion towards the bulk, which therefore reduce total hydrogen retention. In other metals, **helium could enhance mechanical properties of metals.** Helium nano bubbles serve as shearable obstacles of dislocations, therefore slow down the dislocation motion, and active internal dislocation sources which promote the uniform nucleation of dislocations in single crystalline copper.

This presentation will focus on the beneficial effects of helium in tungsten and emphasize that the relevant research efforts could provide new ideas for solving problems related to plasma-wall interactions and tritium self-sustainability in fusion reactors.

[1] Hong-Bo Zhou, Guang-Hong Lu, et al., Acta Materialia 2016, 119: 1-8.

## Effect of co-deposition on helium plasma irradiation to tungsten

Shin Kajita<sup>1,3</sup>, Hirohiko Tanaka<sup>2,3</sup>, and Noriyasu Ohno<sup>3,2</sup>

<sup>1</sup> Graduate School of Frontier Sciences, The University of Tokyo  
Kashiwa, Chiba 277-8561, Japan  
kajita@k.u-tokyo.ac.jp

<sup>2</sup> Institute of Materials and Systems for Sustainability, Nagoya University  
Nagoya 464-8603, Japan

<sup>3</sup> Graduate School of Engineering, Nagoya University  
Nagoya 464-8603, Japan

In fusion devices, the divertor material (tungsten) is subjected to significant heat and particle loads. The particles include helium atoms in addition to hydrogen isotopes due to the nuclear reaction of deuterium and tritium. The interaction of helium with tungsten is special and different from those of hydrogen and hydrogen isotopes. Helium nanobubbles and fiberform nanostructures called *fuzz* can be formed on the surface [1]. In particular, because fuzz can significantly change the physical properties including thermal conductivity, field electron emission property, sputtering yield, particle reflection, and so on, the growth feature has been extensively investigated worldwide. One of the unknown effect on the fuzz growth is the effect of co-deposition. Since co-deposition occurs in fusion devices, it is important to investigate it further.

The co-deposition effect was investigated in the divertor simulator NAGDIS-II. A sputtering source (tungsten wire) was placed near the sample and the growth of fuzz on the sample was studied. It was found that fuzz growth is significantly accelerated, say by several orders of magnitude, and mm thick fuzz is grown on the surface under certain conditions [2]. It was also found that the growth of nanotendrils bundles (NTBs), which are several tens of  $\mu\text{m}$  high bundled fiberform structures, is also related to the deposition effect [3].

Figure 1 shows a scanning electron microscope (SEM) image of fuzz grown on tungsten mesh with tungsten deposition. The growth rate on the mesh was different from that on the tungsten plate. By comparing the growth rate on different sized meshes, it was found that the helium flux and the tungsten deposition rate are two important factors for the initial growth.

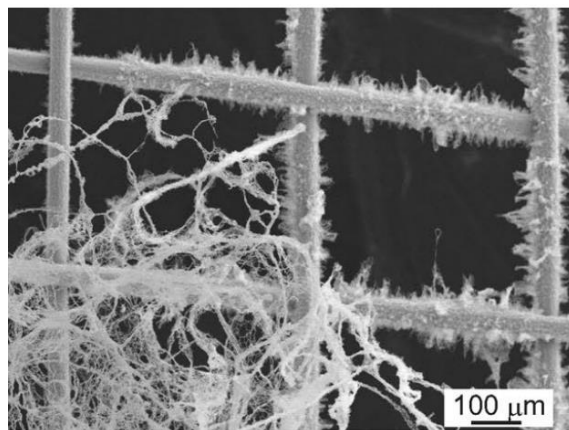


Fig. 1: Fiberform nanostructure grown on tungsten mesh during tungsten deposition in helium plasma [4].

- [1] S Kajita, W Sakaguchi, N Ohno, N Yoshida, T Saeki, Nuclear Fusion 49 (2009), 095005.
- [2] S Kajita, S Kawaguchi, N Ohno, N Yoshida, Scientific Reports 8 (2018), 56.
- [3] D Hwangbo, S Kajita, N Ohno, P McCarthy, JW Bradley, H Tanaka, Nuclear Fusion 58 (2018), 096022.
- [4] K Hori, S Kajita, R Zhang, H Tanaka, N Ohno, Scientific Reports 13 (2023), 5450.

# Performance of tungsten materials under sequential high heat flux loading and deuterium plasma exposure

Yue Yuan<sup>1</sup>, Peng Wang<sup>2</sup>, Henri Greuner<sup>2</sup>, Wei Liu<sup>3</sup>, Long Cheng<sup>1</sup>, Guang-Hong Lu<sup>1</sup>

<sup>1</sup>*School of Physics, Beihang University, Beijing 100191, China*

<sup>2</sup>*Max-Planck-Institut für Plasmaphysik, EURATOM Association, 85748 Garching, Germany*

<sup>3</sup>*Department of Material Science and Engineering, Tsinghua University, Beijing 100084, China*

Tungsten (W) and W based materials, the most promising candidates for plasma facing materials for future fusion reactors, will be exposed to extreme conditions during operations, such as high heat flux (HHF) loads and intense particle irradiations (i.e. hydrogen isotope ions and energetic neutrals). HHF loads can lead to recrystallization, and the more destructive surface melting issue of W materials. Such recrystallized and resolidified W materials should still withstand further deuterium (D) irradiation in subsequent operation. It is thus imperative to assess the D retention in the recrystallized and resolidified W materials after additional D exposure.

In this work, we first prepare recrystallized and resolidified W and W-1 wt% La<sub>2</sub>O<sub>3</sub> samples by applying a HHF loading ( $\leq 23 \text{ MW/m}^2$ ) above the melting threshold in the high heat flux test facility GLADIS (IPP-Garching). Thereafter, they are exposed to D plasma in a low-pressure steady-state electron cyclotron resonance (ECR) plasma chamber ‘PlaQ’. The thermal desorption spectroscopy (TDS) measurements indicate that D retention reduces by ~40% after shallow surface melting for both of the two W grades. On the other hand, D retention in the WL10 is almost double that in the pure W regardless of whether surface melting occurs or not. The TDS spectra exhibit two main desorption peaks at around 550 K and 700 K, which largely corresponds to grain boundaries and voids respectively. However, an additional peak appears unexpectedly around 1070 K for the melted WL10. We attribute this additional high-temperature peak to the formation of the formation of the hydrogen absorbing metal La in the resolidified layer, which is confirmed by transmission electron microscopy and energy dispersive X-ray spectrometry results.

## Low-temperature plasma as a ferroptosis inducer in cancer cells

Shinya Toyokuni<sup>1,2</sup>, Hao Zheng<sup>1</sup>, Yasumasa Okazaki<sup>1</sup>, Kae Nakamura<sup>2</sup>, Hiroaki Kajiyama<sup>2</sup>, Hiromasa Tanaka<sup>2</sup>, Keiji Ishikawa<sup>2</sup> and Masaru Hori<sup>2</sup>

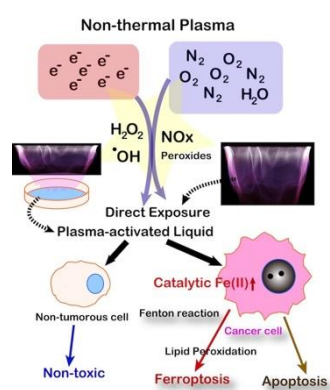
<sup>1</sup> Department of Pathology and Biological Responses, Nagoya University Graduate School of Medicine  
65 Tsurumai-cho, Showa-ku, Nagoya, Japan

<sup>2</sup> Center for Low-temperature Plasma Sciences  
Furo-cho, Chikusa, Nagoya 464-8603, Japan

Iron is an essential nutrient for every species on the earth. However, iron provides double edged sword; its deficiency causes anemia in mammals but its excess leads to toxic effects. Indeed, excess iron has been associated with carcinogenesis [1]. Ferroptosis is defined as a form of regulated necrosis, characterized by lipid peroxidation through high iron (oxidants)/sulfur (antioxidants) ratio [2]. Considering that cancer cells generally reserve more catalytic Fe(II) than non-tumorous counterparts, many iron-induced carcinogenesis models, including asbestos-induced mesothelioma, suggest that cancer is a state of “iron addiction with ferroptosis-resistance.” [3] The concept of ferroptosis is now expanding, and ferroptosis is observed not only in pathological conditions (cancer cells after chemotherapy; neurons with aging, etc.) but also in certain physiological conditions.

Low-temperature plasma (LTP) is a novel physical technique that emits abundant electrons, resulting in a variety of ROS products by reaction with ambient air. Exposure of LTP to biomolecules, cells or tissues causes oxidative stress *in situ*, leading to DNA breaks and lipid peroxidation products, such as HNE. We found that NTP exposure is highly dependent on Fe(II) *in situ*, causing cancer cell-specific ferroptosis, which was associated with autophagy activation and lysosome genesis. We are trying to visualize ferroptosis in formalin-fixed paraffin-embedded pathology specimens with new monoclonal antibodies, which revealed physiological ferroptosis [4].

NTP-activated Ringer’s lactate (PAL) is another modality at the preclinical stage as cancer therapeutics, based on more stable reactive species. PAL specifically kills



malignant mesothelioma (MM) cells, employing lysosomal nitric oxide as a switch from autophagy to ferroptosis [5]. Here we studied cytosolic iron regulations in MM and other cancer cells in response to PAL exposure. PAL can sensitize MM cells to ferroptosis by remodeling not only nitric oxide but also cytoplasmic iron homeostasis, where glutathione and poly(rC)binding protein 1/2 (PCBP1/2) play critical roles. PCBPs can be novel targets for cancer therapeutics.

(Funding: JSPS Kakenhi JP19H05462)

Fig. 1 Low-temperature plasma as a ferroptosis inducer in cancer cells

- [1] Toyokuni S, *et al.* Ferroptosis at the crossroads of infection, aging and cancer. *Cancer Sci* 2020;111(8):2665-2671.
- [2] Stockwell BR, *et al.* Ferroptosis: A Regulated Cell Death Nexus Linking Metabolism, Redox Biology, and Disease. *Cell* 2017;171(2):273-285.
- [3] Toyokuni S, *et al.* Iron and thiol redox signaling in cancer: An exquisite balance to escape ferroptosis. *Free Radic Biol Med* 2017;108:610-626.
- [4] Zheng H, *et al.* Embryonal erythropoiesis and aging exploit ferroptosis. *Redox Biol* 2021;48:102175.
- [5] Jiang L, *et al.* Lysosomal nitric oxide determines transition from autophagy to ferroptosis after exposure to plasma-activated Ringer's lactate. *Redox Biol* 2021;43:101989.



# Assessment of Probability Estimation on Human Tissue-Derived Fibroblast/Stromal Cells Response to Non-Thermal Biocompatible Plasma

Ihn Han<sup>1,2</sup> and Eun Ha Choi<sup>1,2</sup>

*1 Department of Plasma-Bio Display, Kwangwoon University, Kwangwoon University, Seoul 01897, Republic of Korea*

*2 Plasma Bioscience Research Center, Kwangwoon University, Kwangwoon University, Seoul 01897, Republic of Korea*

*I.Han [hanihn@kw.ac.kr](mailto:hanihn@kw.ac.kr)*

Non-thermal nano-biocompatible plasma (NBP) has emerged as a powerful biomedical tool with the potential to revolutionize tissue regeneration strategies. This study delves into the effects of NBP on human tissue-derived fibroblasts and mesenchymal stem cells (hMSCs), examining their responses in terms of cellular mobility, collagen synthesis, and osteogenic differentiation.

NBP treatment has been demonstrated to significantly enhance fibroblast mobility, facilitating their directed migration towards wound sites. This phenomenon holds the potential to expedite wound healing by ensuring the effective recruitment of essential cells to the site of injury. Moreover, NBP treatment stimulates the production of collagen, a critical extracellular matrix component essential for tissue remodeling. Collagen generation not only reinforces tissue structure but also supports the regenerative processes vital for complete healing.

Furthermore, this study uncovers NBP's impact on hMSCs, revealing its potential to promote osteogenic differentiation. NBP-treated hMSCs exhibit an increased propensity to differentiate into osteoblasts, the cells responsible for bone formation. Additionally, these differentiated osteoblasts show heightened mineralization capacity, indicating their potential in accelerating bone tissue regeneration.

This research contributes to our expanding knowledge of NBP's potential in tissue engineering and regenerative medicine. By enhancing fibroblast mobility and collagen generation while also promoting osteogenic potential, NBP presents an integrated approach to expedite wound healing and tissue remodeling. The quantified estimate of enhanced cellular responses obtained through statistical analysis offers a solid foundation for harnessing NBP's potential in innovative biomedical applications.

In conclusion, this study bridges the gap between non-thermal nano-biocompatible plasma and tissue regeneration by elucidating its multifaceted effects on fibroblasts and hMSCs. By addressing cellular mobility, collagen synthesis, and osteogenic differentiation, NBP holds promise as a transformative approach for advancing tissue healing and regenerative therapies.

## Cold atmospheric plasma facilitates wound healing for type 2 diabetes and skin flap treatments

BS Lou<sup>1,2</sup>, SH Chen<sup>3</sup>, CW Hou<sup>1</sup>, TP Chu<sup>4</sup>, and JW Lee<sup>4,5,6</sup>

<sup>1</sup> Chemistry Division, Center for General Education, Chang Gung University, Taoyuan, Taiwan

<sup>2</sup> Department of Orthopaedic Surgery, New Taipei Municipal TuCheng Hospital Chang Gung Memorial Hospital, Taoyuan, Taiwan. [blou@cgu.edu.tw](mailto:blou@cgu.edu.tw)

<sup>3</sup> Department of Plastic and Reconstructive Surgery, Chang Gung Memorial Hospital, Chang Gung University and Medical College, Taoyuan, Taiwan

<sup>4</sup> Department of Materials Engineering, Ming Chi University of Technology, New Taipei City, Taiwan

<sup>5</sup> Center for Plasma and Thin Film Technologies, Ming Chi University of Technology, New Taipei City, Taiwan

<sup>6</sup> Department of Mechanical Engineering, Chang Gung University, Taoyuan, Taiwan

Cold atmospheric plasma jet (CAPJ) has been employed in various biomedical applications based on their functions in bactericidal activity and wound healing. The effect of CAPJ generated by a particular composition of gases on wound closure and the underlying mechanisms that regulate wound healing signals had been investigated. He/Ar-CAPJ effectively induced keratinocyte proliferation and migration mediated through the activation of epithelial-to-mesenchymal transition (EMT) and cell cycle progression, which was evidenced by a decrease in E-cadherin levels and increases in N-cadherin, cyclin D1, Ki-67, Cdk2, and p-ERK levels. Rat wound healing studies showed that He/Ar-CAPJ treatment facilitated granulation tissue formation and mitigated inflammation in cutaneous tissue, resulting in accelerated wound closure. Furthermore, animal models were developed to evaluate the CAPJ treatment effect for diabetic rats in different stages as it progresses and angiogenesis for skin flap.

[1] BS Lou, JH Hsieh, CM Chen, CW Hou, HY Wu, PY Chou, CH Lai, JW Lee *Bioengineering and Biotechnology* 8, 683. 1-11 (2020).

[2] BS Lou, CH Lai, TP Chu, JH Hsieh, CM Chen, YM Su, CW Hou, PY Chou, JW Lee. *Journal of Clinical Medicine*, 1930 (2019).

## **In vivo toxicity test of DBD plasma activated water by using Zebrafish**

Ying-Hung Chen<sup>1</sup>, Yi-Jun Chung<sup>2</sup>, Chen-Shin Chen<sup>2</sup>, Yen-Lun Chung<sup>2</sup>, Yu-Ren Wei<sup>2</sup>, Ping-Yen Hsieh<sup>1</sup> and Ju-Liang He<sup>1,2</sup>

<sup>1</sup> *Institute of Plasma, Feng Chia University*  
*No. 100, Wenhwa Road, Seatwen District, Taichung City 407102, Taiwan.*  
[jlhe@o365.fcu.edu.tw](mailto:jlhe@o365.fcu.edu.tw)

<sup>2</sup> *Department of Materials Science and Engineering, Feng Chia University*  
*No. 100, Wenhwa Road, Seatwen District, Taichung City 407102, Taiwan.*

Climate change increases the need for efficient and sustainable technologies in food and agriculture. Plasma-activated water (PAW) is a new and emerging technology with potential applications in food and agriculture. PAW is water that has been treated with cold atmospheric plasma (CAP). The presence of reactive oxygen and nitrogen species (RONS) can produce a variety of synergistic effects on animals, plants, and food. PAW has been verified to effectively improve plant growth, crop preservation, food sterilization, and animal cell activation. However, humans will eventually eat these processed animals, plants, or food, and PAW's biotoxicity must be considered. The biotoxicity of PAW is an important indicator for evaluating its safety. The zebrafish embryo acute toxicity test is a commonly used evaluation method, which can assess the impact of PAW on fish in the early stages of development.

Here we present the results of the in vivo toxicity study on dielectric barrier discharge (DBD) plasma activated water by using Zebrafish as the test sample. The motive of such a study is to understand how the concentration of main active species  $\text{NO}_3^-$  and RONS in PAW can affect Zebrafish survival, so as to laterally figure out how the toxicity brought by  $\text{NO}_3^-$  can be tolerated by animal body. Experimentally, a set of  $\text{NO}_3^-$  water solution make-up with different concentrations was deployed for comparison, and a set of PAW with different  $\text{NO}_3^-$  concentrations was prepared at different plasma treatment time. Both sets were underwent Zebrafish test. The results of the tests will be reported. The research results will provide a scientific basis for the safety evaluation of PAW and provide guidance for the application of PAW in food and agriculture.

## Chemically Active Compounds Formed in Low-temperature Plasma Treated Liquids for Cancer Treatment

Camelia Miron<sup>1</sup>, Hiromasa Tanaka<sup>1</sup>, Taishi Yamakawa<sup>1</sup>, Du Lyin<sup>1</sup>, Hiroki Kondo<sup>1</sup>, Hiroshi Hashizume<sup>1</sup>, Takashi Kondo<sup>1</sup>, Kenji Ishikawa<sup>1</sup>, Shinya Toyokuni<sup>1,2</sup>, Masaaki Mizuno<sup>3</sup>, and Masaru Hori<sup>1</sup>

<sup>1</sup> Center for Low-temperature Plasma Sciences, Nagoya University,  
Furo-cho, Chikusa-ku, Nagoya 464-8603, Japan  
camelia@plasma.engg.nagoya-u.ac.jp

<sup>2</sup>Department of Pathology and Biological Responses, Nagoya University,  
Graduate School of Medicine, 65 Tsurumai-cho, Showa-ku, Nagoya 466-8550, Japan

<sup>3</sup>Center for Advanced Medicine and Clinical Research, Nagoya University Hospital,  
65 Tsurumai-cho, Showa-ku, Nagoya 466-8560, Japan

With the promising perspective of becoming a new type of oncological therapy, low-temperature plasma (LTP) has recently gained much attention [1,2]. The liquids treated with LTP contain a variety of reactive species, including molecular, atomic, radical, and ionic compounds. These interactions are changing the chemical properties of the irradiated liquids, reported to have anti-cancer activity [3]. Chemically active species identified in various plasma-treated liquids, such as Ringer's lactate or chitosan depend on the irradiation time and on the feeding gas mixture (argon, nitrogen, and oxygen) used in the discharge. The degree of polymerization is also modified by plasma treatment, depending on the chemical composition of the initial compounds used in the experiments.

The cleavage of radicals from the liquid precursors, such as methyl radicals, is followed by the formation of key intermediate products (peracetic acid, 2-2-dihydroxyacetic acid, carboxymethyl radicals, or oligosaccharides). Further interactions in plasma result in the formation of more complex compounds, such as glyceric acid, acetic anhydride, ethyl acetate, or tricarballic acid with stimulatory or inhibitory effects on cell viability. The killing selectivity towards cancer cells is influenced by the gas mixture used in the discharge, but also by the chemical composition of liquids, higher molecular weight compounds used in our studies being very effective in destroying the cancer cells. Plasma generates a mixture of certain chemically active species in the exact amount able to induce cytotoxic effects on breast cancer cell lines (MCF-7), leaving the non-tumorigenic epithelial cell lines (MCF-10A) unharmed. The adjustment of the plasma parameters gives the possibility of engineering liquids that induce a selective generation of chemical compounds responsible for the antitumor activity.

[1] S. Toyokuni, Y. Ikehara, F. Kikkawa, and M. Hori, *Plasma medical science* (AP, Elsevier, 2018).

[2] Y. Liu, K. Ishikawa, C. Miron, H. Hashizume, H. Tanaka, and M. Hori, *Plasma Sources Sci. Technol.*, **30**, 04LT03 (2021).

[3] C. Miron, K. Ishikawa, S. Kashiwagura, Y. Suda, H. Tanaka, K. Nakamura, H. Kajiyama, S. Toyokuni, M. Mizuno, M. Hori, *Free Radical Research*, **57**,104 (2023).

## **Recent trends of plasma deposition technologies for the development of next-generation electronic devices**

Jaeho Kim

*Samsung Electronics Co., Ltd  
1-1 Samsungjeonja-ro, Hwaseong-si, Gyeonggi-do 18448, Korea  
jplasma.kim@samsung.com*

Recently, the development of advanced electronic materials are required to realize next-generation electronic devices. In special, 2D materials such as graphene, MoS<sub>2</sub> and h-BN have been listed as strong candidates in the roadmap for future electronic devices [1]. Plasma-based technology is the most promising method for the lab-to-fab transition of 2D materials in semiconductor industry.

In this talk, we will review recent trends of plasma deposition technology including PECVD (plasma enhanced chemical vapor deposition) and PEALD (plasma enhanced atomic layer deposition) for the deposition of 2D materials. The growth mechanisms of 2D materials in plasma and the limitation of conventional plasma technology are discussed. The strategies to develop an advanced plasma deposition equipment which allows the lab-to-fab transition of 2D materials will be also discussed.

[1] International Roadmap for Devices and Systems (IRDS™) 2022 Edition.

## On the mechanism of Arcing phenomenon in low temperature plasma

Shinjae You<sup>1,2</sup>, Sijun Kim<sup>1,2</sup>, Chulhee Cho<sup>1</sup>, Daewoong Kim<sup>3</sup>, and Sanghoo Park<sup>4</sup>

<sup>1</sup> *Department of Physics, Chungnam National University  
Daejeon 34134, Republic of Korea  
sjyou@cnu.ac.kr*

<sup>2</sup> *Institute of Quantum Systems (IQS), Chungnam National University  
Daejeon 34134, Republic of Korea*

<sup>3</sup> *Department of Plasma Engineering, Korea Institute of Machinery and Materials (KIMM),  
Daejeon 34103, Republic of Korea*

<sup>4</sup> *Department of Nuclear and Quantum Engineering, Korea Advanced Institute of Science and  
Technology (KAIST), Daejeon 34141, Republic of Korea*

For more than 120 years, arcing, a transient high-density discharge, has attracted significant attention in both industrial and academic fields. Arcing leads to substantial damage on material surfaces, regardless of material properties. However, its underlying physics, particularly in moderate-density plasmas (ranging from  $10^{09}$  to  $10^{11}$   $\text{cm}^{-3}$ ), remains not entirely understood.

This study explored the mechanism triggering arcing on an arcing-inducing probe (AIP) within a radio frequency capacitively coupled plasma environment (RF-CCP). Detailed information about the experimental setup can be found elsewhere [1]. We examined arcing by measuring its voltage ( $V_{\text{AIP}}$ ) and current waveforms, capturing spatiotemporal images, and analyzing optical emission spectra. We found that electron emission from the arcing spot dominates both the arcing current and the emitted light, despite the existence of energetic ions and electrons produced by the capacitively coupled plasma. Additionally, we observed peaks in the emission lines caused by evaporated metals in the optical emission spectra, suggesting a sufficiently high temperature at the arcing spot to induce surface vaporization.

Based on these results, we propose that the initiation of arcing in a moderate-density plasma results from thermo-field emission and metal evaporation at the arcing spot, driven by intense Ohmic heating. This interplay triggers ionization collisions between emitted electrons and vaporized atoms, initiating an electron cascade near the emission point and eventually leading to the generation of arcing. While our proposed mechanism aligns with conventional understanding in vacuum arc scenarios, its significance lies in its examination under the RF-CCP environment with direct measurement of arcing voltage and current, as well as its spatiotemporal image analysis. Furthermore, our experimental results imply the presence of yet-unveiled mechanisms, such as the initiation of field emission, transition to thermo-field emission, and the influences of arcing on RF-CCP.

[1] S. -J. Kim, Y. S. Lee, C. -H. Cho, M. -S. Choi, I. -H. Seong, J. -J. Lee, D. -W. Kim, and S. -J. You, *Scientific Reports*, **12**, 20976 (2022).

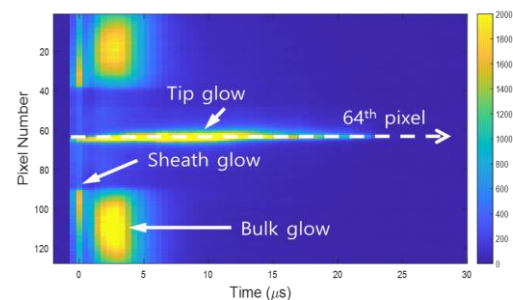


Fig. 1: Spatiotemporal image of arcing at  $V_{\text{AIP}}$  of -75 V, pressure of 171 mTorr, and RF power of 40 W.

# Enterprise Intelligentization of Semiconductor Manufacturing in Taiwan

Shu-Kai S. Fan

*Department of Industrial Engineering and Management, National Taipei University of Technology  
No. 1, Sec. 3, Zhongxiao E. Rd., Taipei 106344, Taiwan  
[morrisfan@ntut.edu.tw](mailto:morrisfan@ntut.edu.tw)*

This talk will discuss state-of-the-art technologies related to data science and their applications in the current semiconductor practice, particularly focused on the front-end-of-line processes. It addresses a new transformation framework, by making the transition from process transformation to artificial intelligence (AI) transformation. The major purpose is to harness the volatility, uncertainty, complexity and ambiguity (VUCA) situations in an attempt to encourage radical innovation in front-end-of-line (FEOL) semiconductor manufacturing. It will explore the advantages of these technologies and how they can create insights and values for semiconductor fabrication during the era of AI Economy.

## Ammonia-free Plasma-enhanced MOCVD for Nitride Semiconductors

Hisashi Yamada<sup>1,2</sup>, Naoto Kumagai<sup>1,2</sup>, Tetsuji Shimizu<sup>1,2</sup>, Xue-lun Wang<sup>1,2</sup>, Jaeho Kim<sup>1,2\*</sup>,  
and Hajime Sakakita<sup>1,2</sup>

<sup>1</sup> *AIST-NU GaN Advanced Device Open Innovation Laboratory (GaN-OIL),  
National Institute of Advanced Industrial Science and Technology (AIST),  
Furo-cho, Chikusa, Nagoya, Aichi 464-8601, Japan  
hisashi-yamada@aist.go.jp*

<sup>2</sup> *Research Institute for Advanced Electronics and Photonics (RIAEP),  
National Institute of Advanced Industrial Science and Technology (AIST),  
Tsukuba Central 2, 1-1-1 Umezono, Tsukuba, Ibaraki 305-8568, Japan*

Nitride semiconductors, such as gallium nitride (GaN), aluminum nitride (AlN), indium nitride (InN), and these alloy compounds, can contribute the SDGs society that meets an environmentally friendly manufacturing process without using toxic precursors, such as AsH<sub>3</sub> and PH<sub>3</sub> for InGaAs/InP system. InN has the bandgap of ~0.7eV, the smallest effective mass (0.07 m<sub>0</sub>), the highest electron mobility (>4000 cm<sup>2</sup>/Vs), and the highest saturation drift velocity (>5 × 10<sup>7</sup> cm/s) among nitride semiconductors. These features are promising not only for next-generation (6G) high-frequency devices but also for near-infrared opt-electronic devices. Furthermore, by layer stacking with InGaN and GaN, it is expected to realize full-color light-emitting diodes (LEDs) and tandem-type solar cells. However, the conventional metal-organic chemical vapor deposition (MOCVD) consumes large amounts of NH<sub>3</sub> (ex. for the GaN case, 1000-10,000 times more than the Group III elements) due to its low decomposition efficiency and elimination of residual impurities. The situation is more severe for InGaN and InN owing to the weaker In-N bonds, which requires lower growth temperatures. This results in almost no growth windows for high-In-content (In>0.4) InGaN and InN.

In order to overcome these issues, we have developed a microstrip-line microwave nitrogen plasma source<sup>[1]</sup> and integrated with MOCVD<sup>[2]</sup>. The plasma source provides an active nitrogen radical density of ~2 × 10<sup>14</sup> cm<sup>-3</sup>. This leads to the NH<sub>3</sub> consumption down to 1/100 or less using NH<sub>3</sub> plasma, and ultimately NH<sub>3</sub>-free manufacturing process using N<sub>2</sub> plasma. Furthermore, the plasma-enhanced MOCVD can expand the growth window toward the lower growth temperature range.

InN crystal growth was demonstrated on a 2-inch GaN/Al<sub>2</sub>O<sub>3</sub> (0001) template using trimethyl indium (TMI) and N<sub>2</sub> as the precursors. The growth temperature and pressure were 650°C and 2kPa, respectively. The plasma power and nitrogen gas flow rates were 90W and 2 L/min, respectively. The ω/2θ of the X-ray diffraction pattern confirms a (0002) peak. The full-widths-at-half-maximum (FWHMs) of the X-ray rocking curve (XRC) for (0002) / (10-12) are 618 / 999 arcsec, respectively. The total threading dislocation density is calculated as 2.4 × 10<sup>9</sup> cm<sup>-2</sup>, which agrees with the cross-sectional TEM result. The photoluminescence at room temperature reveals the peak energy and the FWHM of 0.687eV and 0.1 eV, respectively. The plasma-enhanced MOCVD makes it possible to obtain high crystalline InN without using NH<sub>3</sub>.

[1] J. Kim, H. Sakakita, H. Ohsaki, and M. Katsurai, Jpn. J. Appl. Phys. 54, 01AA02 (2015).

[2] H. Sakakita, N. Kumagai, T. Shimizu, J. Kim, H. Yamada, and X.-L. Wang, Appl. Mater. Today 27, 101489 (2022).

\*Present affiliation: Samsung Electronics Co., Ltd.



# Property control of Ge and Si nanostructured films by high-pressure He sputtering process for next-generation Li ion battery

Giichiro Uchida

Faculty of Science and Technology, Meijo University  
1-501 Shiogamaguchi, Nagoya 468-8502, Japan  
uchidagi@meijo-u.ac.jp

Electric vehicles powered by Li-ion batteries are increasingly replacing gasoline-powered vehicles toward the realization of a carbon-neutral society, and the development of high-performance Li-ion batteries that have high capacity for long-distance driving, high power for rapid charging, and low degradation for long-term use is encouraged worldwide. Group-IV Si and Ge are promising anode materials for Li-ion batteries because they have very high theoretical capacities of 4200 and 1600 mAh/g, respectively, which are 4–11 times higher than the 372 mAh/g capacity of commercial carbon. However, the high-capacity Si and Ge materials suffer large volume expansion during Li alloying reactions, and repeated cycling leads to material pulverization from the current collector, resulting in performance degradation. In the present study, we propose an alternative plasma bottom-up process to fabricate Ge and Si nanostructured films for Li-ion-battery anodes using plasma sputtering PVD. The important advantage of our plasma sputtering PVD is that it employs a simple single-step procedure that enables the direct fabrication of anode, where our method enables control of material properties such as crystallinity, conductivity, and morphology.

The Ge and Si anode films were fabricated on a Cu disk using 13.56 MHz radiofrequency magnetron sputtering.<sup>1,2)</sup> The Cu disk had a diameter and thickness of 15 mm and 80  $\mu\text{m}$ , respectively, and was placed at the center of the substrate holder. The sputtering target of 1 inch diameter was used. Ar or He gas was supplied from the direction of the target to the substrate holder, and the gas pressure was set to a high value of 100 to 500 mTorr. The distance between the target and the substrate holder was 10 or 20 mm. The substrate holder was not heated or cooled during film deposition. As shown in fig. 1, the film morphology could be controlled from a 3D nanoporous to a 1D nanowire morphology by changing plasma condition. In particular, 1D nanowire films were obtained under the special sputtering conditions of a SiSn (3–6 at%) target and He discharge gas at a high pressure of 100–500 mTorr. The 1D nanowires consisted of an amorphous Si core with high Li-ion capacity and a crystalline Sn shell with high electrical conductivity, which were suitable structures for Li-ion-battery anodes.<sup>2)</sup> We will discuss in detail the properties of nanomaterials and the performance of lithium-ion batteries.

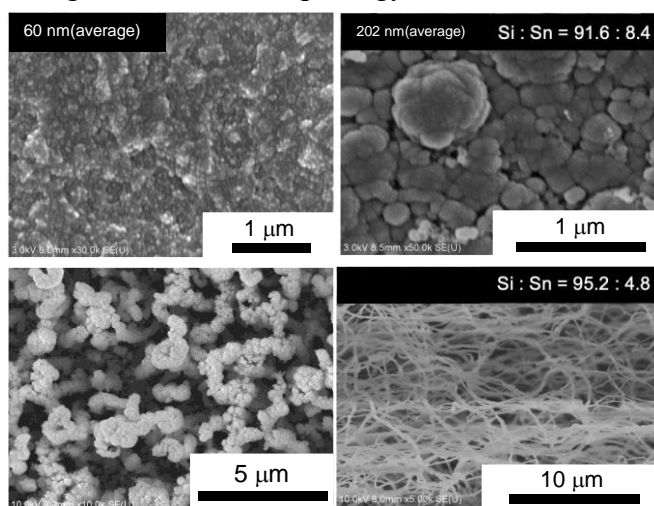


Fig. 1: Various morphology of Si nanostructured films fabricated in the low-temperature plasma process.

[1] G. Uchida *et al.*, *Sci. Rep* **12**, 1742 (2022).

[2] G. Uchida *et al.*, *Sci. Rep.* **13**, 14280 (2023).

## A process for synthesizing melted tin-carbon core-shell nanoparticles using dusty plasma

Munaswamy Murugesh and Koichi Sasaki

*Division of Applied Quantum Science and Engineering,  
Graduate School of Engineering, Hokkaido University, Sapporo 060-8628, Japan  
murugesh@elms.hokudai.ac.jp*

Energy management is a common interest in recent years with increasing awareness over sustainable development goals and increased utilization of energy resources. Particularly, phase changing materials (PCM) for thermal storage have gained wide attention from recent decades. The latent heat storage method is considered as one of efficient methods of thermal energy storage; it relies on the storage material absorbing or releasing heat when it undergoes the phase change between solid and liquid. This work is addressing the process development for synthesizing tin-carbon core-shell nanoparticles that can be used as PCM.

To realize the robustness of the shell against the volume expansion of the core at the melting, we constructed a process to deposit shell films around melted tin cores. As shown in figure 1(a), dc magnetron sputtering at a high pressure was used for synthesizing tin nanoparticles. The gravity transported nanoparticles to the bottom of the chamber, where a capacitively coupled rf plasma was generated using a ring electrode. Tin nanoparticles were trapped on the sheath boundary, and they were heated by the rf plasma. After the heating, we introduced methane to deposit amorphous carbon films around melted tin nanoparticles. Finally, core-shell nanoparticles thus synthesized were collected by applying a positive bias voltage to a circular electrode placed inside the ring rf electrode. Figure 1(b) shows TEM images of collected nanoparticles. The spherical shapes of cores suggest that they were melted when trapped in the rf plasma. We examined the melting characteristics of core-shell nanoparticles using TEM with the sample heating ability. We observed the melting (the transition from crystalline to amorphous structures) of cores at the melting temperature of metallic tin, indicating negligible oxidation of tin cores. In addition, we did not observe the break of shell films at the melting of cores. The present work has demonstrated the usefulness of dusty plasma to deposit shell films around melted cores.

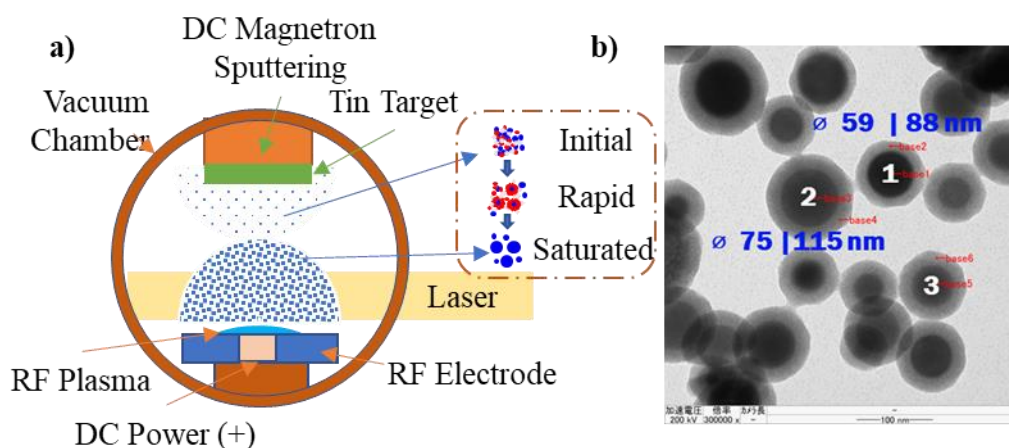


Figure 1. a) Schematic of synthesis apparatus and b) TEM images of synthesized core-shell nanoparticles.

## Controlling the synthesis, transport, and surface coverage of carbon nanoparticles using plasma CVD

Shinjiro Ono<sup>1</sup>, Manato Eri<sup>1</sup>, Takamasa Okumura<sup>1</sup>, Kunihiro Kamataki<sup>1</sup>, Naoto Yamashita<sup>1</sup>, Haruto Kiyama<sup>1</sup>, Naho Itagaki<sup>1</sup>, Kazunori Koga<sup>1</sup>, and Masaharu Shiratani<sup>1</sup>

<sup>1</sup> *Kyushu University, Motoooka 744, Nishi-ku, Fukuoka 819-0395, Japan  
s.ono@plasma.ed.kyushu-u.ac.jp*

Controlling the deposition properties of nanoparticles is a fundamental and important topic in plasma nanotechnology. In particular, carbon nanoparticles (CNPs) are widely applied in optical and chemical applications such as photocatalysis and electrode materials [1, 2]. There are many methods for synthesis of CNPs, including liquid-phase and spraying methods. Plasma processes are useful methods through a simple process with little contamination [3]. So far, we have revealed growth mechanism of Si nanoparticles in SiH<sub>4</sub> plasmas and realized to synthesized Si nanoparticles of 2 nm in size with a narrow size dispersion [4]. In this study, we studied the synthesis, transport and deposition of CNPs using CH<sub>4</sub> capacitively coupled plasma CVD, which allows large-area deposition and is highly compatible with semiconductor front-end processes.

The experiments were performed using a plasma CVD reactor [5]. A powered electrode was installed at 115 mm above a grounded substrate electrode. Mixture gas of Ar and CH<sub>4</sub> was introduced from the top of the chamber. The flow rate of Ar and CH<sub>4</sub> were 19 sccm and 2.6 sccm, respectively. Total pressure was set at 300 mTorr. A discharge frequency and voltage were 28 MHz and 280 V<sub>pp</sub>, respectively. To prevent unexpected agglomeration during CNPs fabrication using plasma CVD, we performed a pulse-like discharge method with a cycle of 1 min ON and 1 min OFF. The CNPs were observed using transmission electron microscopy (TEM).

We have measured the size of CNP deposited on the substrate from the TEM image and obtained size distribution. The results show that the distribution of the formed CNPs is divided into two groups. One group was small, with an average size of about 5 nm, while the other group was relatively large, with an average size of about 20 nm. From the size distribution, we calculated the coverage  $C_p$  of CNPs by following equation.

$$C_p = \pi r_p^2 n_p$$

where  $r_p$  is radius of CNPs and  $n_p$  is area number density of CNPs. The  $C_p$  shows the ratio of projected area of CNPs and total area. The  $C_p$  was linearly increased with the cycle number  $N_d$  of discharge. The CNP deposition takes place from  $N_d=10$ . The delay time of the CNPs deposition might suggest the time to increase the temperature of the discharge electrode to generate thermophoretic force exerted on the CNPs[6].

- [1] K. Koga et al., J. Phys, Conf. Ser., **518**, 012020 (2014).
- [2] L. Cao et al., J. Am. Chem. Soc., **133**(13), 4754-4757 (2011).
- [3] S. Nunomura et al., J. Appl. Phys., **99**, 083302 (2006).
- [4] T. Takeya et al., Thin Solid Films, **506**, 288 (2006).
- [5] S. H. Hwang et al., Thin Solid Films, **729**, 138701 (2021).
- [6] S.H. Hwang et al., Diam. Relat. Mater., **109**, 108050 (2020).

## Plasmonic Plasma Process using Nanoparticles on Substrate

Takeshi Kitajima and Toshiki Nakano

*National Defense Academy of Japan  
1-10-20 Hashirimizu, Yokosuka, Kanagawa 239-8686, Japan  
kitajima@nda.ac.jp*

With the sophistication of various surface processes by non-equilibrium plasma in the gas phase, it is a certain necessity in the direction of scientific and technological development to incorporate extended reaction fields due to the non-equilibrium nature of solid plasma and to design integrated non-equilibrium reaction fields.

In this talk, we introduce the plasmon resonance of nanoparticles on silicon wafers and chemical reactions on the surface layer enabled by radicals supplied by plasma. Plasma deposition can be performed at room temperature using plasmon resonance of nanoparticles on Si substrates. The case using gold nanoparticles and the case using HfN nanoparticles are shown.

Gold is a typical plasmonic nanoparticle [1], and it is known that the energy accumulated by surface plasmon resonance induced by light in the green region can induce various chemical reactions through hot electron emission [2].

In the study, gold is irradiated onto the silicon substrate from the deposition cell in a vacuum, and gold nanoparticles with an average diameter of 5 nm are grown by a self-assembly. Low pressure inductively coupled nitrogen plasma delivers nitrogen radical species onto the substrate through a stainless-steel mesh. Light for plasmon excitation is supplied either from the plasma itself or from a light emitting diode. In this configuration, adsorbed radical species are irradiated by hot electrons produced by plasmon de-excitation at the substrate surface, causing conversion of chemical bonds in the substrate. In the nitridation process of silicon substrates, uniform and ultra-thin low defect SiON films were formed at room temperature using green excitation light at 530 nm. In the oxidation process, similar low defect SiO<sub>2</sub> films were formed at room temperature using oxygen plasma and 850-nm near-infrared light.

HfN nanoparticles are known as an alternative plasmonic material to gold. By nitridating Hf nanoparticles generated by the self-assembly method and forming HfN nanoparticles, it is possible to deposit films on silicon substrates in the same way, in which case HfSiON films can be formed. Hot electrons from plasmon deexcitation allow dissociation of the SiO<sub>2</sub> passive layer at room temperature, resulting in interlayer transport of Si to enable film deposition.

This talk will also introduce the future vision of surface processes enabled by plasmonic plasma processes.

[1] V. Amendola, R. Pilot, M. Frascioni, O.M. Maragò, and M.A. Iati: J. Phys.: Condens. Matter 29, 203002 (2017).

[2] C. Clavero: Nature Photonics 8, 95 (2014).

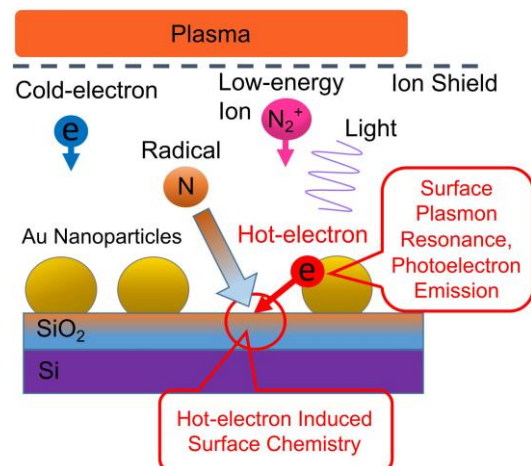


Fig. 1: Basic design of plasmonic plasma process with nanoparticles.

***Exploration of Atmospheric Pressure Plasma Technique in the Surface Modification on Anode Material for High-rate Lithium-ion Battery and Rapid Organic Fertilizer Manufacturing for Sustainable Farming***

Yuan-Tai Lai<sup>1</sup>, Che-Ya Wu<sup>1</sup>, Shih-Nan Hsiao<sup>2</sup>, Masaru Hori<sup>2</sup>, Shao-Hsuan Chin<sup>1</sup>, Pin-Hao Huang<sup>1</sup>,  
Yun-Chen Chan<sup>1</sup>, Jenq-Gong Duh<sup>1\*</sup>

1. Department of Materials Science and Engineering, National Tsing-Hua University, Hsinchu, Taiwan

2. Center for Low-temperature Plasma Sciences (cLPS), Nagoya University, Nagoya, Japan

\*Corresponding Author e-mail: jgd@mx.nthu.edu.tw

Atmospheric pressure plasma (APP) is an emerging technology, which has attracted the attention of scientists globally due to its combination of low cost, simplicity, and wide applications. It is shown that APP could be successfully used in materials science and manufacturing for the deposition of coatings, surface modifications, and treatments. In this study the recent developments in the applications of APP on energy materials and novel agriculture field would be presented.

Lithium ion batteries (LIBs), as the key technology in electrical energy storage systems, are applied in wide possibilities for next-generation electronics because of their high energy density, long lifespan, high operating voltage. Nowadays, with the rapid development of electric vehicle, the demands for battery have been focused on high power density and long cycle life. The APP has been used for LIBs anode materials treatment to meet requirements. The surface modification could result in the enhancement of electrochemical performance with stable capacity retention and high columbic efficiency and APP irradiation introduced into the manufacturing process of lithium ion batteries is a facile, green and scalable post-fabrication treatment approach.

Recent studies reveal that APP improves the electrochemical performance by N-doped decoration on conductive carbon, electrolyte wettability enhancement on PVDF binder, and defects manufacturing in  $\text{TiNb}_2\text{O}_7$  anode materials. Good wettability of surface free energy to  $51.0 \text{ mJ/m}^2$  in the APP-treated sample contributes to improved cycling performance. Both N-doped carbon and the modified TNO promote the high-rate capability. The C-rate performance of APP treated improves by over 250 % at 10 C as compared to the non-treated one. This work demonstrates a potential solution to achieve a roll-to-roll modification without any complex synthesis processes, which is a promising technology for the affordable manufacturing of lithium-ion battery anode.

In addition, APP applications could be extended into the agriculture field as a powerful tool for non-thermal processing. For the enhancement of germination and seedling stages, direct and indirect plasma treatment can interact with seeds and change their surface characteristics by etching, introducing functional groups or giving the essential nutrients. Recently, enhanced utilization of organic waste for fertilizer has significant impact for worldwide economy and ecology. The exploration of APP has also been expanded into food recycling areas. Using the plasma can help to promote the utilization and efficiency. Recent study has revealed that the plasma activated water (PAW) could rapidly react with organic waste to produce extra nitrate fertilizer ( $\text{NO}_3^-$ ). Herein, it is reported for the first time on organic wastes treated with PAW, implying an innovation way to rapid organic fertilizer manufacturing processes for sustainable farming in the novel agriculture related field.

## Plasma-Enhanced Atomic Layer Etching for Metals and Dielectric Materials

Heeyeop Chae

School of Chemical Engineering, Sungkyunkwan University (SKKU),

Suwon, 16419, Republic of Korea

The critical dimensions of semiconductor devices are continuously shrinking with 3D device structure and are approaching to nanometer scale. The demand for dimension control in angstrom level is drastically increasing also in etching processes. Atomic layer etching (ALE) processes are being actively studied and developed for various semiconductor and dielectric materials as well as metals. In this talk, various plasma-enhanced ALE (PEALE) processes will be discussed for isotropic and anisotropic patterning of metals and dielectric materials such as molybdenum, ruthenium, cobalt, titanium nitride, tantalum nitride, hafnium oxide, zirconium oxides. [1-9] Typical ALE processes consist of surface modification step and removal step. For the surface modification, various fluorination, chlorination and oxidation schemes were applied including fluorocarbon deposition, halogenation, oxidation with radicals generated plasmas. For the removal or etching step, various schemes were applied including ion-bombardment, heating, ligand volatilization, ligand exchange, and halogenation. The surface characteristics and requirements of plasma-enhanced ALE will be also discussed.

- 1) K. Koh, Y. Kim, C.-K. Kim, H. Chae, *J. Vac. Sci. Technol. A*, 36(1), 10B106 (2017)
- 2) Y. Cho, Y. Kim, S. Kim, H. Chae, *J. Vac. Sci. Technol. A*, 38(2), 022604 (2020)
- 3) Y. Kim, S. Lee, Y. Cho, S. Kim, H. Chae, *J. Vac. Sci. Technol. A*, 38(2), 022606 (2020)
- 4) D. Shim, J. Kim, Y. Kim, H. Chae, *J. Vac. Sci. Technol. B*, 40(2) 022208 (2022)
- 5) Y. Lee, Y. Kim, J. Son, H. Chae, *J. Vac. Sci. Technol. A*, 40(2) 022602 (2022)
- 6) J. Kim, D. Shim, Y. Kim, H. Chae, *J. Vac. Sci. Technol. A*, 40(3) 032603 (2022)
- 7) Y. Kim, H. Chae, *Appl. Surf. Sci.*, 619, 156751 (2023)
- 8) Y. Kim, H. Chae, *Appl. Surf. Sci.*, 627, 157309 (2023)
- 9) Y. Kim, H. Chae, *ACS. Sustain. Chem. Eng.*, 11, 6136 (2023)

## Overview of plasma heat exhaust studies in the DIFFER linear devices

I.G.J. Classen<sup>1</sup>, T.W. Morgan<sup>1</sup>, H.J. van der Meiden<sup>1</sup>, G.G. van Eden<sup>1</sup>, J. van den Berg<sup>1</sup>, K. Schutjes<sup>1</sup>, P. Rindt<sup>2</sup>, K.J. Loring<sup>1,3</sup>, J. Vernimmen<sup>1</sup> and the Magnum-PSI team<sup>1</sup>

<sup>1</sup> Dutch Institute For Fundamental Energy Research (DIFFER)  
De Zaale 20, 5612 AJ Eindhoven, The Netherlands  
First author email: [I.G.J.Classen@diffier.nl](mailto:I.G.J.Classen@diffier.nl)

<sup>2</sup> Science and Technology of Nuclear Fusion Group, Eindhoven University of Technology, Eindhoven, Netherlands

<sup>3</sup> Stanford University, Palo Alto, California, United States of America

The biggest challenge in the development of a reliable fusion reactor is the handling of large heat and particle loads on the reactor wall. To solve this heat exhaust problem, two different approaches can be taken:

- 1) The development of advanced reactor wall concepts that are capable of surviving the heat fluxes in future reactors, for example using liquid metal plasma facing components.
- 2) Developing plasma scenarios that greatly mitigate the fluxes before they hit the reactor wall, most notably *detachment*. Key to understanding detachment is the interaction of the plasma with a background of neutral particles in the divertor region.

Linear plasma devices are often used for studying the various aspects of the heat exhaust problem, as they offer divertor relevant conditions in a controlled, accessible and well diagnosed environment. Currently, two linear devices are operational at DIFFER: Magnum-PSI (see fig. 1) and UPP. Magnum-PSI is the main plasma facility at DIFFER, capable of producing reactor relevant heat and particle fluxes. The smaller UPP device, operational since 2021, will enable operando ion beam analysis of the plasma target, and is a valuable testbed for new diagnostics. A third linear device, LiMeS-PSI, is under development. LiMeS-PSI will be dedicated to testing liquid metal divertor concepts.

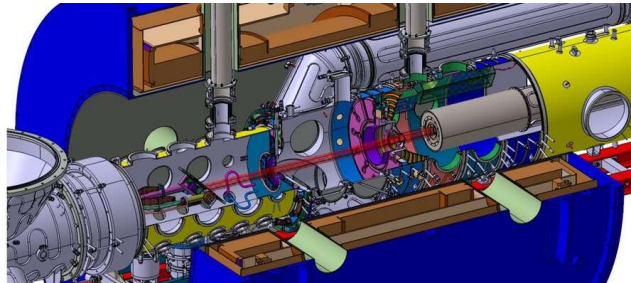


Fig. 1: The Magnum-PSI linear device [1] simulates the divertor conditions of future fusion reactors.

In this talk a selection of DIFFER linear device studies will be presented, all aiming at developing solutions to the heat exhaust problem. These studies include:

- Material testing of conventional Tungsten plasma facing components [2];
- Development of liquid metal divertor concepts, including vapor shielding [3,4];
- Detachment physics and divertor plasma characterization studies [5];
- Development of active spectroscopy methods to diagnose the neutrals in the divertor.

- [1] H. van Eck *et al.*, *Fusion Eng. Des.* **142** (2019) 26–32  
 [2] T.W. Morgan *et al.*, *Phys. Scr.* **T171** (2020) 014065  
 [3] G.G. van Eden *et al.*, *Phys. Rev. Lett.* **116** (2016) 135002  
 [4] P. Rindt *et al.*, *Nucl. Fusion* **59** (2019) 056003  
 [5] J. van den Berg *et al.*, *Nuclear Fusion* **61** (2021) 096007

## Review on DiPS-2 as a Linear Plasma Device: Source, Diagnostics, Physics and PMI

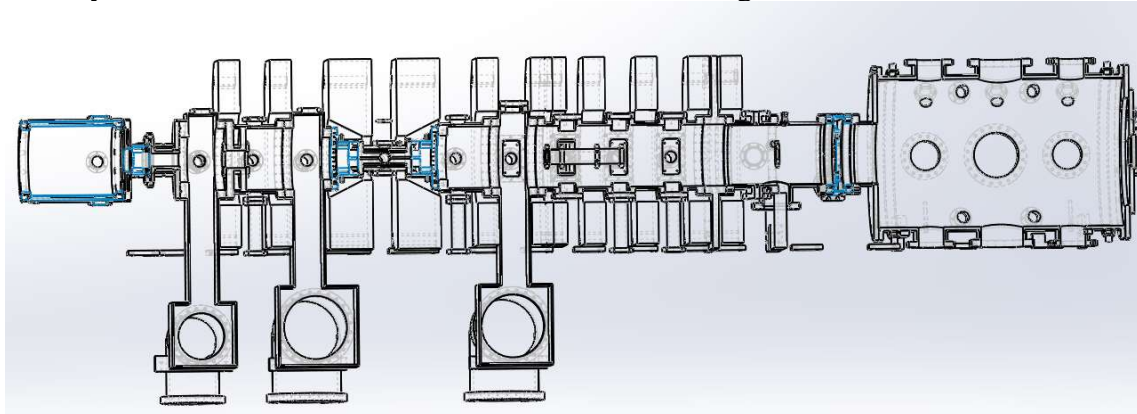
Kyu-Sun Chung<sup>1</sup> and APLers<sup>2</sup>

<sup>1</sup> Department of Electrical Engineering, Hanyang University  
222, Wangsimni-ro, Seongdong-gu, Seoul 04763, Korea  
[kschung@hanyang.ac.kr](mailto:kschung@hanyang.ac.kr)

<sup>2</sup> Former Members of Applied Plasma Laboratory of Hanyang University

DiPS-2 is a linear plasma device for simulating divertor and scrape-off layer (SOL) plasmas, which has been evolved as the following: (1) Diversified Plasma Simulator (DiPS) has been developed for simulations of divertor and space plasmas with various electric probes, such as single, triple, and Mach probes and gridded energy analyzer. DiPS consists of two major parts: a divertor plasma simulator with a LaB6 DC plasma source and a space plasma simulator with a helicon RF plasma source; (2) Divertor Plasma Simulator-1 (DiPS-1) is a part of DiPS with only a LaB6 cathode, where a low-power laser-induced fluorescence (LIF) is added and more electric probe diagnostics are augmented. It is dedicated only for fusion edge and divertor plasmas; and (3) Divertor Plasma Simulator-2 (DiPS-2) has been modified from the DiPS-1 by adding a magnetic nozzle with a limiter structure. DiPS-2 has a plasma source with a 4-inch LaB6 cathode, the same source as DiPS-1, and it is focused on plasma-material interactions (PMIs) and the development of various diagnostics such as LIF, laser Thomson scattering (LTS), and laser photo-detachment (LPD) along with various electric probes.

Although DiPS-2 could not generate ions with high temperature and toroidicity with much less power density compared to toroidal devices, it has been used for a few fusion-relevant physics experiments, including edge localized mode (ELM) simulation and edge transport of diffusion and convection: (1) an ELM simulation has been performed by modulating the magnetic field relevant to the pressure modulation of toroidal devices; and (2) the diffusion coefficients of free and bounded presheaths have been measured by simulating divertor or limiter transport. Moreover, the convection of the filament or the bubble expansion to the first wall of toroidal devices has been analyzed. PMIs have also been studied in terms of the following elements or processes: (1) boronizations, both for dust interactions with the surface chamber (DiSC) and KSTAR device, are analyzed; and (2) tungsten as a divertor-tile material is analyzed via laser ELM simulations in terms of dust generation and surface modification.



Schematic diagram of the DiPS-2, where LaB6 plasma source is on the left side, a magnetic nozzle is located in the middle, and DiSC is augmented on the right side.



# Plasma Fundamental Research Activities based on Atomic and Molecular Data in Korea Institute of Fusion Energy

Mi-Young Song<sup>1\*</sup>, Young Choon Park<sup>1</sup>, Heechol Choi<sup>1</sup>, Yeunsoo Park<sup>1</sup>, Young-Rock, Choi<sup>1</sup>, Dae-Chul Kim<sup>1</sup>, Jongsik Kim<sup>1</sup>, Yonghyun Kim<sup>1</sup>, Hyonu Chang<sup>1</sup>, Nidhi Sinha<sup>1</sup>, Swati Bharti<sup>1</sup>, HyunYeong Lee<sup>1</sup>,  
Jun-Hyoung Park<sup>1</sup>, Sun Min Han<sup>1</sup>

<sup>1</sup> *Institute of Plasma Technology, Korea Institute of Fusion Energy, 37 Dongjangan-ro  
Gunsan, Rep. of Korea*

\*Corresponding Author e-mail: mysong@kfe.re.kr

Through this opportunity, we would like to introduce the fundamental research of low-temperature plasma at KFE.

In recent years, we have utilized our research base to study the chemical and physical properties of candidate gases for the development of new alternative gases.

In particular, the properties of low GWP process gases in the semiconductor process were studied using the density functional theory DFT (wB97X-D/aug-cc-pVTZ) calculation using the Gaussian 09 program. In addition, the scattering cross-section by the electron collision gas was calculated using the R-matrix method.

Standard reference data for the spectral characteristics of the visible light region in ICP 13.56MHz argon plasma and nitrogen plasma were developed, and through this, wavelengths with high correlation with spectral signals and plasma temperature and density were secured.

In addition, the relationship between the atomic and molecular state characteristics of the plasma generation gas and the characteristics in the plasma was identified through the measurement of neutral species and ion species in CxFy plasma.

In addition, the International Data Evaluation Group has developed various scattering cross-section data sets for electron collisions with CH<sub>4</sub>, NF<sub>3</sub>, N<sub>x</sub>O<sub>y</sub>, and N<sub>2</sub> molecules. It can be used as basic data required for plasma analysis.

This work was supported by the R&D Program Plasma BigData ICT Convergence Technology Research Project through the Korea Institute of Fusion Energy (KFE) funded by the Government, Republic of Korea.

## REFERENCES:

- [1] Mi-Young Song, Hyuck Cho, Grzegorz P. Karwasz, Viatcheslav Kokoouline, Jonathan Tennyson, J. Phys. Chem. Ref. Data 52, 023104 (2023)
- [2] Heechol Choi, Young Choon Park, Yeon-Ho Im, Deuk-Chul Kwon and Sang-Young Chung, Plasma Chemistry and Plasma Processing, 43, 47-66, 2023
- [3] Nidhi Sinha, Heechol Choi, Mi-Young Song, Hyun-Jae Jang, Yeon-Ho Oh, Ki-Dong Song, Computational and Theoretical Chemistry 1225, 114159, 2023

# Multi-scale deep learning for estimating horizontal velocity fields on the solar surface

Ryohtaroh T. Ishikawa<sup>1</sup>

<sup>1</sup> *National Institute for Fusion Science,  
322-6 Oroshi-cho, Toki, GIFU 509-5292, Japan  
ishikawa.ryohtaro@nifs.ac.jp*

The dynamics on the solar surface are governed by thermally driven convection. This in turn produces cellular patterns that are observed in visible light continuum images. The bright areas with hot upflows are surrounded by darker and cooler downflows. The turbulent nature of the surface convection inherently creates flow structures that are smaller than the typical size of the convection.

We can obtain the line-of-sight (LOS) component of the flow velocities by spectroscopic observation via the Doppler effect. Conversely, there are no direct methods for observing the components perpendicular to the LOS to date. These components correspond to the horizontal velocity on the solar surface in disk center observations. There is a classical method called Local Correlation Tracking (LCT) [1] to estimate the horizontal velocity from intensity maps, but it has been pointed out that the LCT underestimates the velocity [2].

We developed a convolutional neural network that predicts the spatial distribution of horizontal velocity from the spatial and temporal variations of vertical velocity and temperature [3]. This model includes multi-scale deep learning architectures: the convolution layers have receptive fields of various sizes. This deep learning model is trained with numerical simulation data of the solar surface convection [4]. Moreover, we also developed coherence spectrum that can evaluate the correlation between the output image of the deep learning model and the original simulation data.

The multi-scale deep learning method successfully predicts the horizontal velocities. The correlation coefficient between the output of our model and the simulation was 0.77 which is better than the accuracy of LCT. We also found that the coherence spectrum has a strong dependence on the spatial scales; coherence is higher than 0.9 on large scales but it rapidly decreases to less than 0.3 on smaller scales. This decrease in coherence seems to occur near the energy injection scales that are comparable to the typical size of the convective cells.

- [1] L. J. November and G. W. Simon, *The Astrophysical Journal*, **333**, 427 (1988)
- [2] M. Verma, M. Steffen, and C. Denker, *Astronomy & Astrophysics*, **555**, A136 (2013)
- [3] R. T. Ishikawa, M. Nakata, Y. Katsukawa, Y. Masada, and T. L. Riethmüller, *Astronomy & Astrophysics*, **658**, A142 (2022)
- [4] T. L. Riethmüller, et al., *Astronomy & Astrophysics*, **568**, A13 (2013)

# Interpretable AI Supporting Scientists' Insight into Large-Scale Dynamics

Yoh-ichi Mototake

*Graduate School of Social and Data Sciences, Hitotsubashi University,  
Kunitachi-shi, Tokyo 186-8601, Japan  
y.mototake@r.hit-u.ac.jp*

I will introduce our efforts to elucidate the mechanism of large-scale dynamics using a framework of machine learning called interpretable AI. In recent years, machine learning models such as deep neural networks, which are widely used for their high performance, generally become black boxes that are difficult to interpret. In this talk, I explain two machine learning frameworks that reduce the large-scale system to a small-scale Hamiltonian system using a neural network, and, by interpreting the obtained neural networks model, reveal the system's mechanism.

The first framework is a framework to support the construction of reduced coordinates of a system using trained neural networks [1]. In this framework, a neural network that has learned the time series data of a large-scale system estimates the continuous symmetry of the system in a given reduced coordinate system (Fig). In Hamiltonian systems, the continuous symmetry of the system corresponds to conserved quantities, so the goodness of the reduced coordinate system can be evaluated in a physically interpretable form. I will show that this method can be used to support the construction of a reduced model of quasi-stable states of collective motion of fishes, which is a kind of active matter.

The other framework is for constructing reduced Hamiltonians using Hamiltonian neural networks [2]. Hamiltonian neural networks can estimate corresponding Hamiltonians as reduced models by taking reduced coordinate systems as inputs. Furthermore, combining them with autoencoders makes it possible to simultaneously estimate the reduced coordinate system and the reduced model by taking the original coordinate as input. By analyzing the properties of the Hamiltonian obtained as a neural network, interpretable information can be obtained. I introduce our trials of applying this framework to large-scale systems such as magnetic domain formation or fluid system.

In this talk, I will also introduce some points to note when extracting interpretable physics information from neural networks based on our empirical experience. Along with these insights, I would like to introduce the effectiveness and limitations of general frameworks that support physics research using neural networks.

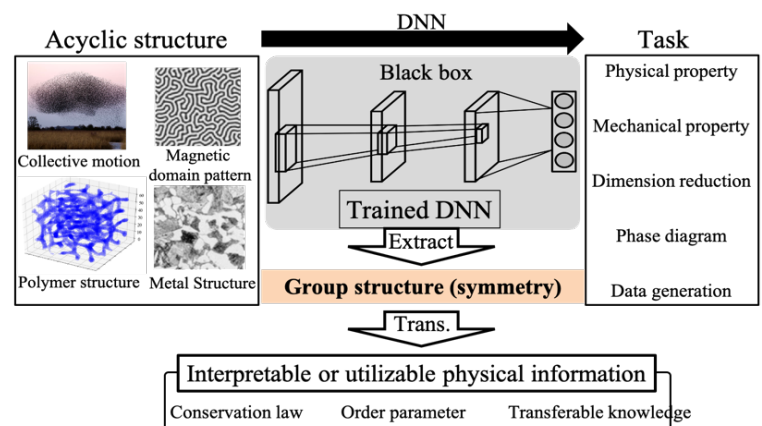


Fig. Extraction of interpretable information from trained DNNs

[1] Y. Mototake, *Phys. Rev. E* **103**, 033303 (2021).

[2] S. Greydanus, M. Dzamba, and J. Yosinski, *Neurips* **32** (2019).

## Plasma processing for diamond wafers

Hideaki Yamada

*National Institute of Advance Industrial Science and Technology, Japan.  
1-8-31 Midoriga-ooka, Ikeda, Osaka 563-8577, Japan.*

Several material constants of diamond which are the best amongst competitive materials have attracted researchers to realize several wonderful applications in industry in addition to mechanical tools and gem stones. Diamond is one of the ultra-wide-bandgap materials, which are expected to realize power devices with higher performance than those made of Si, SiC, and even GaN. Quantum information of Nitrogen-Vacancy center in diamond can be controlled under steady state, which may realize future information technology and quantum sensing.

For such purposes, it is indispensable to establish the way to produce the wafers with sufficient quality for each purposes under acceptable cost. The “man-made-diamond“ was firstly reported by using high-pressure-high-temperature method [1]. Then, plasma CVD was found to be another option to obtain diamond crystals artificially [2]. At present, mono-crystalline diamond substrates with even more than 10millimeter square, which were homo-epitaxially grown, are commercially available [3]. Hetero-epitaxial diamond with almost 4-inch diameter was also reported [4]. Mosaic wafer is another option to obtain homo-epitaxially grown inch size wafer [5]. Figure 1 shows companies which produces CVD mono- and poly- crystalline diamond raw material (colored in blue) and some products made of diamond (colored in red). Most of them started their activity in this 20 years. For this progresses, development of plasma CVD is indispensably important.

In this presentation, current state of the art of the plasma CVD for diamond growth is reviewed, which is followed by related R&D to develop techniques to realize diamond wafers for above mentioned several purposes.

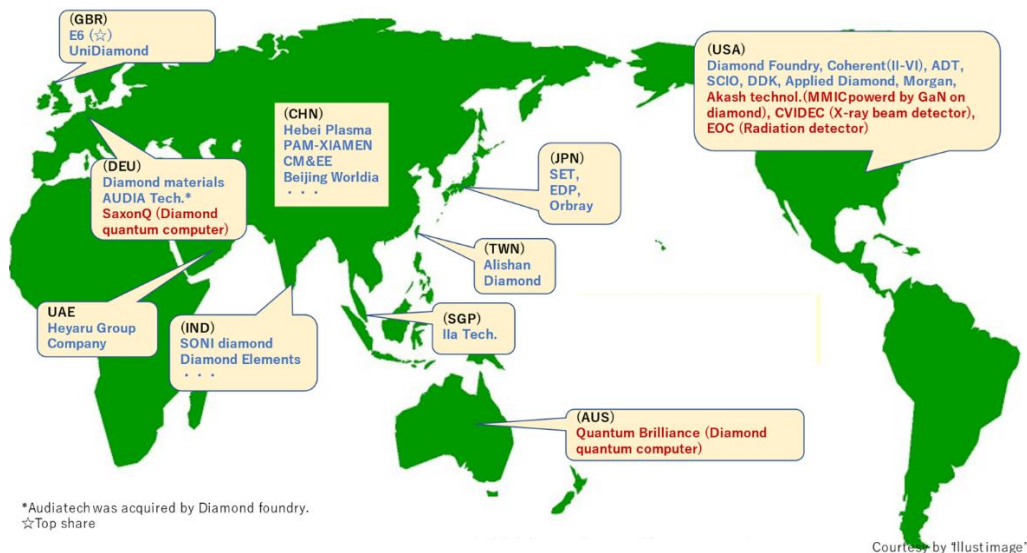


Fig. 1 Companies which produce diamond raw materials and products made of diamond.

### References

- [1] F. P. Bundy, H. T. Hall, H. M. Strong, et al., *Nature* 176 (1955), 51.
- [2] M. Kamo, Y. Sato, S. Matsumoto, and N. Setaka, *J. Cryst. Growth* 62 (1983) 642.
- [3] EDP Corporation, <https://www.d-edp.jp/en/> (last accessed at Sep. 8, 2023).
- [4] Diamond Foundry, <https://diamondfoundry.com/> (last accessed at Sep. 8, 2023).
- [5] H. Yamada, A. Chayahara, Y. Mokuno, et al., *Appl. Phys. Lett.* 104, 10 (2014) 102110.

# Nitrogen doped and undoped $Ti_3C_2T_x/Co_3O_4$ hybrid composites synthesis for application as anode materials in flexible Supercapacitor

A. Ali<sup>\*1)</sup>, L.M.C.H.P. Nguyen<sup>1)</sup>, Sosiawati Teke<sup>1)</sup>, Y.S. Mok<sup>1)</sup>

<sup>1)</sup> Department of Chemical Engineering, Jeju National University, South Korea

**Keywords:** MXene,  $Co_3O_4$ , hybrid composites, doping, supercapacitor

**Corresponding author\*:** [adnanaligohar@gmail.com](mailto:adnanaligohar@gmail.com)

## Abstract

Freestanding and flexible electrodes are vital for the development of flexible and wearable devices that store energy. But the significant trade-off between mechanical flexibility and electrode electrochemical performance limits the fabrication of efficient energy storage systems. In this research, we report the synthesis of a nitrogen undoped and doped hybrid composite made of 2D material i.e.  $Ti_3C_2T_x$  and  $Co_3O_4$ . Nitrogen doped hybrid composite is synthesized by reacting it with Urea in a hydrothermal unit at  $180^\circ C$  for 18 hours. These hybrid composite materials were characterized by scanning electron microscopy (SEM) Energy Dispersive Spectroscopy and X-Ray Diffraction for morphology and phases analysis. Besides these Transmission electron microscopies (TEM) and X-ray Photoelectron spectroscopy (XPS) were also done. For electrochemical analysis these hybrid composites materials were applied on the  $1\text{ cm}^2$  carbon cloth as active material (Working electrode). Their electrochemical i.e. cyclic voltammetry (CV), galvanic charge/discharge (GCD) and electrochemical impedance spectroscopy (EIS) were carried out in a three electrode set-up by immersing working electrode, counter electrode (Pt) and reference electrode (Ag/AgCl) in  $1M\ H_2SO_4$  electrolyte. We have studied the effect of different weighted ratios of N-doped and undoped  $Ti_3C_2T_x/Co_3O_4$  while doping while keeping the working electrode Ti weight constant. Furthermore, we have studied the effect of different weighted ratios of N-doped and undoped  $Ti_3C_2T_x$  and  $Co_3O_4$  nanoparticles and carried out the same set of characterizations and analyzed as active material for applying as active material in supercapacitor.

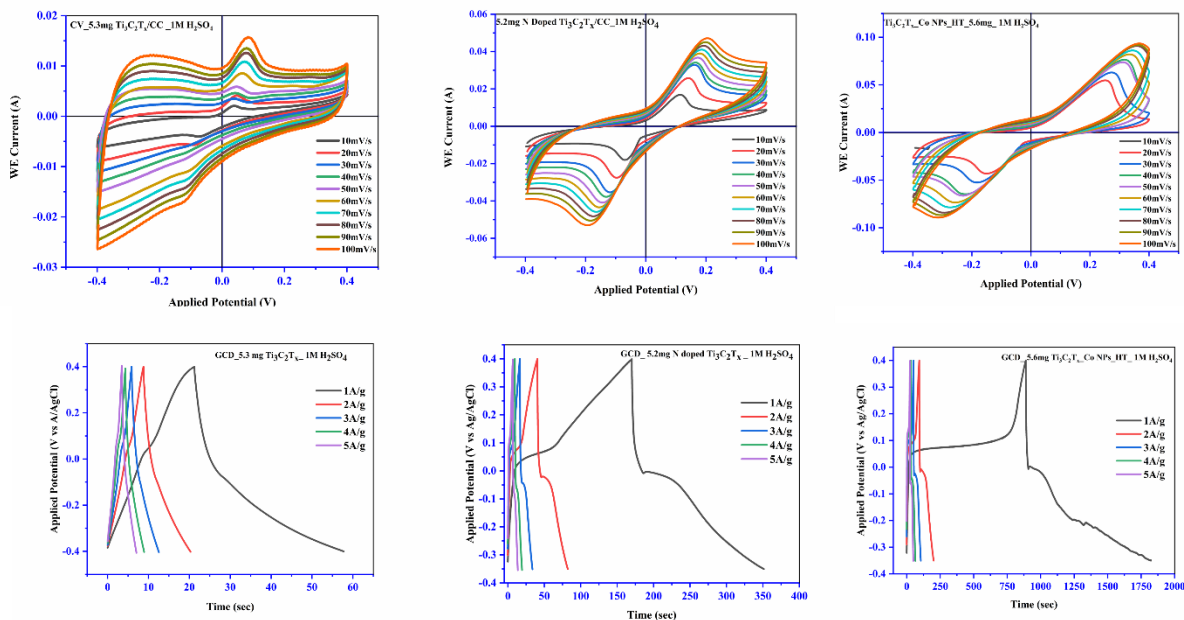


Figure 1.  $Ti_3C_2T_x$ , N-doped and Co Doped  $Ti_3C_2T_x$  anode material deposited on CC for flexible supercapacitor

## Development of Plasma Catalysis System for Reducing the Emissions of GHGs and Air Pollutants

Amir Machmud, and Moo Been Chang

*Graduate Institute of Environmental Engineering, National Central University, No. 300, Zhongda Rd, Zhongli District, Taoyuan City 32001, Taiwan*  
[mbchang@ncuen.ncu.edu.tw](mailto:mbchang@ncuen.ncu.edu.tw)

Plasma catalysis offers potential solutions for reducing the emissions of greenhouse gases (GHGs) and air pollutants. This emerging technology shows promise in improving current technologies across various applications. The advantages of plasma catalysis stem from its capability to combine the high selectivity of catalyst with the reactivity of plasma [1]. Dielectric barrier discharge is commonly used as a plasma source for this application, operating mainly under a filamentary regime where millions of microdischarges occur throughout the reactor with spatial and temporal non-uniformity. Recent studies have heavily focused on understanding these mechanisms and applying them effectively. Consequently, significant research efforts have focused on exploring the mechanisms and applications of plasma catalysis. A multitude of comprehensive reviews have been published over the years covering various aspects including specific applications such as: NO<sub>x</sub> abatement, VOC abatement, PFC (perfluorocarbon) abatement, and CO<sub>2</sub> conversion, or highlighting the importance of modeling and simulation to enhance our understanding of this field [2-4]. Despite gaining considerable interest for its diverse range of applications, vast majority of tests were conducted on a laboratory size. Considerable progress is being made in gaining an understanding of the intricacies of the mechanism of plasma catalysis, and this is significantly assisted by the theoretical and computational studies. In order to maximize the potential of plasma catalysis, it is essential to harness its distinctive attributes such as simplified catalyst preparation, rapid response times, low-temperature operation, and the synergistic effects between plasma and catalysis. These unique features offer numerous advantages that can be leveraged in various environmental applications. In this talk, several possible strategies to enhance the effectiveness and energy efficiency of plasma catalysis will be presented and discussed, i.e., (i) aligning the power supply with the reactor, (ii) optimizing and adopting suitable catalysts, (iii) utilizing computer-aided investigation of reaction mechanisms, and (iv) exploring potential pathways for achieving high activity and selectivity.

- [1] H. H. Kim, Y. Teramoto, A. Ogata, H. Takagi, and T. Nanba, *Plasma Chem. Plasma Process.*, **36**, 45-72, (2016).
- [2] X. Tu, J. C. Whitehead, and T. Nozaki, (Eds.). *Plasma Catalysis: Fundamentals and Applications*. (Berlin, Springer, 2019).
- [3] H.L. Chen, H.M. Lee, S.H. Chen, Y. Chao, and M.B. Chang, *Appl. Catal. B*, **85**, 1-9, (2008).
- [4] H.L. Chen, H.M. Lee, S.H. Chen, M.B. Chang, S.J. Yu, and S.N. Li, *Environ. Sci. Technol.* **43**, 2216-2227, (2009).

## Gradient-descent-method Analysis of Mie-scattering Ellipsometry during Fine-particle Growth in Plasma

Yasuaki Hayashi and Akito Miya

*Yamato University  
Katayama, Suita, Osaka 564-0082, Japan  
hayashi.y@yamato-u.ac.jp*

Mie-scattering ellipsometry had been developed for the analysis of growth of fine particles in plasmas [1-3]. It can analyze not only the size of fine particles but the growth process and other physical phenomena about fine particles suspended in space such as plasma. In Mie-scattering ellipsometry, analogous to thin film ellipsometry, the parameter angles  $\Psi$  and  $\Delta$  are defined by the ratio of the scattering amplitude function of a parallel polarization component,  $S_p$ , in scattering plane and to that of a perpendicular one,  $S_s$ , as

$$\tan \Psi \cdot e^{j\Delta} = \frac{S_p}{S_s} .$$

Those two amplitude functions are calculated for a single or monodisperse spherical fine particles by the Mie scattering theory. For polydisperse fine particles,  $\Psi$  and  $\Delta$  are calculated through the four Stokes parameters [1,3].

The growth process of fine particles are analyzed by the comparison correspondence between experimental and calculated results. Many unknown variables, such as particle size, size-distribution, refractive index, scattering angle, as well as the azimuth adjustment errors of polarizer and analyzer, are related to the change of  $\Psi$  and  $\Delta$  during particle growth. In order to determine these multiple unknown variables, the machine learning method is a powerful analytical method.

We have carried out the analysis of variation of  $\Psi$  and  $\Delta$  during fine-particle growth using regression analysis method as gradient-descent-method. Figure 1 shows an experimental result of variation of  $\Psi$  and  $\Delta$  during carbon fine particle growth in a methane plasma. The result of the analysis revealed that the particle size dispersion decreased with growth. It suggests that fine particles grew by coating of carbon films on smaller ultra-fine particles.

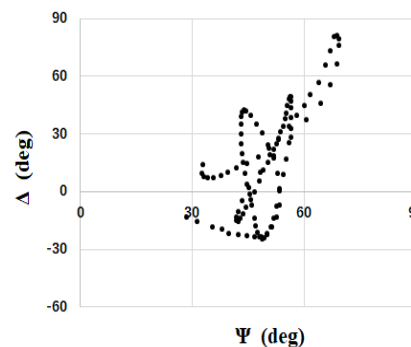


Fig. 1: Variation of  $\Psi$  and  $\Delta$  during particle growth in a methane plasma.

- [1] Y. Hayashi and K. Tachibana, *Jpn. J. Appl. Phys.* 33 (1994) L476.
- [2] Y. Hayashi and K. Tachibana, *Jpn. J. Appl. Phys.* 33 (1994) 4208.
- [3] Y. Hayashi and A. Sanpei, Chap.1 in *Ellipsometry*, INTECH, 2017.

## Analyses of Coulomb Crystals in Dusty Plasmas under Gravity and Microgravity

Kazuo Takahashi

*Faculty of Electrical Engineering and Electronics, Kyoto Institute of Technology  
Matsugasaki, Sakyo-ku, Kyoto 606-8585, Japan  
takahash@kit.jp*

Coulomb crystals of dusty plasmas have been investigated by projects utilizing facilities under microgravity for the past 20 years. An European Space Agency project of PK-4 has been working on the International Space Station since 2014. The apparatus of PK-4 enables to analyze dynamics of dust particles in a cylindrical discharge plasma. The author is engaging in experiments of the PK-4 on the ground and parabolic flights. Figure 1 shows the structures of Coulomb crystal in detail, which have been obtained in ground-based experiments [1]. In a cylindrical discharge plasma (Ar, 33 Pa, 700 V<sub>p-p</sub> at 1 kHz), spatial distribution of dust particles formed a cylinder with cross section of ellipse. Lower part of the cylinder consists of layers including the hexagonal closed-packing structure, which clearly appears in the region of  $2 < y < 4$  mm. The closed-packing structure around center of the cylinder indicates that compressive force toward to center confines the dust particles. Furthermore, outline of the cross section is not identical to potential contour of the plasma without dust particles in the cylindrical discharge, which the dust particles produce potential to confine themselves by self-consistent interaction with the plasma. A structure of liner chains formed under microgravity will be discussed in the presentation.

[1] Kazuo Takahashi and Hiroo Totsuji, *IEEE Trans. Plasma Sci.* 47, 4213 (2019).

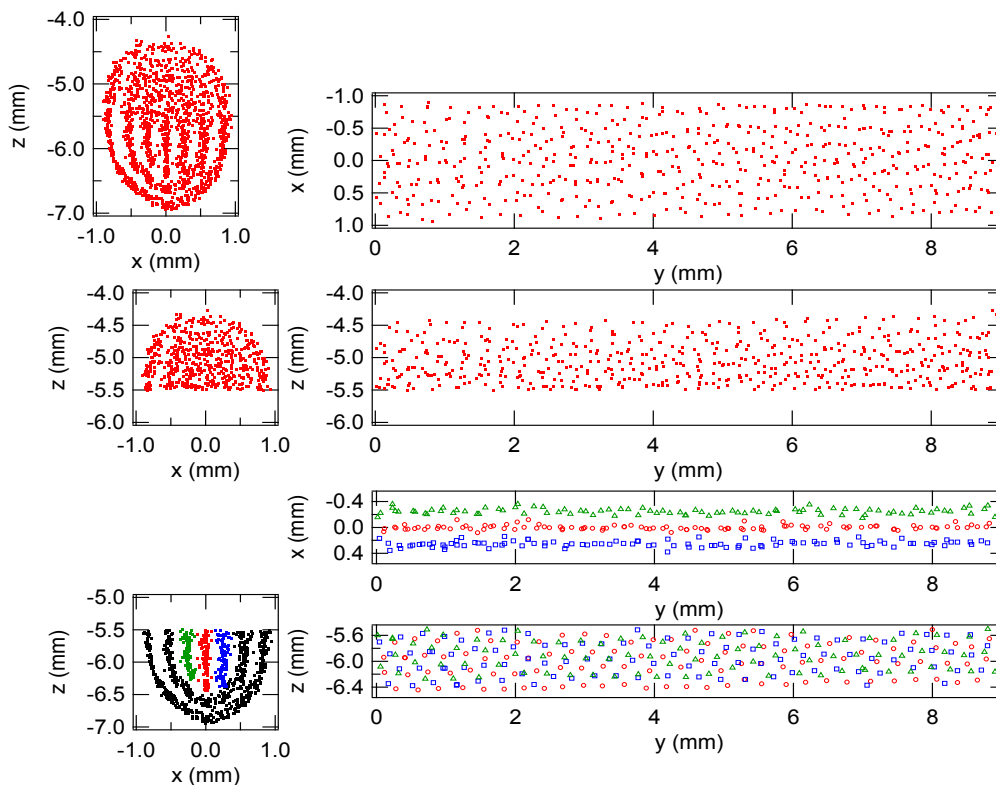


Fig. 1: Coordinates of dust particles in a cylindrical discharge plasma [1].



## Highly Sensitive Electric Field Vector Measurements Using an Optically Trapped Fine Particle

M. Shiratani<sup>1</sup>, T. Sato<sup>1</sup>, K. Kamataki<sup>1</sup>, S. W. Fitriani<sup>1</sup>, K. Tomita<sup>2</sup>,  
P. Yiming<sup>2</sup>, D. Yamashita<sup>1</sup>, N. Yamashita<sup>1</sup>, N. Itagaki<sup>1</sup>, and K. Koga<sup>1</sup>

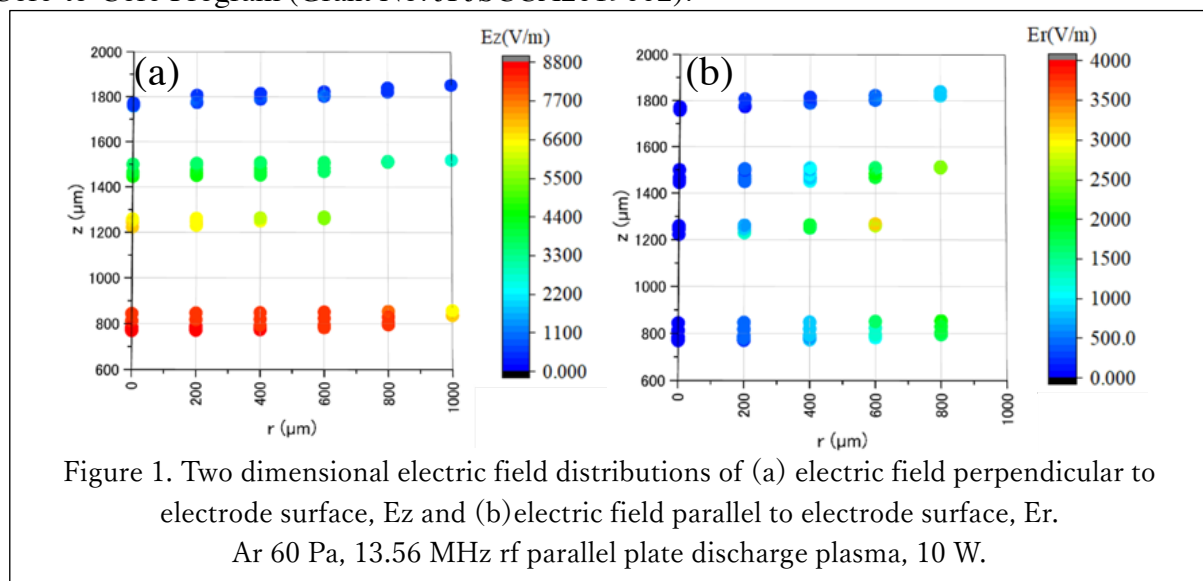
<sup>1</sup> Graduate School of Information Science and Electrical Engineering, Kyushu University,  
Motooka 744, Nishi-Ku, Fukuoka 819-0395, Japan  
siratani@ed.kyushu-u.ac.jp

<sup>2</sup> Graduate School of Engineering, Hokkaido University,  
Kita 8, Nishi 5, Kita-ku, Sapporo, Hokkaido, 060-0808 Japan

In low pressure processing plasmas, ions impinging on substrates often play key roles in the plasma processes. Ions are accelerated by electric field in pre-sheath and sheath before reaching substrate. Therefore, kinetic energy and incident angle of ions are predominantly determined by the electric field there. Especially, information on electric field and its fluctuation in a direction parallel to electrode surface are important, whereas it is difficult to obtain the information because electric field parallel to electrode surface is much smaller than that perpendicular to electrode surface.

To obtain such information, here we have developed a method of electric field vector measurements using an optically trapped fine particle [1, 2]. The electric field vector is deduced from force balance exerted on the fine particle. The method has a high sensitivity because of zero method as well as a high spatial resolution of the order of 20  $\mu\text{m}$ . Figure 1 shows an example of two dimensional profile of electric field near the plasma-sheath boundary using an acrylic fine particle of 10, 15, 18, 20  $\mu\text{m}$  in diameter, optically trapped with laser tweezers. The unique advantage of the method is to measure simultaneously high  $E_z$  around 8000 V/m together with low  $E_r$  below 20 V/m as well as their fluctuation.

This work was partly supported by JSPF KAKENHI (Grant No. JP20H00142) and JSPS Core-to-Core Program (Grant No. JPJSCCA2019002).



[1] T. Ito, et al., J. Phys. Conf. Ser. 518, 012017 (2014).

[2] M. Shiratani, et al., Mater. Sci. Forum 879, 1772 (2017).

## Laser-induced breakdown spectroscopy for wall diagnosis in nuclear fusion devices

Hongbin Ding

*Key Laboratory of Materials Modification by Laser, Ion and Electron Beams,  
Chinese Ministry of Education, School of Physics,  
Dalian University of Technology, Dalian, 116024, P.R. China  
hding@dlut.edu.cn*

In recent years, Laser-Induced Breakdown Spectroscopy (LIBS) has been developed for diagnosis of the co-deposition of impurities, fuel retention and wall conditioning on the first wall in fusion devices such as EAST, HL-2A[1] and KSTAR tokamaks[2] as well as W7X stellarator[3]. The main challenges faced by the LIBS diagnosis approach in fusion wall elemental analysis arise from two issues: firstly, LIBS spectral intensity is strongly affected by laser-plasma interaction such as the prompt electrons emissions, plasma shielding, charge separation, plasma sheath, self-absorption in vacuum environment such like Tokamaks; secondly, the matrix effect arising from the hardness and temperature of the substrate sample, which is due to laser-target interaction such as the nonlinear features in the different ablation regions: optical, thermal, phase-explosion; To achieve high accuracy of LIBS analysis, the laser-plasma interaction and the fluctuation of transient plasma parameters, which affect the LIBS stability and analysis accuracy, must be eliminated or reduced by the hardware or the algorithm software. So far, various approaches to improve LIBS signal strength and the plasma stability have been investigated in our team and others, including polarization-resolution constraint, magnetic field constraint, double-pulse and DC-discharge enhancement using micro-, nano-, pico- and femo-second lasers. For understanding matrix effect, recently the influence of the chemical sates, hardness, conductivity and temperature of the substrate sample on LIBS have been investigated. Above-mentioned, an in-situ endoscopic LIBS system has been successfully developed for the wall diagnosis study in EAST tokamak. The results show optimistic prospects and more details will be discussed in this forum.

[1] C.Li et al., *Frontiers of Physics*, **11**,114214(2016)

[2] L.Sun, et al., *Nuclear Materials and Energy*, **31**, 101174(2022)

[3] C.Li et al., *Physica Scripta*, **T170**, 014004 (2020)

## Development of Plasma Application Technology in IPT-KFE

Yong Sup Choi<sup>1</sup>

<sup>1</sup> *Institute of Plasma Technology, Korea institute of Fusion Energy  
37 Dongjangan-ro, Gunsan, 54004, Korea  
yschoi@kfe.re.kr*

Plasma Technology is widely used in various fields such as semiconductor, display, particle processing, surface modification, environment, bio, agriculture, and so on.

The Korean government-funded Institute of Plasma Technology at Korea institute of Fusion Energy(IPT-KFE) is developing the fundamental, core, and convergence technologies of plasma. The fundamental plasma technologies are cross section measurement and calculation, plasma material interaction, plasma modeling and simulation, and diagnostics and control. The core technology is development of new type plasma sources and innovation in applied plasma sources. The convergence technology is industrial applications of core technology.

Current research activities and applications of technologies will be presented, including plasma farming, semiconductor and display application, waste treatment, and so on.

# Surface morphology and grain structure changes induced by helium ion implantation and subsequent thermal annealing

Jia-Guan Peng\*, Long Cheng, Yue Yuan, and Guang-Hong Lu

*School of Physics, Beihang University,  
Beijing 100191, China  
peng1919@buaa.edu.cn*

Plasma-wall interaction (PWI) originated from high-flux plasma irradiation together with high heats load has been recognized as a critical concern for ITER which could impact both plasma operation and divertor component lifetime. Helium (He) is one of the main impurities in fusion edge plasma. In previous work, distinct changes in the surface morphology of tungsten (W) were observed under He plasma irradiation with a low incident energy of 80 eV and a low fluence of  $4 \times 10^{24} \text{ m}^{-2}$  at a high surface temperature of 1400 K [1]. After He plasma irradiation, it was also found that He nano-bubbles could retard recrystallization through the Zener drag force during annealing [2]. He could also be in bulk W in ways of energetic He ion implantation or transmutation. It has been found that the irradiation of W by He ion with an incident energy less than 100 keV can induce complex surface morphology changes [3]. Despite these findings, precise alterations in grain structure and surface morphology resulting from the effect of He and heat treatment remain unclear. In this work, the effect is investigated by using He ion implantation and subsequent thermal annealing.

Mirror-polished rolled W samples were exposed to He ions with energies ranging from 10 keV to 100 keV and ion fluences ranging from  $10^{19} \text{ m}^{-2}$  to  $10^{22} \text{ m}^{-2}$  followed by subsequent annealing at temperatures ranging from 1373 K to 1973 K. The results indicate that a low concentration of 40 appm He in W could significantly retard the recrystallization process in W. Moreover, the grain boundary (GB) motion transitions from shear-coupled migration to pure sliding migration at a higher He concentration. No distinct surface morphology change was found right after ion irradiation. However, when W samples were exposed to fluence larger than  $1 \times 10^{21} \text{ m}^{-2}$  and annealing at temperatures above 1473 K, a distinctive wave-like structure, measuring 3 nm in height, emerged in {111}-oriented grains, while {100}- and {110}-oriented grains exhibited no noticeable changes. Underlying mechanisms of the microstructure evolution are discussed based on ion channeling effects, He-vacancy interactions and dislocation loop-punching.

The results show that helium ion implantation retards grain boundary migration and induces surface morphology evolution during the annealing process. This contributes to understand the effects of helium on tungsten in ITER divertor. The temperature window of divertor operation might be enlarged by He in W.

- [1] C.M. Parish, H. Hijazi, H.M. Meyer, F.W. Feyer, *Acta Mater.* 62 (1) (2014).
- [2] Guo W, Cheng L, De Temmerman G, Yuan Y, Lu G.-H, *Nucl. Fusion* (2018).
- [3] Y. Ueda, H. Peng, H. Lee, N. Ohno, S. Kajita, *J. Nucl. Mater.* 442 (1–3) (2013).

## **MD simulation of the interaction between hydrogen and helium bubble in bcc iron**

Ze Chen\*, Zhengyang Ming, Chao Yin, Shifeng Mao, and Minyou Ye

*School of Nuclear Science and Technology, University of Science and Technology of China  
Anhui, Hefei 230026, China  
zchen@ustc.edu.cn*

It is of vital importance to understand the interaction between hydrogen (H) and helium (He) bubbles in reduced activation ferritic-martensitic (RAFM) steels for future fusion reactors. This work used molecular dynamics (MD) simulations to evaluate the H retention behavior of nano-sized spherical/cubic He bubbles, both of which have been observed in experiments. For spherical He bubbles, the effect of He-to-vacancy (He/V) ratio, bubble size, H concentration, and temperature on the H retention were studied in detail. The simulation results suggest that H prefers to reside at the bubble interface, with only a small fraction of trapped H inside the bubble. H<sub>2</sub> molecules were observed inside the He bubbles and the relation between H<sub>2</sub> formation and the He/V ratio within the bubble is discussed. The binding energy of atomic H to a 2 nm He bubble with a He/V ratio of 1.0 was calculated to be 0.73 eV by molecular statics (MS). Besides, for cubic He bubbles, the dependence of bubble orientation ((110) and (100)) on H trapping behavior was also investigated with the same He/V ratio of 1.0, size of 6 nm, and at the temperature of 923 K. Results indicated that the (110) bubble was more stable with less trapped H atoms than the (100) one. H prefers to be trapped at the edge regions instead of face center regions for both situations, which can be explained by the local stress distribution near the bubble. The difference of H trapping behavior between cubic bubbles and cubic voids was also discussed.

# Data Assimilation in Semiconductor Crystal Growth: Chemical Reaction Network Modeling

Akira Kusaba

*Research Institute for Applied Mechanics (RIAM), Kyushu University,  
Kasuga, Fukuoka 816-8580, Japan  
kusaba@riam.kyushu-u.ac.jp*

In semiconductor crystal growth, accurate modeling of vapor phase chemical reactions is crucial to control impurity concentrations. In general, those reactions form a complex network. The reaction rate constants for each reaction have been determined by first-principles calculations based on density functional theory (DFT) and transition state theory (TST). This is due to the difficulty of in situ measurement experiments in a reactor. However, the rate constants determined by calculations are often not quantitative enough to meet the requirement of concentration control in semiconductor engineering.

On the other hand, recent advances in measurement technology have made it possible to obtain concentrations of chemical species that could not be measured before. But it is still impossible to determine rate constants only from experimental data. Therefore, it is necessary to make good use of both computational and experimental data. In this research area, experimental data are generally more accurate as absolute values than computational data. Conversely, computational data are generally more comprehensive than experimental data. Thus, fitting to experimental data needs to be performed while preserving the trend of computational data.

Such an approach corresponds to the well-known data assimilation in meteorology. This study shows that such tuning of rate constants is possible simply by multi-objective optimization, rather than by using advanced statistical theory. In addition, the importance of reducing the size of reaction network to prevent overfitting is mentioned (Fig. 1). In the forum, more details will be presented, focusing on the methodology.

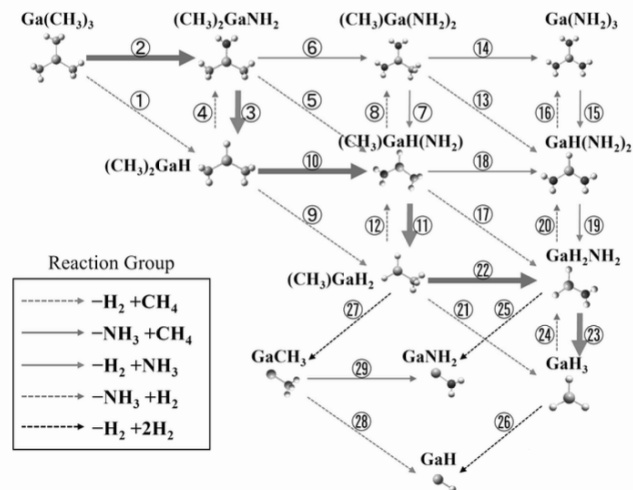


Fig. 1: Reduced reaction network in GaN MOVPE.

# A new approach to mixed-domain and higher-order dependence modeling

Keisuke Yano<sup>1</sup> and Tomonari Sei<sup>2</sup>

<sup>1</sup> *The Institute of Statistical Mathematics  
Micori cho, Tachikawa City, Tokyo, 190-8562, Japan  
yano@ism.ac.jp*

<sup>2</sup> *The University of Tokyo,  
Bunkyo-ku, Hongo, Tokyo 113-8656, Japan  
sei@mist.i.u-tokyo.ac.jp*

In data analysis, we frequently encounter mixed-domain data. This refers to multivariate data spanning various domains such as real values, categorical values, manifold values, and functional values. Categorical variables denote qualitative data, while manifold-valued variables typically manifest as directional or axial data. On the other hand, functional variables can be observed in forms such as power spectra.

In this presentation, we will introduce the minimum information dependence model [1]. This statistical model is tailored to analyze potential higher-order dependencies in mixed-domain data. We will highlight its utility through its application in the ecological study of penguins [2] and in the analysis of earthquake catalogs [3].

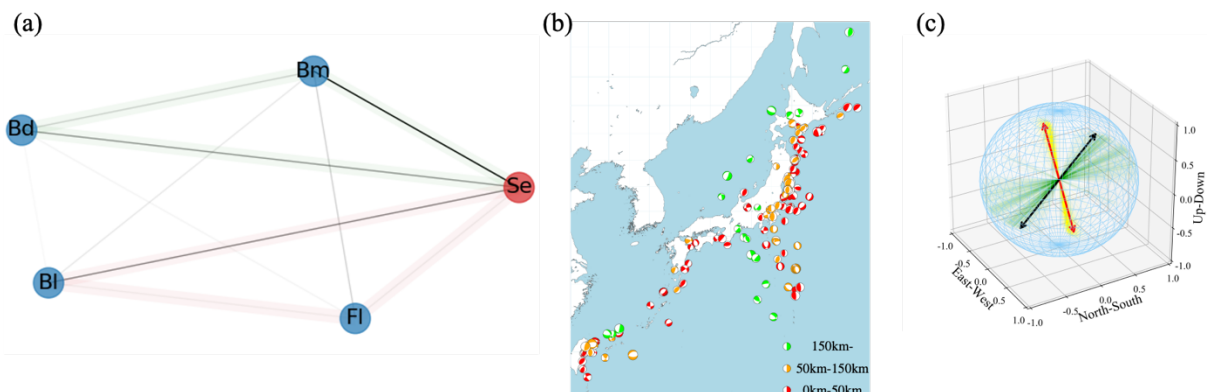


Figure 1: (a) Application to the ecological study of penguins for extracting the first and the second order dependencies; (b) The map of rupture patterns of 158 earthquakes that occurred in Japan during the period from January 1st, 2021 to December 8th, 2021 (c) Extracted dependence between the rupture patterns and the source depths.

[1] T. Sei and K. Yano, Minimum information dependence modeling for arbitrary product spaces, arXiv:2206.06792

[2] Horst, A. M., Hill, A. P. and Gorman, K. B. (2020). palmerpenguins: Palmer Archipelago (Antarctica) penguin data R package version 0.1.0.

[3] Japan Meteorological Agency (2022). The seismological bulletin of Japan. [https://www.data.jma.go.jp/svd/eqev/data/bulletin/index\\_e.html](https://www.data.jma.go.jp/svd/eqev/data/bulletin/index_e.html).

## Monolayer Graphene, an ideal material for exploring out-of-equilibrium phenomena involved in plasma-surface interactions

Pierre Vinchon<sup>1</sup>, Luc Stafford<sup>2</sup> and Satoshi Hamaguchi<sup>1</sup>

<sup>1</sup>Center for Atomic and Molecular Technologies, Osaka University  
2-1 Yamadaoka, Suita, Osaka 565-0871, Japan  
[vinchon@ppl.eng.osaka-u.ac.jp](mailto:vinchon@ppl.eng.osaka-u.ac.jp)

<sup>2</sup>Département de Physique, Université de Montréal, Montréal, QC H2V 0B3, Canada

With the ever-decrease in semiconductor devices dimensions, the precise understanding of plasma-surface interactions becomes crucial. It is especially necessary to study how low-pressure plasma can generate defects despite the low-energy ions which can be used in certain processes. Upon contact with the sample, plasma excited species generate out-of-equilibrium phenomena on surfaces, of which influences are difficult to quantify. Furthermore, synergistic phenomena can arise with the simultaneous irradiations of the sample by other plasma-excited species such as metastable and VUV photons. These effects are often invoked but rarely understood. As a result, a mechanistic understanding of plasma-surface interactions involving all excited species remains a challenge.

Since its experimental discovery in 2004, tremendous research effort worldwide has been focused on monolayer graphene to harness its remarkable properties. There are now numerous characterization methods that enable a precise understanding of its structure. Raman spectroscopy is particularly successful in providing a clear view of defect concentration and nature without altering the graphene state. Graphene will be particularly affected by any surface treatment which makes it ideal for the observation of phenomena affecting the extreme surface.

It has been shown that low-pressure Argon plasma irradiation of graphene induces a significant amount of defects despite the ultralow energy ions (~12 eV). This is even more remarkable considering that the threshold energy to generate defects in graphene is well established at 18-22 eV [1]. There is reason to believe that ion neutralization to the surface may contribute to defect generation [2]. On the other hand, Argon metastable influence, often overlooked for 3D materials treatment, has been observed to have a non-negligible influence on graphene, promoting vacancies migration and nucleation [3]. Both ions and metastable are suspected to generate transient hot electrons and holes in graphene, leading to out-of-equilibrium physics in graphene.

We will present how Molecular Dynamics simulations can support experiments involving graphene, enabling a better understanding of mechanisms that are in play at extreme surfaces during plasma-surface interactions. This would also contribute to shedding light on synergistic effects related to the combined influence of plasma-excited species. More generally, it is expected that experiments conducted with monolayer graphene could benefit other plasma processes in which atomic control is required.

- [1] F. Banhart, J. Kotakoski, and A. V. Krasheninnikov, *Structural Defects in Graphene*, ACS Nano **5**, 26 (2011).
- [2] P. Vinchon, X. Glad, G. Robert Bigras, R. Martel, and L. Stafford, *Preferential Self-Healing at Grain Boundaries in Plasma-Treated Graphene*, Nat Mater **20**, 49 (2021).
- [3] P. Vinchon, X. Glad, G. R. Bigras, A. Sarkissian, R. Martel, and L. Stafford, *Plasma-Graphene Interactions: Combined Effects of Positive Ions, Vacuum-Ultraviolet Photons, and Metastable Species*, Journal of Physics D: Applied Physics **54**, 295202 (2021).



# Poly-diagnostics of a nanosecond He-based atmospheric plasma

Nikolay Britun, Michael K. T. Mo, Shih-Nan Hsiao, Masaru Hori

Center for Low-temperature Plasma Sciences, Furo, Chikusa, Nagoya 464-8603, Japan  
britun@plasma.engg.nagoya-u.ac.jp

Discharges with pulse-on duration shorter than the glow-to-spark transition time normally possess high degree of non-equilibrium, where the temperature of heavy gas particles (e.g. He, Ar, N<sub>2</sub>, etc.) may be close to 300 K. The non-equilibrium regime in this case favours vibrational kinetics and efficient plasma radical production. In turn, the burst pulse regime of plasma operation may further increase molecular decomposition as well as the radical production.

This work deals with poly-diagnostic characterization of a ns- He-based plasma discharge [1], both in space and time. The study is targeted at various plasma parameters which are sparsely measured in literature (for same discharge). The optical emission, absorption and laser-based spectroscopy techniques are involved to our work in order to cover the dynamics of emission lines and ionization wavefronts, the electron density, rotational, vibrational and gas temperature, the evolution of He 2s <sup>3</sup>S<sub>1</sub> metastable state and electric field, as well as the discharge performance toward molecular decomposition (CO<sub>2</sub>) and synthesis (NO).

Among the main results, it was shown that the rotational excitation of N<sub>2</sub><sup>+</sup> ions precedes the electron excitation of the He (3p <sup>3</sup>P<sub>1</sub>) state at the pulse beginning [2], which is followed by electron avalanche with density exceeding 5×10<sup>15</sup> cm<sup>-3</sup>. The peak of the electric field (about 25 kV/cm) follows shortly after the electron avalanche [3]. At the same time, He 2s <sup>3</sup>S<sub>1</sub> metastable state gets abruptly populated during the pulse with number density exceeding 10<sup>14</sup> cm<sup>-3</sup> [4]. The typical evolution of the electron density, the discharge current and the population of He <sup>3</sup>S<sub>1</sub> state are shown in Figure 1.

The efficiency of CO<sub>2</sub> decomposition is found very low at small CO<sub>2</sub> admixtures in He, being at the same time > 20% at high admixtures (CO<sub>2</sub>/He > 3%) [5]. Since the thermal decomposition pathway should be likely excluded in our case, such decomposition behaviour can be associated with rather high electron temperature at low CO<sub>2</sub> admixtures, whereas at higher admixtures the (lower) electron energy may be predominantly channelized towards the vibrational excitation of CO<sub>2</sub> [6] also resulting in a higher energy efficiency.

The work is supported by the JSPS KAKENHI Tokusui project (19H05462).

[1] V. Gamaleev *et al.*, Rev. Sci. Instr. **93**, 053503 (2022)

[2] N. Britun *et al.*, PSST, **31**, 125012 (2022)

[3] N. Britun *et al.*, J. Appl. Phys., **133**, 183303 (2023)

[4] N. Britun *et al.*, (2023) *in preparation*.

[5] N. Britun *et al.*, (2023) *in preparation*.

[6] A. Fridman *Plasma Chemistry*, Cambridge University Press (2005)

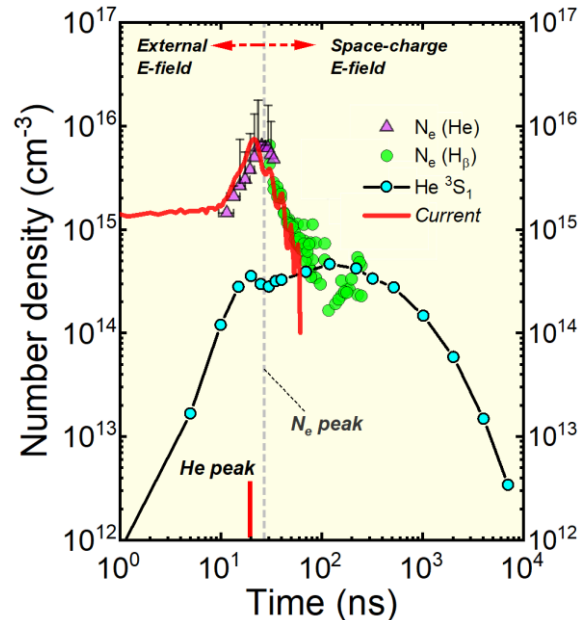


Fig. 1: The time-resolved evolution of the electron density, He <sup>3</sup>S<sub>1</sub> density and discharge current in the electrode gap.

# Application of Gliding Arc Plasma in Nitrogen fixation: Conversion of Atmospheric Nitrogen into Nitro compounds

Avik Denra<sup>1</sup>, Young Sun Mok<sup>1,\*</sup>

<sup>1</sup>Department of Chemical Engineering, Jeju National University, Jeju 63243, Republic of Korea

## Abstract

The substantial increase in the investigation of suitable ways for nitrogen fixation can be attributed to the need for higher agricultural productivity. Moreover, the abundant nitrogen in the atmosphere is not directly accessible to the living organisms. Currently, the commercial method of N<sub>2</sub> fixation is the Haber Bosch process for the conversion of N<sub>2</sub> into ammonia. However, the requirement of high amount of energy along with tons of CO<sub>2</sub> production are some of the major drawbacks of this process. This work implements the application of rotational gliding arc plasma to convert N<sub>2</sub> into nitro compounds. The generation of high energy electrons and radicals in the plasma mixture is effective to convert N<sub>2</sub> into Nitrogen oxides (NO<sub>x</sub>) in the presence of oxygen (O<sub>2</sub>). Herein, the effect of various input parameters (inlet gas flow rate, applied power, inlet gas composition) on the overall NO<sub>x</sub> yield were studied to investigate the optimum conditions for better energy efficiency. The NO<sub>x</sub> generation for an inlet composition of 3:2 N<sub>2</sub> to O<sub>2</sub> ratio was found to be higher compared to 1:1 feed ratio. For practical applications, the effect of water content in the feed was also investigated. The resultant NO<sub>x</sub> generated in the reactor was oxidized and dissolved into water to form Nitric Acid (HNO<sub>3</sub>). Thus, this work demonstrates a sustainable pathway for nitrogen fixation at atmospheric conditions.

**Keywords:** Rotational gliding arc plasma, N<sub>2</sub> fixation, Non-thermal plasma, NO<sub>x</sub> generation.

\* Correspondence: smokie@jejunu.ac.kr; Tel: +82-64-754-3682

## The Potential of a Simple Microplasma Reactor in Cobalt Oxide Nanoparticle Synthesis.

*Sosiawati Teke, Roshan Mangal Bhattarai, Avik Denra, Mai Cao Hoang Phuong Lan Nguyen, Young Sun Mok\**

*Department of Chemical Engineering, Jeju National University, Jeju-63243, Republic of Korea.  
corresponding author: [smokie@jejunu.ac.kr](mailto:smokie@jejunu.ac.kr)*

Cobalt oxide nanoparticles have gained widespread attention due to their unique properties, including an increased surface area, heightened reactivity, and exceptional optical, electronic, and magnetic attributes compared to their bulk counterparts. To precisely control particle size, traditional bottom-up synthesis in liquid media has been favored. In this study, we exploit the capabilities of microplasma technology for the production of  $\text{Co}_3\text{O}_4$  nanoparticles, eliminating the need for hazardous reducing agents while ensuring both efficiency and cost-effectiveness. The resultant nanoparticles were subjected to a thorough characterization process involving UV-Vis spectroscopy, X-ray diffraction (XRD), X-ray photoelectron spectroscopy (XPS), field emission scanning electron microscopy (FESEM), and transmission electron microscopy (TEM). Our findings demonstrate the successful synthesis of  $\text{Co}_3\text{O}_4$  nanoparticles through the implementation of microplasma technology.

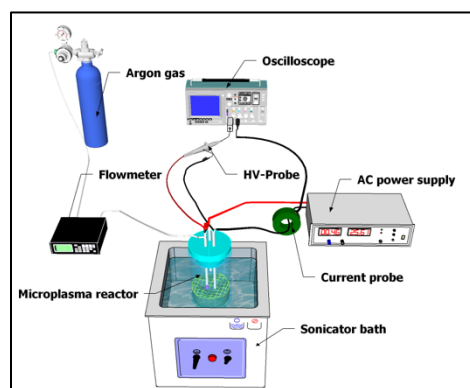


Figure 1. Schematic diagram of the microplasma setup.

# Sputter-Grown Size-Selected Nanocluster Synthesis: Deposition and Characterization for Material Science

Masahiro Shibuta

Osaka Metropolitan University, 3-3-138, Sugimoto, Sumiyoshi-ku, Osaka 558-8585, Japan  
shibuta@omu.ac.jp

High-temperature plasma, which is achieved by strong laser irradiation or ion sputtering, provides an important field for the synthesis of new functional nanomaterials with a bottom-up method. For example, C<sub>60</sub> fullerene is first generated in vacuum plasma and extracted as a functional chemical compound. After the discovery of C<sub>60</sub>, many researchers have explored artificial nanoclusters (NCs) composed of a few to several tens of atoms exhibiting distinct chemical functionalities to be used as nanomaterials in the next generation.

Here, I introduce several examples of atomically controlled NCs generated in the plasma field implemented by a magnetron sputtering (MSP) technique (Fig. 1 left) [1], where the NCs are deposited onto the substrate. In the MSP system, not only NCs with single atomic species (e.g. Ag<sub>n</sub>[2], Al<sub>n</sub>[3]), but also binary NCs (X<sub>m</sub>Y<sub>n</sub>) can be synthesized using alloy targets. Fig. 1 center shows the mass distribution of cationic NCs generated from a Ta-Si alloy target, providing selective generation of Ta<sub>1</sub>Si<sub>16</sub> NCs ( $m/z = 630$ ). The selective formation originates from both electronic and geometric factors, namely, an electron shell closure is satisfied with 68 e<sup>-</sup> at cationic species, and close-packed metal encapsulation is available with the Si<sub>16</sub> cage to be Ta@Si<sub>16</sub><sup>+</sup>. The amount of NC flux reaches several nA as an ion current, whose generation amount can fabricate “pure” Ta@Si<sub>16</sub> film on a substrate with several 10 min. deposition time.

The NC film can be characterized using conventional methods in the field of material science. The X-ray photoelectron spectra for Si 2*p* and Ta 4*f* core levels indicate 1:16 atomic ratio of the deposited NCs and their preferable +1 charge state on the substrate (Fig. 1 right). Furthermore, it revealed that the favorable charge states and chemical stabilities of M@Si<sub>16</sub> NCs can be tuned by changing the central metal atom (M = Lu, Hf, Ta (period 6), and V, Nb, Ta (group 5))[4,5]. These systematic studies will open up new material science based on a periodic table of NCs synthesized in the plasma field.

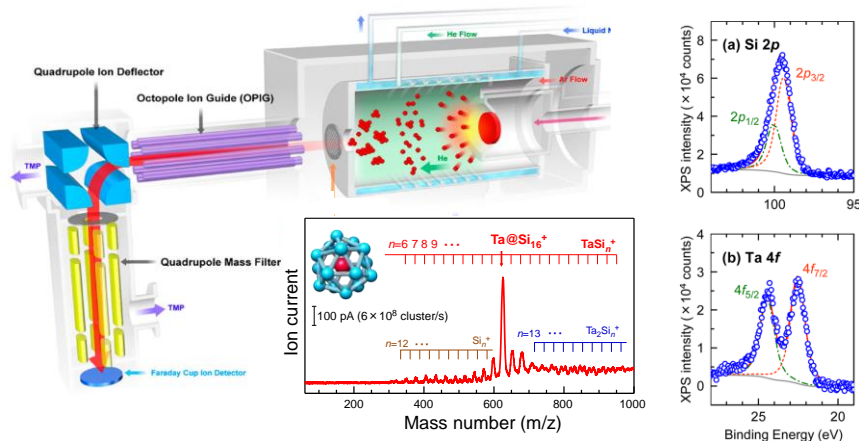


Fig. 1: (left) MSP NC deposition system, (center) Mass distribution of Ta<sub>m</sub>Si<sub>n</sub><sup>+</sup> NCs and (right) XPS spectra of the Ta@Si<sub>16</sub> film.

## References

- [1] H. Tsunoyama, M. Shibuta, et al., *Acc. Chem. Res.* **51**, 1735 (2018)
- [2] K. Yamagiwa, M. Shibuta, A. Nakajima, *ACS Nano* **14**, 2044 (2020).
- [3] M. Shibuta, et al., *Nat. Commun.* **13**, 1336 (2022).
- [4] M. Shibuta, et al., *J. Am. Chem. Soc.* **137**, 14015 (2015). *Phys. Chem. C* **120**, 15265 (2016).
- [5] M. Shibuta, et al., *Commun. Chem.* **1**, 50 (2018). *Phys. Chem. C* **126**, 4423 (2022).

## A microplasma-based approach for the growth of highly crystalline carbon nanotubes

Takashi Tsuji<sup>1</sup>, Guohai Chen<sup>1</sup>, Yoshiki Shimizu<sup>1</sup>, Hajime Sakakita<sup>1</sup>, Kenji Hata, Don Futaba<sup>1</sup>, Shunsuke Sakurai<sup>1</sup>

<sup>1</sup>*National Institute of Advanced Industrial Science and Technology (AIST)  
1-1-1 Higashi, Tsukuba, Ibaraki 305-8565, Japan  
takashi.tsuji@aist.go.jp*

The synthesis of defect-free, highly crystalline carbon nanotubes (CNTs) is crucial to fully harness the exceptional properties of this material. The primary methods for growing CNTs include substrate-based growth and gas-phase growth. In substrate-based growth, CNTs are grown from a dense array of catalyst nanoparticles on a substrate, allowing for the growth of CNTs in high areal density. However, defects in the graphitic lattice occur due to stress concentration at the CNT-catalyst interface from the contact with adjacent CNTs [1]. In contrast, gas-phase processes involve the growth of CNTs from catalyst nanoparticles “floating” through the reactor chamber. While this method yields highly crystalline CNTs, the areal density of the resulting CNTs is low, which limits its productivity. This is attributed to the agglomeration of catalyst nanoparticles at higher concentrations.

To address these challenges, I will discuss the development of a multi-step, gas-phase synthesis reactor composed of a micro-plasma based nanoparticle generator, a precision carbon feeding system, and a thermal reactor [2]. Each of these components are critical in generating the high density flow of size-controlled catalyst nanoparticles, which can be used to grow high crystalline single-walled carbon nanotubes. In short, catalyst particles, are formed by flowing the catalyst precursor through a microplasma for decomposition and nucleation. Then, the formed nanoparticles are mixed with a carbon feedstock within a very short time (a few milliseconds) after formation to modulate the level of agglomeration. Employing this approach, the growth of catalyst particles is effectively constrained to a scale of several nanometers even with catalyst precursor concentrations higher than those typically used in conventional gas-phase growth. Consequently, we could grow highly crystalline single-walled CNTs from these small particles. Characterization of the crystallinity by far-infrared spectroscopy (FIR) showed that the crystallinity is on par with arc-discharge synthesized CNTs.

We envision that the high-density aerosol growth of highly crystalline CNTs can be achieved through further enhancements in catalyst activity (ratio of particles growing CNTs to total particles).

[1] T. Tsuji, G. Chen, T. Morimoto, Y. Shimizu, J. Kim, H. Sakakita, K. Hata, S. Sakurai, K. Kobashi and D. N. Futaba: *Nanomaterials* 11, 3461 (2021).

[2] G. Chen, T. Tsuji, M. Yamada, J. He, Y. Shimizu, H. Sakakita, K. Hata, D. N. Futaba, S. Sakurai: *Chem. Eng. J.* 444, 13664, (2022).

# Discharge Mode Transition Triggered by Three-Wave Coupling in Partially Magnetized Cross-Field Plasma

JongYoon Park<sup>1</sup> and Jung Young Kim<sup>2†</sup>

<sup>1</sup> *Department of Nuclear Engineering, Seoul National University, Seoul 08826, Korea  
jongblues@snu.ac.kr*

<sup>2</sup> *Department of AI semiconductor Engineering, Korea University, Sejong 30019, Korea  
juneyoungkim@korea.ac.kr*

In this study, we discovered that the discharge mode transition in a partially magnetized cross-field plasma originates from a three-wave coupling between azimuthally rotating large- and small-scale spokes and the radially propagating breathing mode. By examining the frequency spectra and spectrograms of probe signals, we traced the simultaneous evolution of the rotating spokes into a turbulent state and the excitation of the breathing mode as the magnetic field strength intensified. Bi-spectral analysis offers conclusive evidence of the nonlinear coupling between the turbulent large- and small-scale spokes and the breathing mode. Significantly, the nonlinear spectral power transfer noted during the excitation of the breathing mode highlights an energy exchange among different modes. Ultimately, the radially propagating breathing mode induces an oscillation in the discharge current, driving the discharge mode transition.

## Non-neutral plasmas in Penning-Malmberg traps: fundamental studies and applications

Massimiliano Romé

<sup>1</sup> *Department of Physics, University of Milano, and INFN-Milano, Italy*  
*massimiliano.rome@mi.infn.it*

Contrary to the more common neutral plasmas, the dynamics of non-neutral plasmas is dominated by the electric field of their net charge [1]. The simplest non-neutral plasmas are composed of a single charged species. As an important example of the use of single-species plasmas, one can cite the CERN experiments aimed at the production and study of antihydrogen, where positron plasmas [2] and antiproton plasmas are confined in Penning-Malmberg traps (PMTs). Such traps use a strong axial magnetic field for radial confinement and an electrostatic field for axial confinement; the latter is produced by biasing a series of electrically isolated, hollow cylindrical conductors aligned along the magnetic axis.

The plasma density and total particle number in PMTs can be controlled by applying rotating electric fields at frequencies close to the azimuthal rotation frequency of the plasma, or by using evaporative techniques. The rotating fields are produced by applying suitably phased oscillating potentials to azimuthally sectored electrodes, while an evaporative cooling is performed by lowering one of the potential barriers confining the plasma such that the most energetic particles escape axially [3,4].

From the point of view of basic physics, the analogy between the transverse dynamics of a single-species plasma in a PMT and that of an incompressible, non-viscous 2D fluid [5] allows to carry out investigations of fluid phenomena under carefully controlled conditions and in almost ideal conditions. These experimental investigations, accompanied by related numerical investigations, help to shed light on the dynamic characteristics of fluid flow [6], ranging from the onset and decay of diocotron (Kelvin-Helmholtz) waves to the development of coherent structures and turbulence, in conditions of free evolution or under the effect of an external forcing [7,8].

Recent results [9,10] on the control and manipulation of the dynamics of a pure electron plasma obtained experimentally in the PMT ELTRAP [11] operating at the University of Milano, and numerically with 2D or 3D particle-in-cell numerical simulations [12] are reported.

- [1] R. C. Davidson, *Physics of Nonneutral Plasmas* (World Scientific, 1990).
- [2] J. R. Danielson, D. H. E. Dubin, R. G. Greaves, and C. M. Surko, *Rev. Mod. Phys.* **87**, 247 (2015).
- [3] M. Ahmadi, et al. (ALPHA Collaboration), *Phys. Rev. Lett.* **120**, 025001 (2018).
- [4] J. Fajans and C. M. Surko, *Phys. Plasmas* **27**, 030601 (2020).
- [5] M. Romé and F. Lepreti, *Eur. Phys. J. Plus* **126**, 38 (2011).
- [6] M. Romé, S. Chen, and G. Maero, *Plasma Sources Sci. Technol.* **25**, 035016 (2016).
- [7] M. Romé, S. Chen, and G. Maero, *Plasma Phys. Control. Fusion* **59**, 014036 (2017).
- [8] M. Romé, S. Chen and G. Maero, *AIP Conf. Proc.* **1928**, 020012 (2018)
- [9] M. Romé, G. Maero, N. Panzeri and R. Pozzoli, *ECA Vol. 43C*, P2.4003, *Proceedings of the 46<sup>th</sup> EPS Conference on Plasma Physics* (Milano, Italy, 2019).
- [10] G. Maero, N. Panzeri, L. Patricelli, and M. Romé, submitted to *J. Plasma Phys.* (2023).
- [11] M. Amoretti, G. Bettega, F. Cavaliere, M. Cavenago, F. De Luca, R. Pozzoli, and M. Romé, *Rev. Sci. Instrum.* **74**, 3991 (2003).
- [12] Yu. Tsidulko, R. Pozzoli and M. Romé, *J. Comp. Phys.* **209**, 406 (2005).

## Plasma-assisted Mist CVD for Formation of 3D Nanostructured Zinc Oxide Thin Films

Kosuke Takenaka<sup>1</sup>, Susumu Toko<sup>1</sup> and Yuichi Setsuhara<sup>1</sup>

<sup>1</sup> *Joining and Welding Research Institute, Osaka University, Ibaraki, Osaka, Japan*  
*k\_takenaka@jwri.osaka-u.ac.jp*

Functional oxide materials are expected as a key materials for next generation electronics. In particular, flexible devices with functional oxide thin films have attracted great attention for next-generation FPDs and flexible solar cells. Flexible devices including semiconductor and transparent conducting oxide (TCO) should be formed at a temperature lower than the glass-transition (softening) temperature of polymer substrates. Therefore, development of functional thin film deposition at low temperatures is strongly desired for application to flexible devices on polymer substrates. To overcome these problems in the low-temperature formation of functional thin films, plasma-assisted reactive processes using inductivity-coupled plasma (ICP) has been developed. In this study, functional oxide thin film deposition using plasma-enhanced chemical vapor deposition (CVD) have been studied. In advanced plasma-enhanced CVD, plasma-assisted mist CVD have been developed. This system is combination of mist CVD and plasma-assisted deposition. The surface morphology of the ZnO film deposited by plasma-assisted mist CVD shown by scanning electron microscopy (SEM) images shows that the ZnO films were textured with round grains, which is attributed to the effect of the use of mist with the precursor. [1,2] The plasma-assisted mist CVD is expected to be a film formation method to control the surface structure of functional thin films. Droplet vaporization behavior during plasma-assisted mist CVD of zinc oxide films was investigated. The droplets injected into the plasma are vaporized by the heat flux from the plasma. It was found that micrometric size droplets evaporate completely within several microseconds due to heat flux from the plasma. Moreover, owing to differences in vaporization rates, solid particles were formed from some of the droplets during their passage through the plasma, but other droplets formed incomplete particles or remained as droplets due to incomplete evaporation. Particles formed in the plasma and subsequently deposited on a substrate maintained their shape.[2]

[1] K. Takenaka, Y. Okumura, and Y. Setsuhara, *Jpn. J. Appl. Phys.* **52** 01AC11(2013)

[2] K. Takenaka, and Y. Setsuhara, *Plasma Sources Sci. Technol.* **28**, 065015 (2019).



## Evaluation of Carbon Nanoparticle Adhesion on Substrate Surface Deposited by Plasma CVD

\*Kazunori Koga<sup>1</sup>, Shinjiro Ono<sup>2</sup>, Manato Eri<sup>2</sup>, Takamasa Okumura<sup>1</sup>, Kunihiro Kamataki<sup>1</sup>, Naoto Yamashita<sup>1</sup>, Naho Itagaki<sup>1</sup>, and Masaharu Shiratani<sup>1</sup>

<sup>1</sup> Faculty of Information Science and Electrical Engineering, Kyushu University, 744 Motooka, Nishi-ku, Fukuoka 819-0395, Japan

<sup>1</sup> Graduate School of Information Science and Electrical Engineering, Kyushu University, 744 Motooka, Nishi-ku, Fukuoka 819-0395, Japan

\*[koga@ed.kyushu-u.ac.jp](mailto:koga@ed.kyushu-u.ac.jp)

Keywords: Plasma, Hydrogenated amorphous carbon, Carbon nanoparticle, Young's Modulus

Nanoparticle deposition on a substrate is an important research topic for bottom-up nanosystem fabrication using plasmas as well as nanoparticle synthesis. So far, we have studied the growth of nanoparticles in plasma chemical vapor deposition (CVD) to realize size and transport control [1-4], but information on the nanoparticles adhesion on the substrate is little. Here we analyzed the adhesion status of carbon nanoparticles (CNPs) deposited on the substrate. We have successfully controlled the size of nanoparticles by plasma CVD [1, 2]. Based on the results, we produced CNPs of 20 nm in size using CH<sub>4</sub>+Ar plasma CVD. We deposited CNPs on the surface of a hydrogenated amorphous carbon (a-C:H) film of 150 nm in thickness. The projected area  $C_p$  of the deposited CNPs on the substrate was 10.9% of the total substrate area. The  $C_p$  was controlled by discharge duration for CNP production. We analyzed mechanical characteristics of CNPs on substrate using a nanoindenter. We measured the load-displacement characteristic of samples using a Berkovich indenter. The indentation depth was set to 15 nm to obtain information on the a-C:H film without the influence of Si. The hold time at maximum load was set to 1 s. For the sample without CNPs, the curves showed a typical a-C:H thin film. The Young's modulus and hardness were 200 GPa and 26 GPa, respectively. For the sample with CNPs, the maximum load was about one-fifth of that without CNPs and the modulus and hardness were 50 GPa and 3 GPa, respectively. The differences in the curves are considered to be information that includes the mechanical properties of the nanoparticles as well as changes in the contact conditions of CNPs on the substrate during the indentation. Details will be discussed at the meeting.

[1] S.H. Hwang et al, Processes **9** (2021) 2.

[2] S.H. Hwang et al., Diam. Relat. Mater. **109** (2020) 108050.

[3] M. Shiratani et al., J. Phys. D: Appl. Phys 44 (2011) 174038.

[4] Y. Watanabe, J. Phys. D: Appl. Phys 39 (2006) R329.

## Contribution of Condensation and Coagulation for Nanoparticle Growth in Modulated Induction Thermal Plasmas

Yasunori Tanaka<sup>1</sup>, Yurina Nagase<sup>1</sup>, Yusuke Nakano<sup>1</sup>, Tatsuo Ishijima<sup>1</sup>,  
Shiori Sueyasu<sup>2</sup>, Shu Watanabe<sup>2</sup>, Keitaro Nakamura<sup>2</sup>

<sup>1</sup> Kanazwawa University  
Kakuma, Kanazawa, Ishikawa 920-1192, Japan  
tanaka@ec.t.kanazawa-u.ac.j

<sup>2</sup> Research Center for Production and Technology, Nisshin Seifun Group Inc.,  
Tsurugaoka 5-3-1, Fujimino 356-8511, Japan

Nanoparticles (NPs) have garnered significant attention due to their exceptionally high specific surface area and distinctive physical and chemical properties. The demand for functional nanoparticles produced at high production rates has led us to develop an original and innovative method: the Tandem-Type Modulated Induction Thermal Plasma (Tandem-MITP) with Time-Controlled Feeding of Feedstock (TCFF) [1]. Following our experimental investigations of nanoparticle synthesis by Tandem-MITP+TCFF method, we have also developed a numerical model for the synthesis of silicon nanoparticles employing the Tandem-MITP+TCFF approach [2]. This advanced model enables the simultaneous computation of the modulated electromagnetic thermofluid field, the dynamics of feedstock powder behavior and evaporation, and the nucleation and growth of nanoparticles. It takes into account the intricate interplay among these processes. In the NP synthesis sequence, nucleation is the initial step, followed by subsequent condensation and coagulation, leading to the enlargement of NP size.

The present study revolves around elucidating the roles played by condensation and coagulation in the growth of nanoparticles within the MITP + TCFF method. We delve into the efficient conversion of precursor materials into nanoparticles through meticulously controlled condensation and coagulation processes.

Fig. 1 indicates an example of the distributions of condensation rate (left) and coagulation rate (right) at  $t=0$  ms for considering the nanoparticle growth mechanisms in tandem-MITP+TCFF method. These are the production terms of the second moment of the particle size distribution function [3]. Each indicates the contributions of heterogeneous condensation and coagulation to nanoparticle growth. As seen, condensation rate becomes locally higher at edge region at  $r=35$  mm. On the other hand, coagulation occurs in wider region of  $10 \text{ mm} < r < 60 \text{ mm}$  in the chamber.

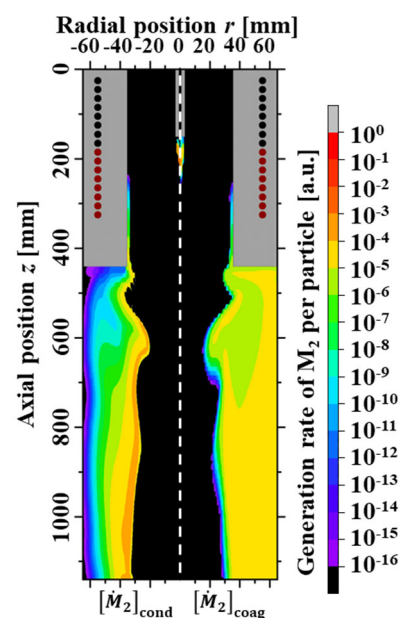


Fig.1 Condensation rate(left) and coagulation rate(right) in tandem-modulated induction thermal plasmas at a certain timing.

[1] K. Kuraishi, et al., J. Phys. Conf. Ser., 441, 012016 (2013).

[2] Y. Tanaka, et al, The 73rd Annual Gaseous Electronics Conference (GEC2020), GT3.00006, (2020).

[3] R. Furukawa, et al, J. Phys. D: Appl. Phys. 55, 044001 (2022).

# Surface Blistering and Deuterium Retention in Chemical Vapor Deposition Tungsten Exposed to Deuterium Plasma

Hao Yin<sup>1,2</sup>, Long Cheng<sup>1,2,\*</sup>, Yue Yuan<sup>1,2</sup> and Guang-Hong Lu<sup>1,2</sup>

<sup>1</sup> School of Physics, Beihang University,  
Beijing 100191, China  
LCheng@buaa.edu.cn

<sup>2</sup> Beijing Key Laboratory of Advanced Nuclear Materials and Physics, Beihang University,  
Beijing 100191, China

One of the key issues in the realization of commercial fusion nuclear power plants is the choice of plasma facing materials. Tungsten (W) is currently the main candidate material for the divertor of the fusion reactor ITER under construction and the first wall of future reactor DEMO and CFETR, as it is resilient against erosion, has the highest melting point of any metal and shows rather benign behavior under neutron irradiation, as well as low tritium retention. Chemical vapor deposition (CVD) technology has recently attracted much attention as it is the main way to produce thick tungsten coatings. CVD-W has characteristics of high density, high purity and high surface coverage with a <001> oriented columnar-grain microstructure. There have studies reported that CVD-W has good performance on thermal conductivity, thermal shock and fatigue resistance. This work focuses on the performance of CVD-W under plasma exposures with a low flux and low fluences to demonstrate the early-stage plasma irradiation effect in CVD-W including surface morphology changes and deuterium (D) retention.

Four grades of W were used including CVD-W with large-size grains (CVD-L) and small-size grains (CVD-S), rolled W (ND-W), and recrystallized W (Rec-W) as the reference material. The average grain size of four samples is ~30.4, 10.9, 10.3, and 55.7  $\mu\text{m}$ , respectively. After surface polishing, samples were irradiated to D plasma in the linear plasma device LEPS with fluences of  $5 \times 10^{24}$ ,  $1 \times 10^{25}$ , and  $2 \times 10^{25}$   $\text{m}^{-2}$ . The ion flux was about  $1.0 \times 10^{21}$   $\text{D m}^{-2}\text{s}^{-1}$  and specimen temperature were set at about 500 K. Thermal desorption spectroscopy was used to measure D desorption and total D retention by heating samples up to 1473 K at a constant heating rate of 1 K  $\text{s}^{-1}$ .

Both types of CVD-W samples featured a columnar grain structure, with the surface normal direction preferred to close to <001>, especially for CVD-L. They showed good resistance to blistering, with no blisters at low fluence and only several sub-micron-diameter blisters at higher fluences detected. In ND-W and Rec-W samples, the number and size of blisters increased with fluence. The D desorption spectra show two desorption peaks in both CVD-W samples at 520 K and 570-604 K. Whereas in ND-W and Rec-W samples, two peaks were at 520 K and 607-700 K. The total D retention in both types of CVD-W samples was less than 30% of that in ND-W and Rec-W samples. The low D retention in CVD-W samples was attributed to the low desorption intensities with the peak at 570-604 K.

In this work, CVD-W has shown an outstanding resistance to D-induced blistering and D retention, which indicates potential advantages as a wall material in terms of surface integrity and tritium inventory. These results provide an experimental reference for the application of CVD-W as the wall material in fusion reactor. Further investigations are undergoing on the depth distribution of D retention and defects to understand the mechanism determining the irradiation effect in CVD-W.

# Time-Dependent Density Functional Theory Simulation for Neutralization Process of Hydrogen Ion Injected onto Graphene

Yuto Toda<sup>1</sup>, Arimichi Takayama<sup>2,1</sup> and Atsushi M. Ito<sup>2,1</sup>

<sup>1</sup> Graduate Institute for Advanced Studies, SOKENDAI  
322-6 Oroshi-cho, Toki 509-5292, Japan  
toda.yuto@nifs.ac.jp

<sup>2</sup> National Institute for Fusion Science, National Institutes of Natural Sciences  
322-6 Oroshi-cho, Toki 509-5292, Japan

In previous molecular simulations for plasma-wall interactions (PWI), incident particles have been approximated as neutral atoms. This was because, due to technical problems, only potentials between atoms were provided. However, incident particles from the plasma are not only atoms but also ions and electrons. In contrast, ions on solid surfaces are expected to be rapidly neutralized. In this study, this process is analyzed in detail using the Time-Dependent Density Functional Theory (TDDFT)[1].

In the TDDFT, the time evolution of electronic wavefunctions is described by the time-dependent Kohn-Sham equation:

$$i \frac{\partial^2 \psi_j(\vec{r}, t)}{\partial t^2} = \left[ -\frac{1}{2} \Delta + \int d\vec{r}' \frac{\rho(\vec{r}', t)}{|\vec{r}' - \vec{r}|} + V_{xc} + V_{ext} \right] \psi_j(\vec{r}, t)$$

where  $V_{xc}$  is the exchange-correlation term and  $V_{ext}$  is external potential. The time evolution of the nucleus is described by the Ehrenfest molecular dynamics (MD) approach [2]. In this approach, the motion of the nuclei is described by Newton's equation in which the forces onto atoms are estimated by electronic density distribution in the DFT.

The SALMON code[3] was used for these calculations, and we modified the code to treat long particle motions. Figure 1 shows a schematic of the normal injection of a hydrogen (H) ion injection onto the graphene. The incident position of the H ion is exactly above the carbon atom. Before the H ion collides with the carbon atom, the H ion is already neutralized due to electron transport from the graphene. The partial charge around the hydrogen nucleus was estimated as  $C_H = \int_{V_H} d\vec{r} \rho(\vec{r})$ , where  $V_H$  is the Bader volume around the H ion. The partial charge  $C_H$  becomes 1 before the collision, while it becomes less than 1 after the collision. This suggests a process of ionization after neutralization, further analysis under the interpretation of the probability density in quantum mechanics in order to compare with experimental observations.

The consideration of electron dynamics allows for more detailed simulations of plasma-wall interactions, taking into account ion neutralization and ionization not limited to conventional simulations with neutral atoms.

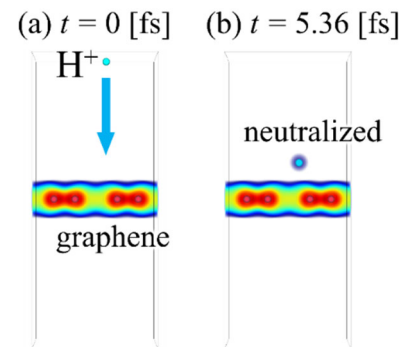


Fig. 1: Hydrogen (H) ion injection onto graphene. (a) Initially, there is no electronic density around the H ion. (b) The electronic density appears around the H ion even before it is close to a typical chemical bonding distance.

[1] E. Runge, E.K. Gross, Phys. Rev. Lett. 52 (12) (1984) 997

[2] B. F. E. Curchod, U. Rothlisberger, and I. Tavernelli, Chem. Phys. Chem. 14, 1314 (2013).

[3] M. Noda, et al., Comp. Phys. Comm., 235, 356-365, (2019)

# Simultaneous measurements of F, O and H ground state atom density in an industry-grade etching plasma

M. K. T. Mo<sup>1</sup>, S.-N. Hsiao<sup>1</sup>, M. Sekine<sup>1</sup>, M. Hori<sup>1</sup>, and N. Britun<sup>1</sup>

<sup>1</sup> Center for Low-temperature Plasma Sciences, Furo, Chikusa, Nagoya, 464-8603, Japan  
[mo@plasma.engg.nagoya-u.ac.jp](mailto:mo@plasma.engg.nagoya-u.ac.jp)

To continue optimizing semiconductor manufacturing processes, accurate gas chemistry analysis is required to be correlated to the surface chemistry during the etching stage; this depends on knowledge of the species that are present as well as their densities in the plasma. Optical actinometry is a well-established technique and has been used to detect and measure the densities of F, O and H [1-3] that play crucial roles in chemical reactions in the etching of materials.

In this work, we report the results of the simultaneous measurements of these atomic ground state densities in a commercial plasma-etching system via actinometry. Emission from multiple argon lines were used to minimize the uncertainty of absolute densities to around 20%. Similarly, electron temperature ( $T_e$ ) values were obtained using a rare gas admixture. Absolute densities were studied over various conditions and different substrate materials (Si, PI, SiO<sub>2</sub>).

The measurements were carried out in an industrial etching system where the plasma was generated between two parallel plates. The conditions studied were: CF<sub>4</sub>/H<sub>2</sub> admixture ratio (8-70% H<sub>2</sub>), total flow rate (25-200 sccm), and the applied powers at the bottom electrode connected to both the low (LF, 0.4 MHz) and high (HF, 40 MHz) frequency power supplies, from 3.0-7.2 kW and 2.2-5.4 kW, respectively. All were carried out at 3.3 Pa.

Using peak intensity values, the ratios from at least 10 Ar lines were taken with emission from F(703), O(777), O(844), and H $\alpha$ , H $\beta$ , and H $\gamma$ . The results were then averaged to determine the species densities. For the studied transitions, electron impact excitation cross sections were taken from [4] for Ar and H, [5] for F, and [6] for O.

The F density typically had the highest population, ranging from  $1\text{-}5 \times 10^{13} \text{ cm}^{-3}$ . In comparison, O densities were more than an order of magnitude smaller, and both decreased with higher H<sub>2</sub> proportion. Conversely, H grew with increasing H<sub>2</sub> content from  $2 \times 10^{12}$  -  $5 \times 10^{13} \text{ cm}^{-3}$ , overtaking F at ~50% admixture. Increasing the LF power also promoted all densities linearly, but at a lesser rate for H<sub>2</sub>. Changing to SiO<sub>2</sub> substrate gave higher O density than Si. Only O saw a noticeable decrease as the total flow increased, while the others remained fairly constant.

This work is supported by the JSPS KAKENHI Tokusui project (grant 19H05462) and Tokyo Electron Miyagi Ltd.

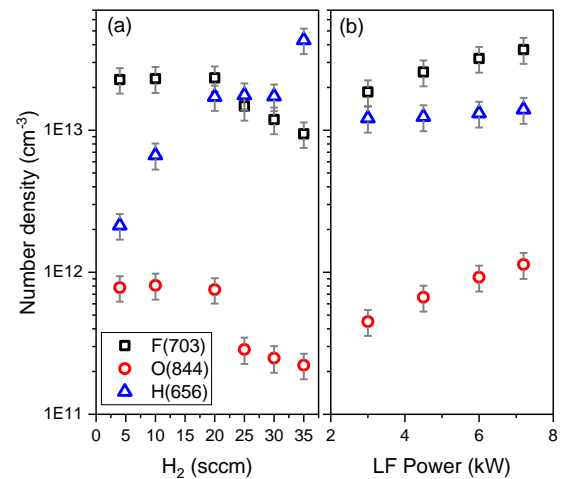


Fig. 1: Number densities as a function of (a) H<sub>2</sub> flow and (b) LF power. Total flow at 50 sccm,  $T_e = 4 \text{ eV}$ , Si substrate.

[1] D. R. Boris, et al., Journal of Vacuum Science & Technology A **35**, 01A104 (2017).

[2] M. A. Worsley, et al., Journal of Applied Physics **100**, 083301 (2006).

[3] D. V. Lopaev, et al., Journal of Physics D: Applied Physics **50**, 075202 (2017).

[4] Biagi, www.lxcat.net, Last accessed on 26 Jul 2022.

[5] D. R. Boris et al., J. Vac. Sci. Tech. A **35**, 01A104 (2017).

[6] R. R. Laher, F. R. Gilmore J. Phys. Chem. Ref. Data, **19**, 277 (1990).

## Machine learning prediction of plasma parameters from optical emission spectra in argon plasma

Fatima Jenina Arellano<sup>1</sup>, Minoru Kusaba<sup>2</sup>, Stephen Wu<sup>2,3</sup>, Zoltán Donkó<sup>1,4</sup>, Márton Gyulai<sup>4</sup>  
Peter Hartmann<sup>4</sup>, Tsanko Vaskov Tsankov<sup>5</sup>, Uwe Czarnetzki<sup>5</sup>, Ryo Yoshida<sup>2,3</sup>, and Satoshi  
Hamaguchi<sup>1</sup>

<sup>1</sup>*Graduate School of Engineering, Osaka University, Osaka, Japan*

<sup>2</sup>*The Institute of Statistical Mathematics, Research Organization of Information and Systems, Tachikawa, Japan*

<sup>3</sup>*Department of Statistical Science, The Graduate University for Advanced Studies, Tachikawa, Japan*

<sup>4</sup>*Wigner Research Centre for Physics, Budapest, Hungary*

<sup>5</sup>*Institute for Plasma and Atomic Physics, Ruhr University Bochum, Bochum, Germany*  
*Email: arellano@ppl.eng.osaka-u.ac.jp*

The continuing reduction of micro/nano-electronics device dimensions and the increasing complexity of their 3D structures necessitate precise control of semiconductor manufacturing processes with atomic-scale accuracy [1]. Automated process control based on sensor data can significantly facilitate such high-accuracy manufacturing processes. Plasma-assisted processes are widely used in semiconductor manufacturing. Optical emission spectroscopy (OES) for processing plasmas can be a simple and noninvasive diagnostic tool but deriving the plasma parameters from the OES is not a simple task. Optical emission spectra can be modelled with a collisional-radiative model (CRM) [2] for specific gaseous species if the electron density ( $n_e$ ), electron energy distribution function (EEDF), and densities of the ground state gases are provided. In this study, we construct a model to perform the inverse operation of the CRM for argon (Ar) plasmas, which predicts the  $n_e$  and EEDF from OES data at a given Ar gas density (or the Ar gas pressure and temperature), using machine learning (ML). The ML model was trained with the  $n_e$  and the EEDF data obtained from Particle-in-cell/Monte Carlo Collisions (PIC/MCC) simulations [3] and the corresponding OES obtained from the CRM [4]. The ML model used in this study is based on multiple kernel ridge regression and random forest. The simulations were performed for radiofrequency-driven Ar capacitively-coupled plasmas in the pressure range of 2-100 Pa, enclosed in a chamber having an electrode gap of 4 cm. It was found that the ML-based inverse CRM predicts the  $n_e$  and EEDF correctly from given OES data.

[1] K. Arts et al, Plasma Sources Sci. Technol., **31**, 103002, (2022).

[2] S. Siepa, S. Danko, T. Tsankov, T. Mussenbrock, and U. Czarnetzki, J. Phys. D: Appl. Phys., **47**, 445201 (2014).

[3] Z. Donko, Plasma Sources Sci. Technol., **20**, 024001 (2011).

[4] F. Arellano et al., First-principles simulation of optical emission spectra for low-pressure argon plasmas and its experimental validation, Submitted (2023).

## Numerical Simulation of RF-driven Capacitively Coupled Argon Plasmas and Comparison with Experimental Observations.

Sarah Alamri<sup>1a</sup>, Hsing-Che Tsai<sup>2</sup>, Michiro Isobe<sup>1</sup>, Fatima Jenina Arellano<sup>1</sup>,  
Charisse Marie D. Cagomoc<sup>1</sup>, Kazumasa Ikuse<sup>1</sup>, Tomoko Ito<sup>1</sup>, Satoshi Sugimoto<sup>1</sup>, Jong-Shinn Wu<sup>2</sup>,  
Satoshi Hamaguchi<sup>1</sup>

<sup>1</sup>Centre for Atomic Molecular and Technology, Osaka University, 2-1 Yamadaoka, Suita, Osaka 565-0871, Japan

<sup>a</sup> sarah.alamri@ppl.eng.osaka-u.ac.jp

<sup>2</sup>Department of Mechanical Engineering, National Yang Ming Chiao Tung University, 1001 University Road, Hsinchu, Taiwan

This work aims to understand radio-frequency (RF) argon (Ar) capacitively coupled plasmas (CCPs) by comparing experimental measurements of the plasmas with the results of numerical simulation based on a two-dimensional (2D) self-consistent fluid-based plasma model coupled with an external circuit model. In this plasma model, the electron dynamics is governed by the electron continuity, momentum, and energy density equation where the momentum equation is simplified as the drift-diffusion approximation and combined with the electron continuity. The transport coefficients and reaction rate constants, including the ionization rates, are evaluated from BOLSIG+. The ion dynamics is governed by the full mass and momentum conservation equations, including the ion convection. The system is assumed to be electrostatic and the plasma equations coupled with Poisson's equation are solved on unstructured grids via the finite-volume method with a parallel computing platform Ultrafast Parallel Processing (ultraMPP). [1]

Following the existing experimental plasmas system, 2D-axisymmetric Ar CCPs between unequal-sized electrodes were simulated in this study. The neutral Ar gas was assumed to be uniformly distributed and constant in time with a gas temperature of 300 K. The electrode gap distance was 30 mm, the diameter of the grounded electrode was 80 mm, and the diameter of the powered electrode was 190 mm. The chamber wall was also grounded. The applied voltage had a sinusoidal form with a frequency of 13.56 MHz. The voltage applied to the electrode was measured close to the electrode but outside the chamber wall, so the measured voltage was slightly different from the actual voltage applied to the electrodes. Therefore, an external circuit model was used to estimate the exact voltage applied to the powered electrode. In the simulation, the pressure, the peak-to-peak voltage  $V_{pp}$  (i.e., half of which is the applied voltage amplitude), and the direct current (DC) bias voltage  $V_{DC}$  were specified as input parameters. The impedance values of circuit elements of the external circuit model were determined experimentally with a network analyzer. It has been found that, with the experimentally measured  $V_{pp}$  and  $V_{DC}$ , the numerically simulated current at the location of the current measurement probe, including the stray current, is found to be in reasonable agreement with the experimentally measured current. The simulation also shows that a large volume of plasma is generated in space below the powered electrode, in addition to the main plasma generated between the upper and electrode.

### References

[1] K. -L. Chen *et al.*, IEEE Trans. Plasma Sci. 49 (1) pp. 104-119 (2021).

## Preliminary Investigation of Methane Plasmatolysis in an Atmospheric Pressure Gliding Arc Plasma

Pierre MATHIEU<sup>1</sup>, Abhyuday CHATTERJEE<sup>1</sup>, Nepal CHANDRA ROY<sup>1</sup>, Rony SNYDERS<sup>1,2</sup>

<sup>1</sup>*Chimie des Interactions Plasma-Surfaces, University of Mons, Mons, Belgium*

<sup>2</sup>*Materia Nova Research Center, Mons, Belgium*

One of today's most important challenges is the reduction of our greenhouse gas emissions below the maximum storage capacity of our Planet's natural carbon wells. In this line, we must insure our energy mixes' decarbonation through the implementation of clean technologies to harvest solar, wind, hydraulic and geothermal energies.

But if we want to activate the switch from fossil fuels toward clean electricity, we will have to adopt efficient electricity storage technologies as well, and hydrogen is foreseen to be one of them. However, the current main production method of this fuel remains problematic, as it is estimated to emit about 12 kg of CO<sub>2</sub> for only 1 kg of H<sub>2</sub> synthesized.<sup>[1]</sup> This industrial process consists in reforming methane in water vapour:  $\text{CH}_4 + \text{H}_2\text{O} \rightarrow \text{CO} + 3 \text{H}_2$ , followed by the water-gas shift reaction:  $\text{CO} + \text{H}_2\text{O} \rightarrow \text{CO}_2 + \text{H}_2$ , and is known as steam methane reforming (SMR). It produces large amounts of CO<sub>2</sub> and costs about 285 kJ of energy per mole of H<sub>2</sub>.

There is another approach to achieve methane reforming to produce H<sub>2</sub>, with no CO<sub>2</sub> emissions, and that has an energy cost of only 74.58 kJ per mole of H<sub>2</sub>. This approach is the pyrolysis of methane in an electric discharge, using non-oxidative conditions:  $\text{CH}_4 \rightarrow \text{C}_{(s)} + 2 \text{H}_2$ . It was also shown with this process that one can tune its selectivity toward several other value-added products, such as acetylene and ethylene, by implementing the proper experimental parameters (plasma power, gas flow, gas mix composition, catalysts).<sup>[2]</sup>

This work presents the results of a preliminary study of plasma-assisted methane reforming, conducted in an atmospheric pressure gliding arc discharge, using CH<sub>4</sub>/Ar mixtures. The CH<sub>4</sub>/Ar ratio varied from 0.2 to 0.4 to insure the stability of the discharge and as a result of optical signals quality optimisation. Optical Emission Spectroscopy was used to evaluate the impact of the plasma power, the total injected gas flow and the CH<sub>4</sub>/Ar ratio on the rotational and vibrational temperatures ( $T_{\text{rot}}$  and  $T_{\text{vib}}$ ) of the C<sub>2</sub> species and on the electronic density ( $n_e$ ). The observed correlation between  $n_e$  and  $T_{\text{rot}}$  suggests that, in our experimental window, the average amount of energy brought to heavy particles by an electronic impact allows rotational excitations (implying more gas heating), but does not promote vibrational excitations (activating a more energy-efficient chemistry).

Finally, the CH<sub>4</sub> conversion rate and H<sub>2</sub> selectivity of the process were determined through gas chromatography. Maximum values of 30% and 57.6% were achieved for these parameters, respectively. The lowest energy cost obtained was therefore about 150 kJ/L<sub>CH<sub>4</sub></sub>.

[1] M. Gautier *et al.*, *International Journal of Hydrogen Energy*, **42(47)**, 28140–28156 (2017)

[2] M. Scapinello *et al.*, *Chemical Engineering & Processing: Process Intensification*, **117**, 120–140 (2017)



## Broadening plasma polymerization process for functional coatings

Ju-Liang He<sup>1,2</sup>, Xuan-Xuan Chang<sup>1</sup>, Yu-Han Wei<sup>1</sup>, Ping-Yen Hsieh<sup>1,2</sup>, Ying-Hung Chen<sup>1,2</sup>  
and Meng-Heng Lai<sup>3</sup>

<sup>1</sup> *Department of Materials Science and Engineering, Feng Chia University  
No. 100, Wenhwa Road, Seatwen District, Taichung City 407102, Taiwan.  
jlhe@o365.fcu.edu.tw*

<sup>2</sup> *Institute of Plasma, Feng Chia University  
No. 100, Wenhwa Road, Seatwen District, Taichung City 407102, Taiwan.*

<sup>3</sup> *Qual-Inno Technology Corporation  
16F.-7, No. 241, Sec. 3, Wenxin Road, Seatwen District, Taichung City 407330, Taiwan.*

With the growing need for broadening the applications of surface modification, the evolution of plasma power generators has led to the progress of plasma coating techniques, particularly generating a very short and stable impulse waveform to improve film quality or architect coating structure. Considering the Yasuda factor to predict the structure of obtained plasma polymerized films, the power output waveform is a key factor that affects the structure and thus the performance of the plasma polymerized films. With implementation of an impulse power supply, featuring a very short pulse (in a few microseconds), low duty cycle, and low plasma power, using impulse plasma polymerization (iP3) to grow plasma parylene coating (iP4C) on silicone rubber is proposed in this study. The iP4C is able to provide low friction, anti-sticking, and biocompatibility properties on silicone catheters for reducing the pain and foreign sensation during invasion. To further meet the demand for antibacterial function, hollow cathode discharge (HCD) in combination with iP3 to synthesize silver containing plasma parylene coating (Ag-iP4C) was also developed, where the silver HCD tube serves as the silver incorporating source *in situ*. Hence, this report will adequately investigate the mechanism of molecular structure modulation for iP4C by adjusting pulse time; in addition, the control of silver containing level and the characteristics of Ag-iP4C will also be discussed in detail. Finally, such iP4C technique is currently transferred to realize the commercial activity as well as providing total solution service of plasma polymerized functional surface modification.

## Development of Atmospheric Pressure Plasma Sources for Material Modification

Magdaleno R. Vasquez Jr., Mark D. Ilasin, Marlo Nicole R. Gilos, Bryndell J. Alcantara, Eunice G. Ramirez, Gericca M. Dol, Mary Mark Jeffrey D. De Leon, Kathrina Lois M. Taaca

*Department of Mining, Metallurgical, and Materials Engineering, College of Engineering, University of the Philippines Diliman, Quezon City 1101 Philippines*  
*mrvasquez2@up.edu.ph*

Atmospheric pressure plasma systems have been gaining considerable attention due to their potential uses in various fields and industries. These systems are simple, inexpensive, easy to use, low-maintenance, fast, and generally safe, making them an attractive option. These systems are used to treat or modify surfaces because of their ability to produce metastable active species. The vacuum-less operation allows for the processing of different materials, including liquids. In addition, large-area treatment is also realized by taking advantage of the flexibility of atmospheric pressure plasma systems. In this report, different custom-built plasma system configurations (Fig. 1), such as arc discharge plasma and dielectric barrier discharge (DBD), were developed and used to modify material surfaces using different gases. A cold atmospheric pressure plasma jet was used to condition polymeric surfaces such as high-density polyethylene (HDPE) to improve the adhesion of water-based paints [1]. Another configuration was used to treat chitosan-arcylic acid hydrogels [2]. Pretreatment of low-density polyethylene (LDPE) sheets using plasma accelerated LDPE biodegradation. A DBD system was used to treat rice seeds and the effect on germination was evaluated. A plasma jet made of 3D printed components was able to generate an argon:air plasma jet. This was used to modify bamboo surfaces to improve the adhesion of polyvinyl acetate. The same system was used to clean and disinfect metallic surfaces used in food processing. Continuous development and advancement of versatile atmospheric pressure plasma systems will improve surface processing technologies and reduce operating costs.

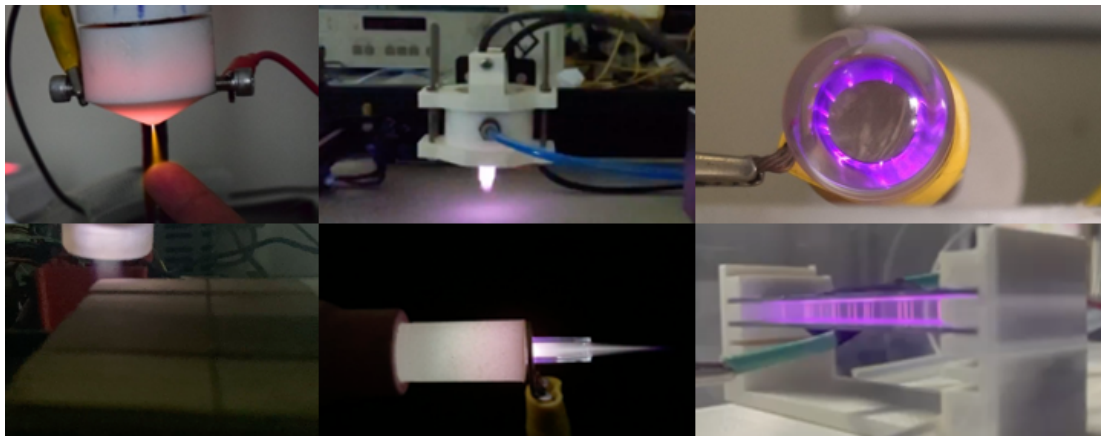


Fig. 1: Images of custom-built atmospheric pressure plasma systems for material modification.

[1] M. J. D. De Leon and M. R. Vasquez, *Mater. Res. Exp.* 8,105306 (2021).

[2] K. L. M. Taaca, M. J. D. De Leon, K. Thumanu, H. Nakajima, N. Chanlek, E. I. Prieto, and M. R. Vasquez, *Colloids Surf. A: Physicochem. Eng.* 637, 128233 (2022).

# Surface Modification by Non-Thermal Plasma for Gaseous Mercury

## Removal

Jinjing Luo, Lurong Ye, Mingchang Jin

*College of the Environment & Ecology*

*Xiamen University, China*

*luojj27@xmu.edu.cn*

Dielectric barrier discharge plasma pre-treatment was conducted to introduce typical functional groups on the surface of carbonaceous materials. Plasma generated from five different discharge gases were investigated their effects on surface modification. Ocean optics spectrometers (OES) and fourier transform infrared spectrometer (FTIR) were used to analyze the generated plasma and gases. X-ray photoelectron spectroscopy (XPS), FTIR, scanning electron microscope (SEM) and X-ray absorption fine structure (XAFS) were used to analyze physical and chemical properties of adsorbents.  $\cdot\text{OH}$  and  $\cdot\text{O}$  were believed to generated by discharge gases and reacted with carbonaceous materials and introduce oxygen-containing functional groups on the surface. Mercury absorption mechanism was also discussed in this study and the schematic diagram of the surface modification mechanism was shown in Figure 1.

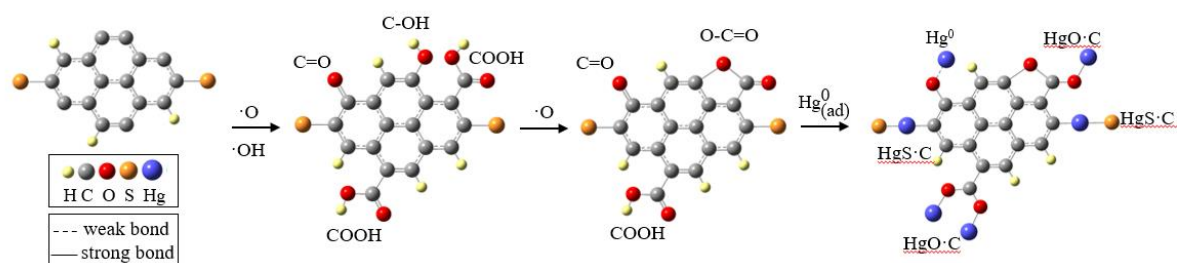


Figure 1 Schematic diagram of the principle of  $\text{Hg}^0$  adsorption by DBD modified carbonaceous material

- [1] Estupiñán E G, Stickel R E, Wine P H J C P L. An investigation of  $\text{N}_2\text{O}$  production from quenching of  $\text{OH}(\text{A } 2\Sigma^+)$  by  $\text{N}_2$ . 2001,336(1):109-117.
- [2] Sun R, Zhu H, Shi M, et al. Preparation of fly ash adsorbents utilizing non-thermal plasma to add S active sites for  $\text{Hg}^0$  removal from flue gas. *Fuel*, 2020,266(11):6936-6942.
- [3] Frentiu T, Ponta M, Mihaltan A I, et al. Quenching of the OH and nitrogen molecular emission by methane addition in an Ar capacitively coupled plasma to remove spectral interference in lead determination by atomic fluorescence spectrometry. 2010,65(7):565-570.

## Amorphous Carbon Film Deposition using Low-energy Ions

Mark D. Ilasin, Lance Tristan Oliver R. Pengson, and Magdaleno R. Vasquez Jr.

*Department of Mining, Metallurgical, and Materials Engineering, College of Engineering,  
University of the Philippines Diliman, Quezon City, Philippines  
mdilasin@up.edu.ph*

Amorphous carbon (C) films have been of particular interest in recent years because of its applications in tribology and in electronics [1] due to its chemical inertness, high hardness, and optical transparency in visible light and infrared [2,3]. In this study, low-energy ion beams were extracted to deposit amorphous C films. A custom-built hot cathode ion source [4] with a cylindrical multi-cusp configuration was used to extract ions with energies around 100 eV. Figure 1 shows the uniformity the extracted ion beam from the 4-cm diameter extractor at different extraction potential. An admixture of acetylene ( $C_2H_2$ , 99.95%) and argon (Ar, 99.999%) with predefined pressure ratio were ionized and eventually extracted in a highly transparent two-electrode ion extractor. Silicon (Si) substrates were positioned downstream opposite the extractors where thin C films were deposited. The deposited material was characterized using Raman spectroscopy, atomic force microscopy (AFM), and nanoindentation. Raman spectral analysis revealed the presence of up to 70%  $sp^3$  C. AFM characterizations of the thin films showed very smooth surfaces with a maximum root-mean-square roughness of 0.57 nm. Nanoindentation modulus and hardness revealed a mean value of approximately 216 and 10 GPa, respectively.

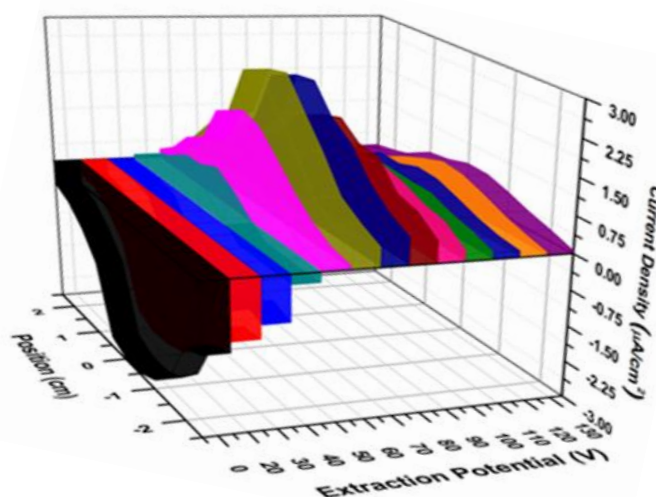


Fig. 1. Current density profile of ion beams at different extraction potential.

- [1] J Robertson, *Surface and Coatings Technology* **50** (1992)
- [2] J Robertson, *Mater. Sci. Eng.* **R 37** (2002) 129-281
- [3] A Hamdan, et al., *Thin Solid Films* **599** (2016) 84-97
- [4] M Vasquez, et al., *Vacuum* **187** (2022) 110067

# Selective removal of graphene by irradiation of remote oxygen plasma

Liugang Hu<sup>1</sup>, Kenji Ishikawa<sup>2</sup>, Takayoshi Tsutsumi<sup>2</sup>, Thi-Thuy-Nga Nguyen<sup>2</sup>, Shih-Nan Hsiao<sup>2</sup>, Hiroki Kondo<sup>2</sup>, Makoto Sekine<sup>2</sup>, and Masaru Hori<sup>2</sup>

<sup>1</sup> Graduate School of Engineering, Nagoya University  
Furo, Chikusa, Nagoya 464-8603, Japan  
[hu.liugang.k5@s.mail.nagoya-u.ac.jp](mailto:hu.liugang.k5@s.mail.nagoya-u.ac.jp)

<sup>2</sup> Center for Low-temperature Plasma Sciences  
Furo, Chikusa, Nagoya 464-8603, Japan

## 1. Introduction

Control of layers of stacked graphene is plausible for realizing next-generation single-layer electronic devices. We reported in-situ electron microscopic observation of continuous etch of multilayer stacked graphene using an exposure of oxygen radicals [1]. Defects on plane of single layer of graphene (SLG) were formed during oxygen radical irradiation [2]. To realize atomic layer etching (ALE) technology, Selective removal of SLG between bilayer graphene (BLG) was discovered and the etch mechanism has been investigated by Raman spectroscopy, atomic force microscopy (AFM), X-ray photoelectron spectroscopy (XPS).

## 2. Experimental

The oxygen plasma was generated using the microwave (2.45 GHz) cavity in flowing O<sub>2</sub> gas with a flow rate of 2.5 sccm and at a pressure of approximately 5 Pa. The microwave power was 50 W to generate plasma in remote plasma system, distanced 29 cm from discharge to the sample position. The irradiation time was 60 and 120 minutes. CVD-grown (Chemical vapor deposition) graphene (EM Japan, G-45R-4) was used. In this preparation, an as-grown graphene sheet was transferred to a coated polymer and then onto a SiO<sub>2</sub> film on Si substrate [3].

## 3. Results and Discussion

Figure 1 (a) shows an optical image of the initial sample. Inset shows overlay of a mapping of Raman signals for BLG and SLG. The BLG area is labeled **A**, and the SLG area is labelled **B**. AFM images at the identical position are shown in Figure 1, taken before irradiation (b) and after 120-min-irradiation (c). Raman spectra at different positions A and B are different in increase of D peak at 1350 cm<sup>-1</sup> and 2D peak at 2700 cm<sup>-1</sup>. The 2D peak intensity almost disappeared at the SLG position. On the other hand, at BLG position, the D peak increased but unchanged 2D peak. Selectively, SLG was removed by etching, while BLG remained on the surface after the 120-min-irradiation. A control of layers of stacked graphene can be realized. Meanwhile, the etching of SLG/BLG occurred at the plane dominantly but considering the dangling bonds should exist at the edge of graphene, we supposed that some bonding formed (C-OH) during CVD-grown or because of the nature of graphene.

## References

- [1] H. Sugiura et al., Carbon **170**, 93-99 (2020).
- [2] C-H. Huang et al., Carbon **73**, 244 (2014).
- [3] X. Liang et al., ACS Nano **5**, 9144 (2011).

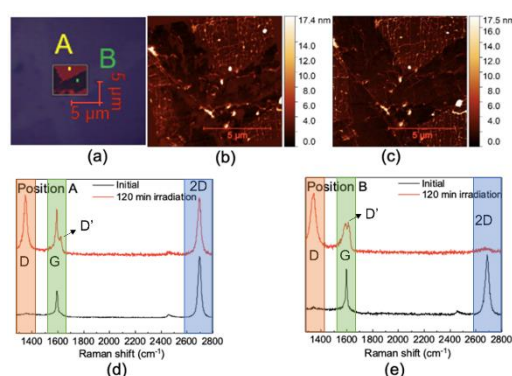


Fig. 1 (a) A optical microscopic image of graphene overlays a mapping of the Raman signals from BLG (labelled 'A') and SLG (labelled 'B'). (b, c) AFM images and (d, e) Raman spectra at the A and B positions of the initial and the remote plasma-treated graphene.

# Synthesis and characteristics of carbon nanowalls using two-step growth combining different plasma chemical vapor deposition methods

Ngo Quang Minh<sup>1</sup>, Ngo Van Nong<sup>2</sup>, Osamu Oda<sup>2</sup>, Masaru Hori<sup>2</sup> and Kenji Ishikawa<sup>2</sup>

<sup>1</sup> Graduate School of Engineering, Nagoya University, Nagoya, 464-8601, Japan

<sup>2</sup> Center for Low-Temperature Plasma Sciences, Nagoya University, Japan

Furo-cho, Chikusa-ku, Nagoya, Aichi, 464-8601, Japan

e-mail: ngo.minh.quang.j6@s.mail.nagoya-u.ac.jp

## 1. Introduction

Carbon nanowalls (CNWs) are self-supported nanostructures of graphene sheets grown almost vertically on substrates. To date, CNWs can be synthesized by various plasma methods such as microwave plasma enhanced chemical vapor deposition (MPCVD), inductively coupled plasma chemical vapor deposition (ICP-CVD), and capacitively coupled plasma chemical vapor deposition (CCP-CVD) [1]. The morphology and density of CNWs have a strong influence on their unique properties. However, using a single plasma method, it is difficult to either control the morphology or improve the density of CNWs. One solution is to apply plasma treatment (e.g., oxygen plasma treatment), but this has a high etching effect and thus reduces the thickness of CNWs.

In this study, CNWs were grown using an innovative two-step plasma method that combined radical injection plasma enhanced chemical vapor deposition (RI-PECVD) and CCP-CVD.

## 2. Experimental

CNWs were grown in two steps: step 1 (RI-PECVD) and step 2 (CCP-CVD). The temperature (700 °C), growth period (10 mins), and gas flow rates (CH<sub>4</sub>/H<sub>2</sub>) were the same parameters for both two steps. While the pressure in step 1 was kept at 1 Pa, it was 10 Pa in the second step. The morphology of CNWs was observed by scanning electron microscopy (SEM – SU-8230 model, Hitachi High-Technologies), and Raman spectra were used to investigate CNWs' structural properties (Renishaw inVia system). The static water contact angle was measured by a sessile drop method to investigate CNWs' surface wettability.

## 3. Results and discussion

**Figure 1** shows the wall density of CNWs synthesized by single plasma methods of either RI-PECVD or CCP-CVD in comparison with the CNWs grown by the two-step plasma methods combining RI-PECVD and CCP-CVD. As can be seen, the wall density of branched CNWs grown by the two-step combined plasma method exhibited the highest density of 74 wall units/ $\mu\text{m}^2$ , which is more than 5 times larger than the CNWs synthesized by the RI-PECVD single-step methods.

## 4. Conclusion

Combining two different plasma methods of RI-PECVD and CCP-CVD in a proper order could create CNWs with highly dense and multi-branched morphology.

## References

[1] M. Hiramatsu and M. Hori, ISBN 978-3-211-99718-5

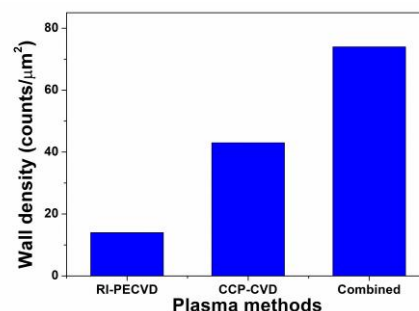


Fig. 1: Wall density of the CNWs grown by: RI-PECVD, CCP-CVD and the two-step plasma methods combining RI-PECVD and CCP-CVD.

October 18  
(Wednesday)

## Beryllium Dust Preparation to Mimic Particle Formation in Fusion Devices

Cristian P. Lungu, Corneliu Porosnicu, Paul Dinca, Oana Pompilian, Bogdan Butoi, Cornel Staicu

*National Institute for Laser, Plasma and Radiation Physics Atomistilor 409, Magurele, Ilfov, 077125 Romania  
cristian.lungu@inflpr.ro*

The safety and performance of the fusion machine operation [1] could be affected by the sputtering or vaporization of some “particulates that might have been produced by blistering or abrasion of wall in previous discharges” [2]. The dust formation in the fusion machine in case of accidental leaks could be influenced by air and water, as possible coolant candidates to be used in ITER. The dust formation and release mechanisms have a direct impact on dust dynamics by dictating both the initial conditions and the regimes of plasma particle collection by the dust. In particular, dust and droplets in metal machines are relatively large sizes, implying inhibition of electron collection due to the presence of strong magnetic fields and, leading to significant release speeds, an inertia-dominated motion.

We studied the influence of air and water leaks over the dust production of beryllium in order to improve the prediction of Be dust generation. Using a ball milling as well as an arching procedure, beryllium dust was obtained starting from a beryllium pebble/2 inch target in air and water environment. The dust shape and size obtained in our experiments were similar with the ones collected from the JET machine.

The crystalline phase composition analysis shows peaks of Be, BeO, Al<sub>2</sub>O<sub>3</sub> and SiO<sub>2</sub>. The observed shifts to small angles suggest the modification of the interplanar spacing of the Be crystalline lattice, due the presence of an uniform stress state responsible for the lattice strain. The BeO diffraction peaks are observed for wet conditions prepared samples. Alumina (Al<sub>2</sub>O<sub>3</sub>) and agate (SiO<sub>2</sub>) used in the milling process appeared too: more obvious under wet conditions.

Different dust powders prepared in wet and dry conditions were studied using the Thermal Desorption Spectroscopy (TDS). Formation of oxides and nitrides: BeO, H<sub>2</sub>O, N<sub>2</sub>, Be(OH)<sub>2</sub> were found in higher content for wet environment prepared samples. Be, O<sub>2</sub> and Be<sub>3</sub>N<sub>2</sub> content was higher for samples prepared in dry condition, suggesting that the water is present in Be dust as: non-reacted pure H<sub>2</sub>O, oxygen that forms BeO and as hydroxide to form Be(OH)<sub>2</sub>. The maximum desorption temperatures were 190°C for H<sub>2</sub>O and 540°C for BeO.

The results presented in this work prove the capability to obtain Be dust samples that mimic the real dust collected from JET after the ILW campaigns. Since the collected real dust is limited in quantities, their properties and varying result in measurement values will contribute in prediction of their behavior in extreme conditions of plasma operation in fusion devices.

The talk will also focus on investigating the impact of fusion plasma on the first wall tiles, as well as exploring the production techniques using High-power impulse magnetron sputtering (HiPIMS) and characterizing Be reference coatings with different composition, morphology, and grain structure. The findings from the research presented offers valuable insights into the dust formation and deposition phenomena occurring in large-scale beryllium structures.

[1] M. Shimada, R.A. Pitts, S. Ciattaglia, et al., J. Nucl. Mater, 438 (2013),p.S996.

[2] S. Ratynskaia, A. Bortolon, et al, Rev of Modern Plasma Physics (2022) 6:20.



## Plasma Treatment of Water for Agricultural Production

Juergen F. Kolb, Marcel Schneider, Henrike Brust, Raphael Rataj, Nicola Wannicke,  
Volker Brüser and Klaus-Dieter Weltmann

*Leibniz Institute for Plasma Science and Technology (INP)  
Felix-Hausdorff-Strasse 2, 17489 Greifswald, Germany  
juergen.kolb@inp-greifswald.de*

Water is a crucial resource for the cultivation and processing of crops. However, a sustainable supply is challenged by increasing scarcity, e.g. due to climate change, and pollutants, e.g. agrochemicals. Accordingly, mitigation and management practices need to be developed to address the problems. Plasma treatments can offer technical solutions, which, on the one hand, can be used for water cleaning, and, on the other hand, provide environmentally benign means to replace pesticides and fertilizers. In addition, they can also be applied to improve current processes in crop farming, food production, and biomass valorization. The different possible applications of plasma methods along the entire food value chain “from farm to fork” require dedicated and special approaches, which take into account respective processes, in particular with respect to treatment volumes. Therefore, the INP develops plasma methods for different applications in crop cultivation and processing in several projects and in particular the comprehensive activity “Physics for Food” [1].

The basis of all these efforts is a thorough understanding of the mechanisms of action for the treatment of aqueous solutions with plasma. Primarily interesting are the chemical species that are generated. Hence, we have carefully investigated the correlation of discharge mechanisms, especially for discharges in water, with reaction rates of hydrogen peroxide in particular, which can serve as a quantitative measure to compare different plasma treatment concepts [2]. However, not all of the approaches, that are promising in the laboratory, can be reasonably transferred towards the treatment of larger volumes [3]. For the process development for water cleaning and reuse, we have, therefore, deployed a pilot water treatment system, which combines established methods with a plasma or ultrasound treatment for throughputs of up to 2000 ltr/h. In addition to the efficacy, an important result was the proof of economic competitiveness of the plasma treatments. A similar approach was also successful for the improved degradation of residual biomass to increase biogas production by combining a microwave plasma together with an ultrasound exposure, which were both operated in fermentation residues with up to 1 kW for each. The objective of a more recent effort is the fixation of nitrogen as an alternative to synthetic fertilizers, especially concerning the Haber-Bosch process. However, the benefits of the application of plasma-treated water are not limited to fertilization. Other reactive oxygen and nitrogen species, introduced into the water, have the potential to stimulate plant metabolic processes and even induce a memory or tolerance, respectively, regarding drought stress [4]. These processes can and should conceivably also be expanded towards preserving and restoring soil health.

The presentation will discuss, based on basic mechanisms, the need for the different outlined applications and report on our experience of specific approaches for relevant volumes, environments, and possible solutions to emerging challenges in agricultural production.

[1] <https://physicsforfood.org/english-summary>

[2] R. Rataj, M. Werneburg, H. Below, J.F. Kolb, *ChemPhysChem*, e202300143 (2023).

[3] M. Schneider, R. Rataj, L. Blàha, J.F. Kolb, *Chem. Eng. J.*, **451**, 138984 (2023).

[4] F. Bussmann, A. Krüger, C. Scholz et al., *J. Plant Growth Regulation*, **42**, 3274 (2023).

## Mechanism of blistering and retention in recrystallized tungsten exposed to deuterium plasma in the linear plasma device STEP

Long Cheng\*, Yi-Wen Sun, Hao Yin, Yue Yuan and Guang-Hong Lu

*School of Physics, Beihang University,  
Beijing 100191, China  
LCheng@buaa.edu.cn*

Blistering in tungsten (W) is a typical observation of fusion plasma and material interaction during low-energy and high-flux hydrogen (H) plasma exposure, which could degrade material's integrity and tritium fuel retention. It is therefore important to understand blistering mechanisms and find a way mitigating blistering. In this work, blistering and deuterium (D) retention in W were investigated using the linear plasma device STEP at Beihang University. Defect and microstructure in the vicinity of blisters were investigated using electron microscopes. D retention was studied using thermal desorption spectroscopy (TDS) and modeled using the rate theory code. Mechanism of blistering based on the dislocation nucleation is proposed and D retention was understood with the presence of blister-induced defects.

A linear plasma device STEP was constructed at Beihang University, which could deliver a flux up to  $1 \times 10^{23}$  ions  $\text{m}^{-2}\text{s}^{-1}$ . A series of D plasma exposures was performed using recrystallized W samples exposed at 500 K with fluences up to  $1.0 \times 10^{28}$  ions  $\text{m}^{-2}$  at a flux of  $\sim 10^{22}$  ions  $\text{m}^{-2}\text{s}^{-1}$  and a surface temperature of  $\sim 500$ -500 K. Transmission electron microscope (TEM) observations demonstrated dislocations and dislocation tangles in the vicinity of intra-granular blisters. In TEM,  $\langle 001 \rangle$  edge dislocations were identified and supposed to form via  $\langle 111 \rangle$  edge dislocations interaction. Considering the high tendency to crack for a  $\langle 001 \rangle$  edge dislocation, its formation is proposed as the nucleation of a blister. An increase in both blister density and D retention was observed with increasing fluence. Based on the simulation of TDS using the rate theory code, defects were found to be located at a depth of tens of microns, which coincided with the average grain size. The majority of defects was supposed to be dislocations as identified in TEM. It is suggested that these defects can diffuse deep into the material but were hindered by grain boundaries at a certain depth, which resulted in the evolution of both peak desorption intensity and temperature with the increasing fluence. Regarding the contribution of blister-induced defects on retention, a blister-dominated retention mechanism is proposed to describe retention in conditions when blistering is severe.

To summarize, blistering and D retention in recrystallized W were systematically investigated using the linear plasma device STEP at Beihang University. A  $\langle 001 \rangle$  edge dislocation nucleating mechanism and a blister-dominated retention mechanism are proposed to understand experimental findings. This work helps improving the understanding of the plasma-induced defect production and hydrogen isotopes retention in W in the context of fusion edge plasma and wall interaction, and indicates the potential contribution of plasma-induced defects to the tritium inventory in the stage of steady-state operation in fusion devices.

# Spectroscopic measurement of deuterium recycling at molybdenum surfaces

Dogyun Hwangbo<sup>1</sup> and Daisuke Nishijima<sup>2</sup>

<sup>1</sup> Faculty of Pure and Applied Sciences, University of Tsukuba,  
1-1-1 Tennodai, Tsukuba, Ibaraki 305-8577, Japan  
hwangbo@prc.tsukuba.ac.jp

<sup>2</sup> Center for Energy Research, University of California San Diego,  
9500 Gilman Dr., La Jolla, CA 92093-0417, USA

In a fusion device, hydrogen isotope recycling [1] plays an important role in determining the edge plasma condition and ELM (edge localized mode) behavior [2], as well as volume recombination processes in the divertor [3]. Note that hydrogen isotope recycling occurs in several mechanisms [1], including reflection, sputtering, desorption, etc. Depending on the mechanism, the released form is either atom or molecule, which has some translational and internal (electronic and rovibrational) energy distributions. Thus, spectroscopic measurements have been used to investigate hydrogen isotope recycling.

In this study, we aim to better understand how hydrogen isotope recycling is affected by the following factors: sample temperature,  $T_s$ , neutral gas pressure,  $P_{D2}$ , incident ion energy,  $E_i$ , and surface morphology. Experiment was performed in the linear plasma device PISCES-A. Deuterium (D) plasma light emission was measured near a molybdenum (Mo) target using an Echelle-type spectrometer and a hyperspectral imaging (HSI) camera (SpecimIQ). The line-of-sight of both systems was set to be parallel to the target surface. To explore the effect of surface nanostructures, fuzz, on D recycling, a  $\sim 1 \mu\text{m}$  thick Mo fuzz layer was formed due to He plasma exposure prior to D plasma measurements.

Preliminary HSI analyses show that the emission from both D atomic Balmer series and the Fulcher band (580-640 nm) of  $D_2$  molecules is not clearly affected by the presence of fuzz on the surface. Instead, the emission appears to depend on the other factors,  $P_{D2}$  and  $E_i$ . Fig. 1(a) presents an example of 2 dimensional image of  $D_\alpha$  line intensity extracted from HSI spectra, which is normalized at  $\sim 84$  mm. Using the HSI spectra, The intensity ratio of  $D_\gamma/D_\alpha$  is surveyed with varying  $P_{D2}$  and  $E_i$ . Fig. 1(b) shows different trends of  $D_\gamma/D_\alpha$  along the distance from the surface. At higher  $P_{D2}$ , the ratio has a sudden decrease near the surface, whereas it gradually decreases from  $\sim 80$  mm at lower  $P_{D2}$  and increases within several mm from the surface due probably to reflected D atoms at the excited states. For further understanding, effects of  $T_s$ ,  $P_{D2}$ , and  $E_i$  on the internal energy states of recycled D atoms and  $D_2$  molecules will be analyzed in detail.

[1] Ph. Mertens et al., Plasma Phys. Control. Fusion **43**, A349 (2001).  
[2] S. Brezinsek et al., Phys. Scr. **T167**, 014076 (2016).  
[3] K. Sawada et al., Contrib. Plasma Phys. **60**, 153 (2020).

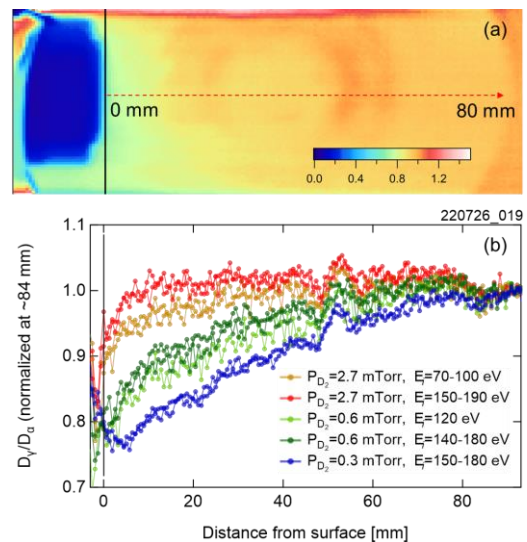


Fig. 1: (a) An example image of 2-dimensional  $D_\alpha$  line intensity. (b)  $D_\gamma/D_\alpha$  ratio distribution against the distance from the surface.

## Study on effects of neutral particle behavior on detached plasma formation using linear plasma device and modeling

Yuki Hayashi<sup>1,2</sup>, Noriyasu Ohno<sup>3</sup>, Hirohiko Tanaka<sup>3</sup>, Hiroki Natsume<sup>4</sup>, Kento Sugiura<sup>3</sup>, Ryoji Mano<sup>3</sup>, Shota Masuda<sup>5</sup>, Ryusei Migita<sup>5</sup>, Keiji Sawada<sup>5</sup>, Shin Kajita<sup>6</sup>, Tadashi Thujihara<sup>3</sup>, Hiroshi Ohshima<sup>3</sup>, Mitsutoshi Aramaki<sup>7</sup> and Gakushi Kawamura<sup>1,2</sup>

<sup>1</sup> National Institute for Fusion Science, Toki 509-5292, Japan

<sup>2</sup> SOKENDAI, Toki 509-5292, Japan

<sup>3</sup> Nagoya University, Nagoya 464-8603, Japan

<sup>4</sup> National Institutes for Quantum Science and Technology, Naka 311-0193, Japan

<sup>5</sup> Shinshu University, Nagano 380-8553, Japan

<sup>6</sup> The University of Tokyo, Kashiwa 277-8561, Japan

<sup>7</sup> Nihon University, Chiba 275-8575, Japan

hayashi.yuki@nifs.ac.jp

Neutral particle plays an important role in determining the edge plasma property especially under high neutral pressure condition associated with plasma detachment. In detached plasma regime with low temperature, neutral temperature,  $T_n$ , is an important parameter acting as the lower limit of  $T_e$ . The purpose of the present study is to elucidate the influence of  $T_n$  on detached plasma formation by experiments using the linear plasma device NAGDIS-II and the modeling which couples plasma fluid code with the neutral transport code.

A DC arc discharge produced helium plasma in a steady-state in NAGDIS-II. The plasma was terminated with a target plate. When the additional helium gas was injected from the second gas puffing port behind the target plate, the neutral pressure,  $P_n$ , increased and the detached recombining plasma was obtained due to the enhanced plasma-neutral interactions.

Figure 1 shows the  $P_n$  dependence of total ion current into the negatively-biased target plate,  $I_{\text{target}}$ . The measurements were conducted under high and low  $T_n$  conditions achieved by changing the neutral gas puffing and pumping rates. When the puffing and pumping rates increase,  $T_n$  should decrease. Fig 1 shows  $I_{\text{target}}$  decreased by increasing the puffing and pumping rates. The result indicated the enhancement of volume recombination processes by increasing the puffing and pumping rates even in the similar  $P_n$ . It could be concluded that the detached plasma formation was affected by  $T_n$  which was controlled by the puffing and pumping.

On the other hand,  $T_n$  of meta-stable atoms is measured by using a laser absorption profile with Doppler broadening at the transition of  $2^3S-2^3P$  [1]. In the case of high puffing and pumping rates,  $T_n$  ( $2^3S$ ) was higher than that in low puffing and pumping rates. The enhanced recombination in the high puffing and pumping rates might increase the number of meta-stable atoms with  $2^3S$  state which reflects the ion temperature.

[1] M. Aramaki, *et al.*, AIP Advances **8** (2018) 015308.

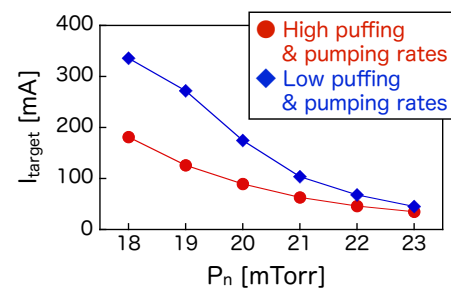


Fig. 1  $P_n$  dependences of  $I_{\text{target}}$  with high and low puffing and pumping rates.

## Newly developed integrated transport code for detached plasma simulation

Hirohiko Tanaka<sup>1</sup>, Hiroki Natsume<sup>2,3</sup>, Shota Masuda<sup>4</sup>, Kento Sugiura<sup>3</sup>, Hideya Umezawa<sup>4</sup>,  
Ryoji Mano<sup>3</sup>, Yuki Hayashi<sup>5</sup>, Kazuo Hoshino<sup>6</sup>, Keiji Sawada<sup>4</sup>, Noriyasu Ohno<sup>3</sup>

<sup>1</sup> *Institute of Materials and Systems for Sustainability, Nagoya University,  
Furo, Chikusa, Nagoya 464-8603, Japan  
h-tanaka@ees.nagoya-u.ac.jp*

<sup>2</sup> *National Institutes for Quantum Science and Technology, Naka Fusion Insutitute,  
801-1 Mukoyama, Naka, Ibaraki 311-0193, Japan*

<sup>3</sup> *Graduate School of Engineering, Nagoya University, Furo, Chikusa, Nagoya 464-8603, Japan*

<sup>4</sup> *Institute of Engineering, Shinshu University, Nagano 380-8553, Japan*

<sup>5</sup> *National Institute for Fusion Science, National Institutes of Natural Sciences, Toki 509-5292, Japan*

<sup>6</sup> *Faculty of Science and Technology, Keio University, Yokohama 223-8522, Japan*

Sufficient divertor heat load reduction is an important issue for future fusion reactors. In the research fields of scrape-off layer (SOL) and plasma-wall interaction (PWI), the establishment of reliable simulation code for the detached plasma, which is expected to be one of the promising solutions to reduce divertor heat flux, has become a hot topic that will determine the success of the reactor. Although many simulation codes have been developed, quantitative reproduction of experimentally observed detached plasmas has not yet been achieved.

In this study, a new integrated transport code named DISCOVER (Detached plasma Integrated Simulation Code with Various Elastic/inelastic Reactions) [1] has been developed to examine the effects of atomic and molecular processes on the formation of detached plasmas in a linear magnetic field geometry. This code consists of a plasma fluid code [2], a kinetic neutral transport code, and a collisional radiative code. The linear plasma device NAGDIS-II is used as the simulation target.

As a first step, attached and detached helium plasmas were calculated in which the transport of metastable atoms was solved. Compared to the case where metastable-atom transport is ignored, ionization is enhanced upstream in the case where the transport is taken into account, and the density rollover position shifts upstream. In the presentation, the formation process of detached plasma in the linear device and future plans will also be explained.

[1] H. Natsume et al., submitted to Nucl. Fusion.

[2] H. Tanaka et al., Phys. Plasmas **27**, 102505 (2020).

## Development of a Plasma Fluid Model Covering a Range of Coulomb Collisionality by Comparison with a Particle-in-cell Model

Satoshi Togo<sup>1</sup>, Kenzo Ibano<sup>2</sup>, Tomonori Takizuka<sup>2</sup>, Yuki Homma<sup>3</sup>, Keishi Homma<sup>1</sup>, Kazuma Emoto<sup>1</sup>, Naomichi Ezumi<sup>1</sup> and Mizuki Sakamoto<sup>1</sup>

<sup>1</sup> Plasma Research Center, University of Tsukuba,  
1-1-1 Tennodai, Tsukuba, Ibaraki 305-8577, Japan  
togo@prc.tsukuba.ac.jp

<sup>2</sup> Graduate School of Engineering, Osaka University,  
1-1 Yamadaoka, Suita, Osaka 305-8577, Japan

<sup>3</sup> National Institutes for Quantum Science and Technology,  
2-166 Obuchi-Omotodate, Rokkasho, Aomori 039-3212, Japan

Plasma fluid models are useful tools to compute profiles of macroscopic quantities of plasmas such as the density, flow, and pressure, with comparatively low computational cost, and thus have been used in various plasma applications. In simulations for the divertor design of plasma fusion reactors, the Braginskii model [1] is widely used to model the fuel plasmas. However, it was pointed out in a DEMO reactor that the kinetic-effect modeling for the parallel-to- $\mathbf{B}$  ion conductive heat flux had a large impact on the plasma profiles due to the marginal Coulomb collisionality [2]. In addition, a particle-in-cell (PIC) simulation showed that, in such a marginal-collisionality plasma, the ion temperature anisotropy tends to be remarkable [3], indicating that an individual treatment of the parallel and perpendicular components of the ion energy would be essential in a simulation for a DEMO reactor.

We have developed a plasma fluid model based on the anisotropic ion pressure (AIP model) [4] combined with the virtual-divertor model [5] for open-field systems. At present, the parallel-to- $\mathbf{B}$  ion conductive heat fluxes for the parallel and perpendicular-energy components are evaluated individually by heat-flux-limiting models similar to those used in Ref. [2]. In this study, the accuracy of the AIP model was investigated by directly comparing its solutions with a PIC code PIXY [6] over a range of Coulomb collisionality. The AIP model solutions were also compared directly with the Braginskii model by using the VFA-AIP scheme [7]. It was shown that the solutions of the AIP model were in good agreement with PIXY over the low to high Coulomb collisionality range, and that they were more similar to the PIXY solutions than Braginskii-model ones. However, qualitative differences were found in the parallel-to- $\mathbf{B}$  ion conductive heat flux profiles. We will also present our plan to incorporate the heat-flux equations [8] directly into the AIP model to address this issue.

This work was performed with the support and under the auspices of the NIFS Collaboration Research Program (NIFS23KIST050 and NIFS21KUGM164).

- [1] S.I. Braginskii, *Transport Processes in a Plasma*, vol. 1 (Consultant Bureau, New York, 1965) 205.
- [2] Y. Homma, *Plasma Phys. Control. Fusion* **64** (2022) 045020.
- [3] A. Froese *et al.*, *Plasma Fusion Res.* **5** (2010) 026.
- [4] S. Togo *et al.*, *Nucl. Fusion* **59** (2019) 076041.
- [5] S. Togo *et al.*, *J. Comput. Phys.* **310** (2016) 109.
- [6] K. Ibano *et al.*, *Nucl. Fusion* **59** (2019) 076001.
- [7] S. Togo *et al.*, *Plasma Fusion Res.* **18** (2023) 1203005.
- [8] W. Fundamenski, *Plasma Phys. Control. Fusion* **47** (2005) R163.

## The feasibility of using ions and charges in the medical field.

Sanae Ikehara<sup>1,2</sup>, Ken Wakai<sup>1</sup>, Shinsuke Akita<sup>1</sup>, Takashi Yamaguchi<sup>1</sup>, Kazuhiko Azuma<sup>1</sup>, Syota Ohki<sup>1</sup>, Nobuyuki Mitsukawa<sup>1</sup>, Hajime Sakakita<sup>2</sup>, Komei Baba<sup>3</sup>, Yuzuru Ikehara<sup>1,2</sup>

<sup>1</sup> Graduate School of Medicine, Chiba University 1-8-1 Inohana, Chuo-ku, Chiba, 260-8670, Japan  
yuzuru-ikehara@chiba-u.ac.jp

<sup>2</sup> National Institute of Advanced Industrial Science and Technology, Tsukuba, 305-8565, Japan.

<sup>3</sup> DLC Research Institute LLC, Nagasaki, 850-0011, Japan.

The life sciences explain that information transfers in the nervous system occur through the transmission of electrical signals and that neuronal activation and muscle contraction result from charge and ion transfer into the cell via the activation of ion channels and receptors. From a broader perspective, biomolecules present in the blood, such as hormones and antibodies, their dispersion and accumulation, binding, and aggregation occur through the alterations of charges on functional domains of molecules and ions in living organisms. The evolution of technology to generate plasma at low temperatures in an atmospheric pressure environment will not only control physiological functions such as neuronal activation and muscle contraction caused by the transfer of electrical charges and ions into cells but also may solve Alzheimer's disease caused by the abnormal accumulation and aggregation of biomolecule. Based on the above understanding, the presenter, a pathologist, will present the following three studies he has conducted to open the feasibility of using ions and charges in the medical field.

We have previously discovered the phenomenon of 1) the aggregation of proteins in solution in a dispersed state by the donation of ions and charges by using a low-temperature atmospheric pressure plasma generator [1]. From this phenomenon, we have conceived of a new medical device that can stop bleeding and exudation of serous fluid by coagulating blood components, and 2) realized a minimally invasive hemostatic device that does not cause cauterization at the treatment site [2]. Furthermore, donating ions and charges may provide a means of overcoming the limitations of ultrastructural analysis performed using electron microscopy, and 3) established a pretreatment technique using plasma for scanning electron microscopy observation [3]. Pathologists use an optical microscope to diagnose formalin-fixed paraffin-embedded thin-sections (FFPE-ts) on slide glasses but not using scanning electron microscopy (SEM) because of their dielectric nature. Therefore, we have developed a method to change the dielectric natures of FFPE-ts to conductive by reacting ions derived from plasma on glass slides. Consequently, in FFPE-ts specimens of pathological autopsy tissue of SARS-CoV2 infected patients, we succeeded in seeing damage on the tunica media of pulmonary arteries due to budding of SARS-CoV2 particles (Fig.1), which was a severe pathology of COVID-19 [4]. Notably, our plasma technology will not only allow pathologists to use SEM to diagnose viral infections but also raise the possibility that the architecture of automated testing of semiconductors using SEM will carry the automated diagnosis of viral infections.

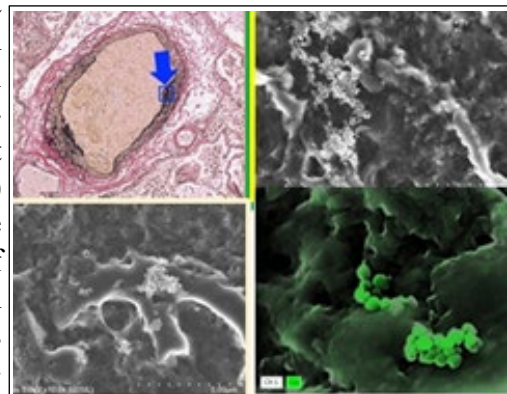


Fig.1, Referred from [4] Proc Natl Acad Sci U S A, 119, e2203437119 (2022).

- [1] Ikehara, S., et al., Plasma Processes and Polymers, 12, (2015).
- [2] Ikehara, Y., et al., J. Photopolym. Sci. Tehnol., 26(4), (2013).
- [3] Wakai, K., et al., Sci Rep, 12, (2022).
- [4] Iwamura, C., et al., Proc Natl Acad Sci U S A, 119, e2203437119 (2022).

## Low-temperature and thermal plasma research at PEwave, Walailak University

M. Nisoa, S. Kaewpawong, W. Kongsawat, R. Taleh, Karaket Wattanasit and D. Srinoum

*Plasmas and electromagnetic wave research laboratory,  
Walailak University: 222 Taiburi, Tasala, Nakhon si thammarat, 80160, Thailand  
mnisoa@gmail.com*

Applications of plasmas for agriculture, food, medical, environment, nanotechnology and material processing have been increasing in the recent years in Thailand. However, shortage of fundamental technologies, such as vacuum system, high-power DC, RF and microwave power supplies and diagnostics tools, cause difficulty for commercial scale development. The plasma and electromagnetic wave(PEwave) research center, at Walailak University, has been developed various plasma sources at low and atmospheric pressures since 2000[1,2,3,4]. In this paper, atmospheric cold plasmas produced by surface barrier discharge and plasma jets, DC thermal plasma torch and high-power helicon plasmas will be presented. Atmospheric cold plasmas are successfully applied for research in food safety, shelf life extension of snacks, fruits and fish, and induce apoptosis in cancer cells. Thermal plasma produced by DC plasma torch has temperature more than 1200 °C will be used for gasification of medical and plastic wastes. High-density helicon plasmas, produced by home-made 5 kW, 13.56 MHz RF power supply, has density more than  $10^{13}$  cm<sup>-3</sup> will be utilized for plasma-material interaction study to develop materials for fusion reactor and plasma heating research.

### Reference

- [1] M. Nisoa, D. Srinoum and P. Kerdthongmee, Development of high voltage high frequency resonant inverter power supply for surface glow barrier discharges: Solid State Phenomena, 107(2005), 81 – 86
- [2] M. Nisoa and T. Srinoum, Characteristics of ozone production by using atmospheric surface glow barrier discharge, Walailak J. Sci. Tech. 6(2), 283 – 292 (2009)
- [3] P. Kerdthongmee ,1 D. Srinoum and M. Nisoa, Development of compact high voltage switched mode power supply for microwave plasma sources supply for low pressure plasma, JINST, 6, 2011
- [4] P. Kerdthongmee, D. Srinoum and M. Nisoa, Development of a compact permanent magnet helicon plasma source for ion beam bioengineering, Rev. Sci. Instrum. 82, 103503 (2011)



## Atmospheric-pressure Plasma Effects on Cancer Cells and RONS Generation for Medical Applications

Yun-Chien Cheng<sup>1</sup>

<sup>1</sup>*Department of Mechanical Engineering, National Yang Ming Chiao Tung University  
Hsinchu 30010, Taiwan  
yccheng@gmail.com*

We compared the effects of plasma with thermal therapy on lung cancer with malignant pleural effusion. This study find out that the plasma can selectively kill lung cancer cells and the benign cells remain its viability. Besides, the thermal therapy kills both cancer cell and benign cells. To investigate what is the plasma factor that inhibits cancer cells, we investigated the effects of plasma-generated short-lived species, long-lived species, and electric fields on skin melanoma and basal cell carcinoma cells (A2058 cells, BCC cells) and normal cells (BJ cells, Detroit 551 cells) and found that the short-lived species do make selective inhibition to the benign and malignant cells. The second part of my study is that we mix water aerosol with plasma jet at downstream region makes the plasma jet generate more  $\bullet$ OH. We designed different mixing chambers and adjusting the water aerosol flow rate maximize the  $\bullet$ OH generated by plasma jet for biological applications. We also constructed an impedance matching circuit for a partial-discharge calibrated (PDC) atmospheric-pressure plane-to-plane DBD equivalent circuit. The last part of my work is that we used machine learning to distinguish the discharge current of different plasma. The plasma discharge can be different depending on the conditions, and the resulting discharge current has quite different electrical features. Hence, a real-time and cost-effective diagnosis of atmospheric-pressure plasma discharge can be possibly provided via current classification with deep learning model.

The reactive radical such as  $\bullet$ OH can penetrate a medium for limited thickness. This phenomenon can be used to control the concentrations of such radicals. By controlling the thickness between cells and water surface, we can treat cancer cells with different concentrations of the reactive radicals. By adding agarose gel on surface, we applied only electric field but no RONS on cells. By comparing experimental results, we can get the effects of short-life RONS, long-life RONS and electric field on cancer cells. relation between the PBS thickness and penetrated  $\bullet$ OH concentration. We observed that  $\bullet$ OH concentration decreased with increasing PBS thickness. The maximum penetration depth of  $\bullet$ OH was about 0.6 mm. In the SLE experiment, we used 0.2 mm and 0.5 mm as the experimental parameter. In the LE experiment, we used 1.4 mm as the experimental parameter. Fig. 4 showed that the The viability of normal skin cells was not affected by the treatments of plasma and the electric field generated by plasma. Fig. 5 showed that the viability of cancer cells was not affected by the electric field and the treatments of plasma (1.4 mm), but decreased with water-layer thickness (i.e. the increase of  $\bullet$ OH concentration). In this work, an experimental setup was designed to be used to investigate the effects of CAP generated short-life RONS, long-life RONS and electric field on cancer cells. We investigated the relation between the PBS thickness and penetrated  $\bullet$ OH concentration. In our study, plasma-generated electric field and long-life RONS did not affected cells, while the short-life RONS has selectively damage on cancer cells.

- [1] R.B. Gadri, R.J. Roth, T.C. Montie et al., *Surface and Coatings Technology*, **131**, 528-541 (2000).
- [2] A. Mishra, P. Tummala, A. King et al., *Tissue Engineering Part C: Methods*, **15**, 431-435. (2009).
- [3] S. Mirpour, H. Ghomi, S. Piroozmand, M. Nikkhah, S.H.Tavassoli, S.Z. Azad, *IEEE Transactions on Plasma science*

## Effect of accumulated charge on the dynamics of plasma bullet propagation

Jun Sup Lim<sup>1</sup> and Eun Ha Choi<sup>2</sup>

<sup>1</sup>*Kwangwoon University, Plasma Bioscience Research Center (PBRC)  
20 Gwangun-ro, Nowon, Seoul 01897, Republic of Korea  
[Junsup117@gmail.com](mailto:Junsup117@gmail.com)*

<sup>2</sup>*Kwangwoon University, Electrical and biological physics department  
20 Gwangun-ro, Nowon, Seoul 01897, Republic of Korea*

Dynamics of plasma behavior is interesting field in the atmospheric pressure plasma jet. In the atmospheric pressure capillary plasma jet, initial plasma bullet generated between the electrodes and pass through the grounded ring region toward the gas exhaust nozzle. Although, plasma bullet escaped from the high electric field region between the electrodes, it continues to propagate as a streamer to the nozzle of the gas outlet. In this experiment, the guided capillary tube which consists of dielectric material can be accumulate the charge from the discharge phenomena with modified sinusoidal waveform of voltage.

The electric field resulting from the charge accumulation on the inner dielectric wall and residual charge on the discharged space could be affect to the propagating plasma bullet for their kinetic energy.<sup>[1]</sup> In this report, we applied the bipolar and unipolar voltage of sinusoidal wave for the separation of accumulated charge by pre-ionization of opposite polarity, and report the effect of charge accumulation to the propagating plasma bullet behavior. In the results of these separation showed the changes of breakdown voltage of discharge and plasma bullet shape in this experiment.

[1] J. Li, B. Lei, J. Wang, B. Xu, S. Ran, Y. Wang, T. Zhang, J. Tang, W. Zhao and Y. Duan, *Commun. Phys.*, **4**, 64 (2021)

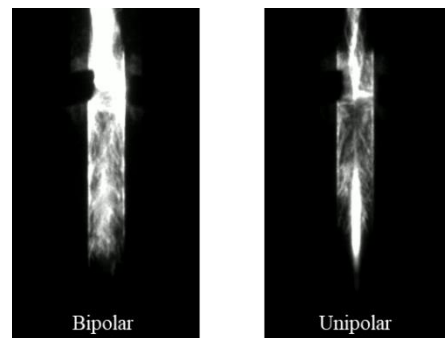


Fig. 1: Plasma bullet propagation with voltage polarity

# **Ion flux reduction factor at the sheath edge as a function of ion-neutral collisions in low temperature Ar or He DC plasmas**

Young-chul Ghim and Yegeon Lim

*Department of Nuclear and Quantum Engineering, Korea Advanced Institute of Science and Technology, Daejeon, S. Korea*

We expect a reduction of ion flux toward a plasma boundary as the ion-neutral collisions increase in partially ionized low-temperature plasmas. Nevertheless, experimentally quantifying how much it will be is a challenging task, while there exists a recent report based on particle-in-cell simulations [Beving et al., *Plasma Sources Sci. Technol.* 31 084009 (2022)]. As a complementary effort to such a numerical study, we have performed experiments with systematic parameter scans aimed at directly inferring the reduction factors in ion flux caused by the collisions. DC Ar or He plasmas are generated in a multidipole chamber with different gas pressures to control the collisionality and with various discharge currents to investigate the ion flux reduction factor in a wide range of the plasma conditions. In this work, we discuss the similarities and discrepancies between the experimentally obtained ion flux reduction factor and the numerical results.

This work was supported by National Research Foundation of Korea (NRF) funded by Ministry of Science and ICT, Grant Nos. RS-2022-00155917 and No. 2021R1A2C2005654.

# Quantification of Causality Among Frequency Modes in Linear Plasma Using Vector Autoregressive Models

Fumikazu Miwakeichi<sup>1</sup> and Makoto Sasaki<sup>2</sup>

<sup>1</sup> *Department of Statistical Science, The Institute of Statistical Mathematics,  
Tachikawa, Tokyo 190-8562, Japan  
miwake1@ism.ac.jp*

<sup>2</sup> *Nihon University, College of Industrial Technology, Chiba 275-8575, Japan*

Linear plasmas exhibit a large number of frequency modes (Fig.1). The mechanisms by which these modes emerge and how they interact with each other are not fully understood. To investigate the interaction between modes, we employed a vector autoregressive (VAR) model. This model allows for a more detailed and quantitative understanding of causal relationships between modes, and in this study we constructed both a full model that considers all variables (modes) and a reduced model that excludes certain modes. By comparing the Akaike information criterion for these models, we were able to assess significant causal relationships between modes (Fig.2). We found that the combination of modes with a causal relationship changes under different pressure conditions.

In the presentation, we will further introduce methods for model selection and techniques for data preprocessing.

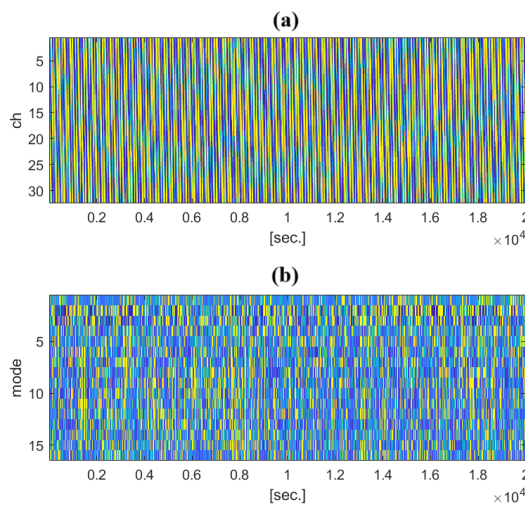


Fig.1:  
(a) 2D representation of cylindrical plasma data  
(b) Fourier mode decomposition over time

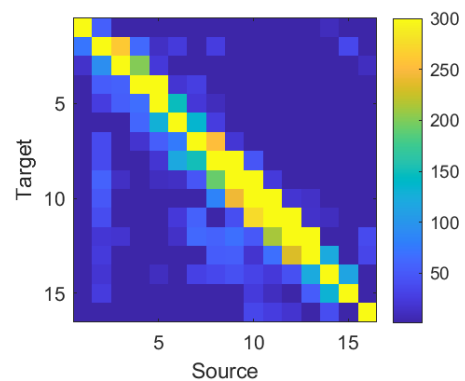


Fig.2:  
Significant causality between modes through the comparison of the full model and reduced model constructed by the VAR model.

## Basis function analysis technique for the two-dimensional structure of fluctuation in magnetized plasma

K. Yamasaki<sup>1</sup>, A. Fujisawa<sup>2</sup>, Y. Nagashima<sup>2</sup>, C. Moon<sup>2</sup>, Y. Kawachi<sup>3</sup>, D. Nishimura<sup>2</sup>, T-K. Kobayashi<sup>2</sup>, S. Inagaki<sup>4</sup>, M. Sasaki<sup>5</sup>, Y. Kosuga<sup>2</sup>, T. Yamada<sup>6</sup>, and N. Kasuya<sup>2</sup>

<sup>1</sup> Graduate school of Advanced Science and Engineering, Hiroshima University  
Higashihiroshima, Hiroshima 739-8527, Japan  
kotaro-yamasaki@hiroshima-u.ac.jp

<sup>2</sup> Research Institute for Applied Mechanics, Kyushu University  
Kasuga, Fukuoka, 816-8580, Japan.

<sup>3</sup>Department of Electronics, Kyoto Institute of Technology  
Kyoto, Kyoto, 611-0011, Japan

<sup>4</sup>Institute of Advanced Energy, Kyoto University  
Uji, Kyoto, 611-0011, Japan

<sup>5</sup>Department of Electrical and Electronic Engineering, Nihon University  
Narashino, Chiba, 275-8575, Japan

<sup>6</sup>Faculty of Arts and Science, Kyushu University  
Fukuoka, Fukuoka, 819-0395, Japan

Fluctuations are a crucial player in heat and particle transport in magnetized plasmas. Recent studies have revealed that the fluctuations emerging from different free energy sources, such as the gradient of density and flow, can interact with each other and coexist at different radial locations [1,2]. These results indicate the necessity of entire and simultaneous plasma observation to improve the understanding of fluctuation-induced transport. For this purpose, we have developed tomography systems to observe two-dimensional structure of fluctuations in the linear magnetized plasma device PANTA. This enables us to obtain the temporal evolution of the emission intensity profile of the whole cross-section of the linear magnetized plasma.

Since the reconstruction data is huge, an efficient analysis method is required to manage the data that is composed of various fluctuations with a wide range of frequency and wavenumber, together with intermittency. For the cylindrical geometry, we developed a basis function decomposition technique, called Fourier-Rectangular Function (FRF) analysis [3], which allows us to obtain the temporal and radial profile of the amplitude and spatial phase for each azimuthal mode.

An example of the FRF analysis on the tomographic reconstruction data is shown in Figure 1. The FRF analysis revealed that the nonlinearly coupled fluctuations show different spatial and temporal behavior. In this talk, we discuss the details of the FRF and further analysis results, including the spatio-temporal behavior of the nonlinear coupling.

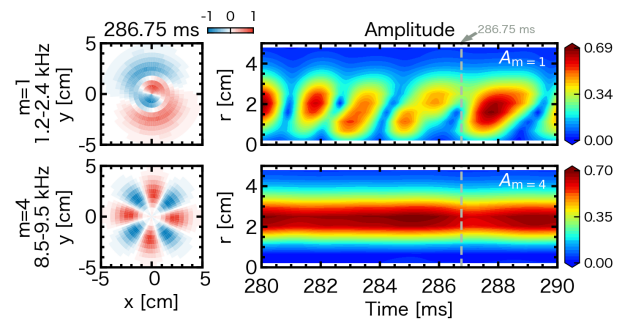


**Figure 1** The two-dimensional spatial structure of nonlinearly coupled fluctuation and temporal evolution of the amplitude of each modes obtained by the tomographic reconstruction data and FRF analysis.

### References

1. T. Kobayashi, *et al.*, Phys. Plasmas **23**, (2016).
2. M. Sasaki, *et al.*, Phys. Plasmas **24**, 112103 (2017).
3. K. Yamasaki, *et al.*, J. Appl. Phys. **126**, 043304 (2019)

## Applications of conditional sampling technique to time series of experimental plasma data

Yuichi Kawachi

*Department of Electronics, Kyoto Institute of Technology  
Matsugasaki, Sakyo Ward, Kyoto 606-8585, Japan  
kawachi@kit.ac.jp*

Various time series analyses have been established to extract plasma dynamics, which is crucial for controlling plasma behavior. The widely used Fourier analysis assumes that the observed data consists of stationary periodic waves and provides time-averaged information. However, nonlinear plasma dynamics often exhibit quasi-periodic or intermittent features, such as blobs, edge-localized modes (ELMs), and various turbulent phenomena. Fourier analysis is often inadequate for comprehending such behaviors.

As an alternative method to analyze quasi-periodic phenomena, the conditional sampling technique has been developed and applied extensively [1]. This technique involves digital processing akin to a lock-in amplifier. Initially, the method detects the emergence timing of the target phenomena from a reference signal. Then, based on this timing, other time series data are resampled. Finally, the resampled data undergo statistical analysis. This approach is simple yet widely applicable. For instance, it can enhance time resolution in measurements and data analysis when dealing with low time resolution data.

The conditional sampling technique offers flexibility in detecting the target phenomena and analyzing the resampled data. In the former case, the conventional approach has been to detect phenomena by setting a threshold for large-amplitude and intermittent events[2]. However, a recent method has emerged for detecting quasi-periodic and sinusoidal waveforms. The latter method, commonly used, involves simple averaging, though combinations with linear regression and Fourier analysis have also been explored[3].

This presentation will outline the analysis procedure flow for the conditional sampling technique and highlight its applications.

[1] G. Fuchert et al., Plasma Phys. Control. Fusion 55, 125002 (2013).

[2] S. Inagaki et al., Plasma Fusion Res. 9, 1201016 (2014)

[3] Y. Kawachi et al, Physics of Plasmas 28, 112302 (2021)

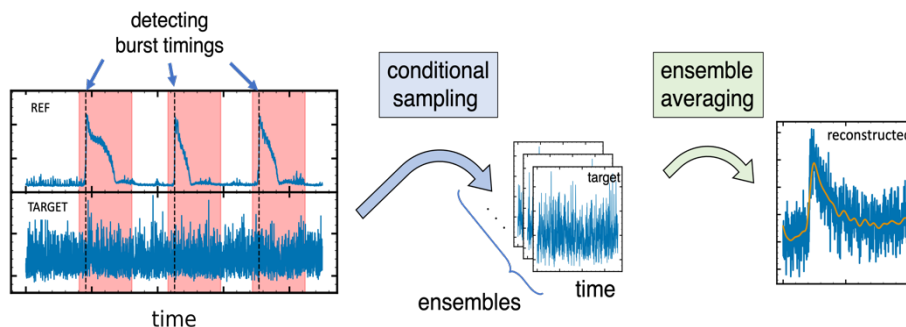


Fig. 1: An example of the conditional sampling procedure.

## Multiple correlation analysis of nonlinear dynamics in plasma turbulence

Takuma Yamada<sup>1</sup>, Makoto Sasaki<sup>2</sup>, Hiroyuki Arakawa<sup>3</sup>, Kosuke Kikuta<sup>4</sup>,  
Takashi Nishizawa<sup>5</sup>, Chanho Moon<sup>5</sup>, Yoshihiko Nagashima<sup>5</sup>,  
Yusuke Kosuga<sup>5</sup>, Naohiro Kasuya<sup>5</sup>, and Akihide Fujisawa<sup>5</sup>

<sup>1</sup> Faculty of Arts and Science, Kyushu University, Nishi-ku, Fukuoka 819-0395, Japan  
takuma@artsci.kyushu-u.ac.jp

<sup>2</sup> College of Industrial Technology, Nihon University, Narashino, Chiba 275-8575, Japan

<sup>3</sup> Faculty of Medical Sciences, Kyushu University, Higashi-ku, Fukuoka 812-8582, Japan

<sup>4</sup> Interdisciplinary Grad. Sch. of Engineering Sciences, Kyushu University, Kasuga, Fukuoka 816-8580, Japan

<sup>5</sup> Research Institute for Applied Mechanics, Kyushu University, Kasuga, Fukuoka 816-8580, Japan

Meso-scale structures such as streamers and zonal flows are produced by nonlinear interaction between microscopic drift wave turbulence in fusion plasmas. Since these structures significantly influence the plasma radial transport, to study the nonlinear dynamics of meso-scale structures is important in plasma physics and fusion reactors.

By using the linear plasma device in Kyushu University, our group succeeded in finding the streamer structure for the first time [1]. The cross-sectional structures of the streamer, its mediator mode, and carrier drift waves were revealed by multiple correlation analysis [2]. While the streamer structure and carrier drift waves were radially elongated, the mediator mode had a node in the radial direction. Additionally, the axial dimensional research revealed that while the carrier drift waves had an axial mode number one (propagation direction from the end to the source), the streamer and mediator were revealed to have an axial mode number zero [3].

To compare the observed meso-scale structures with theoretical and numerical studies more precisely in the phase space, local information of the wave number is required. In this study, we tried to observe the local wave number (poloidal mode number  $m$ ) of plasma turbulence. Furthermore, local information of the results of multiple correlation analysis were obtained.

Figure 1 well shows that when the streamer exists, the amplitude of mode number three (one of the carrier waves) is poloidally localized and the localized region is rotating in the poloidal direction with the frequency of 1.2 kHz, which is the same frequency with the rotation of streamer.

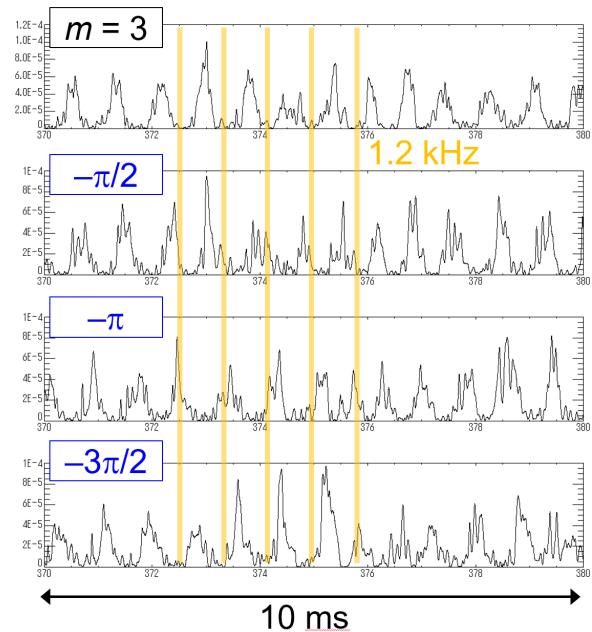


Fig. 1: Time evolution of the  $m = 3$  amplitude. Window function is applied in the poloidal direction. The windows are phase shifted for  $-\pi/2$ ,  $-\pi$ ,  $-3\pi/2$ , compared to the top figure.

- [1] T. Yamada *et al.*, Nat. Phys. **4**, 721 (2008).  
[2] T. Yamada *et al.*, Phys. Rev. Lett. **105**, 225002 (2010).  
[3] T. Yamada *et al.*, J. Phys. Soc. Jpn. **87**, 034501 (2018).

# Beam-assisted Atomic Layer Etching

Doo San Kim<sup>†</sup>, Yun Jong Jang<sup>†</sup>, Ji Eun Kang<sup>†</sup>, and Geun Young Yeom<sup>†‡\*</sup>

<sup>†</sup> School of Advanced Materials Science and Engineering, Sungkyunkwan University, Suwon 16419, Republic of Korea

<sup>‡</sup> SKKU Advanced Institute of Nano Technology (SAINT), Sungkyunkwan University, Suwon 16419, Republic of Korea

\*E-mail: [gyyeom@skku.edu](mailto:gyyeom@skku.edu)

## Abstract

The atomic layer etching technology is currently being researched in various ways by academia, the research community, and semiconductor equipment/device companies. It is expected to be the next-generation precision etching technology due to its characteristics of low damage, high selectivity, low aspect ratio dependent etching (ARDE), and high uniformity. In this presentation, we used a remote plasma source-type energetic particle beam source to etch various semiconductor materials (silicon, oxides, III-V, 2D materials) and evaluated their properties. We aim to summarize the research results in this presentation. Neutral beams do not cause charging effects due to ions, and electron beams have minimal momentum exchange due to ion collisions, reducing the potential for material damage during etching. In this presentation, we intend to provide the results of etching of semiconductor materials using these energetic particles.



## Past, Present, and Future Plasma Solutions to Semiconductor Challenges

Sang Hoon Ahn

*Semiconductor R&D Center, Semiconductor, SAMSUNG ELECTRONICS Co., Ltd.  
San #16 Banwol-Dong, Hwasung-City, Gyeonggi-Do 445-701, Korea  
sanghoona.ahn@samsung.com*

Plasma has been used as a key enabling technology for thin film deposition and etch in the semiconductor device manufacturing since the birth of the semiconductor devices. The traditional semiconductor device trend can be characterized by 2D down-scaling but 3D up-scaling. The traditional scaling continues to reduce the size in 2D, but it keeps increasing in 3D to ensure the device or interconnect density improvement every node. Nonetheless, these trends drive the process temperature down as well as enhances the structural aspect ratio very high, which, in turn, requires increasingly high gap-fill capability and highly conformal deposition together with high integrity etch. This paper will review how deposition plasma technology has evolved to address the semiconductor device challenges such as high quality film at low temperature, high aspect ratio gapfill, highly conformal deposition, low k dielectrics, and wiggly lines over the time. Plasma enhanced chemical vapor deposition (PECVD) was introduced to deposit high quality dielectrics at relatively lower temperature than 500C. Typically, films deposited by PECVD has a poor step coverage with large overhang, creating voids. This inability to fill up the trenches resulted in inventing high density plasma CVD which has both deposition and etch components simultaneously. HDPCVD have been applied to diverse gap-fill applications for many nodes. As HDPCVD has run out of its steam at an advanced node, flowable CVD has adopted the remote plasma for reactant gases while the CVD precursors are introduced to a reactor without being exposed to plasma. Its gapfill capability improved dramatically. Dielectric film qualities can also be engineered by an appropriate selection of the deposition plasma frequency. For example, at the superfine line pitch, patterned line can be wiggly under the compressive stress. VHF PECVD can boost its density as well as its stress in a tensile direction to overcome the risk of wiggly line. Pulsed PECVD can also reduce the sticking coefficient of the CVD precursor, boosting its deposited film step coverage up to 95% at the pattern. Mixed plasma frequency can be used as a knob to boost the deposition rate as well as the film density. Throughout the history of the plasma application to semiconductor, the engineering of dielectric film properties by plasma have been nicely demonstrated to address diverse challenges of ever scaling semiconductor devices. Moving forward, the mega trend is expected to continue in lowering temperature, increasing higher aspect ratio, and improving higher qualities (k, stress) and there are even more opportunities for plasma technology to contribute to the semiconductor applications.

# Plasma-enhanced atomic layer processing for semiconductor processing

Satoshi Hamaguchi, Tomoko Ito, and Kazuhiro Karahashi

*Graduate School of Engineering, Osaka University, Osaka, Japan  
Email: hamaguch@ppl.eng.osaka-u.ac.jp*

The most advanced generation of semiconductor devices that are already in mass production (as of mid-2023) is said to be 3nm technology node devices. As the mass production of the subsequent generations of semiconductor devices, i.e., 2nm node devices and beyond, is already in sight and new and complex device structures such as those for gate-all-around field effect transistors (GAA-FETs) need to be mass-produced, highly innovative plasma processing techniques with atomic-scale accuracy must be developed expeditiously and cost-effectively. For this purpose, a large part of the conventional try-and-error approach for process development must be replaced with more logical approaches based on a better understanding of the fundamental mechanisms of surface processing. In this presentation, recent analyses of plasma-material interactions based on atomic-scale numerical simulations and surface reaction experiments will be discussed with atomic-layer etching (ALE)<sup>1,2,3</sup> and atomic-layer deposition (ALD)<sup>4</sup> as examples.

## References

1. E.T.C. Tinacba, *et al.*, *J. Vac. Sci. Technol.* **A39**, 042603 (2021).
2. A. Hirata, *et al.*, *Jpn. J. Appl. Phys.* **62** S11015 (2023).
3. A. H. Basher, *et al.*, *J. Vac. Sci. Technol.* **A38**, 052602 (2020); **A39**, 057001 (2021).
4. T. Ito, *et al.*, *Jpn. J. Appl. Phys.* **61**, S11011 (2022).
5. K. Arts, *et al.*, *Plasma Sources Sci. Technol.* **31**, 103002 (2022).

## Adsorptive removal of cationic and anionic dyes using nanocomposite of graphene oxide/zinc oxide from aquatic environment.

Ghayas Uddin Siddiqui\*, Adnan Ali, Youn Sun Mok

Department of Chemical Engineering, Jeju National University, Jeju 63243, Republic of Korea.

[gsiddiqi@jejunu.ac.kr](mailto:gsiddiqi@jejunu.ac.kr)

### Abstract

Today water contamination has become one of the most serious problems due to discharge of hazardous dyes into the aquatic environment. There are numerous methods to remove those dyes, but adsorption is considered one of the most facile and feasible methods to remove the pollutants from the water. Researchers have been making many efforts to develop and synthesize adsorbents that can eliminate contaminants from water but selecting an adsorbent is difficult task because some adsorbents can only remove cationic dyes and some can remove only anionic dyes. This study aimed to remove the cationic (Methylene Blue) and anionic (Eosin Y) dyes using a nanocomposite of graphene oxide and zinc oxide. Results showed that 0.23 mg/ml GO/ZnO nanocomposite adsorbed 0.1 mg/ml EY and 0.04 mg/ml MB dyes simultaneously from the aqueous solution in 10 and 15 minutes respectively. These are the appreciable results showing highly efficient removal of pollutants using GO/ZnO nanocomposite via adsorption method.

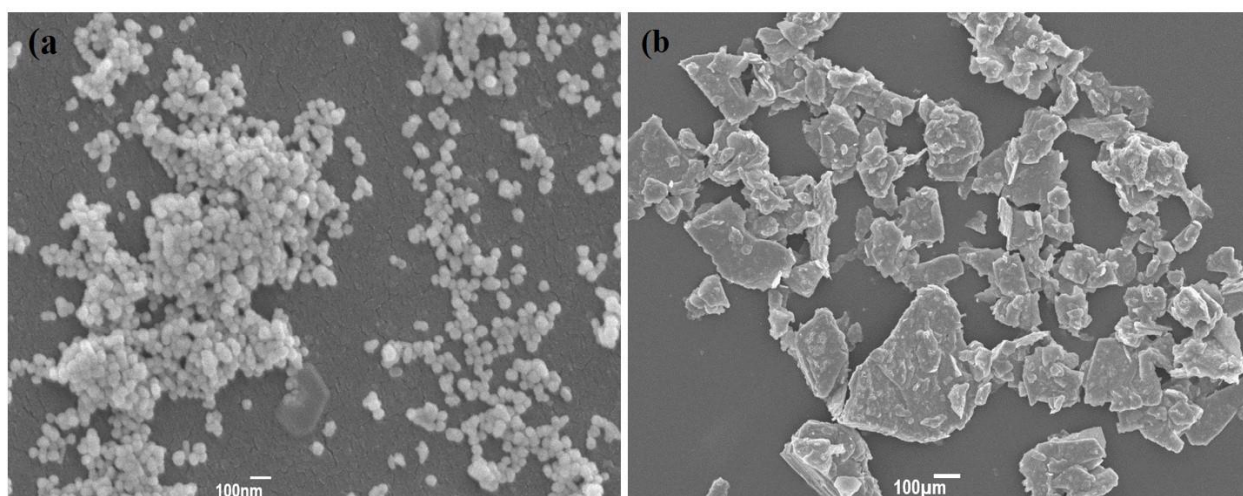


Figure 1. a) ZnO nanoparticles used for the adsorption, b) graphene oxide synthesized by modified Hummer's method

## 3D-Graphene Networks: Synthesis and Applications

Mineo Hiramatsu<sup>1</sup>, Keigo Takeda<sup>1</sup>, Hiroki Kondo<sup>2</sup> and Masaru Hori<sup>2</sup>

<sup>1</sup> *Department of Electrical and Electronic Engineering, Meijo University  
1-501 Shiogamaguchi, Tempaku, Nagoya 468-8502, Japan  
mnhmmt@meijo-u.ac.jp*

<sup>2</sup> *Center for Low-temperature Plasma Sciences, Nagoya University  
Furo-cho, Chikusa, Nagoya 464-8603, Japan*

3-dimensional (3D) graphene network called as carbon nanowalls (CNWs) and vertical graphenes represents an aggregate of vertically standing graphenes. CNWs and related sheet nanostructures are composed of self-supported few-layer graphene sheets with open boundaries, standing almost vertically on the substrate. CNWs are characterized by large specific surface area and space surrounded by vertical graphene sheets. The wall maze-like architecture or disordered honeycomb structure of CNWs with large-surface-area graphene planes could be applied as electrodes for energy storage devices and electrochemical sensors as well as scaffold for cell culturing. CNWs have been grown using various CVD methods employing CH<sub>4</sub> and H<sub>2</sub> mixtures on a variety of heated substrates [1]. The morphology of CNWs depends on the source gas mixtures, pressure, process temperature as well as the type of plasma used for the growth of CNWs. Isolated nanosheets, vertical maze-like structure, highly branched type, and a kind of porous film have been fabricated. We can expect a wide variety of applications based on their structure as illustrated in Fig. 1.

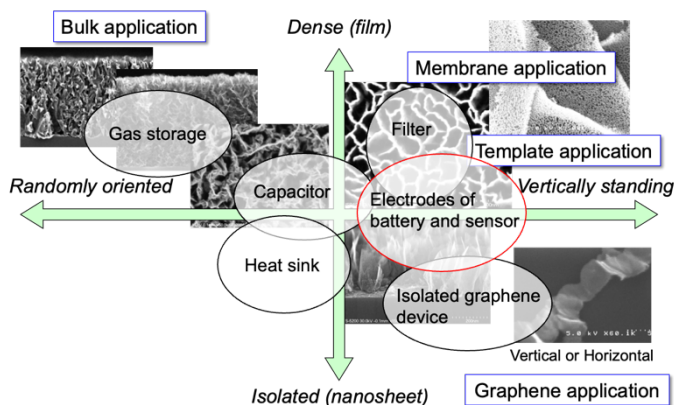


Fig. 1 Schematic illustration of expected applications of CNWs vs. morphologies.

In the typical case of wall maze-like CNW growth, after the nucleation, the height of CNWs increases almost linearly with the growth period, while the thickness of each sheet and interspaces between adjacent sheets are almost constant. From TEM observation, each sheet is composed of nanographene domains. These domain boundaries and graphene edges are chemically reactive, and metal nanoparticles such as Pt nanoparticles stick selectively at the grain boundaries and graphene edge (top of CNWs). Therefore, combined with surface functionalization, CNWs can be suitable as platform in electrochemical and bio applications. For this purpose, we have carried out CNW growth using inductively coupled plasma-enhanced CVD with CH<sub>4</sub>/H<sub>2</sub>/Ar mixture. Moreover, CNW surface was decorated with Pt nanoparticles by the reduction of chloroplatinic acid. Alternatively, conformal coating of CNW surface with metal oxide nanoparticles/films such as ZnO and SnO<sub>2</sub> was carried out using mist CVD or thermal decomposition. As examples of applications, we report the performances of hydrogen peroxide sensor and fuel cell, where CNW electrode was used. Electrochemical experiments demonstrate that CNWs can be promising electrode materials for electrochemical sensing, biosensing and energy conversion applications.

[1] M. Hiramatsu, M. Hori, *Carbon Nanowalls, Synthesis and Emerging Applications* (Springer Verlag, Wien, 2010).

# Near-future industrial innovation Digital transformation (DX) to Quantum transformation (QX)

Masahiro Horibe

*Global Research and Development Center for Business by Quantum-AI Technology (G-QuAT),  
National Institute of Advanced Industrial Science and Technology  
1-1-1 Umezono, Tsukuba, Ibaraki 305-8563, Japan  
masahiro-horibe@aist.go.jp*

Japanese government has been serious of quantum strategy since 2020. The first strategy, “Quantum Innovation and Technology Strategy“ has been published in 2020 and focused on basic technical research in quantum information science[1]. In 2021, some of foreign quantum computing vendors released gate-type quantum computer through cloud platform. This means that quantum R&D activities is started to move to social implementations. The government released “Vision of Quantum Future Society“ in 2022[2], and “Strategy of Quantum Future Industry Development“, as a roadmap of implementation of quantum technology to society, in 2023[3]. In the vision and strategy, the METI decided to build new R&D center (G-QuAT) in AIST.

G-QuAT is not only focusing on research and development but also business development. Especially, valuable applications are going to be created using quantum computing technology and G-QuAT plans the next generation large-scale quantum computer and related system level developments by collaborating with quantum computing vendors and components suppliers. As the results of the activities, quantum business ecosystem will be created in future.

In the case of quantum application development, G-QuAT is now starting to collaborate with various industrial users to create new solution by quantum computing algorithms combined with existing classical computing technology. We try to implement quantum computing technology to materials informatics, bioinformatics, and process informatics. Plasma process and control technology are one of valuable R&D target as quantum computing applications.

Other activity in G-QuAT also research quantum sensing system technology to realize accurate and precision measurements. The sensing is also support to plasma research activity.

- [1] “Quantum Innovation and Technology Strategy“, Japanese government (2020).
- [2] “Vision of Quantum Future Society“, Japanese government (2022).
- [3] “Strategy of Quantum Future Industry Development“, Japanese government (2023).

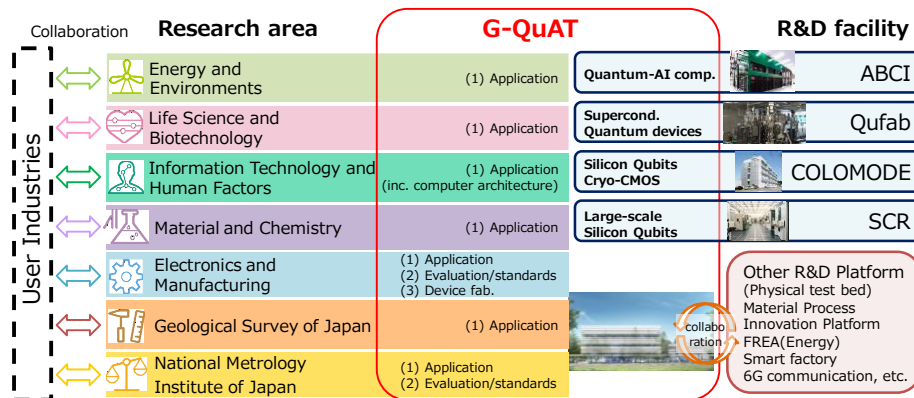


Figure 1: Application development framework in AIST coordinated G-QuAT

## Divertor detachment: Fusion plasma physics meets plasma chemistry

Detlev Reiter<sup>1</sup>

<sup>1</sup> *Heinrich-Heine-University Düsseldorf,  
D-40225 Düsseldorf, Germany  
reiterd@uni-duesseldorf.de*

It was recognized as early as 1968 by Bo Lehnert [1] that a zone of powerful gas - plasma interaction, formed near intensely plasma exposed surface elements, can be the key to solving the still critical plasma surface interactions (PSI) issue for sustainable nuclear fusion reactor operation. Today the „divertor detachment" regime in large magnetic fusion devices (tokamaks, stellarators) is characterized by strong volumetric exchanges of particles, momentum and energy, provided by such a gas-plasma interaction zone near target surfaces. Computational separation of plasma chemistry from the typically only empirically known plasma transport (intermittent or turbulent) allows to quantify the latter experimentally.

Firstly, by resorting to highly accurate atomic and molecular (AM) collision data [2] This builds on rate equation concepts well established e.g. in astrophysical and chemical kinetics (aka: non-equilibrium collision radiative modelling). Secondly by building on the high standards in (kinetic) transport theory and its wide range of applications, e.g. in the nuclear (neutronics) or radiation transfer sciences. This has meanwhile led to quite mature fusion boundary plasma (often partially “Monte Carlo” based) multi-physics and multi-scale simulation tools [3].

It is shown that the dominant gas-plasma friction force in typical “detached divertor conditions” is to be expected from (ro-vibrationally excited) molecule - ion collisions, rather than from the often-quoted resonant charge exchange between fuel atoms and their ions.

In conditions relevant for the boundary region in fusion devices a high sensitivity of the friction forces and energy exchange rates (kinetic and chemical energy exchanges between plasma components) between the gas and plasma phases is observed. Originating from a combination of electron collisions via various resonant  $H_2^-$  anion states and the near resonant heavy particle ion conversion channels, such as particle rearrangement or charge transfer. The former electron collisions have recently been theoretically re-investigated and completed in [4] for a wide set of intermediate resonant states, with the Local Complex Potential approach.

Direct contributions from dissociating molecules and their ions to atomic spectral lines, typically with overlapping kinetic energy releases, complicate visible light spectroscopy. Furthermore, quite unexpected kinetic isotope effects may arise in the D-T mixture of a future reactor divertor plasma: This effect might be well accessible experimentally in dedicated small laboratory plasma devices, e.g., when operated in H/D mixtures.

[1] B.Lehnert, Journal Nuclear Fusion **8**, 173, (1968)

[2] IAEA Vienna, Atomic and Molecular Data Unit, <https://amdis.iaea.org> (2023)

[3] R.Pitts, X.Bonnin, et al., Nuclear Materials and Energy **20**, 100696 (2019)

[4] V.Laporta, R.Agnello et al., Plasma Phys. Control. Fusion **63**, 085006 (2021)

## Verification of Birth Process of Primordial Organic Molecules in the Solar System from Molecular Clouds using Molecular Dynamics Simulations

Hiroaki Nakamura<sup>1,2</sup>, Masayuki Murai<sup>2</sup>, Yuki Goto<sup>1</sup>, Miyuki Yajima<sup>1</sup>, Masahiro Kobayashi<sup>1</sup>, Masahiro Katoh<sup>1,3,4</sup>, Kensei Kobayashi<sup>5</sup>

<sup>1</sup> National Institute for Fusion Science, 322-6 Oroshi, Toki GIFU 509-5292, Japan  
hlnakamura@nifs.ac.jp

<sup>2</sup> Nagoya University, Furo, Chikusa, Nagoya 464-8603, Japan

<sup>3</sup> Hiroshima Synchrotron Radiation Center, Hiroshima University, Higashi-Hiroshima, 739-0046, Japan

<sup>4</sup> UVSOR Synchrotron Facility 38 Nishigo-Naka, Myodaiji, Okazaki, 444-8585, Japan

<sup>5</sup> Yokohama National University, Tokiwadai, Hodogaya-ku, Yokohama 240-8501, Japan

The prevailing theory for the origin of life on the earth is that the amino acids (or more precisely, amino acid precursors, named "garakuta molecules" [1]), that make up proteins came from extraterrestrial sources[2-5]. To confirm this theory, it is necessary to clarify the reaction pathway of how amino acids are synthesized extraterrestrially.

The following proposal, named the bottom-up scenario, was proposed as a candidate scenario for the synthesis reaction of amino acids. The bottom-up scenario assumes a process in which organic dust scattered in the vicinity of a nova that has reached the end of its life is incorporated into a molecular cloud and reacts to become the garakuta molecule.

The study of this reaction pathway has confirmed that amino acid precursors are synthesized from small molecules through experiments using an accelerator. We attempt to corroborate the reaction in this experiment using a molecular dynamics simulation. Specifically, hydrogen, carbon monoxide, and ammonia were randomly arranged as small molecules in the ratio of 100:10:1, the temperature was raised to 1000 K, and then cooled to 10 K.

The results of the MD simulation for the 80 ps show that large molecular weight molecules are produced, as shown in Fig. 1.

*Acknowledgment:* The computation was performed using Research Center for Computational Science, Okazaki, Japan (Project: 22-IMS-C104) and Plasma Simulator of NIFS. The research was supported by Japan Society for the Promotion of Science (Grant Nos. JP19K14692, JP22H05131, JP23H04609, JP22K18272, JP23K03362), by the NINS program of Promoting Research by Networking among Institutions, by the NIFS Collaborative Research Programs (NIFS22KIIP003, NIFS22KIGS002, NIFS22KISS021) and by the ExCELLS Special Collaboration Program of Exploratory Research Center on Life and Living Systems.

[1] K.Kobayashi, et al., *Astrobiology: Emergence, Search and Detection of Life* (Ed.:Basiuk, V. A.), p. 175, American Scientific Publishers, Stevenson Ranch, CA, USA (2010).

[2] S. L. Miller, *Science*, 118(1953) 528.

[3] G. Schlesinger and S.L. Miller, *J. Mol. Evol.*, 19 (1983) 376.

[4] J.E. Elsila, et. al., *ACS Cent. Sci.*, 2 (2016) 370.

[5] C.R. Cronin, S. Pizzarello, *Science*, 275 (1997) 951.

[6] I. Endo, I. Sakon, et al., *Astrophys. J.*, 917 (2021) 103.

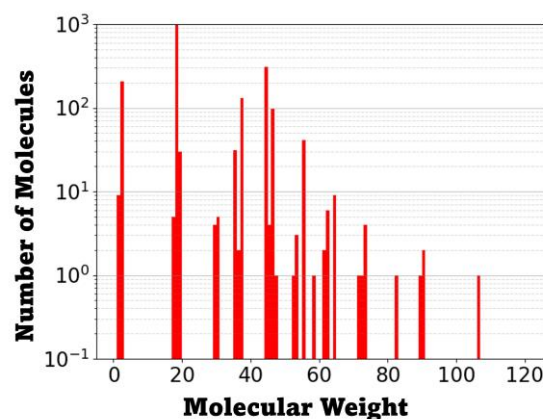


Fig. 1: molecular weight distribution of product molecules.

## Angular Momentum Coupling of Tilted Gaussian Beam with Waveguide Mode

Yoshihisa Fujita<sup>1</sup>, Hiroaki Nakamura<sup>2</sup>, Hideki Kawaguchi<sup>3</sup> and Yuki Goto<sup>2</sup>

<sup>1</sup> College of Industrial Technology, Nihon University,  
1-2-1 Izumi, Narashino, Chiba 275-8575, Japan  
fujita.yoshihisa@nihon-u.ac.jp

<sup>2</sup> National Institute for Fusion Science,  
322-6 Oroshi, Toki, Gifu 509-5292, Japan

<sup>3</sup> Muroran Institute of Technology,  
27-1 Mizumoto, Muroran, Hokkaido 050-8585, Japan

An optical vortex is an electromagnetic wave with a spiral wavefront. Since the phase of an optical vortex has higher degrees of freedom than that of a plane wave, applications in measurement and heating have been proposed. The possibility of propagating in plasmas above the cutoff density has been suggested [1], and its application is expected. Various methods of excitation of optical vortices have been proposed [2, 3], all of which are realized by shifting the phase of the plane wave using interaction with the medium. High-power millimeter wave is necessary to adapt to high-temperature plasmas. When high power is used, Joule losses in the medium cannot be ignored. Therefore, this study aims to propose a new excitation method for optical vortices.

Waveguides are used to transmit electromagnetic waves over long distances. The superposition of eigenmodes of cylindrical waveguides with different phases can be used to represent vortex modes such as optical vortices [4]. Nevertheless, it is difficult to excite arbitrary eigenmodes simultaneously. Generally, a Gaussian beam is incident parallel to the waveguide axis when exciting a waveguide mode. It is known that multiple higher-order modes are generated when the axes are misaligned. Therefore, it would be possible to control the excitation modes by clarifying the relationship between misalignment and higher-order modes.

By calculating the coupling between the Gaussian beam and the eigenmodes of the waveguide, the fraction of excitation modes can be calculated. Ohkubo et al. clarified the relationship between incident angle and excitation modes by calculating couplings [5]. However, vorticity has not been evaluated. The orbital angular momentum of the Gaussian beam is zero, but the optical vortex is not. In addition, the oblique incidence of the Gaussian beam will most likely have orbital angular momentum. Therefore, the purpose of this study is to clarify the angular momentum coupling in a misaligned waveguide.

Details will be presented at the conference.

- [1] T. I. Tsujimura et al., Phys. Plasmas 28, 012502 (2021).
- [2] H. Chung et al., Sci Rep 10, 8289 (2020).
- [3] B. He et al., J. Opt. Soc. Am. B 38, 1518 (2021).
- [4] D. Mao et al., APL Photonics 4, 060801 (2019).
- [5] K. Ohkubo et al., Int. J. Infrared Milli. Waves 18, 23 (1997).



## A simple method for modifying the surface morphology of various semiconductors and its application in random lasing

Quan Shi<sup>1</sup>, Hideki Fujiwara<sup>2</sup>, Shin Kajita<sup>1</sup>, Ryo Yasuhara<sup>3</sup>, Hirohiko Tanaka<sup>4</sup>, Noriyasu Ohno<sup>4</sup>, Hiyori Uehara<sup>3</sup>

<sup>1</sup> The University of Tokyo, 5-1-5 Kashiwanoha, Kashiwa, Chiba 277-8561, Japan  
shi.quan@edu.k.u-tokyo.ac.jp

<sup>2</sup> Faculty of Engineering, Hokkai-Gakuen University, 1-1, Nishi 11, Minami 26, Chuo-ku, Sapporo 064-0926, Japan

<sup>3</sup> National Institute for Fusion Science, 322-6, Oroshi-cho, Toki 509-5292, Japan

<sup>4</sup> Graduate School of Engineering, Nagoya University, Nagoya, 464-0863, Japan

As the development of high technology progresses, the social demand for semiconductor products has been expanding. The demand for nano/micro-meter surface modification that can be applied to a wide range of semiconductors has increased. However, specific structures or patterns are not always necessary for all conditions. Therefore, it is necessary to look for a simple method to fabricate structures on semiconductors.

This study introduces a one-step method called co-deposition etching (CoED). Semiconductors substrate was exposed in noble gas plasma such as helium (He) and argon (Ar), as shown in the experimental step in figure 1(a). Molybdenum impurities were introduced from a sputtering wire with bias. Structures are formed mainly due to the preferential sputtering after heavy impurities deposited on the substrate. This idea came out from the formation of cone structures on silicon after He plasma irradiation, which was because of the presence of heavy impurities. This method can be applied to various semiconductors, such as gallium arsenide, germanium, zinc selenide, and gallium nitride, as long as the sputtering rate of impurity species is smaller than that of the substrate. Besides, characteristics of structures, such as size, height, and density, can be controlled by the deposition rate of impurities, which increase the possibility for application.

One of the successful examples is performing random lasing on GaN treated by CoED. As shown in figure 1(b-c), an emission at 365 nm with a narrow linewidth can be observed from the GaN surface with particles of micrometer size, excited by a UV pulse laser. The lasing intensity increasing with the size of structures.

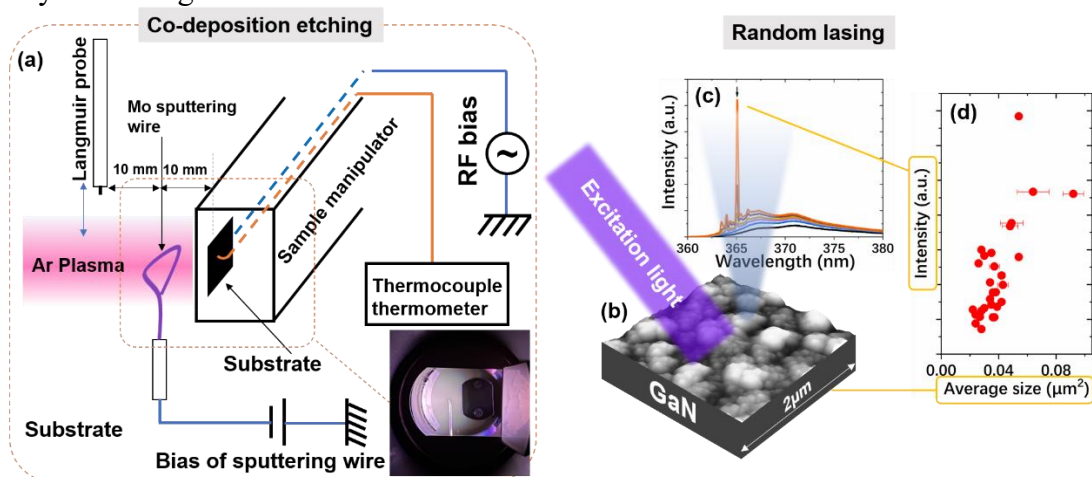


Fig. 1. (a) Schematic of the experimental setup of the co-deposition etching (CoED) method. (b) Topography of GaN treated by CoED. (c) Spectrum of random lasing from GaN excited by a pulse laser with a wavelength of 355 nm. (d) Correlation between the intensity of lasing and size of structures on GaN.

## Applications of Cold Plasma Technology in the Agri-food Industry

Roopesh Mohandas Syamaladevi (M. S. Roopesh)<sup>1</sup>

*<sup>1</sup>Food Safety & Sustainability Engineering Lab  
Department of Agricultural, Food & Nutritional Science  
University of Alberta  
Edmonton, Alberta, T6G 2P5, Canada  
roopeshms@ualberta.ca*

Cold plasma (CP) technology has gained a huge interest in the agriculture and food industry recently. The applications of cold plasma range from seed germination to disinfection in the agri-food sector. This presentation will focus on some of the most researched and emerging applications of cold plasma in the agri-food sector.

This presentation also aims to introduce some of the research works conducted at the University of Alberta on cold plasma applications in seed germination and plant growth as well as for disinfection. In the seed germination research, details on germination improvement of cold plasma treated seeds (e.g., peas, lentils) and greenhouse trial results will be discussed.

In the disinfection research, the effectiveness of plasma activated water bubble technology with different hydrodynamic flow regimes on the inactivation of microbial biofilms inside pipelines will be discussed. The presentation ends with an overview of the activities of certain companies working on the scale-up of cold plasma technologies in the food and agriculture sectors.

# Behavior of Gas Flow and Characteristics of Atmospheric Pressure Plasma Jet for Bio-Applications

Hiromasa Yamada<sup>1</sup>

<sup>1</sup> *National Institute of Technology, Nagano College  
716 Tokuma, Nagano city, Nagano 381-8550, Japan  
h\_yamada@nagano-nct.ac.jp*

Atmospheric pressure plasma jets (APPJs) are plasmas  $\sim 10^0$  mm in diameter and  $\sim 10^1$  mm in length that are generated at atmospheric pressure using noble gases as the working gas. The APPJ can be easily generated using a low-cost power supply without the constraints of a chamber. It is also possible to generate plasma with a low gas temperature that can be touched by hand, and is being applied to various fields such as hemostasis, cancer treatment, and other medical applications. APPJ generated in a working gas stream generates reactive species, which are important in many bio-applications, by mixing with ambient air and being transported by the working gas stream. In addition, plasma generation has been reported to promote turbulence in the working gas stream (jet stream) <sup>[1]</sup>. Such an effect of plasma generation on the gas flow also affects the plasma generation path, i.e. the plasma size and the generation and transport of reactive species. Therefore, it is important to understand the relationship between the APPJ and the gas flow in order to effectively promote each bio-application by controlling the size of the APPJ and efficiently transporting reactive species.

The effect of plasma generation on the gas flow, such as increased turbulence, is caused by the action of charged particles (ions and electrons) accelerated by an electric field on the neutral particles that make up the gas flow. However, the electric field acting on the charged particles is spatially complex, being formed between the plasma itself, the high-voltage electrodes used to generate the plasma, the surrounding equipment, etc. Therefore, the understanding of the mechanism of the effect of plasma generation on gas flow in APPJ is not fully understood. In this study, we analyzed the effect of the electric field on the working gas flow in the APPJ by placing external electrodes between the generated plasma from above and below and applying an external electric field with a constant direction and magnitude in space and time to the plasma to better understand the behavior of charged particles. The presentation will discuss the results for other conditions and the relationship to plasma properties such as emitting species and temperature.

<sup>[1]</sup> H. Yamada, et al., Jpn. J. Appl. Phys., Vo. 55, No. 1 (2016), pp. 01AB08-1 - 01AB08-5.

## Environmental control for plant growth and preservation using high-voltage pulsed discharges

Katsuyuki Takahashi<sup>1</sup> and Koichi Takaki<sup>1,2</sup>

<sup>1</sup> Faculty of Science and Engineering, Iwate University  
4-3-5, Ueada, Morioka, Iwate, 020-8551, Japan  
ktaka@iwate-u.ac.jp

<sup>2</sup> Agri-Innovation Center, Iwate University  
3-18-8, Ueada, Morioka, Iwate, 020-8550, Japan

Agricultural applications of high-voltage pulsed discharges have been widely investigated and have become one of the most attractive research topics in plasma science [1]. Atmospheric pressure plasma can produce various types of chemical active species, which have various effects on the cell membrane of bacteria, activity of a living plant body and chemical structure of organic compounds.

As a production process of fruits and vegetables, hydroponics, which is the method of growing plants without soil using nutrient solution, has been widely used. In hydroponics, the nutrient solution is re-circulated in a closed system in to reduce the cost and the environmental load. In the system, plant diseases caused by microbial contamination of the artificial nutrient solution rapidly spread in the circulation system and cause serious damage to the entire plant. During the entire period of plant growth, contamination with pathogens can never be excluded, since the pathogens are introduced in the nutrient solution via the irrigation water supply. Therefore, the nutrient solution should be remedied by continuous water treatment system operation during the cultivation period.

In transportation and preservation of fruits and vegetables, it is desired to store several kinds of productions in one place because it can reduce the cost due to the effective utilization of space. In these cases, ethylene ( $C_2H_4$ ) is responsible for the changes in texture, softening and color, depending on how sensitive the plant is to  $C_2H_4$ .  $C_2H_4$  is thought of as an aging hormone in plants. Since ethylene sensitive fruits such as persimmon and the others naturally emit a lot of  $C_2H_4$  to the air such as apple are loaded together in one container, ethylene sensitive fruits should be kept in an extremely low  $C_2H_4$  level during transportation.

In this study, water and gas treatment systems using non-thermal plasmas generated by pulsed high voltages are developed for practical use in hydroponic cultivation as shown in Fig. 1 [2,3] and preservation of fruits and vegetables as shown in Fig. 2 [1]. These system shows high performance for improving the environment of production and preservation of fruits and vegetables.

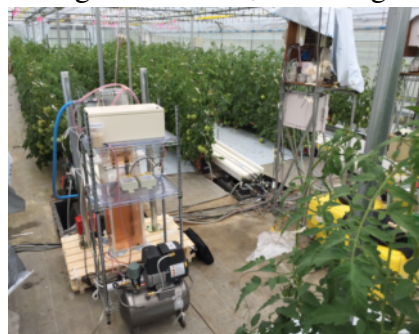


Fig. 1: System for treatment of nutrient used in hydroponics.

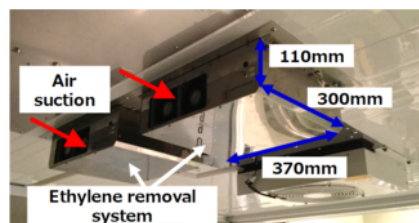


Fig. 2: Ethylene removal system for practical use installed in container.

- [1] K. Takaki, K. Takahashi, D. Hamanaka, R. Yoshida, and T. Uchino, *Jpn. J. Appl. Phys.*, **60**, 010501 (2021),.
- [2] K. Takahashi, Y. Saito, R. Oikawa, T. Okumura, K. Takaki and T. Fujio, *J. Electrostat.*, **91**, 61-69 (2018), 61-69.
- [3] K. Takahashi, S. Kawamura, R. Takada, K. Takaki and T. Fujio, *J. Appl. Phys.*, **129**, 143301 (2021).

# Simultaneous inference of multiple plasma parameter profiles by utilizing transport properties

Takashi Nishizawa

*Research Institute for Applied Mechanics, Kyushu University,  
Kasuga, 816-8580, Japan  
t.nishizawa@riam.kyushu-u.ac.jp*

Numerical techniques for the computation of a posterior distribution ease restrictions on inference models, and multiple plasma parameters can be simultaneously inferred with detailed modeling of uncertainties[1]. In addition, data that depend on multiple parameters in a complex fashion can also be utilized[2]. This contribution reviews the frameworks that further expand the capability of inference by including transport properties in plasmas.

In addition to the smoothness conditions, the particle conservation law given by a transport model provides a prior belief. Specifically, sets of plasma parameter profiles that satisfy the particle conservation law are likely to be true. This information can be utilized as the prior belief within the Bayesian frame. Ref[3] employs a prior probability function that takes large values when the particle source and sink terms are balanced by the divergence of a diffusive particle flux. Through synthetic data analyses, it is shown that one-dimensional profiles of the electron density, electron temperature, and neutrals can be inferred even when only a few line integrated quantities are observable. Furthermore, if local measurements of plasma parameters, e.g. Thomson scattering diagnostic, are available, the diffusion coefficient can be treated as unknown, and estimated together with the other plasma parameters.

The second example[4] considers the measurements of the diffusion coefficient and the convection velocity of impurities in a tokamak plasma. In this case, the profiles of these transport coefficients for given source and sink can be obtained by solving linear equations. By taking advantage of this low computation cost, the transport coefficients can be directly inferred from data without considering the profiles of impurities. As is the case with conventional techniques for impurity transport measurements, this inference problem is ill-conditioned. To address this issue, a non-parametric Bayesian approach is employed. In this framework, all spatial points that represent smooth profiles have their own degrees of freedom. Therefore, all solutions that are consistent with data and prescribed smoothness conditions can be considered. The red solid lines shown in Fig. 1 are the 50% percentiles of those solutions.

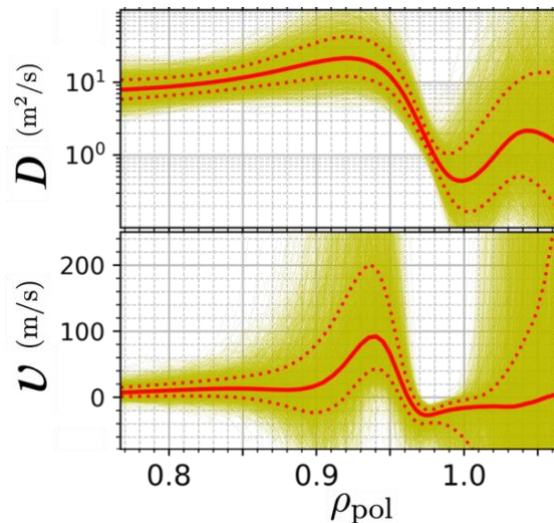


Figure 1. Profiles of the impurity diffusion coefficient (top) and convection velocity (bottom) obtained by the non-parametric inference.

[1] S. Kwak, et.al, Nucl. Fusion, **60**, 046009 (2020).

[2] C. Bowman, et.al., Nucl. Fusion, **62**, 045014 (2020).

[3] T. Nishizawa, et.al., Phys. Plasmas, **28**, 032504 (2021).

[4] T. Nishizawa, et.al, Nucl. Fusion, **62**, 076021 (2022).

# Information Thermodynamics of Plasma Wave Turbulence

Eiichirou Kawamori

*Institute of Space and Plasma Sciences, National Cheng Kung University  
1, Ta-Hsueh Road, 70101 Tainan, Taiwan  
kawamori@isaps.ncku.edu.tw*

Information thermodynamics treats information and thermodynamic functions in the same framework of thermodynamics, enabling to decrease entropy using information (i.e. exchange between thermodynamic entropy and information entropy) without any energy cost. Historically, this idea was initiated by J. C. Maxwell, who considered a gedankenexperiment that a thermodynamic system immersed in a heat bath is measured and manipulated by an external intelligence called Maxwell daemon to decrease the entropy. With appropriate usage of information perpetual heat engines of the second kind can be realized, that is, extraction of work from the heat bath [1].

Turbulence is a highly energy-rich state sustained by steady energy injection. However, the stored energy in turbulence cannot be extracted as work, but rather dissipated as heat because of its highly incoherent property. This is analogous to the prohibition of perpetual heat engines of the second kind referred to as the second law of thermodynamics. However, with the use of information on turbulence and thermodynamics, the extraction of coherent work from turbulence may be possible. This study aims at the verification of the theory of information thermodynamics of plasma wave turbulence employing numerical experiments, demonstration of extraction of coherent work from turbulence, and an analogous perpetual heat plasma engine of the second kind using the theory.

The developed code simulates one-dimensional (1D) wave turbulence and traces the motion and trajectory of a particle immersed in the turbulence. The particle motion is governed by the electrostatic potential of the wave turbulence.

Wave turbulence applied this time is Kuramoto-Sivashinsky (K-S) turbulence with a periodic boundary condition. We manipulate the phase of the wave turbulence according to a protocol based on information about the particle in the phase space. Figure 1 shows the time evolution of kinetic (red), potential (blue), and total (black) energies of the particle in the K-S turbulence for the cases of (left) no feedback control application and (right) the feedback control application using the measured information about the particle, respectively. The kinetic energy is saturated at  $\sim 3.0$  and the particle shows a kind of Brownian motion after  $t \sim 400$  when no feedback control is applied (left). On the other hand, when the feedback control is applied, the kinetic energy of the particle is monotonically increased in time as shown by the black in Fig. 1 (right), indicating an extraction of coherent work from the turbulence.

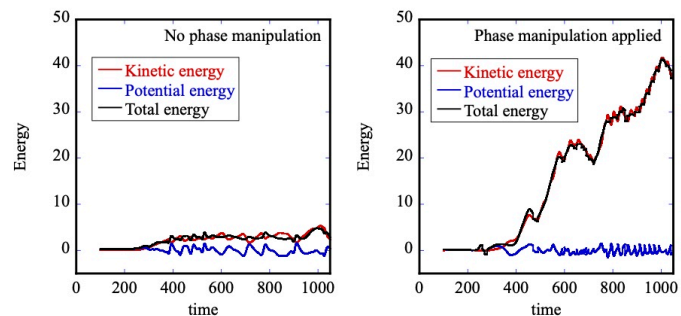


Fig. 1. Time evolution of kinetic (red), potential (blue), and total (black) energies of the particle in the K-S turbulence for the cases of (left) no feedback control application and (right) the feedback control application, respectively.

[1] Juan M. R. Parrondo, et al., *Nature Physics* **11**, p.p. 131–139 (2015).

## On the mechanism of high-speed SiO<sub>2</sub> etching using hydrogen fluoride-contained plasmas at cryogenic temperature

Shih-Nan Hsiao<sup>1</sup>, Makoto Sekine<sup>1</sup>, Nikolay Britun<sup>1</sup>, Michael Kin-Ting Mo<sup>1</sup>, Yusuke Imai<sup>1</sup>, Takayoshi Tsusumi<sup>1</sup>, Kenji Ishikawa<sup>1</sup>, Yuki Iijima<sup>2</sup>, Masahiko Yokoi<sup>2</sup>, Ryutaro Suda<sup>2</sup>, Yoshihide Kihara<sup>2</sup> and Masaru Hori<sup>1</sup>

<sup>1</sup> Center for Low-temperature Plasma Sciences  
Furo, Chikusa, Nagoya 464-8603, Japan

<sup>2</sup> Tokyo Electron Miyagi Ltd.  
Techno-Hills, Taiwa-cho, Kurokawa-gun, Miyagi, 981-3629, Japan  
(Corresponding authors: Shih-Nan Hsiao, e-mail: hsiao@plasma.engg.nagoya-u.ac.jp)

Plasma etching is a key process in the manufacturing of semiconductor integrated circuit devices. Conventionally, the reactive ion etching (RIE) processes rely on the formation of radicals or ions which are transported or accelerated by plasma sheath to react with the surface being etched. Recently the low-temperature or cryogenic temperature etching has drawn much attentions for the structure with high aspect ratio contact, owing to its unique feature that the radicals and etchants can physisorbed on the surface. However, the mystery for the dramatic enhancement of SiO<sub>2</sub> using CHF<sub>3</sub> plasma at cryogenic temperature still remains unsolved [1]. In this work, the dependence of etch rate (ER) of SiO<sub>2</sub> on substrate temperature ( $T_s$ ) using CF<sub>4</sub> plasma mixed with H<sub>2</sub> additive (H<sub>2</sub> percentage ranged from 30 to 70 %) was investigated. A home-made reactor equipped with a dual frequency capacitively coupled plasma was used. The  $T_s$  was controlled by circulant cooling system from 20 to -60 °C. An *in situ* spectroscopic ellipsometry (SE) and Fourier Transformation infrared spectroscopy (FTIR) was implemented to the reactor to provide real time etching data and surface structure information. The neutral HF density and F atomic density was measured by FTIR and actinometry based on optical emission spectroscopy. Figure 1 illustrates the dependence of the SiO<sub>2</sub> ER etched at 20 and -60 °C on H<sub>2</sub> content in the CF<sub>4</sub>/H<sub>2</sub> plasmas. For the samples etched at 20°C, the ER decreased monotonically from 2.6 to 1.3 nm/s as the H<sub>2</sub> content was increased from 20 to 70 %, which is attributed to the well-known scavenging reaction of H atoms with F [2]. Due to the reactions, the concentrations of the main etchants for SiO<sub>2</sub>, such as F and CF<sub>x</sub> radicals/ions decrease with increasing H concentrations, which results in the decrease of ER. On the contrary, when the SiO<sub>2</sub> film was etched at -60 °C, the ER increased and reached to the maximum of approximately 3.4 nm/s as H<sub>2</sub> concentration increased to 33 %. Based on the results of HF and F atomic density, the trend in ER at -60 °C depends on the HF molecules formed by the plasmas rather than the F radicals or other etchants like CF<sub>x</sub> ions. The *in situ* FTIR shows that the absorption of H<sub>2</sub>O and HF molecules on the SiO<sub>2</sub> surface after plasma etching at -60 °C. Based on the results, an etching mechanism, so-called pseudo-wet plasma etching, based on plasma-assisted reaction between SiO<sub>2</sub>, HF and H<sub>2</sub>O was proposed.

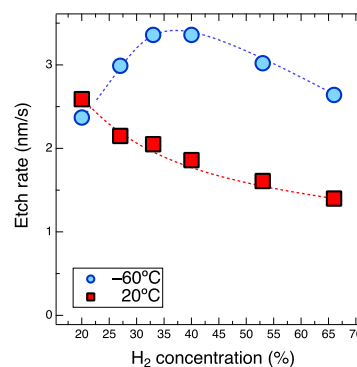


Fig. 1 Dependence of etch rate of SiO<sub>2</sub> etched by CF<sub>4</sub>/H<sub>2</sub> plasma at  $T_s = 20$  and -60 °C.

- [1] T. Ohiwa et al., Jpn. J. Appl. Phys., **31**, 405 (1992).  
[2] D. C. Marra, et al., J. Vac. Sci. Tech. A **15**, 2508 (1997).

# Feasibility of applying non-thermal plasma to the degradation of pharmaceuticals in real medical wastewater

Wei-Cheng Lin<sup>1</sup>, Chih-Yu Ko<sup>1</sup>, Jang-Hsing Hsieh<sup>2</sup> and Wen-Hui Kuan<sup>1\*</sup>

<sup>1</sup> Department of Safety, Health and Environmental Engineering, Ming Chi University of Technology, Taishan, New Taipei, Taiwan

\*Corresponding author. whkuan@mail.mcut.edu.tw

<sup>2</sup> Center for Plasma and Thin Film Technologies, Ming Chi University of Technology, Taishan, New Taipei, Taiwan

Due to the limitations of traditional wastewater treatment processes in effectively degrading pharmaceuticals and personal care products (PPCPs), these pollutants have been identified to be discharged into environmental water bodies from urban wastewater treatment. PPCPs not only induce antibiotic resistance in bacteria in natural ecosystems but also have the potential to promote the formation of superbugs. Although the concentrations of these compounds or their disinfection byproducts in the environment are not high, long-term exposure may lead to biological mutations.

In this study, a non-thermal plasma system reactor using dielectric barrier discharge (DBD) was developed for wastewater treatment to degrade various pharmaceuticals present in medical wastewater. The concentrations of reactive species O<sub>3</sub>, H<sub>2</sub>O<sub>2</sub>, and OH radicals and the degradation of target pollutants (amoxicillin) were investigated in terms of the reactor layout and the water quality conditions. Real wastewater discharged from a hospital with 1500 beds in north of Taiwan were sampled and subjected into the developed non-plasma reactor. The results showed that the removal efficiency reached 90% or above at five different frequencies, with energy efficiency ranging from 0.38 to 0.42 gkW<sup>-1</sup>h<sup>-1</sup>, indicating the effectiveness of the module system in amoxicillin degradation. In the treatment of actual hospital wastewater with the spike of standard samples, the removal efficiency also reached 82%-93%, demonstrating the feasibility of plasma in actual hospital wastewater treatment.



## **Novel plasma source for atomic scale processing**

JY Park, MS Kim, and ChinWook Chung

<sup>1</sup> *Plasma electronics Lab., Dept. of Electrical Engineering, Hanyang University,  
222, Wangsimni-ro, Seongdong-gu, Seoul, 04763, Korea  
joykang@hanyang.ac.kr*

Semiconductor processing has been advancing from the nano to the atomic scale. For atomic-scale processing, the plasma source need to be precisely controlled to minimize damage, such as UV radiation damage, ion-induced damage, and charge accumulation damage. In this presentation, we will introduce an Ultra Low Electron Temperature (ULET) plasma ( $T_e < 0.5$  eV) as a novel plasma source enabling us to perform damage-free plasma processing. We will also explain how to produce the ULET plasma. It is demonstrated that charge accumulation even in a patten with high aspect ratio is almost eliminated, and graphene remains undamaged in the ULET plasma, while it is heavily damaged in conventional plasma processes. The ULET plasma shows great promise for applications in atomic-scale plasma processing.

## Yttrium-based plasma etching resistant coating obtained by gas flow sputter deposition

Ping-Yen Hsieh<sup>1,2</sup>, Tzu-Chun Lin<sup>1</sup>, Ying-Hung Chen<sup>1,2</sup> and Ju-Liang He<sup>1,2</sup>

<sup>1</sup> *Department of Materials Science and Engineering, Feng Chia University  
No. 100, Wenhwa Road, Seatwen District, Taichung City 40724, Taiwan.  
pyhsieh@fcu.edu.tw*

<sup>2</sup> *Institute of Plasma, Feng Chia University  
No. 100, Wenhwa Road, Seatwen District, Taichung City 40724, Taiwan.*

In the semiconductor plasma etching process, the plasma gas not only reacts with silicon wafers for circuit patterning but also reacts with process equipment, including pipelines, shower heads, chambers, and all components in contact with plasma. This results in device contamination, reduced service life of parts, and failure of IC devices, ultimately affecting the etching efficiency, wafer performance, and production yield. Among other plasma etching resistant materials, yttrium oxide ( $Y_2O_3$ ) is a promising material for providing oxygen and/or fluorocarbon plasma etching resistance. By taking advantage of high plasma density, high throwing power, and high deposition rate, this study aims to use gas flow sputtering (GFS) technique to deposit yttrium-based coating,  $Y_2O_3$ , on silicon substrate. The anti-plasma etching ability of the obtained  $Y_2O_3$  coatings in  $CH_4/O_2$  mixture was further evaluated.

Experimental results show that, without additional heating, the obtained GFS- $Y_2O_3$  coating possesses a crystalline dense columnar structure with a (111) preferred orientation under an oxygen-rich atmosphere. The deposition rate for GFS- $Y_2O_3$  coatings can reach  $3.0 \mu\text{m/h}$ , which is substantially higher than those many other sputtering processes. Based on the  $CH_4/O_2$  plasma etching test results, the GFS prepared  $Y_2O_3$  coatings exhibit low plasma etching rate than bare Si wafer, demonstrating their excellent plasma resistance. These results indicate the potential of the GFS prepared yttrium-based coating as a novel plasma etching resistance material for surface modification on semiconductor process components.

Posters

October 17

(Tuesday)

## Design of a Thomson scattering system for atmospheric plasma sources

Y.-G. Kim<sup>1</sup> and S. Park<sup>1</sup>

<sup>1</sup> *Institute of Plasma Technology, Korea Institute of Fusion Energy,  
Gunsan 54004 Korea  
ykim@kfe.re.kr*

In the plasma chemistry and biomedical field, reactive oxygen and nitrogen species (RONS), including oxygen atoms, ozone, hydroxyl radicals, nitric oxide, and nitrogen dioxide, play an important role because of their high reactivity [1, 2]. Cold atmospheric plasma is known to produce a wide range of RONS. Numerous techniques, such as corona discharge, dielectric barrier discharge (DBD), radio-frequency discharge, and microwave discharge, have been developed and explored to generate plasma under atmospheric pressure and room temperature condition. However, study on the relationship between “plasma parameters” and “radical generation” is relatively rare possibly due to the difficulty of direct quantification of the plasma parameters such as velocity distribution function, temperature, or density.

Recently, the Korea Institute of Fusion Energy (KFE) has embarked on the development of a complex plasma diagnostic system aimed at enabling quantitative research on the production of radicals and metastable species, along with their relationship with electron kinetics. It will include spectroscopic systems, including laser-induced fluorescence (LIF), tunable diode laser absorption spectroscopy (TDLAS), cavity ring-down spectroscopy (CRDS), and Thomson scattering (TS). Among the various methods, the TS diagnostic system takes precedence as the primary focus of development, as it is a key diagnostic for plasma measurement.

The TS system is widely recognized as a powerful diagnostic method for measuring the absolute electron temperature and the density within a given scattering volume [3-6]. However, owing to the extremely small cross section of Thomson scattering ( $6.65 \times 10^{-29} \text{ m}^2$ ), the TS system requires a stable laser source, careful alignment, efficient optical components, and highly sensitive detectors to ensure accurate measurement. Furthermore, care must be taken on high background pressure, low electron temperature, and density. Foremost among these concerns is the constraint imposed by air breakdown and multi-photon ionization, which restricts the maximum permissible laser energy to approximately 20 mJ [7]. For successful measurement of TS signal with a favorable signal-to-noise ratio, the proposed approach involves employing an emCCD, a combination of electron multiplier charge-coupled device (emCCD) and image intensifier (I-) while accumulating a number of scattered signals over a long period or laser repetition.

- [1] A. G. Volkov et al., *Journal of the Royal Society Interface*, **16**, 20180713 (2019).
- [2] D. B. Graves and G. Bauer, *Key Roles of Reactive Oxygen and Nitrogen Species*. In: H.-R. Metelmann, et al. (eds) *Comprehensive Clinical Plasma Medicine*, Springer, Cham, 11 Jan 2018.
- [3] M. J. van de Sande, *Laser scattering on low temperature plasmas: high resolution and stray light rejection*, PhD Thesis, Eindhoven University of Technology (2002)
- [4] H. Yoshida et al., *Japanese Journal of Applied Physics*, **42**, 439 (2003)
- [5] J. H. Lee et al., *Review of Scientific Instruments*, **81**, 10D528 (2010)
- [6] A. F. H. van Gessel et al., *Plasma Sources Science and Technology*, **21**, 015003 (2012)
- [7] Y. Sonoda et al., *The Japan Society of Plasma Science and Nuclear Fusion Research*, **8**, 696 (2009).

## Irradiation experiment of new type of divertor heat removal component fabricated by AMSB to LHD divertor plasma

Masayuki Tokitani<sup>1</sup>, Yukinori Hamaji<sup>1</sup>, Yutaka Hiraoka<sup>2</sup>, Yuki Hayashi<sup>1</sup>, Suguru Masuzaki<sup>1</sup>, Hiroyuki Noto<sup>1</sup>, Tatsuya Tsuneyoshi<sup>3</sup>, Yoshiyuki Tsuji<sup>3</sup>, Gen Motojima<sup>1</sup>, Hiromi Hayashi<sup>1</sup>, Takanori Murase<sup>1</sup>, Takeo Muroga<sup>1</sup> and Tomohiro Morisaki<sup>1</sup>

<sup>1</sup> National Institute for Fusion Science, Toki, Gifu 509-5292, Japan

<sup>2</sup> Okayama University of Science, Okayama 700-0005, Japan

<sup>3</sup> Nagoya University, Furo-cho, Chikusa, Nagoya 464-8603, Japan

The novel method “Advanced Multi-Step Brazing (AMSB)” has been developed to fabricate a new type divertor heat removal component in the National Institute for Fusion Science (NIFS), in which the fabricated new component showed an excellent heat removal capability with  $\sim 30$  MW/m<sup>2</sup>. As a next step, the component was exposed to repetitive heat loading in the Large Helical Device (LHD) to demonstrate a durability in the large sized plasma confinement device.

The principle of the AMSB is a repetitive application of the advanced brazing technique (ABT). The ABT was originally developed to braze tungsten (W) to ODS-Cu (GlidCop<sup>®</sup>) with the BNi-6 (Ni-11%P) filler material, in our previous work [1]. Later we developed the leak tightness joint procedures of GlidCop<sup>®</sup> (GlidCop<sup>®</sup>/GlidCop<sup>®</sup>), and stainless steel (SUS) and GlidCop<sup>®</sup> (SUS/ GlidCop<sup>®</sup>) accompanied with high enough joint strength to be comparable with bulk GlidCop<sup>®</sup>. One of the special feature of in the ABT joints of GlidCop<sup>®</sup>/GlidCop<sup>®</sup> and the SUS/GlidCop<sup>®</sup> is strong tolerance against the repetitive brazing heat-cycle, i.e., the repetitive application of the ABT can be applied for fabricating a single heat removal component.

“New type of divertor heat removal component“ with the rectangle-shaped fluid flow path and the V-shaped staggered rib structure were successfully produced by the AMSB; therein a pre-processed rectangle-shaped cooling flow path channel was sealed with a GlidCop<sup>®</sup> and SUS lid structure with leak-tight conditions. the new component was installed in the divertor strike position of the Large Helical Device (LHD) as shown in Fig. 1, and exposed to neutral beam injection–heated plasma discharges with 1180 shots ( $\sim 8000$  s) in total. After the exposure, several microstructural analyses were conducted by using a dual-beam type of focused-ion beam/scanning electron microscopy (FIB-SEM) device on the W armor plate.

An extremely high heat removal response in the component was demonstrated through the quick increase and decrease of the temperature of the W plate located on the divertor strike point during discharges. Though submillimeter scale damages, such as unipolar arc trails and microscale cracks, were identified on the W surface, such a high heat removal response did not show any sign of degradation during the 1180 shots ( $\sim 8000$  s) of plasma discharges.

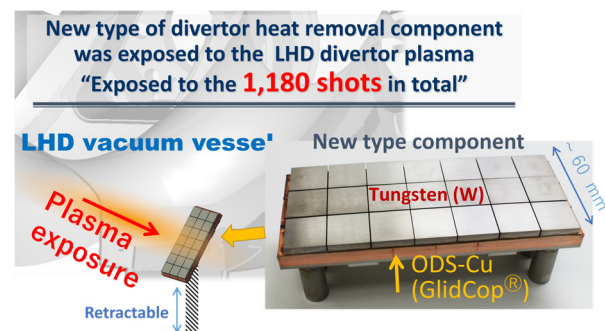


Fig. 1 Schematic figure for an exposure experiment of new type of divertor heat removal component to a LHD divertor plasma. The component was installed in the divertor leg position in the LHD and exposed to plasma discharges with 1180 shots ( $\sim 8000$  s) in total.

## Theoretical issue of the electron cyclotron emission with decay process in a waveguide

Yuki Goto<sup>1</sup> and Tomio Petrosky<sup>2,3</sup>

<sup>1</sup>*National Institute for Fusion Science, National Institute of Natural Sciences  
322-6, Oroshi-cho, Toki 509-5292, Japan  
goto.yuki@nifs.ac.jp*

<sup>2</sup>*Center for Complex Quantum Systems, The University of Texas at Austin,  
2515 Speedway, Stop C1609, Austin 78705, USA*

<sup>3</sup>*Institute of Industrial Science, The University of Tokyo,  
5-1-5, Kashiwanoha, Kashiwa 277-8574, Japan*

Electron cyclotron motion and its emission are observed in various places such as the Earth's magnetosphere represented by auroras, neutron stars in space, free electrons within metals, and magnetic confinement fusion plasmas, and are playing a crucial role in astrophysics, condensed matter physics, and fusion science. As is well known, cyclotron motion is a typical example of the classical radiation damping. And phenomenological Lorentz-Abraham (LA) equation has established in classical mechanics to deal with this phenomenon of radiation damping in classical mechanics. However, this classical radiation damping has not been solved yet. Because the LA equation includes a third-order time derivative term of the electron's position in the equation of motion, which causes difficulty in finding a physically meaningful solution.

Thus, we treat this issue by using classical Friedrichs model without perturbation analysis. The Hamiltonian known as the Friedrichs model in quantum mechanics reveals that the phenomenon of decay of a harmonic oscillator while emitting photons can be derived as an exact solution of the Heisenberg equation in Fock space [1]. In our approach, by "classicalization" the conclusions of Friedrichs's quantum theory, we analyzed the electron cyclotron emission by using classical Friedrichs model in waveguide [2]. In this talk, we will present the essence of classical radiation dumping problem and show how to solve the difficulty for deriving a decay solution with mathematically consistently that violates the time symmetry from the fundamental equations of physics that originally has time symmetry.

[1] K. Friedrichs, *Commun. Pure Appl. Math.*, **1**, 361 (1948).

[2] T. Petrosky, C. O. Ting, and S. Garmon, *Phys. Rev. Lett.*, **94**, 043601 (2005).

## Simulation analysis of lithium transport in the peripheral plasma during impurity powder injection in the Large Helical Device

Mamoru Shoji<sup>1,2</sup>, Gakushi Kawamura<sup>1,2</sup>, Tomoko Kawate<sup>1,2</sup>, Suguru Masuzaki<sup>1,2</sup>, Naoko Ashikawa<sup>1,2</sup>, Robert Lunsford<sup>3</sup>, Erik P. Gilson<sup>3</sup>, Federico Nespoli<sup>3</sup>, and Novimir Pablant<sup>3</sup>

<sup>1</sup> National Institutes of Natural Sciences, National Institute for Fusion Science  
322-6 Oroshi-cho, Toki, Gifu 509-5292, Japan  
shoji.mamoru@nifs.ac.jp

<sup>2</sup> The Graduate University for Advanced Studies, SOKENDAI, Shonan Village, Hayama, Kanagawa 240-0193, Japan

<sup>3</sup> Princeton Plasma Physics Laboratory, 100 Stellarator Road, NJ 08540, United States of America

Multi-species impurity powder dropper (IPD) [1] has contributed to the improvement of the ion energy confinement in the plasma in the Large Helical Device (LHD) [2]. As another promising usage of the IPD, lithium coating on the surface of the in-vessel components was tried by lithium powder injection in the last experimental campaign for the first time. The purpose of the lithium coating was to reduce the recycled particles on the plasma-facing components and to sustain them during long plasma discharges. A stereoscopic fast-framing camera has been installed in an upper port close to the IPD for monitoring the trajectories of dropped lithium powders and the ablation positions in the peripheral plasma. Figure 1 shows an image of the ablation of a dropped lithium powder (850  $\mu\text{m}$  in diameter) observed with the camera. It indicates an oblique bright line along a magnetic field line, which is initiated from the ablation position of the lithium powder. The change of the ablation positions toward the outboard side of the torus was observed with the increase in the plasma density.

The analysis of the lithium powder trajectories in the peripheral plasma was performed using a three-dimensional edge plasma simulation code (EMC3-EIRENE) [3] coupled with a dust transport simulation code (DUSTT) [4, 5] in a full-torus model for LHD [6]. It has successfully reproduced the change of the ablation position of the lithium powder by the deflection of the trajectories due to the effect of the plasma flow in an upper divertor leg. The simulation also calculates the three-dimensional density profile of lithium ions in the peripheral plasma, providing the line-integrated intensity profiles of lithium-ion emission along the line of sight of spectrometers. In the forum, the lithium-ion transport in the plasma is investigated by comparing the simulations with the spectroscopic observations.

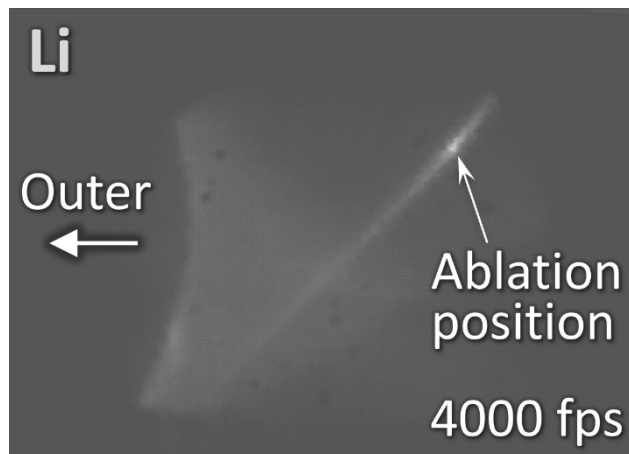


Fig. 1: An image of the ablation of a lithium powder injected by the IPD for a high plasma density ( $\bar{n}_e \sim 6 \times 10^{19} \text{ m}^{-3}$ ).

- [1] A. Nagy et al., Rev. Sci. Instrum., **89**, 10K121 (2018).
- [2] F. Nespoli et al., Nat. Phys., **18**, 350 (2022).
- [3] Y. Feng et al., Plasma Phys. Control. Fusion, **44**, 611 (2002).
- [4] A. Y. Pigarov et al., Physics of Plasmas, **12**, 122508 (2005).
- [5] R. Smirnov et al., Plasma Phys. Control Fusion **49**, 347 (2007).
- [6] M. Shoji et al., Contrib. Plasma Phys., **60**, e201900101 (2020).

# Molecular Dynamics Simulation for Elucidation of Vacancy Coalescence in Tungsten Crystal

Sotaro Tsuru<sup>1</sup>, Hiroaki Nakamura<sup>1,2</sup>, Yuki Goto<sup>2</sup>, Miyuki Yajima<sup>2</sup>,  
Seiki Saito<sup>3</sup>, and Shunsuke Usami<sup>2</sup>

<sup>1</sup> School of Engineering, Nagoya University, Furo-cho, Chikusa-ku, Nagoya 464-8603, Japan  
tsuru.sohtaro@nifs.ac.jp

<sup>2</sup> National Institute for Fusion Science, National Institute of Natural Sciences 322-6, Oroshi-cho, Toki 509-5292, Japan

<sup>3</sup> Graduate School of Science and Engineering, Yamagata University, 4-3-16, Jonan, Yonezawa, 992-8510, Japan

In a fusion reactor environment, tungsten, which is used as the plasma-facing material, is irradiated with neutrons and high-energy hydrogen isotopes that result from the D-T fusion reaction. This irradiation leads to the formation of defects known as vacancies in the tungsten. In the previous research conducted by Yajima *et al.*, phenomenon of vacancy coalescence was discovered experimentally [1]. The report indicates that vacancies tend to coalesce more readily when hydrogen atoms are contained in the vacancies compared to when they are not. In order to understand the atomic-level effect of hydrogen atoms on vacancy coalescence, we analyzed the behavior of vacancies formed in tungsten using the molecular dynamics simulation by LAMMPS [2].

As a first attempt of understanding the vacancy behavior, the case in which a single vacancy exists in a tungsten crystal was conducted [3]. In this study, we set two vacancies in a tungsten crystal and analyze the interaction between the vacancies in detail. Figure 1 shows the simulation model. In order to elucidate the effect of hydrogen contained in the vacancies on the interaction between the vacancies, simulations are performed with different numbers of hydrogen in vacancies. As the interaction potential between tungsten and hydrogen, we use 2014-Bonny-G-Grigorev-P-Terentyev-D--W-H-He-EAM1 [4]. Our simulations show that the tungsten atoms between the vacancies migrate, and the two vacancies coalesce to form a single large vacancy. In this presentation, we will discuss the results of our simulations in detail.

*Acknowledgment:* The computation was performed using Research Center for Computational Science, Okazaki, Japan (Project: 22-IMS-C104) and Plasma Simulator of NIFS. The research was supported by Japan Society for the Promotion of Science (Grant Nos. JP19K14692, JP22H05131, JP23H04609, JP22K18272, JP23K03362), by the NINS program of Promoting Research by Networking among Institutions, by the NIFS Collaborative Research Programs (NIFS22KIIP003, NIFS22KIGS002, NIFS22KISS021) and by the ExCELLS Special Collaboration Program of Exploratory Research Center on Life and Living Systems.

[1] M. Yajima *et al.*, Phys. Scr., **96**, 4042 (2021).

[2] Aidan P. Thompson *et al.*, Comp. Phys. Comm., **271**, 108171 (2022)

[3] H. Nakamura *et al.*, J. Adv. Simul. Sci. Eng., **10**, 132(2023).

[4] G. Bonny *et al.*, J. Phys. Condens. Matter, **26(48)**, 485001(2014).

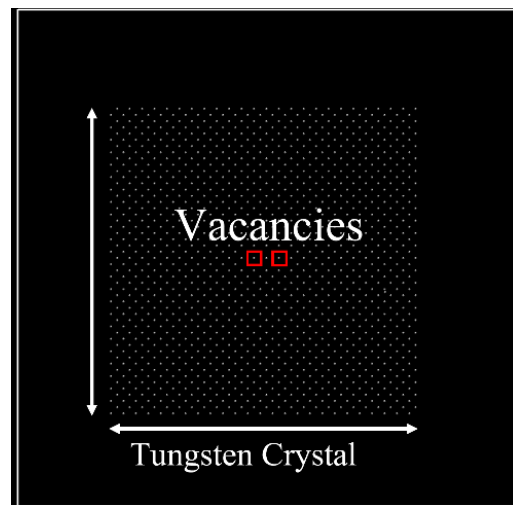


Fig. 1: Arrangement of vacancies in tungsten crystal



## Nanopatterning of Si by low-energy He plasma irradiation

Zhe Liu<sup>1</sup>, Long Li<sup>1</sup>, Zeshi Gao<sup>1</sup>, Ze Chen<sup>1</sup>, Chao Yin<sup>1</sup>, Shifeng Mao<sup>1</sup>, Shin Kajita<sup>2</sup>, Noriyasu Ohno<sup>3</sup>, Minyou Ye<sup>1\*</sup>

<sup>1</sup>*School of Nuclear Sciences and Technology, University of Science and Technology of China, Hefei, Anhui 230026, People's Republic of China*

*\*e-mail: yemy@ustc.edu.cn*

<sup>2</sup>*Graduate School of Frontier Sciences, The University of Tokyo, Chiba 277-8561, Japan*

<sup>3</sup>*Graduate School of Engineering, Nagoya University, Nagoya 464-8603, Japan*

The phenomenon of self-organized nanopatterning on material surfaces, particularly Si, through ion beam irradiation (IBI) has garnered considerable attention in recent decades. Significantly noteworthy progress has been made in elucidating the underlying mechanisms governing ion-material interactions, coupled with notable advancements in experimental results. These outcomes affirm the versatility, expeditiousness, and cost-effectiveness of the IBI method as a bottom-up approach for achieving surface nanopatterning. This technique exhibits promising potential for applications across various domains [1,2].

However, a legitimate constraint emerges concerning the ion-substrate pairing: scenarios arise where no structures manifest when the ion possesses a lower mass than the substrate [3]. This phenomenon substantiates the inadequacy of He and Ne ion beams for Si nanopatterning, contributing to the limited extent of related investigations. Nevertheless, a well-established realization within the past decade reveals that low-energy He plasma irradiation can induce various nanostructure formations on diverse metals and semiconductors [4]. This finding contradicts preceding knowledge, presenting a paradox.

In this study, we experimentally investigate Si substrates exposed to low-energy ( $< 100$  eV) and high-flux ( $\sim 10^{22}$  m<sup>-2</sup>s<sup>-1</sup>) He plasma irradiation under normal incidence. By rigorously maintaining contamination control measures, the irradiated Si surface reveals distinctive mountain-like nanostructures with well-defined facets and grooves extending along mutually perpendicular  $\langle 110 \rangle$  directions. In cases involving pre-deposited metal impurities, notably Ta, which previously exhibited no impact on nanostructure growth during Ar ion beam irradiation trials, a densely packed arrangement of nanocones emerges on the irradiated Si surface. SEM cross-sectional images distinctly illustrate the presence of He bubbles, oriented nearly perpendicular to the irradiated surface. These subsurface He bubbles introduce a novel instability, fostering nanostructure formation on the Si surface, even under normal incidence conditions. This finding necessitates a reassessment of the nanopatterning effects of low-energy He ion irradiation on materials. Furthermore, it calls for a comprehensive investigation into the influence exerted by He bubble formation on the established BH theory and the CV effect in surface evolution.

[1] S. A. Norris, *Appl. Phys. Rev.*, 6, 1 (2019).

[2] L. Vázquez, *J. Phys. Condens. Matter*, 34, 33 (2022).

[3] B. Rauschenbach, *Low-Energy Ion Irradiation of Materials* (Springer Nature, 2022).

[4] S. Kajita, *J. Appl. Phys.*, 132,18 (2022)..

## Growth of micro-pillars on tungsten by helium plasma exposure with impurity gases

Rongshi Zhang<sup>1</sup>, Shin Kajita<sup>2</sup>, Hirohiko Tanaka<sup>3</sup>, Yuta Yamamoto<sup>3</sup> and Noriyasu Ohno<sup>1</sup>

<sup>1</sup> Graduate School of Engineering, Nagoya University  
Furo, Chikusa, Nagoya 464-8603, Japan  
[zhang.rongshi.r1@s.mail.nagoya-u.ac.jp](mailto:zhang.rongshi.r1@s.mail.nagoya-u.ac.jp)

<sup>2</sup> Graduate School of Frontier Sciences, The University of Tokyo, Japan,  
5-1-5 Kashiwanoha, Kashiwa, Chiba, 277-8561, Japan

<sup>3</sup> Institute of Materials and Systems for Sustainability, Nagoya University,  
Furo, Chikusa, Nagoya 464-8603, Japan

Plasma-material interactions have been noticed and investigated for a long time. The interaction between helium (He) and tungsten (W) leads to many morphological changes on W, and one of the most well-known morphology changes is the fuzzy nanostructure [1]. In recently years, a cone-like structure called nanotendrils bundles (NTB) was found to be formed on W by He plasma exposure with additional impurity gases such as neon (Ne), nitrogen (N<sub>2</sub>) and argon (Ar) [2]. Both of the fuzz and NTB enhance the field emission of W, which leads to a possibility of arcing and enhancement of erosion on the divertor plate [3, 4]. Thus, the morphology changes occurring on W are a concern for the fusion reactor.

In this research, W plates were exposed by He plasma with Ne, N<sub>2</sub>, or Ar in linear plasma device NAGDIS-II. The incident ion energy was controlled to be 150 – 200 eV and the partial gas pressure of impurity gas was in a range of 3% - 20%. During the plasma exposure, the surface temperature of the sample was kept to be ~ 1550 K, which was measured by an infrared pyrometer (~1.6 μm).

After the plasma exposure, the morphological change of W surface was confirmed by scanning electron microscopy (SEM). When N<sub>2</sub> impurity was added, a micro-sized pillar-like structure was formed on W with a height of several μm as shown in Fig. 1. When the Ar impurity gas was added, the pillars grown higher to several tens μm. Thus, the type of impurity gas affects the growth of micro-pillars.

The field emission property of micro-pillars was measured in a vacuum chamber. For the sample exposed by He-N<sub>2</sub> mixed plasma, the field emission current from the sample was lower than 1 μA at 2000 V/mm. On the other hand, for the sample exposed by He-Ar mixed plasma, the field emission current became ~ 100 μA at ~ 2500 V/mm, which is a similar value to that of NTBs [5]. It should be investigated whether these micro-pillars can trigger an arcing in a nuclear fusion reactor.

[1] S. Takamura et al., Plasma Fusion Res. **1**, 051 (2006).

[2] D. Hwangbo et al., Nucl. Fusion **58**, 096022 (2018).

[3] D. Sinelnikov et al., IEEE Trans. Plasma Sci. **47**, 5186-5190 (2019).

[4] R. Zhang et al., Plasma Fusion Res. **16**, 2405069 (2021).

[5] R. Zhang et al., Mater. Res. Express **10**, 054002 (2023).

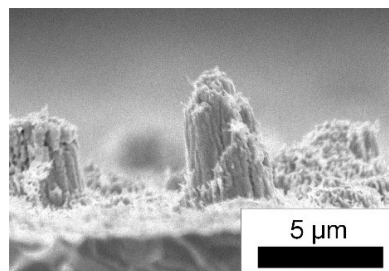


Fig. 1: SEM micrograph of micro-pillars which were formed by He-N<sub>2</sub> mixed plasma

## Surface modification of ZrC dispersion-strengthened W under low energy He plasma irradiation

Long Li<sup>1</sup>, Zhe Liu<sup>1</sup>, Ze Chen<sup>1</sup>, Chao Yin<sup>1</sup>, Shifeng Mao<sup>1</sup>, Xuebang Wu<sup>2</sup>,  
Noriyasu Ohno<sup>3</sup>, Minyou Ye<sup>1,\*</sup>

<sup>1</sup>*School of Nuclear Sciences and Technology, University of Science and Technology of China,  
Hefei, Anhui 230026, People's Republic of China*

<sup>2</sup>*Key Laboratory of Materials Physics, Institute of Solid State Physics, Chinese Academy of Sciences,  
Hefei, Anhui 230031, People's Republic of China*

<sup>3</sup>*Graduate School of Engineering, Nagoya University, Nagoya 464-8603, Japan*

\*e-mail: yemy@ustc.edu.cn

Tungsten (W) is considered as a candidate for plasma-facing materials (PFMs) in fusion devices. However, the brittleness, poor machinability, and low strength at high temperature limit its performance. To resolve these problems, various W with enhanced mechanical properties have been developed over recent decades. ZrC dispersion-strengthened W exhibits high strength/ductility, low ductile-to-brittle transition temperature, and excellent thermal shock resistance, making it a promising candidate PFM for future fusion devices [1]. A recent study of irradiation effect on W-0.5 wt% ZrC using low energy He plasma will be presented.

The W-0.5 wt% ZrC plates were exposed to He plasma with low energy ( $< 100$  eV) at different irradiation fluences up to ( $6 \times 10^{24}$ - $2 \times 10^{26}$  He·m<sup>-2</sup>) in CLIPS (Compact Linear Plasma-Surface interaction device). At 1190 K, the typical fuzz nanostructures were observed on the W matrix. Moreover, the fuzz showed comparable thickness and structure features of pure W, which suggested that the addition of particles did not affect its resistance to high fluence He irradiation at high temperature. While, the sputtering process dominated the behavior of particles. Under  $6 \times 10^{24}$  He·m<sup>-2</sup>, only nanopores appeared on the sub-surface. With the fluence increasing to  $5 \times 10^{25}$  He·m<sup>-2</sup>, the surface was relatively uneven and further eroded, forming larger holes and stalagmitic structures. W was enriched on the top of stalagmitic structures, due to the subthreshold sputtering under He irradiation. With the fluence increasing to  $2 \times 10^{26}$  He·m<sup>-2</sup>, the particles disappeared. In addition, near the W-particle interface, unique layered nanotendrils formed. The inner W-riched skeleton and outer Zr-riched layer indicated that the layered nanotendrils might result from fuzz extension combined with particles sputtering and redeposition. The detail results will be presented in this conference.

[1] Xie, Z.M., et al., Extraordinary high ductility/strength of the interface designed bulk W-ZrC alloy plate at relatively low temperature. *Sci Rep*, 2015. 5: p. 16014.

## Probabilistic modeling of impurity transport based on the drift-kinetic equation

Ryutaro Kanno<sup>1,2</sup>, Gakushi Kawamura<sup>1,2</sup>, Seikichi Matsuoka<sup>1,2</sup>,  
Masanori Nunami<sup>1,3</sup> and Shinsuke Satake<sup>1,2</sup>

<sup>1</sup> National Institute for Fusion Science, Toki 509-5292, Japan  
kanno@nifs.ac.jp

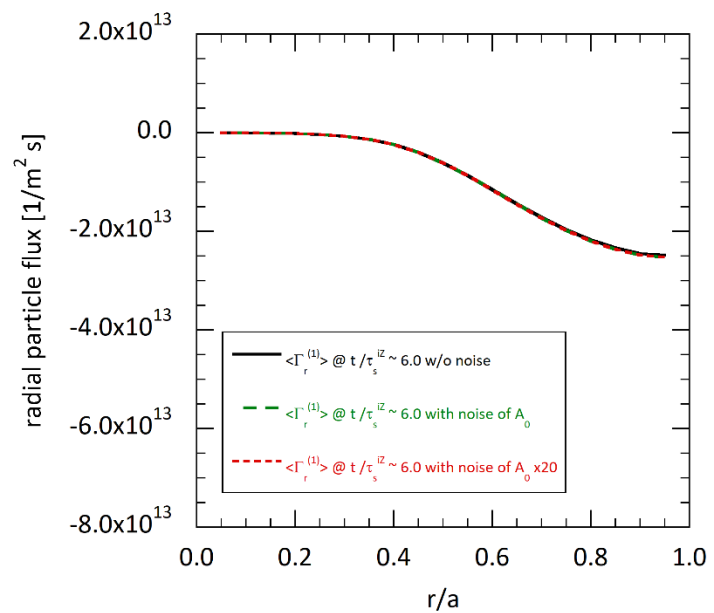
<sup>2</sup> The Graduate University for Advanced Studies, SOKENDAI, Toki 509-5292, Japan

<sup>3</sup> Nagoya University, Nagoya 464-8601, Japan

We are developing a probabilistic model of collisional transport of a heavy impurity like tungsten in the edge of a quasi-steady three-dimensional fusion plasma, based on the drift-kinetic equation [1]. Here, the impurity is assumed to be sufficiently rarefied, i.e., its number density is  $10^{-4}$ – $10^{-5}$  or more times smaller than the number density of the background plasma, and to contribute little to self-consistent electromagnetic field. In such a case, when electromagnetic fluctuation is generated by, for example, turbulence of the background plasma, the distribution function of the impurity is also assumed to be fluctuating. The computational cost of a kinetic simulation of the impurity transport including such an electromagnetic fluctuation is estimated to be high. Considering that the behavior of the distribution function of the impurity is probabilistic, it is helpful for reducing the cost that effect of the electromagnetic fluctuation is modeled as a noise having finite amplitude in the impurity transport. Here, the noise is assumed to have zero expectation and is bounded.

It is known that when considering the distribution function of the impurity only in the velocity space, such a probabilistic fluctuation does not change the distribution. This fact is mathematically guaranteed, as shown in Theorem 8.4.3 in [2]. On the other hand, when effect of the probabilistic fluctuation is considered in the drift-kinetic equation of the impurity, role of the effect has not been explained. Therefore, we first investigate effect of such a noise in the drift-kinetic equation by using a drift-kinetic simulation code, KEATS [1]. When the noise affects the impurity only in the velocity space, we find that the effect is negligible in the drift-kinetic equation, as shown in the figure below, although the noise influences orbits of the impurity particles in the configuration space through the velocities changed. We see that the radial particle flux of the impurity is determined by the friction and thermal forces with the background ions, which is the same result in [1].

On the other hand, when the noise affects the distribution function in the 5-dimensional phase space, the effect becomes complicated. We consider the time-evolution of an ensemble-averaged distribution function of the impurity for understanding how the distribution function becomes quasi-steady. The modeling shows that the noise effect can be ignored in the drift-kinetic equation of the ensemble-averaged distribution function.



[1] R. Kanno et al., Nuclear Fusion **60** (2020) 016033.

[2] B. Øksendal, Stochastic Differential Equations (Springer-Verlag, 2003).

## 2-D spectroscopic measurement of Balmer series in detached plasma with ICR heating

Naonori Okada<sup>1</sup>, Ryuichi Ohonuma<sup>1</sup>, Akira Tonegawa<sup>1</sup> and Kohnosuke Sato<sup>2</sup>

<sup>1</sup> Tokai University,  
4-1-1, Kitakaname, Hiratuka-shi, Kanagawa 259-1292, Japan  
8BSP1107@gmail.com

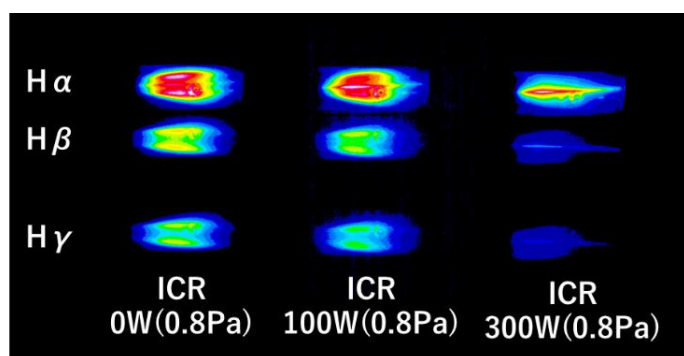
<sup>2</sup> Reserch Institute for Applied Mechanics, Kyusyu University  
7-4-4, Motoooka, Nishi-Ku, Fukuoka-shi, Fukuoka, Japan

The divertor is subject to damage by high heat flow particles emitted from the core plasma. Therefore, it is considered to reduce the heat load on the divertor plates by introducing neutral gas to generate a detached plasma. In the divertor of future DEMO-class devices, further reduction of the heat load is required, and simulation experiments of advanced divertors employing a divergent magnetic field configuration, such as the Super X divertor, are in progress. Therefore, basic research on heat load reduction in detached plasma is being actively conducted in small linear divertor simulators.

However, the ion temperature of the plasma produced by most linear divertors is as low as about 3 eV, which is significantly different from the ion temperature of the divertor plasma of large devices such as the International Thermonuclear Experimental Reactor (ITER), which is 10-20 eV. Therefore, the effect of ion temperature on detached plasma generation has been an open question in basic research using linear divertor simulators. In addition, the process of detached plasma generation in the divergent field configuration used in advanced divertors has also been mainly studied by simulation, and few basic experiments have been conducted.

The objective of this study is to investigate the generation process of detached plasma with respect to ion temperature by ion cyclotron resonance (ICR) heating of high-density sheet plasma generated in a linear divertor simulator (TPDsheet-U) [1].

In this study, we investigated the process of detached plasma formation when the ion temperature is varied by ICR heating in a high-density sheet plasma generated in a divertor-simulator TPDsheet-U. The plasma is heated by ICR, and the ion temperature is varied. The plasma thermal energy was measured with a diamagnetic coil, the electron temperature and density with a Langmuir probe, and the two-dimensional emission intensity distribution of  $H_\alpha$ ,  $H_\beta$ , and  $H_\gamma$  with a high-speed camera equipped with an Arbaa prism spectrometer. The results show for the first time that increasing the ICR heating power decreases  $H_\gamma$  and suppresses the formation of exfoliation plasma.



Reference

[1] Okada Naonori, et al. Fusion Engineering and Design 192 (2023) 113596.

Fig1. Characteristics of 2-D spectroscopy of Balmer series ( $H_\alpha$ ,  $H_\beta$ , and  $H_\gamma$ ) in detached plasmas with increasing ICR heating power at gas pressure of 0.8 Pa.

## Analysis of Molecular Activated Recombination in Hydrogen Plasma Produced in Radio-Frequency Plasma Source DT-ALPHA

Keigo Yoshimura<sup>1</sup>, Hiroyuki Takahashi<sup>1</sup>, Tomohiro Seino<sup>1</sup>, Ryota Nishimura<sup>1</sup>,  
Akihiro Kanno<sup>1</sup>, Yusaku Takahashi<sup>1</sup>, Tomoya Hara<sup>1</sup>, Shigetaka Kagaya<sup>1</sup>,  
Akinobu Matsuyama<sup>2</sup>, Tetsutarou Oishi<sup>1</sup> and Kenji Tobita<sup>1</sup>

<sup>1</sup> Department of Quantum Science and Energy Engineering, Tohoku University,  
6-6-01-2 Aoba, Aramaki, Aoba, Sendai, Miyagi 980-8579, Japan  
keigo.yoshimura.s5@dc.tohoku.ac.jp

<sup>2</sup> Graduate School of Energy Science, Kyoto University,  
Uji 611-0011, Japan

One of the key challenges for future fusion reactors is safe control of power exhaust from burning core plasma to divertor plates. A promising way to control the power exhaust is the formation of detached divertor, which is facilitated by electron-ion recombination (EIR) and molecular activated recombination (MAR). DA-MAR (Dissociative Attachment-MAR) and IC-MAR (Ion Conversion-MAR) are known to be main reaction chains of MAR. Compared with DA-MAR, publications on IC-MAR have been quite limited because of a difficulty in obtaining evidence of the IC-MAR. For this situation, it is of great significance of to establish a methodology to experimentally distinguish the IC-MAR reaction. In our group, we have been conducting divertor plasma simulating experiment on hydrogen MAR using a radio-frequency plasma source DT-ALPHA. Although we have achieved to obtain the experimental results that indicate strong enhancement of MAR [1], DA-MAR and IC-MAR were not distinguished yet. In this paper, we present efforts to explore the methodology to experimentally distinguish the IC-MAR reaction based on experimental results of hydrogen plasma obtained in the DT-ALPHA.

The DT-ALPHA is approximately 2 m in length and plasma is produced by 13.56 MHz radio-frequency (RF) discharge. Hydrogen working gas is supplied at the upstream end of the device. Secondary hydrogen gas is supplied at the downstream region to enhance MAR. The hydrogen neutral pressure at the secondary gas feeding region was controlled up to 3.6 Pa by increasing the amount of the secondary gas. To maintain the discharge condition during the experiment, the upstream neutral pressure was kept almost constant by adjusting the feeding rate of the working and secondary gases. Langmuir probes, spectrometers and a retarding field analyzer (RFA) were used for the measurement.

The electron temperature at the secondary gas feeding region decreased monotonically from 17 eV to 6 eV with increasing the neutral pressure. In the experiment, a rollover of the electron density was clearly observed, showing a sign of enhancement of the plasma recombination. The observed Balmer line intensity ratio ( $H\alpha/H\beta$ ), which is a good indicator of DA-MAR, was almost independent of the neutral pressure. Numerical analysis with a collisional-radiative model indicated that the density rollover was dominated by the IC-MAR reaction. To confirm the results, we plan to measure the hydrogen ion temperature and evaluate the reaction rate of ion conversion. The result of the additional measurement will be presented, as well.

This work was supported by JSPS KAKENHI Grant Numbers JP20H01883 and JP22K18699 and JST Grant Number JPMJFS2102.

[1] K. Yoshimura *et al.*, Plasma Fusion Res. **17**, 1201082 (2022).

## Diffusion Behavior of Adatom on Tungsten Surface Evaluated by Density Functional Theory Calculation

Arimichi Takayama<sup>1,2</sup> and Atsushi M. Ito<sup>1,2</sup>

<sup>1</sup> National Institute for Fusion Science, National Institutes of Natural Sciences,  
322-6 Oroshi-cho, Toki, Gifu 509-5292, Japan  
Takayama.arimichi@nifs.ac.jp

<sup>2</sup> Graduate Institute for Advanced Studies, SOKENDAI,  
322-6 Oroshi-cho, Toki, Gifu 509-5292, Japan

The authors are interested in tungsten nano structure (so called fuzz), which is formed due to helium irradiation with relatively low incident energy (less than about 100 eV) and was firstly reported by Prof. Takamura in 2006 [1]. Its formation mechanism is not clear and is believed to involve multiple elementary processes. Motion of adatom which is trapped on a surface is regarded as one of these processes. In the present work, migration energy of adatom on tungsten surface [2], which is related to surface diffusion is evaluated by *ab initio* calculations based on density functional theory (DFT), and plausible diffusion path is revealed.

The used method is the followings: a target system having supercell of 3x3x6 unit lattice tungsten (BCC) with an adatom on (0 0 1) surface is prepared. Surface is introduced by vacuum region with the size of 6 unit cells in *z*-direction and fixed atoms in the bottom two layers of the system. Periodic boundary condition in (*x*-, *y*-, *z*-) directions are imposed. Brillouin zone sampling (*k*-points) is 4x4x1 and the SCF convergence criterion is  $1.0 \times 10^{-7}$  hartree. Nudged elastic band (NEB) method with 7 images is used for minimum energy path search. DFT calculations are performed by the modified version of OpenMX code which is vectorized and tuned for NEC SX Aurora TSUBASA [3-5].

The evaluated migration energy of the case where tungsten adatom does not jump to the adjoining trapping site but moves onto the lattice point on the surface and the surface atom pops out on the surface is 2.03 eV. On the other hand, the one for the case where the adatom jumps to the adjoining trapping site is 2.85 eV. The similar tendency is obtained for adatom of molybdenum, tantalum, and rhenium. In addition, tungsten with adatom of Ta/Mo is 0.43eV less stable / 0.18 eV more stable than the state where the adatom of Ta/Mo and single W atom are exchanged, respectively. These results imply that it is preferable that an adatom moves onto the lattice point on the surface and the surface atom pops out on the surface, and tantalum adatom prefers to merge into tungsten material.

- [1] S. Takamura, N. Ohno, D. Nishijima, and S. Kajita, Plasma Fusion Res., **1**, 051 (2006).
- [2] Z. Chen and N. Ghoniem, Phys. Rev. B **88**, 035415 (2013).
- [3] T. Ozaki and contributors, <https://openmx-square.org/>
- [4] A. M. Ito, A. Takayama, O. Watanabe, V. Singh, S. Tyagi, and S. S. Singh, Plasma Fusion Res., **15**, 1203085 (2020).
- [5] A. M. Ito, <https://github.com/atsushi-m-ito/openmx-vector-patch>

This work is partly supported by KAKENHI (19H01882 and 19K21870). Calculations are carried out on "Plasma Simulator Raijin" (NEC SX Aurora TSUBASA) of NIFS with the support and under the auspices of the NIFS Collaboration Research program (NIFS20KNSS130, NIFS21KNSS156, and NIFS22KISS027).

## Weighted Sum Estimation of Radiation Power and Toroidal Asymmetry in LHD

Gakushi Kawamura<sup>1,2</sup>, Kiyofumi Mukai<sup>1,2</sup>, Byron Peterson<sup>1,2</sup>

<sup>1</sup> National Institute for Fusion Science, Toki Gifu 509-5292, Japan

<sup>2</sup> The Graduate University for Advanced Studies, SOKENDAI, Toki Gifu 509-5292, Japan  
kawamura.gakushi@nifs.ac.jp

Impurity species act as a radiator in a plasma and affect the plasma transport properties. Especially heavy impurities such as tungsten are quite important for the fusion plasma design because of their strong core radiation. In Large Helical Device (LHD), the total radiation power [1] has been estimated as a linear combination of bolometer powers at different toroidal positions by using a regression analysis of the synthetic data simulating the bolometer diagnostics with the aid of the numerical transport code EMC3-EIRENE [2]. The feasibility of the simple regression analysis of the synthetic dataset has been proved by introducing some artificial variations to the dataset such as noise, toroidal modulation, and core radiation, which are not involved in the EMC3-EIRENE model. Evaluation of toroidal asymmetry, or locality, was also realized by comparison between the estimations with all the bolometers and with a bolometer at a certain toroidal position [3].

In this study, the data dataset of the synthetic bolometer diagnostics was updated to include different magnetic field configurations to cover most of the LHD discharges (see Fig. 1): the magnetic axis position  $R_{ax} = 3.75$  m and 3.9 m in addition to  $R_{ax} = 3.6$  m in the previous study [1]. The influence of each artificial variation type was evaluated, and it was found that all of them contribute to the stability of the regression results, and especially the noise component is important. Tikhonov regularization was newly introduced for further stability.

In order to realize a quantitative evaluation of toroidal asymmetry, Fourier components were introduced as the toroidal variation. The coefficient of each Fourier component was obtained by the regression analysis for it (see Fig. 2). Time development of the degree of asymmetry and its direction becomes available during a discharge.

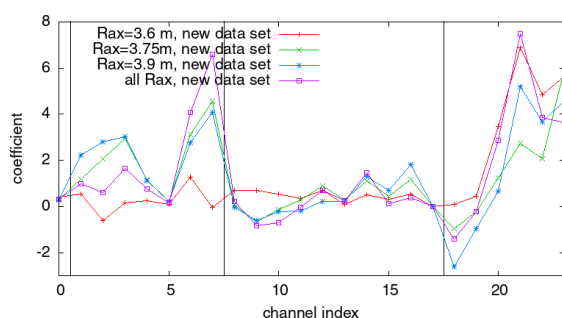


Fig. 1: the coefficients for the bolometer channels in three magnetic configurations. The four groups separated by the vertical lines correspond to the four bolometer systems.

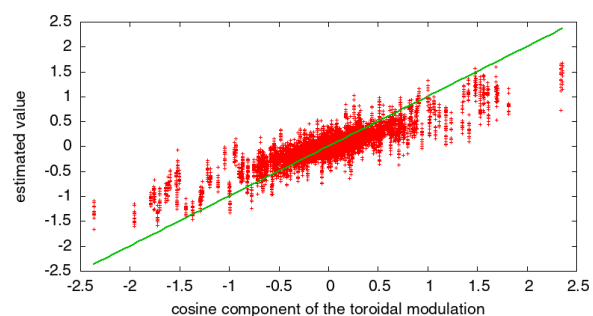


Fig. 2: comparison between the estimation and the input coefficient for the cosine component. A clear correlation was obtained. The green line denotes the perfect match.

[1] P. L. Van De Giessen *et al.*, Rev. Sci. Instrum., **92**, 033518 (2021).

[2] G. Kawamura *et al.*, Plasma Phys. Contr. Fusion, **60**, 3403034 (2018).

[3] B. J. Peterson *et al.*, Nucl. Mater. Energy, **26**, 100848 (2021).



## Evaluation of proton density ratio in a bucket-type ion source based on kinetic code plasma simulation and rate equation for hydrogen ions

Hiroyuki Takahashi<sup>1</sup>, Ryota Nishimura<sup>1</sup>, Tomohiro Seino<sup>1</sup>, Keigo Yoshimura<sup>1</sup>,  
Akihiro Kanno<sup>1</sup>, Tomoya Hara<sup>1</sup>, Yusaku Takahashi<sup>1</sup>, Tetsutarou Oishi<sup>1</sup>,  
Akinobu Matsuyama<sup>2</sup>, Kenji Tobita<sup>1</sup>, Kazuo Hoshino<sup>3</sup>

<sup>1</sup> *Department of Quantum Science and energy Engineering, Tohoku University  
Aobayama, Sendai 980-8579, Japan  
hiroyuki.takahashi.c6@tohoku.ac.jp*

<sup>2</sup> *Graduate School of Energy Science, Kyoto University  
Uji 611-0011, Japan*

<sup>3</sup> *Faculty of Science and Technology, Keio University  
3-14-1 Hiyoshi, Kohoku-ku Yokohama, Kanagawa, 223-8522, Japan*

Future fusion reactors will be operated with detached divertor regime to allow the divertor plates to withstand large plasma heat load. The detached divertor is facilitated by plasma volumetric recombination. Although many toroidal plasma devices and linear divertor plasma simulators demonstrated its capability of the divertor protection, transient behavior of the detached divertor, which is triggered by energetic ion inflow attributed to the edge-localized modes (ELMs), has not yet been understood clearly. We have been conducting ELM-simulating experiments using a radio-frequency plasma source and an ion beam generator. It was found that ELM-simulating helium ion beam decreases reaction rate of the volumetric recombination of helium ions [1]. With respect to hydrogen plasma, recently we succeeded to obtain the experimental results that indicate strong enhancement of hydrogen molecular activated recombination (MAR) [2]. This achievement enables us to conduct similar experiments with hydrogen MAR plasma and hydrogen ion beam ( $H^+$  beam). However, one difficulty in use of intense  $H^+$  beam is that installation of a mass filter is necessary to separate ion species, making decrease of ion beam intensity inevitable. Intensity of  $H^+$  beam depends on  $H^+$  density ratio inside the ion source. Therefore, this study aims to find suitable operation window to obtain high  $H^+$  ratio.

The ion beam source utilized in our device has approximately 80 mm diameter and 90 mm length. Permanent magnets aligned azimuthally produce multi-cusp magnetic field. Plasma is produced with the direct-current arc discharge between its body and hot cathode of tungsten filaments. Ratio of the protons to hydrogen molecular ions in a multi-cusp type ion source can be calculated with its geometry and plasma parameters inside [3]. However, our ion source is not equipped with measurement port. Therefore, we use KEIO-MARC kinetic code [4], which is able to calculate electron temperature and electron density inside a given-size ion source, using neutral pressure and arc power as input parameters. Combination of this analysis and rate equations for hydrogen ions enables to explore suitable operation window for producing intense  $H^+$  beam. In this presentation, we will report results of these analyses.

This work is supported by the Japan Society for the Promotion of Science JSPS KAKENHI (Grant Nos. JP20H01883 and JP22K18699).

- [1] H. Takahashi *et al.*, *Physics of Plasmas* **23**, 112510 (2016).
- [2] K. Yoshimura *et al.* *Plasma Fusion Res.* **17**, 1201082 (2022).
- [3] Y. Okumura *et al.*, *Rev. Sci. Instrum.* **55**, 1 (1984).
- [4] I. Fujino *et al.*, *Rev. Sci. Instrum.* **79**, 02A510 (2008).

## Formation of fiber-form nanostructures and He bubbles/holes on tungsten surfaces by collisional helium arc plasma irradiation

Mitsuo Tajima<sup>1</sup>, Yusuke Kikuchi<sup>1</sup>, Tatsuya Aota<sup>1</sup>, Shiro Maenaka<sup>2</sup>,  
Kazunori Fujita<sup>2</sup>, Shuichi Takamura<sup>2</sup>

<sup>1</sup> University of Hyogo  
2167 Shosha, Himeji, Hyogo 671-2201, Japan  
er22v011@guh.u-hyogo.ac.jp

<sup>2</sup> Yumex Inc.  
400 Itoda, Yumesakichou, Himeji, Hyogo 671-2114, Japan

Recently, it has been found that fiber-form nanostructures are formed on the surfaces of tungsten (W) and other metals by helium (He) plasma irradiation [1]. From the viewpoint of industrial application, a technology for high-speed formation of fiber-form nanostructures using a high-density He plasma generated by a compact device is desirable. So far, we have succeeded in forming fiber-form nanostructures using He arc discharge plasma irradiation under a gas pressure of 5 kPa, where collisions between ions and neutral particles in the sheath cannot be neglected.

One of the properties of fiber-form nanostructures is their high thermal radiation properties. However, there is a problem that nanofibers shrink under high temperature without He irradiation [3]. In this study, in order to improve the thermal radiation properties at high temperatures, we formed micron-sized He bubbles/holes structures [4] obtained by irradiating He plasma at a higher temperature than fiber-form nanostructure formation.

In this experiment, a DC He arc discharge (discharge voltage: 36 V, discharge current: 34 A) was generated between W electrodes placed in a vacuum vessel. The He gas flow rate and gas pressure were 1 L min<sup>-1</sup> and 5 kPa, respectively. A W thin plate sample (10 mm × 15 mm × 0.05 mm) was inserted into a He arc discharge and irradiated for 2 hours, as shown in Fig. 1 (a). In addition, the W sample temperature under He arc irradiation measured with a radiation thermometer was obtained to be approximately 2000°C. A biasing voltage of -60 V was applied between the W sample and the vacuum chamber wall to control the incident He ion energy on the W sample surface.

Fig. 1 (b) shows an FE-SEM image of the W surface after the He arc plasma irradiation. It can be found that open holes of He bubbles with a diameter of about 1 to 2 μm are formed on the W sample surface. On the other hand, the diameter of the open He bubbles/holes formed at a W sample temperature of about 1550°C was less than 0.5 μm, indicating that larger-sized bubbles/holes are formed at higher sample temperatures.

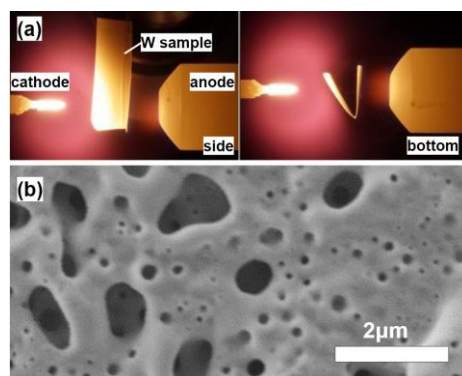


Fig. 1(a) He arc irradiation, (b) He bubbles/holes structure formed on the W surface (ion flux:  $2 \times 10^{22} \text{ m}^{-2}\text{s}^{-1}$ , surface temperature: about 2000°C, bias voltage: -60V)

[1] S. Takamura et al., Plasma Fusion Res. 1, 051 (2006).

[2] Y. Kikuchi et al., J. Appl. Phys. 131, 123301 (2022).

[3] T. Miyamoto, S. Takamura and H. Kurishita, Plasma Sci. Technol. 15, 161 (2013).

[4] S. Takamura, J. Nucl. Mater. 466, 239 (2015).

## Simulation Development for the Next Stage of Plasma-Material Interaction

Atsushi M. Ito<sup>1,2</sup>, Arimichi Takayama<sup>1,2</sup>, and Yuto Toda<sup>2</sup>

<sup>1</sup> *National Institute for Fusion Science, National Institutes of Natural Sciences  
322-6 Oroshi-cho, Toki 509-5292, Japan  
ito.atsushi@nifs.ac.jp*

<sup>2</sup> *Graduate Institute for Advanced Studies, SOKENDAI  
322-6 Oroshi-cho, Toki 509-5292, Japan*

We had been developed the several simulation codes to advance the understanding of the plasma-material/wall interaction (PMI/PWI) phenomena by focusing the classify the mechanisms in atomistic scale. In the presentation, we introduced our simulation codes to find new collaboration partners. In addition, we would like to disclose our future plans for code development, along with the next PMI research agenda we have in mind.

For the sputtering on surfaces, the Binary Collision Approximation (BCA) is better not only in point of calculation speed but also in the reliability of interatomic potential for high energy collision. We have been tackle the modernization of BCA in the BDoG[1] code, especially high accuracy interatomic potential, ReGZ potential[2], was developed and we demonstrate that the recoil cutoff energy, which is corresponding to the sputtering threshold energy, should be moderated by using the Density Functional Theory (DFT). The DFT is better to estimate the microscopic property in viewpoint of nanomaterial. Moreover, to just use the code, the DFT is easy rather than Molecular Dynamics (MD) because users need only input the atomic coordinate and a few parameters. MD requires not a little customization of the code and coding to analyze the results of dynamics. We can support the partners to start the DFT and provide a tuning patch[4] to run the OpenMX code[3] on the vector architecture super computer.

For future simulations in PMI/PWI, we are planning two directions: the first is to further improve the validity between simulation and experiment. The interesting feature of PMI/PWI is the gap of time- and space-scales. By using well controlled plasmas, nanomaterials are generated in microscopic space-scale, while the their generation need seconds and minutes which is relatively macroscopic time-scale[5]. One solution for this gapped-scale problem is the hybrid simulation. The BCA-MD-KMC hybrid method for the helium plasma induced fuzz can achieve 1 minutes or more in elapsed time[6]. An important scheme is to replace some of the MD calculations with KMC or BCA. For versatility, it is important to develop the lattice-free and on-the-fly KMC that can represent a wider variety of atomic motions. The second direction is to clarify quantum electron dynamics in PMI/PWI phenomena. Almost previous simulations were performed under the assumption that all particles are charge neutral because of theoretical limitation. The true pictures of PMI, including the neutralization process of ions flying from the plasma onto surfaces, the electron stopping power for the ion penetrating into the material, and so on, are still unclear. This problem can also be a frontier in terms of nanoscale plasma picture, and we have been trying with the Time-Dependent Density Functional Theory (TDDFT) simulation.

[1] A. M. Ito, A. Takayama, H. Nakamura, *Plasma Fusion Res.* **13**, 3403061 (2018).

[2] A. M. Ito, A. Takayama, Y. Toda, *Jpn. J. Appl. Phys.* **62**, SL1012 (2023).

[3] T. Ozaki, *Phys. Rev. B.* **67**, 155108, (2003).

[4] A. M. Ito, et al., *Plasma Fusion Res.*, **15**, 1203085 (2020).

[5] A. M. Ito, *JSAP Rev.* **2023**, 230412 (2023).

[6] S. Kajita, A. M. Ito, K. Imano, *J. Appl. Phys.* **132**, 181101 (2022).

## Visualization of metastable helium distribution using ghost imaging absorption spectroscopy

Ryusei Koyama and Mitsutoshi Aramaki

*Nihon University, Graduate School of Industrial Engineering  
Narashino, Chiba 274-0072, Japan  
ciry23022@g.nihon-u.ac.jp*

Ghost imaging is a method that employs a single-pixel detector such as a photodiode to capture an image of an object [1]. We are developing a novel 2-D absorption spectroscopy method by integrating computational ghost imaging (CGI) with traditional absorption spectroscopy. Figure 1 shows a schematic diagram of CGI. Structured light with a computer-generated random structure  $I_r(x, y)$  is irradiated onto an object with a transmittance distribution  $T(x, y)$ . The transmitted light is focused on a photodiode (PD) by a lens, and a PC records the integrated intensity  $b_r$ .  $T(x, y)$  is obtained by the following calculation.

$$T(x, y) = \frac{\langle b_r I_r(x, y) \rangle - \langle I_r(x, y) \rangle \langle b_r \rangle}{|\langle I_r(x, y) \rangle|^2}, \quad (1)$$

where  $\langle \dots \rangle$  represents an ensemble average for measurements from  $r = 1$  to  $N$ . In addition to eliminating the need for an expensive camera, this measurement technique offers noise tolerance comparable to lock-in detection. Furthermore, it has the potential to be developed into an absorption spectroscopy method with spatial resolution in the line-of-sight direction. This is accomplished by focusing the structured light in a plasma.

Figure 2 shows a helicon wave plasma device developed to study a detached plasma. A ghost imaging absorption spectroscopy system has been developed to image the distribution of metastable helium atoms near the end plate of the helicon wave plasma (Fig. 3). We used a 1083nm DFB laser as a light source to excite metastable helium atoms. The laser beam is converted to structured light by the DMD. The structured light is focused into a plasma, and the integration of the transmitted light is observed by the lens system and a PD. By calculating eq. (1), we obtained an image of the metastable helium atom distribution. Details of the imaging system and measurement results will be reported.

[1] J. H. Shapiro, Phys. Rev. A **78**, 061802(R) (2008).

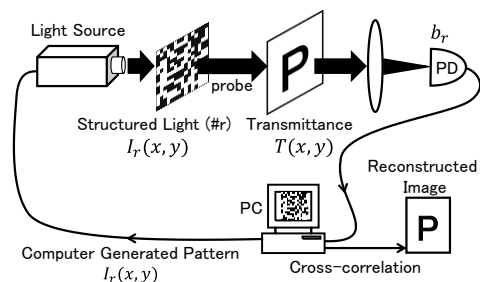


Fig.1 Schematic diagram of CGI

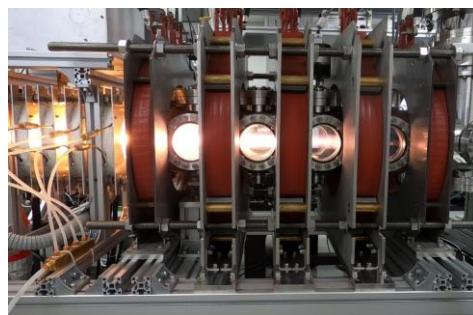


Fig.2 Helicon wave plasma device.

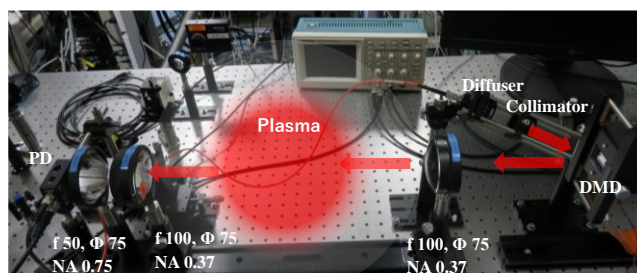


Fig.3 Ghost imaging absorption spectroscopy system.

## Analysis of Scattering of UV Vortex from Helix Conductor Using MoM

Hideki Kawaguchi<sup>1</sup>, Masahiro Katoh<sup>2</sup> and Koichi Matsuo<sup>2</sup>

<sup>1</sup> Muroran Institute of Technology  
27-1, Mizumoto-cho, Muroran 050-8585, Japan  
kawa@muroran-it.ac.jp

<sup>2</sup> Hiroshima University, Hiroshima Synchrotron Radiation Center,  
1-3-2 Kagamiyama, Higashi-Hiroshima City, Hiroshima 739-8511, Japan

Circular dichroism is effectively used for observation and identification of fine structure of chiral materials such as protein, DNA and so on. Then it is pointed out that the phenomena of the circular dichroism appear as a result of interaction between angular momentum of incident circular polarized (CP) wave field and the chiral material<sup>[1]</sup>. During the last decade, so-called optical vortex has attracted strong attentions since it was shown by L.Allen in 1992 that the optical vortex carries well-defined orbital angular momentum which is much stronger than that of standard plane wave. Accordingly it is predicted that optical vortex dichroism can be used for identification of chiral material structure effectively. Indeed experimental study on the optical vortex dichroism using UV light is now planing.

In this paper, the UV vortex dichroism is investigated by using numerical simulation. Then the wavelength of UV light is much larger than typical size of the protein. This means the finite-difference time-domain (FDTD) method, which is the most popular numerical scheme for the scattering phenomena, is not suitable. We here consider to use the method of moments (MoM) in this work. Then the chiral material such as the protein is regarded as infinitesimally thin helical conductor, and electric field  $\mathbf{E}(\omega, \mathbf{x})$  produced by induced surface current  $K_l$  along the thin conductor is expressed by the following frequency domain integral equation, EFIE,

$$\mathbf{E}(\omega, \mathbf{x}) = \mathbf{E}_{ext}(\omega, \mathbf{x}) + \frac{1}{4\pi} \int_S e^{-i\frac{\omega}{c}|\mathbf{x}-\mathbf{x}'|} \left\{ i\omega\mu \frac{K_l \mathbf{l}}{|\mathbf{x}-\mathbf{x}'|} - i \frac{1}{\varepsilon\omega} (\mathbf{x}-\mathbf{x}') \frac{\partial K_l}{\partial l} \right\} dS, \quad (1)$$

where  $\mathbf{l}$  is normal tangential vector of the thin conductor.

In Fig.1, distributions of  $K_l$  on the helical thin conductor and radiation patterns are depicted when the conductor is illuminated by 190nm vortex field with topological charge  $l = 1$ , (a) left and (b) right CP. Big difference in radiation power of scattered field appears for (a) and (b).

[1] S.S.Andrews and J.Tretton, J.Chem.Educ. vol.97 (2020), pp.4370-4376.

### Acknowledgement

This work was supported by JSPS KAKENHI Grant Number 23H04597.

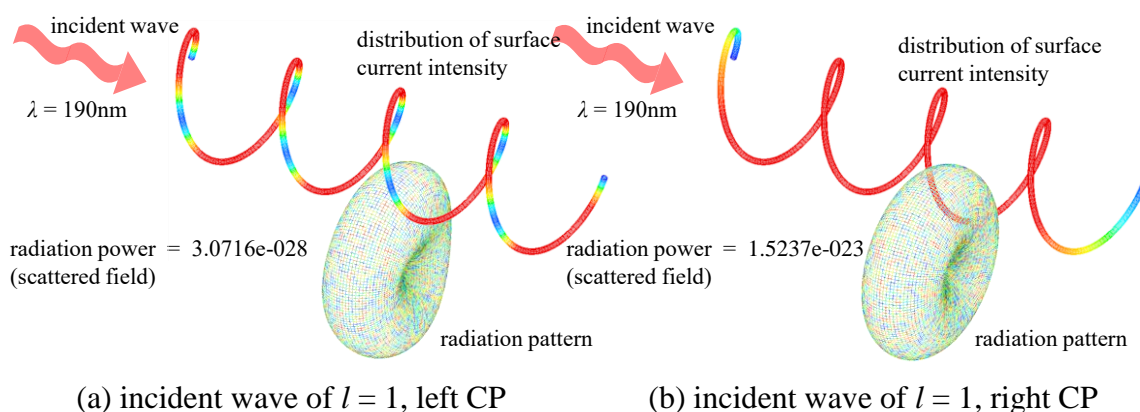


Fig.1: MoM analysis of scattering of UV vortex wave from helical thin conductor.

# Evaluation of Propagation of Millimeter Wave Vortex Using FDTD Method

Chenxu Wang<sup>1</sup>, Hideki Kawaguchi<sup>1</sup> and Hiroaki Nakamura<sup>2</sup>

<sup>1</sup> Muroran Institute of Technology  
27-1, Mizumoto-cho, Muroran 050-8585, Japan  
kawa@muroran-it.ac.jp

<sup>2</sup> National Institute for Fusion Science,  
322-6 Oroshi-cho, Toki-city, Gifu 509-5292, Japan

It was pointed out that millimeter wave vortex can propagate in magnetized weakly ionized plasma, in which normal plane wave can not propagate due to cut-off condition<sup>[1]</sup>. This phenomena may lead to more efficient plasma heating than that of conventional plasma heating by corrugated waveguide HE<sub>11</sub> mode millimeter wave since the millimeter wave vortex can inject wave power to not only propagation region but also the cut-off region in the plasma. Then the millimeter wave vortex was assumed to be Lagarre-Gauss (LG) mode vortex in the original work. In this paper, propagation of the millimeter wave vortex of corrugated waveguide hybrid mode<sup>[2]</sup> is evaluated by finite-difference time-domain (FDTD) method.

The FDTD analysis in 3D grid space consists of two parts, time domain calculation of electromagnetic wave fields  $\mathbf{E}(\mathbf{x},t)$ ,  $\mathbf{H}(\mathbf{x},t)$  based on Maxwell's equation, and behavior of polarization  $\mathbf{P}(\mathbf{x},t)$  and current density  $\mathbf{J}(\mathbf{x},t)$  based on the Drude-Lorentz model.

The numerical model is depicted in Fig.1(a). It is assumed that the hybrid mode millimeter vortex is excited inside the corrugated circular waveguide and illuminated to the plasma region located at downstream. A numerical example of the propagation of the millimeter wave vortex in the magnetized plasma is shown in Fig.1(b). It is also found by the FDTD simulation that plane wave of HE<sub>11</sub> mode can not propagate in the plasma region with the same condition of Fig.2, which means that similar phenomena as in [1] can occur even for the hybrid mode vortex.

[1] T. Tsujimura and S.Kubo, Phys. Plasmas, **28**, 012502 (2021).

[2] H. Kawaguchi, S.Kubo, H. Nakamura, IEEE MWTL, Vol.33. No.2, pp.118-121, (2023).

## Acknowledgement

This work was supported by JSPS KAKENHI Grant Number 23H04609.

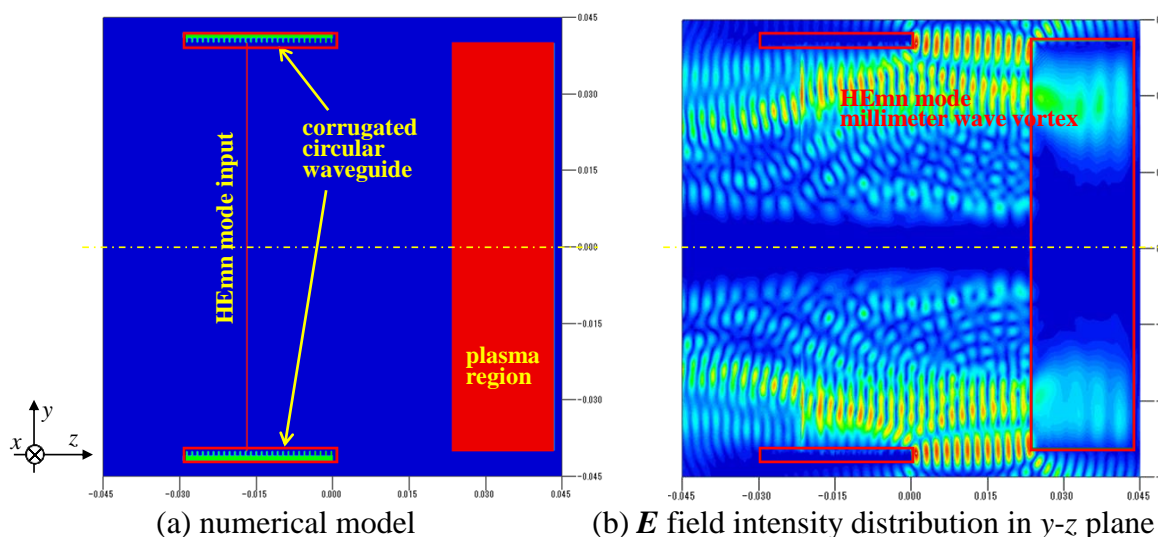


Fig.1: FDTD analysis of millimeter wave vortex propagation in magnetized plasma.

## Observation of Global Structural Changes in Two-dimensional Emission Profiles Associated with Attached and Detached Plasma Transitions

Yuta Uematsu<sup>1</sup>, Hideki Kaizawa<sup>1</sup>, Jielin Shi<sup>1,2</sup>, Hirohiko Tanaka<sup>1,3</sup>,  
Shin Kajita<sup>4</sup>, Noriyasu Ohno<sup>1</sup>

<sup>1</sup> Graduate School of Engineering, Nagoya University, Furo, Chikusa, Nagoya 464-8603, Japan  
uematsu.yuta.g6@s.mail.nagoya-u.ac.jp

<sup>2</sup> School of Physics, Dalian University of Technology, Dalian 116024, China

<sup>3</sup> Institute of Materials and Systems for Sustainability, Nagoya University, Nagoya 464-8603, Japan

<sup>4</sup> Graduate School of Frontier Sciences, the University of Tokyo, Kashiwa, Chiba 277-8561, Japan

In fusion power reactors, the heat flux to the divertor plate is extremely high. One of the solutions to reduce this heat load is generating detached plasmas, in which the plasma is neutralized by increasing the gas pressure near the divertor plate. Detailed measurements of plasma distribution are necessary to understand property of detached plasmas. In this study, global emission profiles of attached and detached helium plasmas were measured by using a 2D spectroscopic measurement system in the radial and axial directions in the linear divertor plasma simulator NAGDIS-II.

Figure 1 shows an overview of the two-dimensional spectroscopy system developed. Emission from the plasma is reflected by a mirror in the head and introduced into an optical fiber via a collimating lens. The optical fiber is connected to a spectrometer. The head can be moved in the axial direction and rotated in the azimuthal ( $\theta$ ) direction.

Figure 2 shows 2D distributions of the emission from helium atoms at a wavelength of 501.4 nm with different gas pressures. The target plate is located at  $z = +10$  mm. It is clearly observed that the plasma transitions from attached to detached plasma as the gas pressure increases. This data can be transformed to the local emission intensity by applying the Abel transformation. The 2D distribution of electron density and electron temperature will be analyzed by comparing with the collisional radiative model.

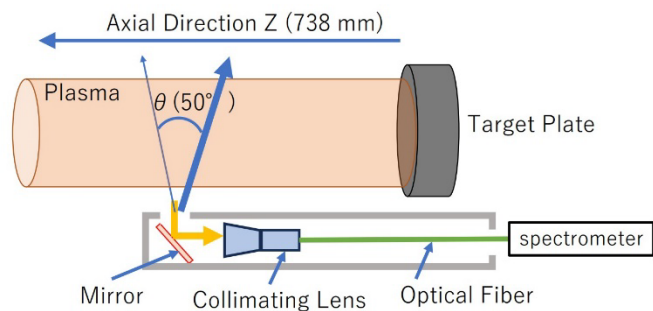


Fig.1 2D spectroscopic measurement system.

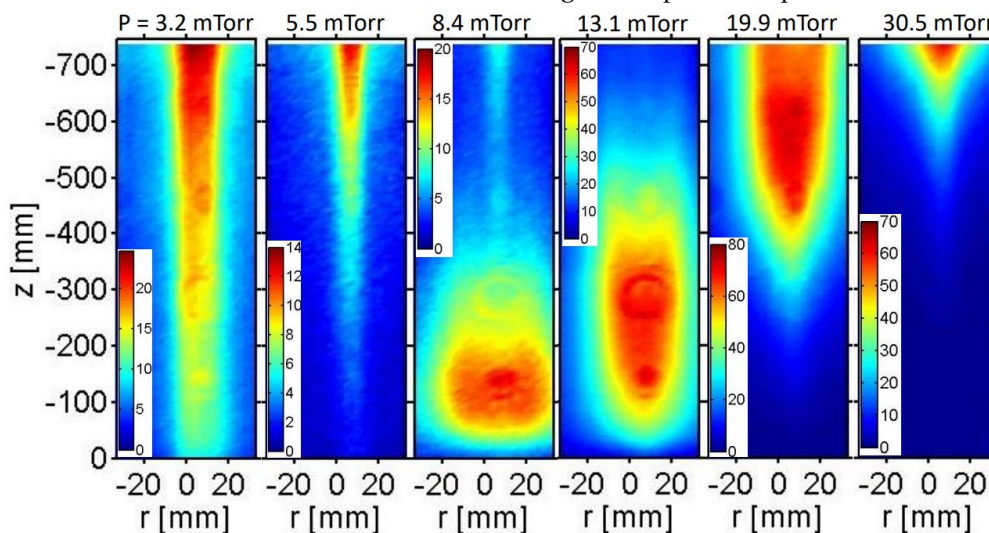


Fig.2 2D emission distributions with different gas pressures. ( $3^1P \rightarrow 2^1S$ , 501.6nm)

## Formation of helium-tungsten co-deposition layers and spectroscopic measurements during sputtering

Masanori Yamamoto<sup>1\*</sup>, Kiho Tabata<sup>1</sup>, Hirohiko Tanaka<sup>2</sup>, Shin Kajita<sup>3</sup>, Quan Shi<sup>3</sup>  
and Noriyasu Ohno<sup>1</sup>

<sup>1</sup> Department of Electrical Engineering, Graduate School of Engineering, Nagoya University,  
Furo, Chikusa, Nagoya 464-8603, Japan

\*yamamoto.masanori.v7@s.mail.nagoya-u.ac.jp

<sup>2</sup> Institute of Materials and Systems for Sustainability, Advanced Measurement Technology Center,  
Nagoya University, Furo, Chikusa, Nagoya 464-8603, Japan

<sup>3</sup> Department of Advanced Energy Engineering, Graduate School of Frontier Sciences, The University of Tokyo,  
5-1-5 Kashiwanoha, Kashiwa, Chiba 277-0882, Japan

Fusion power generation is expected to be the key to realize a decarbonized society. In fusion reactors, tungsten (W), which has a high melting point and a low sputtering rate, will be used as the wall material. A co-deposition layer composed of W and gases such as hydrogen and helium (He) will be formed on the wall, but its physical properties are not well understood.

In this study, we used the compact plasma device called Co-NAGDIS (Fig. 1) to simulate a reactor-wall environment with the formation of a W-He co-deposition layer [1]. A W sample was exposed to a steady state He plasma. At the same time, W wire negatively biased at -300 V was placed in front of the sample to feed the sputtered W onto the sample. Sample temperature was adjusted by plasma heating and air cooling. The porosity of the co-deposition layer was evaluated by the thickness and mass change.

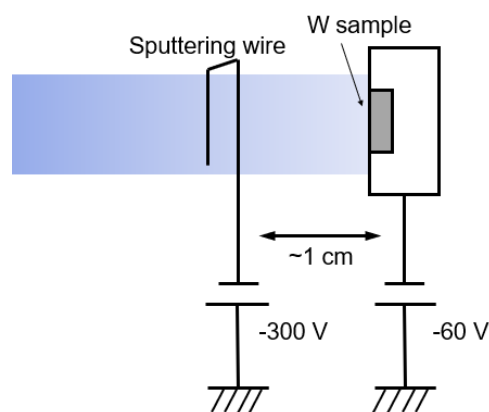


Fig. 1: A schematic of the experiment setup.

After forming the co-deposition layer, we investigated the sputtering property of the co-deposition layer by argon (Ar) plasma exposure as measuring the evolutions of the W and Ar line emissions with a spectrometer. As a result, it was found that the ratio of WI/ArII was ~80% lower on the co-deposition layer compared to the bulk, suggesting that the co-deposition layer has a lower sputtering rate.

[1] S. Kajita et al, J. Nucl. Mater. **540** (2020) 152350.



## A preliminary kinetic study on plasma flow in open magnetic systems using a quasi-one-dimensional particle-in-cell model

Kazuma Emoto,<sup>1</sup> Satoshi Togo,<sup>1</sup> Yoshinori Takao,<sup>2</sup> Kazunori Takahashi,<sup>3,4</sup>  
Isao Katanuma,<sup>1</sup> and Mizuki Sakamoto<sup>1</sup>

<sup>1</sup> *University of Tsukuba, Plasma Research Center  
Tennodai 1-1-1, Tsukuba 305-8577, Japan  
emoto@prc.tsukuba.ac.jp*

<sup>2</sup> *Yokohama National University, Division of Systems Research,  
Tokiwadai 79-5, Hodogaya-ku, Yokohama 240-8501, Japan*

<sup>3</sup> *Tohoku University, Department of Electrical Engineering,  
Aoba 6-6-05, Aramaki, Aoba-ku, Sendai 980-8579, Japan*

<sup>4</sup> *National Institute for Fusion Science, Plasma Apparatus Unit,  
Oroshi-cho 322-6, Toki 509-5292, Japan*

Open magnetic systems are widely applied to plasma devices to confine and extract plasmas, e.g., electric thrusters [1] and divertor simulations [2]. In open magnetic systems, the plasma pressure is converted into directional plasma flow according to the momentum conversion.

For electric thrusters, a two-dimensional numerical model of open magnetic systems has been employed, and the plasma physics in open magnetic systems has numerically been investigated using particle-in-cell (PIC) and Monte Carlo collisions (MCC) techniques, where the electrons and ions were treated as particles in the simulations [3]. The PIC simulations in the two-dimensional model have successfully clarified the mechanisms of plasma acceleration and thrust generation. However, the two-dimensional PIC model has a large calculation cost, and the high-density and large-size plasmas have not been investigated yet.

To reduce the calculation cost and simulate high-density and large-size plasmas, quasi-one-dimensional PIC simulations in open magnetic systems are under development. The axial size in the quasi-one-dimensional model is extended to several tens of centimeters, whereas that in the previous two-dimensional model was several centimeters. Furthermore, the high-temperature plasmas are also simulated in the quasi-one-dimensional kinetic model, where the plasma temperature of several tens of electron volts and an open magnetic field of several teslas are employed. In the conference, preliminary results obtained from the quasi-one-dimensional PIC model will be reported and discussed with axial plasma profiles and velocity distributions.

This work was partly supported by JSPS KAKENHI Grant Number 23H05442 and The Futaba Foundation. The computer simulation was performed on the A-KDK computer system at Research Institute for Sustainable Humanosphere, Kyoto University. This research is partially supported by Initiative on Promotion of Supercomputing for Young or Women Researchers, Information Technology Center, The University of Tokyo.

[1] K. Takahashi, *Rev. Mod. Plasma Phys.*, **3**, 3 (2019).

[2] Y. Nakashima, et al., *Nucl. Fusion*, **57**, 116033 (2017).

[3] K. Emoto, K. Takahashi, and Y. Takao. *Phys. Plasmas*, **28**, 093506 (2021).

## Porous silicon produced with helium plasma for lithium-ion battery anode

Kiho Tabata <sup>1</sup>, Shin Kajita <sup>2</sup>, Teruya Yamada <sup>3</sup>, Kodai Masumoto <sup>3</sup>, Giichiro Uchida <sup>3</sup>, Hirohiko Tanaka <sup>1,4</sup>, Noriyasu Ohno <sup>1</sup>

<sup>1</sup> Graduate School of Engineering, Nagoya University, Furo, Chikusa, Nagoya 464-8603, Japan

[tabata.kiho.j3@s.mail.nagoya-u.ac.jp](mailto:tabata.kiho.j3@s.mail.nagoya-u.ac.jp)

<sup>2</sup> Graduate School of Frontier Sciences, the University of Tokyo, Kashiwa, Chiba 277-8561, Japan

<sup>3</sup> Graduate School of Science and Technology, Meijo University, 1-501, Shiogamaguchi, Tenpaku, Nagoya 468-8502, Japan

<sup>4</sup> Institute of Materials and Systems for Sustainability, Nagoya University, Nagoya 464-8603, Japan

The lithium-ion battery is a rechargeable secondary battery that can be used repeatedly and is required to have high capacity for use in electric vehicles. The capacity of a lithium-ion battery is highly dependent on the material used for the battery's negative electrode, and silicon, which has a theoretical capacity 10 times greater than that of graphite, is being considered as a candidate for higher capacity. However, there is a serious problem when silicon is used: the charge-discharge cycle causes rapid volume expansion, causing peel off of the silicon from the electrode. As a result, the performance drops rapidly after several charge cycles. In contrast, previous studies [1, 2] reported that nanostructured or porous silicon can prevent self-destruction and suppress the performance degradation due to the number of cycles.

In this study, a compact plasma device Co-NAGDIS was used to fabricate the negative electrode. By sputtering silicon with high-density helium plasma, several  $\mu\text{m}$  of silicon with fine or porous structure was deposited on the substrate. Figure 1 shows the surface structure with silicon deposition. It was observed that the surface structure varied greatly depending on the experimental conditions.

Then, we investigated how the different morphology of the silicon structures relates to the battery performance. Figure 2 shows the battery capacity up to  $\sim 100$  times. It is found that the fabricated samples have greatly different performances. The best performing sample (sample 2) successfully maintains its capacity more than five times better than that of conventional materials after more than 100 charge cycles. We investigated what kind of experimental condition and surface structure would result in a high-capacity battery.

[1] Peng Li et al. *Energy Storage Materials*, **35**, 550-576 (2021)

[2] Lin Sun et al. *Energy Storage Materials*, **46**, 482-502 (2022)

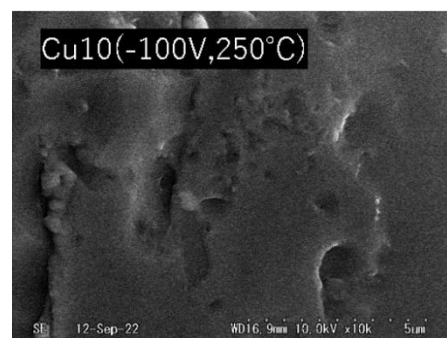


Fig1. Surface structure of Si

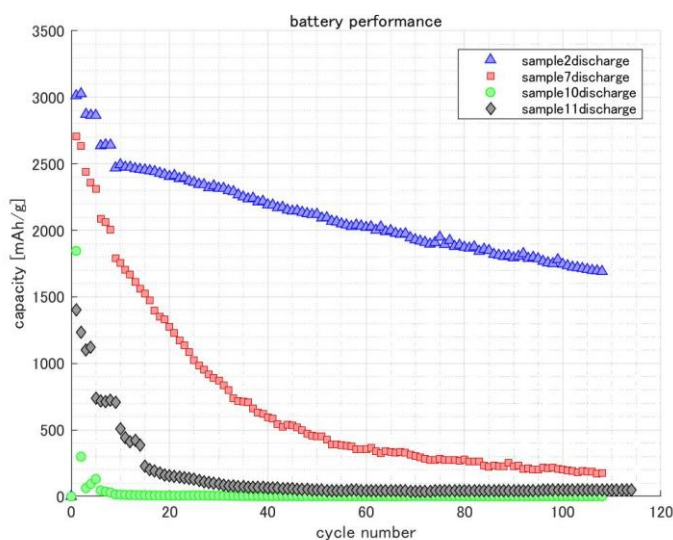


Fig2. The battery performance of several samples

## Phase Structure and Angular Momentum of Cyclotron Radiation

Masahiro Katoh<sup>1,2</sup>, Hideki Kwaguchi<sup>3</sup>

<sup>1</sup> *Hiroshima Synchrotron Radiation Center, Hiroshima University  
2-313 Kagami-yama, Higashi-hiroshima 739-0046, Japan  
mkatoh@hiroshima-u.ac.jp*

<sup>2</sup> *Institute for Molecular Science, National Institutes of Natural Sciences,  
38 Nichigo-naka, Myodaiji-cho, Okazaki 444-8585, Japan*

<sup>3</sup> *Muroran Institute of Technology  
27-1, Mizumoto-cho, Muroran 050-8585, Japan*

Radiation field emitted from electrons, which can be described by Liénard–Wiechert potentials, has characteristic spatial and temporal structures which reflect the electron motion. One of the simplest cases is cyclotron radiation. Electrons are making circular/helical motion in a uniform magnetic field and radiate. They lose not only their energy but also their angular momentum through the radiation. Therefore, both the energy and angular momentum should be carried away by the electromagnetic wave. It is well known that electromagnetic wave carries energy, which is described by Poynting vector. It is also well known that circularly polarized electromagnetic wave carries angular momentum which corresponds to spin angular momentum. On the other hand, it had been less known that electromagnetic radiation carries orbital angular momentum until 30 years ago. In 1992, Allen et al. discussed that Laguerre-Gaussian beam, which has helical phase structure, carries orbital angular momentum [1]. Since then, such a light beam called optical vortex has attract interests of researchers and has been investigated theoretically and experimentally [2].

In this presentation, we review our previous researches on the radiation field emitted from electrons in circular/helical motion [3, 4, 5]. Based on the classical electrodynamics, we show that such radiation field generally possesses helical phase structure and carries both spin and orbital angular momentum. Such topological structure is caused by the relativistic effect. As another consequence of the relativistic effect, the radiation field contains harmonics. Each harmonic component carries well-defined angular momentum depending on the number of harmonic. We attempt an intuitive understanding of this phenomenon.

Electrons in circular/helical motions can be seen in various physical situations such as nuclear fusion plasma, electron accelerators, astrophysical phenomena and so on. They radiate electromagnetic waves possessing helical wavefront and carrying orbital angular momentum. Consequently, such vortex radiation is ubiquitous not only in laboratories but also in the universe. Moreover, we can realize powerful sources of vortex radiation in the entire wavelength range from radio wave to gamma-rays [6, 7, 8].

- [1] L. Allen *et al.*, Phys. Rev. A 45, 8185 (1992)
- [2] Y. Shen *et al.* Light: Science & Applications, 8, 90 (2019)
- [3] M. Katoh *et al.*, Phys. Rev. Lett. 118(9) 094801 (2017).
- [4] H. Kawaguchi, M. Katoh, Prog. Theor. Exp. Phys. 2019(8) 083A02 (2019).
- [5] E. Salehi, M. Katoh, J. Adv. Simulat. Sci. Eng. 8, 1, 87 (2021).
- [6] Y. Goto, S. Kubo, T. Tsujimura, T. Kobayashi, Plasma and Fusion Res., 17, 2401007 (2022)
- [7] M. Katoh *et al.*, Sci. Rep. 7, 6130 (2017)
- [8] Y. Taira, T. Hayakawa, M. Katoh, Sci. Rep. 7, 5018 (2017)

## Spectroscopic measurement of microwave atmospheric pressure nitrogen plasma and the effect of vapor addition on the hydrophilicity of polystyrene surface

Kazutaka Onoda<sup>1</sup>, Hwangbo Dogyun<sup>2</sup>, Katsuhiko Shiraishi<sup>3</sup> and Mizuki Sakamoto<sup>1</sup>

<sup>1</sup>*Plasma Research Center, University of Tsukuba,  
1-1-1 Tennodai, Tsukuba, Ibaraki, 305-8577, Japan  
[onoda\\_kazutaka@prc.tsukuba.ac.jp](mailto:onoda_kazutaka@prc.tsukuba.ac.jp)*

<sup>2</sup>*Faculty of Pure and Applied Sciences,  
Plasma Research Center, University of Tsukuba,  
1-1-1 Tennodai, Tsukuba, Ibaraki 305-8577, Japan*

<sup>3</sup>*Research & Development Group, Hitachi, Ltd,  
7-2-1 Omika, Hitachi 319-1221, Japan*

Controlling the hydrophilicity of cell culture plates has been a key issue in improving cell culture efficiencies. Polystyrene (PS) is one of the most widely used cell culture plates, and contact angle control using PS has been studied for many years [1,2]. In particular, atmospheric pressure plasma jet (APPJ) has accelerated the application of plasma in surface hydrophilicity control, due to its low fabrication cost and ease of development. In this study, a microwave APPJ is developed and the effect of the plasma on the hydrophilic properties of PS plates is evaluated.

This study focused on three main aspects. First, we generated an atmospheric microwave plasma using nitrogen (N<sub>2</sub>) gas. Sometimes water vapor was added to the working gas, which leads to changes in the plasma components. To evaluate the plasma characteristics, spectroscopy was performed with a compact visible spectrometer (AvaSpec-ULS4096CL-EVO, Avantes), measuring the spectra emitted from the plasma source and from the remote jet region. The commercial software Specair was used to identify the plasma species and to evaluate the excitation temperatures. Subsequently, PS samples with different pretreatments were exposed to different types of plasma jets for 1-4 min, then the surface hydrophilicity was analyzed by the contact angle method. In addition, the surface composition due to plasma irradiation was investigated by X-ray photoelectron spectroscopy (XPS). Then, the temporal changes of the contact angles were measured with the samples in different conditions (in ultrapure water, vacuum, air etc.) to see the effect of storage conditions on the hydrophilicity.

The plasma species and excitation temperatures of the plasmas were influenced by the input power, gas flow rate and vapor concentration. The spectra consisted of NO, OH, NH as well as N<sub>2</sub>. The ratio of NO, OH, NH to the total components increased with the vapor concentration, while the intensities of the spectra decreased. The most hydrophilic surface was produced with pure N<sub>2</sub> working gas. On the other hand, when the surface was exposed to the plasma with N<sub>2</sub>+vapor mixture, the contact angle decreased only slightly compared to the pristine surface. Relevant XPS analysis also confirmed the changes in surface composition due to N<sub>2</sub> plasma irradiation, demonstrating the formation of hydrophilic bonds.

- [1] Bo-Lennart Johansson *et al.*, *Journal of Applied Polymer Science*, **86**, 2618-2625 (2002).  
[2] Esmaeil Biazar *et al.*, *International Journal of Nanomedicine*, **6**, 641-647 (2011).

## Effect of argon additive in Cs-free negative hydrogen ion source

Kaito Miura<sup>1</sup>, Ryuichi Onuma<sup>1</sup>, Naonori Okada<sup>1</sup> and Akira Tonegawa<sup>1</sup>

<sup>1</sup> Tokai University, Kitakaname, Hiratsuka, Kanagawa 259-1292, Japan  
[9bsp1214@gmail.com](mailto:9bsp1214@gmail.com).

Most neutral beam injection (NBI) systems in fusion devices use Cs-type negative ion sources, which require careful control and are difficult to operate for long periods of time. As an alternative method, we are developing a volume-production (Cs-free) type negative ion source using sheet plasma[1-4]. In this Cs-free negative ion source, the current ratio of co-extracted electrons to extracted ions  $J_{EG}/J_c$  must be kept below 0.5-1.0 to prevent high heat load on the extraction electrode (EG). Previously, Cs-free negative ions have been proposed using a high-density magnetized sheet plasma produced by TPDsheet-U [1,2]. The purpose of this study is to increase the negative ion current and to reduce the co-electron current by using the following two methods; (1) argon addition method and (2) second anode bias method (Fig.1).

Ar gas additive is effective when the discharge current is low. However, the effect of Ar addition is small because the electron temperature increases with increasing discharge current and the state of Ar shifts from a metastable state to an ionized state, so that resonant excitation of molecular hydrogen by Ar metastable atoms does not occur.

By applying a positive bias to the second anode, the negative ion current  $J_c$  was successfully increased while keeping  $J_{EG}/J_c$  below 1, even when the discharge current was increased. This indicates experimentally that the second anode bias method enhances the effect of Ar gas addition (Fig.2).

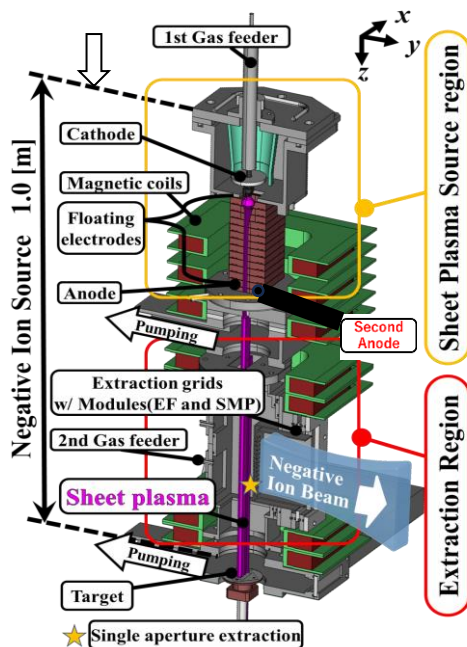


Fig.1 Schematic diagram of Cs-free negative ion source TPDsheet-U.

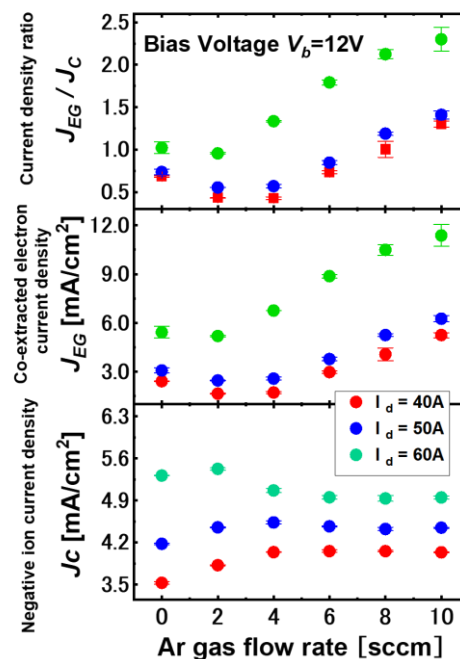


Fig.2 Characteristics of  $J_c$ ,  $J_{EG}$ ,  $J_{EG}/J_c$  vs Ar gas flow rate.

- [1] K.Kaminaga, et. al., Rev. Sci. Instrum. **91** (2020) 113302.  
 [2] A.Tonegawa, et. al., Nucl. Fusion **61** (2021) 106030.

## Correlation of tungsten surface morphology changes and deuterium absorption properties by deuterium plasma exposure with pulsed heat load

Ryo Sasaki<sup>1</sup>, D. Hwangbo<sup>1</sup>, K. Saito<sup>1</sup>, K. Onoda<sup>1</sup>, S. Murakami<sup>1</sup>, H. Yoshida<sup>1</sup>, M. Sakamoto<sup>1</sup>

<sup>1</sup> Plasma Research Center, University of Tsukuba  
Tennodai, Tsukuba, Ibaraki 305-8577, Japan  
sasaki\_ryo@prc.tsukuba.ac.jp

As a plasma facing material (PFM) in future fusion reactors, tungsten (W) must withstand particle and heat loads from collisions by hydrogen isotopes and helium ions, as well as neutron loading. In the study of fusion-relevant plasma-surface interaction (PSI), tritium absorption and surface modification of PFMs are important research issues related to the lifetime of PFMs, operational stability of fusion reactors and fuel efficiency [1].

Under high flux plasma irradiation conditions, surface modification of W can cause the changes in the implantation of hydrogen isotope ions, and both the surface modification and the amount of hydrogen isotope absorption strongly depend on the irradiation parameters such as the target temperature, the incident ion flux and the irradiation fluence. In this study, we focused on changes in the W surface structure and relevant hydrogen isotope absorption characteristics due to changes in sample temperature. Specifically, deuterium (D) plasma and pulsed laser irradiation were simultaneously applied to a W sample to examine the surface modification and D absorption of a W sample undergoing instantaneous temperature changes.

Experiments were conducted with three W samples called (a), (b) and (c), respectively. All three samples were irradiated plasmas with D ion flux of  $6 \times 10^{21}$  D/(m<sup>2</sup>.s) and the incident fluence was  $2 \times 10^{25}$  D/m<sup>2</sup>. The irradiation temperature for (a) was 617 K. For (b), the plasma was irradiated under the same conditions as (a) with an additional heating by Nd:YAG pulsed laser, and the sample temperature was 644 K. For (c), the sample temperature was 644 K. The surface condition of W after plasma irradiation was observed by scanning electron microscope (SEM), and the D absorption amount was measured by thermal desorption spectroscopy (TDS).

Figure 1 shows the results of D amount retained in desorbed from the samples with the three different irradiation conditions. Resultant surface morphologies are also shown. Fig. 1(a) and (c) are the results of D plasma irradiation alone, showing that the blisters were formed on the surface and D absorption was higher than that of Fig. 1(b), where W was exposed simultaneously to the D plasma and the pulsed laser. The total D retention for the sample (b) was one fifteenth to the sample (c) with D plasma only, while no surface changes were observed at the same time. These results suggest that intermittent temperature changes caused the suppression of blistering on the surface, leading to reduced D retention into W body.

[1] J. Roth, E. Tsitrone, and A. Loarte, Nucl. Instr. and Meth. in Phys. Res. B 258 (2007) 253–263

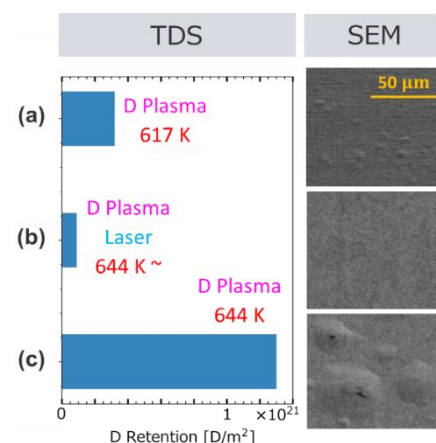


Fig. 1: Results of D absorption amount and surface morphology after irradiation. (a) and (c) are exposed to the sole D plasma, and (b) to the simultaneous D plasma and pulsed laser irradiation.

## The appearance of deuterium low temperature desorption at modified tungsten surfaces under helium pre-exposure conditions

Kota Saito<sup>1</sup>, D. Hwangbo<sup>1</sup>, H. Yoshida<sup>1</sup>, K. Onoda<sup>1</sup>, R. Sasaki<sup>1</sup>, S. Murakami<sup>1</sup>, T. Okugi<sup>1</sup>,  
A. Kataniwa<sup>1</sup>, H. Kida<sup>1</sup>, M. Sakamoto<sup>1</sup> and M. Sakamoto<sup>1</sup>

<sup>1</sup> Plasma Research Center, University of Tsukuba  
Tsukuba, Ibaraki 305-8577, Japan  
saito\_kota@prc.tsukuba.ac.jp

Tungsten (W) as the divertor and the first wall material in future nuclear fusion reactors will be exposed to hydrogen isotopes-helium (He) admixture plasmas. Estimating the amount of hydrogen isotopes absorbed in a W body during/after fusion operation is therefore of importance for the reactor safety regulation as well as to realize the steady state operation [1].

It has been known that He bubbles and He clusters are easily created and stabilized in a W bulk space. Furthermore, fiberform nanostructure, so-called 'fuzz', grows on a W surface [2]. Fuzz and He bubble themselves and W lattice defects made by them has been a long-standing issue for their role in the hydrogen isotopes retention. It is generally understood that pre-irradiated He defects can act as near-surface diffusion barrier against hydrogen isotopes. On the other hand, a recent study has shown that deuterium (D) can agglomerate and settle inside a He bubble, implying that the He defects can play a trapping site of hydrogen isotopes [3].

A previous study has also shown that D and He desorption peaks existed at  $\sim 350$  K on fuzz samples, while the surface temperature during the plasma exposure was much higher [4]. The reason for this desorption is still unclear. Our study aims to understand a potential mechanism of the low temperature desorption on W.

For experiment, the compact RF linear plasma device APSEDAS was used. Three W samples were prepared, named (i) Pristine W, (ii) Bubble W and (iii) Fuzz W. The sample (ii) and (iii) were pre-exposed to He plasmas with different conditions to form He bubbles and Fuzz on the surfaces, respectively. Then, D plasma was set and the samples were retracted  $\sim 10$  cm away from the plasma center, being exposed to not D ions but only D atoms reflected from the vacuum vessel to see if the surface absorption by D atoms are effective. Fig. 1 shows the results of thermal desorption spectra (TDS) of the samples. First, D desorption peaks around  $\sim 360$  K appear by D atom collision, indicating that the desorption is partly due to the surface absorption. Second, D desorption from the sample (i) is 50 or 100 times lower than (ii) or (iii) samples, which is estimated He effect.

The effect of He desorption and fuzz nanostructure to low temperature D desorption peak should be more researched.

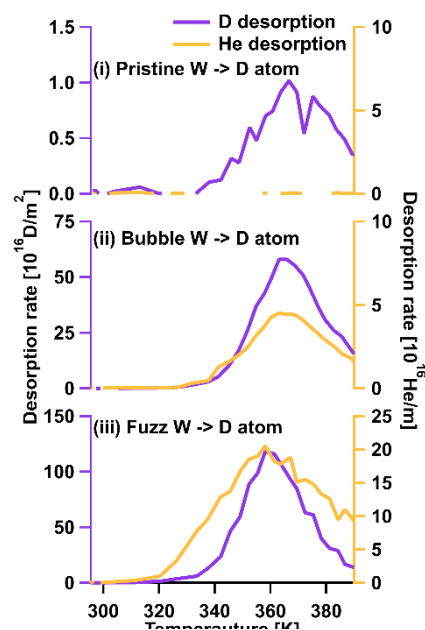


Fig. 1: D desorption spectra for three W samples at 300-400 K.

- [1] T. Tanabe, *Tritium: Fuel of Fusion Reactors* (Springer, 2017).
- [2] S. Takamura et al., *Plasma Fusion Res.*, **1**, 051 (2006).
- [3] M. Miyamoto, et al., *Nucl. Mater. Energy*, **36**, 101484 (2023).
- [4] M. Yajima, et al., *J. Nucl. Mater.*, **449**, 9-14 (2014).

## Investigation of Reaction Process during Combined Seeding of Nitrogen and Hydrogen in Divertor Simulated Plasma

Takuma OKAMOTO, Naomichi EZUMI, Satoshi TAKAHASHI, Satoshi TOGO,  
Kosuke TAKANASHI, Keishi KOUNO, Hiroto KAWAHARA, Takumi SETO,  
Reina MIYAUCHI and Mizuki SAKAMOTO

Plasma Research Center, University of Tsukuba, Tsukuba, Ibaraki 305-8577, Japan  
okamoto\_takuma@prc.tsukuba.ac.jp

One of the challenges in realizing the fusion reactor is protecting the divertor from enormous heat loads. The particle flux toward the divertor plates must be reduced to achieve heat load reduction. For this purpose, forming the detached plasma through the plasma-gas interaction is being considered [1]. The detached plasma is formed by volumetric recombination contributing to the particle flux reduction. Recently, “Nitrogen-induced Molecular-Activated Recombination (N-MAR)” during Nitrogen and Hydrogen seeding has been found effective in ion flux reduction [2,3]. This is because Dissociative Recombination of  $\text{NH}_x^+$  has higher rate coefficients in a few electron temperatures than other recombination processes such as H-MAR, and EIR. However, N-MAR reaction processes are complicated because multiple ions and molecules exist [2,4]. In this study, we investigate the reaction processes during Nitrogen and Hydrogen seeding in the divertor simulated plasma. We conduct the divertor simulated experiments and the particle and reaction balance calculations.

The experiment is conducted with the Divertor simulation experimental module (D-module) installed in GAMMA 10/PDX that is the tandem mirror device. Hydrogen plasma is generated at  $t = 50$  msec and sustained for 400 msec. We conducted the detached plasma experiments with only Hydrogen seeding and the combined seeding of Nitrogen and Hydrogen. As shown in Fig.1 (a) and (b), the ion flux and electron density ( $n_e$ ) show “rollover”, they first increase and then decrease. It can be seen that both the ion flux and  $n_e$  are lower in the combined seeding than in only Hydrogen seeding. In the case of the combined seeding, however, the ion flux decreases greater than  $n_e$ . This result indicates that heavy ions ( $\text{NH}_x^+$ ,  $\text{N}_2\text{H}^+$ ) produced in the N-MAR reaction process affect the ion flux. In this presentation, we also show the results of spectroscopic measurement and particle balance calculation.

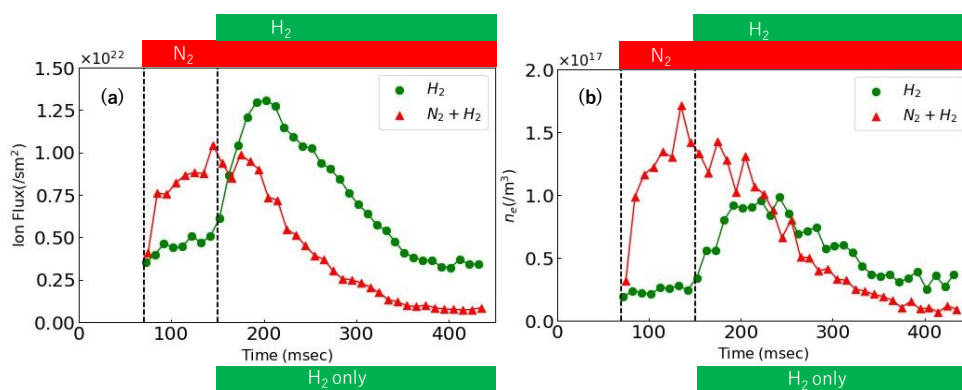


Fig.1 Time evolution of (a) the ion flux and (b) the electron density (green circle: only Hydrogen seeding, red triangle: Nitrogen and Hydrogen combined seeding).

- [1] A.W. Leonard, Plasma Phys. Control. Fusion **60**, 044001 (2018).
- [2] R. Perillo *et al.*, Plasma Phys. Control. Fusion **60**, 105004 (2018).
- [3] N. Ezumi *et al.*, Nuclear Fusion **59** (2019) 066030.
- [4] T. Okamoto *et al.*, Plasma Fusion Research **18**, 1402047 (2023)



## Electrostatic field calculation on a curved surface for gyrokinetic modeling of stellarator edge plasmas

Toseo Moritaka<sup>1</sup>, Robert Hager<sup>2</sup>, Seung-Hoe Ku<sup>2</sup> and C-S. Chang<sup>2</sup>

<sup>1</sup> National Institute for Fusion Science, Toki 509-5292, Japan  
moritaka.toseo@nifs.ac.jp

<sup>2</sup> Princeton Plasma Physics Laboratory, Princeton, NJ 08543, USA

The gyrokinetic model is commonly used to demonstrate plasma transport phenomena under self-consistent field perturbations in global magnetic field equilibria. X-point Gyrokinetic Code (XGC) is developed for whole-volume modeling of tokamaks. It utilizes an unstructured mesh and particle-in-cell method to include the edge magnetic field and the vessel components [1]. We are developing the non-axisymmetric version of XGC, namely XGC-S. XGC-S has been successfully applied for linear and non-linear simulations in the core regions of stellarators [2,3,4]. However, extending the gyrokinetic model to the edge regions remains challenging because of their complex magnetic field structures. The complexity comes not only from the non-axisymmetric configuration but also from the entangled magnetic field lines. In addition, the magnetic field lines divert significantly from the torus direction in the helical divertor configuration.

We present novel computational schemes to calculate electrostatic fields in the edge region of stellarators. The scheme includes curved surface and hierarchical mesh generation. The curved surface is generated using a numerical optimization technique to ensure it is locally perpendicular to the confinement magnetic field. This surface effectively solves the gyrokinetic Poisson equation with the perpendicular gradient operator. The finest mesh is generated by numerical field line tracing on the curved surface. Magnetic field lines with long connection lengths automatically refine important regions such as the divertor leg and the ergodic layer (Fig. 1). The iterative matrix solver using the multi-grid biconjugate gradient stabilized method is improved for electrostatic field calculation on the hierarchical mesh. Here the Jacobian matrix computed at each mesh vertex is considered in solving the Poisson equation on the curved surfaces (Fig. 2).

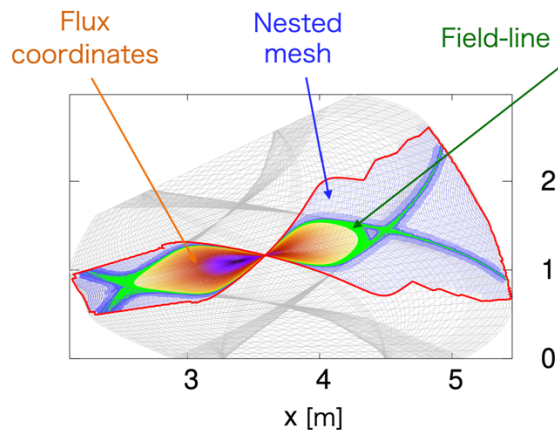


Fig. 1 : Hierarchical mesh on the optimized surface in the Large Helical Device

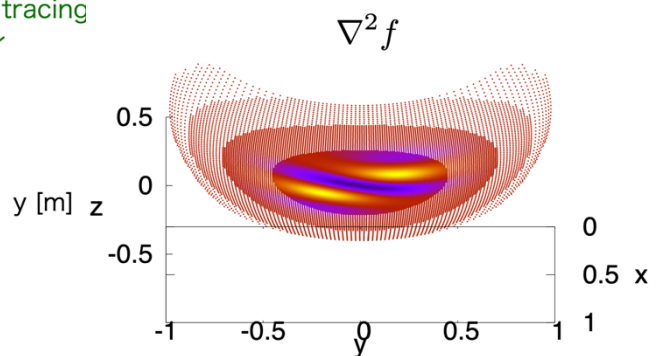


Fig. 2 : Test of the Laplacian operation using a hierarchical mesh on the unit spherical surface

- [1] S. Ku, C. S. Chang, R. Hager, et al., Phys. Plasmas **25**, 056107 (2018).
- [2] T. Moritaka, R. Hager, M. Cole, et al., Plasma **2**, 179-200 (2019).
- [3] M. Cole, R. Hager, T. Moritaka, et al., Phys. Plasmas **26**, 082501 (2019).
- [4] M. Cole, T. Moritaka, R. Hager, et al., Phys. Plasmas **27**, 044501 (2020).
- [5] T. Moritaka, H. Sugama, M. Cole, et al., Nucl. Fusion **62**, 126059 (2022).

## Development of a kinetic transport model in broken flux surfaces

J. X. Li<sup>1</sup>, T. Moritaka<sup>1,2</sup>, R. Kanno<sup>1,2</sup>, G. Kawamura<sup>1,2</sup>, R. Hager<sup>3</sup> and C.S. Chang<sup>3</sup>

<sup>1</sup> The Graduate University for Advanced Studies, SOKENDAI, Toki 509-5292, Japan  
li.joseph@nifs.ac.jp

<sup>2</sup> National Institute for Fusion Science, Toki 509-5292, Japan

<sup>3</sup> Princeton Plasma Physics Laboratory P.O. Box 451, Princeton, NJ 08543, USA

Modern toroidal magnetic fusion devices often have broken flux surfaces with magnetic islands and ergodic layers generated by resonant magnetic perturbations (RMPs). Such broken flux surfaces may play a role in the control of MHD instabilities, such as Edge Localized Modes [1]. In the devices using RMPs, effects of broken flux surfaces on edge turbulence and neoclassical transport are also worthy of interest. In this study, to adequately treat the effects of these structures on kinetic transport phenomena, a kinetic model is developed, based on a kinetic simulation in a toroidal plasma equilibrium including RMPs.

The X-point Gyrokinetic Code (XGC) utilizes particle-in-cell (PIC) methods with an unstructured mesh without assuming flux coordinates for whole volume modeling of tokamaks [2]. A stellarator compatible version, XGC-S [3], can treat broken flux surfaces under non-axisymmetric magnetic field perturbations. We use analytic circular tokamak equilibria [4] wherein islands and ergodic layers changed gradually according to RMPs in XGC-S and calculated the resulting transport coefficients. Additionally, we will extend this study to stellarators using, for example, the equilibrium of the planned CFQS [5], and present preliminary calculations.

The initial simulation result of calculating an electrostatic potential in a circular tokamak plasma without RMPs is shown in the figure below. To stimulate the formation of islands, a magnetic perturbation of the form  $\delta\mathbf{B} = \nabla \times (\alpha\mathbf{B})$ , where  $\alpha = \alpha_0 \cos(m\theta - n\phi) \exp[-(r_{nm}^2 - r^2)^2/\Delta r^4]$ , is applied. Here,  $\alpha_0$  is chosen according to other parameters such as the mode numbers  $m/n$ ,  $\theta$  is the poloidal angle,  $\phi$  is the toroidal angle,  $R_{ax}$  is the toroidal axis, and  $r = \sqrt{(R - R_{ax})^2 + Z^2}$ . The kinetic modeling is performed in magnetic structures with islands/ergodic layers generated gradually according to the strength of RMPs.

With an eye towards complex stellarator geometries, we believe the ability to accurately model perturbative magnetic phenomena will be a great asset in stellarator design and the study of edge plasmas in magnetic fusion devices.

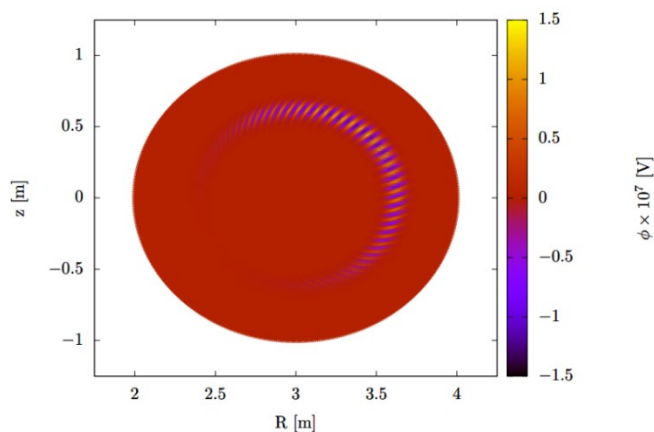


Figure 1: ITG mode electrostatic potential fluctuations from a linear XGC-S simulation with an analytic circular tokamak equilibrium

### References:

- [1] Kirk, A. et. al. Plasma Phys. Contr. Fusion, 55(12), 124003 (2013).
- [2] Ku, S., Chang, C. S., Diamond, P. H. Nucl. Fusion, 49(11), 115021 (2009).
- [3] Moritaka, T. et. al. Plasma, 2(2), 179–200 (2019).
- [4] Kanno, R., et al., Nucl. Fusion 58, 016033 (2018).
- [5] Liu, H. et. al. Nucl. Fusion, 61(1), 016014 (2020).

## Example of Medical and Engineering Collaboration in Data Analysis in the field of the Nuclear Fusion

Yoshihide Shibata<sup>1</sup>, Hoshino Shinsuke<sup>2</sup>, Ryusuke Ae<sup>3</sup>, Tohru Kobayashi<sup>4</sup>  
and Hiromichi Hamada<sup>5</sup>

<sup>1</sup> *National Institute of Technology, Gifu college  
2236-2, Kamimakuwa, Motosu, Gifu, 501-0495, Japan  
shibata.yoshihide@gifu-nct.ac.jp*

<sup>2</sup> *Shiga University of Medical Science,*

<sup>3</sup> *Jichi medical University,*

<sup>4</sup> *National Center for Child Health and Development,*

<sup>5</sup> *Chiba University*

Medical records such as patient data and lab data are stored in data storage in each hospital for medical treatment. The size of medical data stored in each hospital is increasing due to the development of medical devices. However, physicians are not expert for data analysis, many physicians cannot make specialized tools for large-scale analysis to analyze these medical data. In the field of engineering, researchers often use a programming language for making data analysis tools. We consider that a collaboration between medical and engineering could provide the new future of medical data analysis.

Kawasaki Disease (KD) is a unique disease for child and the onset mechanism has not been clarified yet although this disease was discovered almost 50 years ago. There is large data set for KD in Japan for research of etiology in KD, which is called nationwide survey in KD, however large-scale data analysis such as by using AI algorithm has not yet been carried out yet. Our team was focused on this point, we made a collaborative team between medical and engineering departments for large-scale data analysis in KD. In our activities, the epidemiology of KD during COVID-19 pandemic periods was investigated by using nationwide survey in KD and data analysis technics in the nuclear fusion and some papers was published in medical journals[1-2]. In this presentation, we will explain examples of medical and engineering collaboration in KD data analysis by using our activities.

[1] R. Ae, Y. Shibata, *et. al.*, J. Pediatr. 2021;250: P54-60.E5.

[2] S. Hoshino, Y. Shibata, *et. al.*, J. Pediatr. 2022;239:50-58.e2.

## Synthesis of graphitic carbon nitride on carbon nanowalls

Kouta Ishigure<sup>1</sup>, Keigo Takeda<sup>1</sup> and Mineo Hiramatsu<sup>1</sup>

<sup>1</sup> Meijo University, Shiogamaguchi, Tempaku, Nagoya 468-8502, Japan  
223427004@ccmailg.meijo-u.ac.jp

Photocatalytic semiconductor is promising for the purification of environmental organic pollutants because it can effectively decompose pollutants into inorganic compounds such as CO<sub>2</sub> and H<sub>2</sub>O. Recently, graphitic carbon nitride (g-C<sub>3</sub>N<sub>4</sub>) has attracted much attention due to its unique properties such as high chemical and thermal stability, suitable electronic band structure for visible light responsiveness, and cost efficiency [1]. However, g-C<sub>3</sub>N<sub>4</sub> has low photocatalytic performance because of its low specific surface area in visible light. The g-C<sub>3</sub>N<sub>4</sub> can be synthesized by vapor deposition polymerization using guanidine carbonate as a raw material or electrodeposition in acetonitrile solvent, and baking dicyandiamide as raw material has been attempted. Among these methods, vapor phase transport is known as a liquid-free method [2]. Carbon nanowalls (CNWs) are two-dimensional nanostructures with open boundary edges composed of stacks of graphene sheets standing nearly vertically on the substrate. Due to their vertical alignment and interspacing, CNWs have large surface area and act like an electrode network [3]. We aim to develop g-C<sub>3</sub>N<sub>4</sub>-based catalytic material with large specific surface area by combining with CNWs. In this study, we synthesized g-C<sub>3</sub>N<sub>4</sub> on CNWs by the vapor phase transport method using melamine.

CNW film was grown by inductively coupled plasma-enhanced chemical vapor deposition (ICP-CVD) [4] on heated (600 °C) Si substrate for 30 min. RF (13.56 MHz) power was 600 W and a chamber pressure was kept at 15 mTorr with H<sub>2</sub> and CH<sub>4</sub> flow rates of 25 and 5 sccm, respectively. Then, carbon nitride was synthesized on the CNWs using a hot-wall thermal CVD apparatus consisting of a ceramic tube and an electric furnace. Melamine as a raw material was placed on Si substrate, and CNW film grown on another Si substrate was placed 10 mm away from the melamine. These Si substrates were covered with aluminum foil and placed in the ceramic tube. Synthesis of carbon nitride was carried out under atmospheric pressure at 600 °C for 2 h. Synthesized product was characterized using scanning electron microscopy (SEM), photoluminescence (PL), and Fourier-transform infrared spectroscopy (FT-IR).

Figure 1 shows FT-IR spectra of (a) CNWs, (b) product on the Si substrate where the raw material was placed, and (c) product synthesized on CNWs. Regarding the FT-IR analysis for g-C<sub>3</sub>N<sub>4</sub>, CN heterocyclic stretching vibration around 1240-1630 cm<sup>-1</sup> and N-H stretching vibration around 3250 cm<sup>-1</sup> have been reported [5]. Clear absorption peaks due to CN heterocyclic stretching vibration and N-H stretching vibration were observed in the FT-IR spectrum of the product synthesized on CNWs, indicating the synthesis of g-C<sub>3</sub>N<sub>4</sub> on CNWs.

[1] X. Wang et al., *Nature materials* 8, 76 (2009).

[2] J. Wang et al., *Chem. Commun.* 19, 2258-2259 (2002).

[3] M. Hiramatsu et al., *App. Phys. Lett.* 84, 4708 (2004).

[4] M. Hiramatsu et al., *Jpn. J. App. Phys.* 52, 01AK05 (2013).

[5] Y. Bu et al., *Electrochim. Acta* 88, 294-300 (2013).

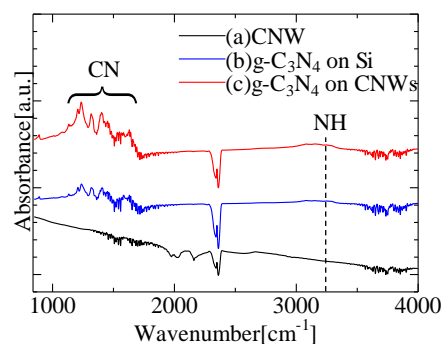


Fig. 1 FT-IR spectra of (a) CNWs and products synthesized on (b) Si and (c) CNWs.

## Nitrogen addition to diamond using radical injection-CVD

Kodai Ishikawa<sup>1</sup>, Keigo Takeda<sup>1</sup> and Mineo Hiramatsu<sup>1</sup>

<sup>1</sup> Meijo university

1-501, Shiogamaguchi, Tenpaku, Nagoya 468-8502, Japan  
223427002@ccmailg.meijo-u.ac.jp

Diamond possesses excellent properties such as a wide bandgap, high thermal conductivity, and high hardness. Additionally, by doping impurities, it exhibits semiconductor characteristics, making it a promising material for next-generation semiconductors. However, the deposition of nitrogen-doped diamond (NDD) which exhibits an n-type conduction is relatively difficult because the efficiency of nitrogen-doping is not so high [1] and the nitrogen-doping into diamond tends to change the crystal structure [2]. To solve this issue, a deposition method utilizing radical injection-CVD (RI-CVD) technique [3] has been applied in this study.

In this study, we utilized microwave plasma (MWP) (ASTeX-Type) combined with inductively coupled plasma (ICP) to deposit nitrogen-doped diamond films. By employing ICP, we aimed to promote the dissociation of nitrogen molecules ( $N_2$ ), facilitating the incorporation of nitrogen-related active species into the diamond film.

Figure 1 shows the schematic of RI-CVD system used in this study. The MWP is used for the main CVD to grow diamond films, and reactive species generated by the remote ICP are introduced into main plasma region. For the MWP, a mixture of  $H_2$  and  $CH_4$  was used as a source gas mixture. For the remote ICP, the main chamber is equipped with a quartz tube of 30 mm in diameter and 250 mm long, which is surrounded by a 5-turn solenoid antenna. A carbon rod connected to the GND is inserted into the quartz tube so that the ICP is generated even under high pressure ( $\sim 55$  Torr). A mixture of  $N_2$  and  $H_2$  ( $N_2/H_2 = 500$  ppm) was flowed through the quartz tube.

NDDs were deposited on the pretreated Si substrate at an  $N_2$  flow rate of 500 ppm relative to  $H_2$ . Figure 2 compares the PL spectra of NDDs deposited by MWP and RI-CVD; a peak at 1.68 eV was observed with and without ICP, whereas a peak due to the N-V center (2.16 eV) was clearly observed in the NDDs deposited by RI-CVD, indicating that the nitrogen addition is enhanced by applying RI-CVD.

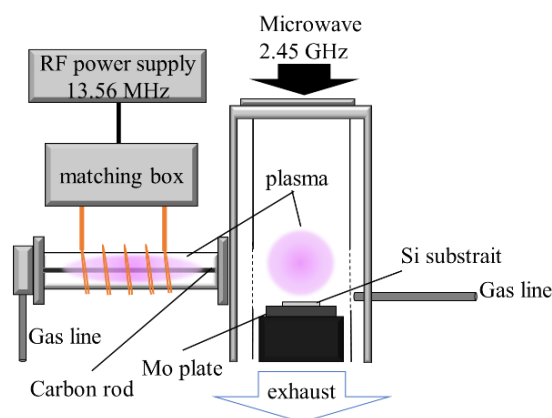


Fig. 1 Schematic of RI-CVD apparatus comprising MWP and ICP

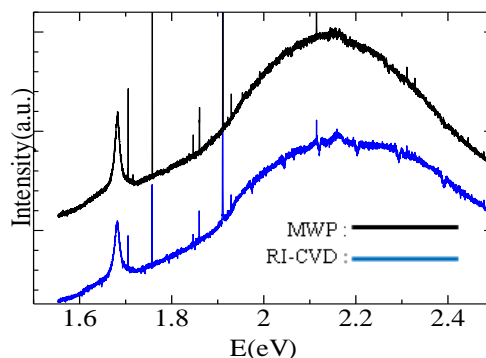


Fig.2 Comparison of PL spectra of NDDs deposited by MWP and RI-CVD

[1] S. Jin, et al., Appl. Phys. Lett., 65, 403 (1994).

[2] R. Locher, et al., Appl. Phys. Lett., 65, 34 (1994).

[3] M. Hori, et al., J. Phys. D: Appl. Phys., 44, 174027 (2011).

## **Defluorinated degradation of per/poly fluoro alkyl substances (PFAS) in water using non-thermal plasma**

Zhe-Wei Gong<sup>1</sup>, Chih-Yu Ko<sup>1</sup>, Jang-Hsing Hsieh<sup>2</sup> and Wen-Hui Kuan<sup>1\*</sup>

<sup>1</sup>*Department of Safety, Health and Environmental Engineering, Ming Chi University of Technology, Taishan New Taipei, Taiwan*

\*Corresponding author: [whkuan@mail.mcut.edu.tw](mailto:whkuan@mail.mcut.edu.tw)

<sup>2</sup>*Center for Plasma and Thin Film Technologies, Ming Chi University of Technology, Taishan, New Taipei, Taiwan*

per/poly fluoro alkyl substances (PFAS) feature carbon chains where all hydrogen atoms have been replaced by fluorine atoms, forming strong and stable carbon-fluorine bonds. The strength of these carbon-fluorine bonds renders PFAS resistant to degradation under common environmental conditions, resulting in high stability. Due to the robustness of the carbon-fluorine bonds, water molecules are unable to effectively interact with them, making PFAS difficult to dissociate or dissolve in water. This property poses potential risks to the environment and health, as the accumulation of perfluorinated compounds can lead to environmental pollution and potential threats to ecosystems and human health.

Non-thermal plasma technology is typically accompanied by the generation of electric fields and reactive chemical radicals, making it suitable for treating stubborn pollutants. Key factors in low-temperature plasma technology include discharge stability, the medium used, and reactor structure. Parameters such as pollutant concentration, pH value, treatment duration, and voltage adjustment can impact degradation efficiency.

This study employs non-thermal plasma technology as an innovative method for defluorinated degradation of the PFAS in water. Perfluorohexanoic acid (PFHxA) was chosen as the target pollutant in the study. Experimental results demonstrated that under positive polar electrode installation, PFHxA can be effectively degraded in 20 min. As plasma treatment progresses over time, the pH of the solution declined, facilitating fluoride degradation. Different modules yielded varying removal efficiencies, with longer-chain fluorinated compounds possessing more carbon atoms exhibiting hydrophobicity and rapid decomposition. Dissolved electron and argon molecule with positive valence were believed to be the key elements for defluorination. However, due to the hydrophobic nature of PFAS, effective aeration was necessary to achieve optimal degradation efficiency.

## Immobilization of glucose oxidase on carbon nanowalls

Jumma Kagami<sup>1</sup>, Keigo Takeda<sup>1</sup> and Mineo Hiramatsu<sup>1</sup>

<sup>1</sup> Department of Electrical and Electronic Engineering, Meijo University,  
1-501 Shiogamaguchi, Tempaku, Nagoya 468-8502, Japan  
223427011@ccmailg.meijo-u.ac.jp

Carbon nanowalls (CNWs) consist of multilayer nanographene grown perpendicularly to the substrate, providing substantial specific surface area, excellent electrical conductivity, and chemical stability. Therefore, CNWs have potential functions as electrodes for batteries and biosensors by applying surface modifications with metal nanoparticles and enzymes [1].

In this study, CNWs were applied to electrode materials for biofuel cells (BFCs). Glucose oxidase (GOD) was chosen as the enzyme, and the surface of CNWs was modified with the GOD. The enzymatic property of GOD immobilized on CNW surface was investigated using UV spectrophotometer.

CNW films were grown on Si substrates using inductively coupled plasma-enhanced chemical vapor deposition (ICP-CVD) system [2] with a mixture of CH<sub>4</sub> and Ar at a pressure of 15 mTorr, a Si substrate temperature 600 °C, and a RF power of 600 W for 30 min. Prior to the immobilization of oxidoreductase enzymes on CNWs, surface treatment using microwave excited atmospheric pressure plasma jet (MW-APPJ) was carried out to modify the CNW surface with hydrophilic groups such as carboxyl groups. Then, hydrophilized CNWs were immersed in buffer solution (pH 6.5) containing GOD for 24 hours to modify CNW surface with GOD.

The hydrogen peroxide (H<sub>2</sub>O<sub>2</sub>) produced by the reaction between GOD and D-glucose react with peroxidase, 4-aminoantipyrine, and phenol, resulting in the formation of a red quinone dye [3]. Since this red quinone dye has an absorption maximum at a wavelength of 505 nm, the amount of H<sub>2</sub>O<sub>2</sub> produced by the reaction between GOD and D-glucose was estimated by measuring the absorbance with a UV spectrophotometer.

Figure 1 shows the results of enzyme activity measurements obtained by an UV spectrophotometer for CNWs with/without surface treatment using MW-APPJ. The absorbance for the surface-treated CNWs was higher than that of the CNWs without surface treatment. Based on a calibration curve obtained using hydrogen peroxide with different concentrations, the amount of H<sub>2</sub>O<sub>2</sub> produced was estimated to be 2.1 mM with surface treatment and 1.2 mM without surface treatment. The surface treatment with MW-APPJ provides hydrophilic groups such as carbonyl and carboxyl groups to the surface of CNWs. This suggests that the amount of immobilized GOD increased due to the dehydration condensation reaction between the carboxyl groups on the surface of the CNWs and the amino groups of the enzyme by the condensation reagent.

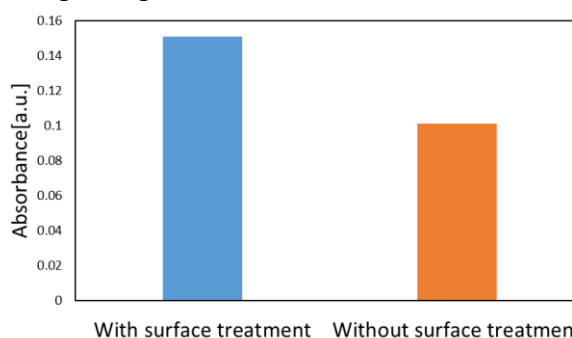


Fig. 1: Absorbance of solution after enzymatic reaction of GOD immobilized on CNWs

[1] M. Hiramatsu, K. Shiji, H. Amano, M. Hori, Appl. Phys. Lett. 84, 4708 (2004).

[2] M. Hiramatsu, Y. Nihashi, H. Kondo, M. Hori, Jpn. J. Appl. Phys. 52, 01AK05 (2013).

[3] M. Shimomura, H. Kikuchi, T. Yamauchi, S. Miyauchi, Pure Appl Chem. 33, 1687 (1996).

## Protein aggregation driven by atmospheric pressure plasma between needle electrode and surface of albumin solution

Yukei Ishihara<sup>1,2</sup>, Tetsuji Shimizu<sup>1</sup>, and Hajime Sakakita<sup>1,2</sup>

<sup>1</sup> National Institute of Advanced Industrial Science and Technology (AIST),  
Central2, 1-1-1 Umezono, Tsukuba, Ibaraki 305-8568, Japan  
S2220826@s.tsukuba.ac.jp

<sup>2</sup> University of Tsukuba,  
1-1-1 Tennodai, Tsukuba, Ibaraki 305-8577, Japan

Low-temperature atmospheric pressure plasma allows a surface treatment without causing thermal damage. Due to this characteristic, low-temperature atmospheric pressure plasmas have been investigated for application in the biological and medical fields. As an example of promising applications, hemostasis by low-temperature plasma treatment was proposed [1]. In many cases, cauterization is used to stop bleeding in surgery. However, cauterization causes heat injury even outside of the hemostasis area. To reduce such thermal damage on tissues, the usage of low-temperature atmospheric pressure plasmas has been proposed and discussed [1].

Previous studies showed that the aggregation of blood proteins is one factor in hemostasis by plasma treatment. Additionally, it was suggested that electrical property of the plasma treatment is important for protein aggregation [2]. However, the detailed mechanism of the protein aggregation is still not clear. This study aims to understand the mechanism of protein aggregation by low-temperature atmospheric pressure plasma.

Plasma treatments were conducted using the setup as shown in Figure 1. The plasma was produced between a needle electrode and the surface of albumin solution by applying high voltage. Albumin solution was used in the treatment because albumin is the most abundant protein in blood. The plasma treatment results in aggregation of albumin as shown in the inset in Figure 1. The growth process of aggregate was recorded and analyzed. Dependences of time evolution of aggregate on plasma treatment conditions were investigated. The relationship between the growth process and the conditions will be discussed in the conference.

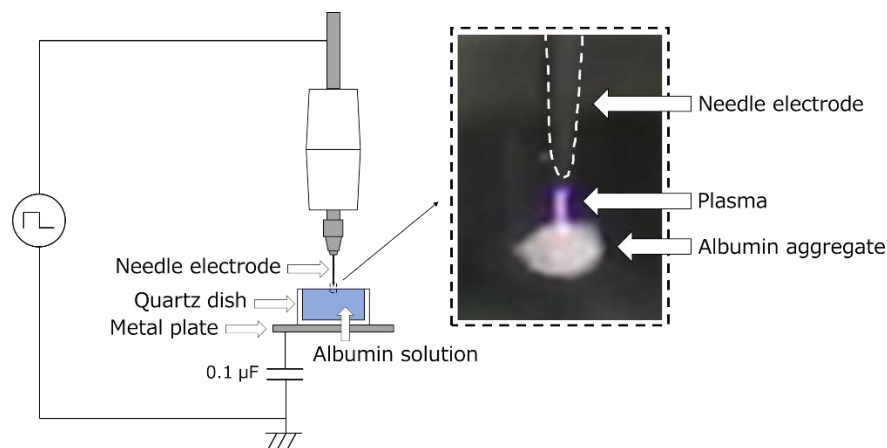


Fig. 1: Experimental setup for protein aggregation. The inset shows the aggregate on the albumin solution.

- [1] References: H. Sakakita and Y. Ikehara, *Plasma and Fusion Research* **5**, S2117 (2010).  
[2] H. Sakakita, H. Yamada, T. Shimizu, M. Fujiwara, S. Kato, J. Kim, S. Ikehara, N. Shimizu, and Y. Ikehara, *J. Phys. D: Appl. Phys.* **54**, 215201 (2021).



## Advances in Development of Quasi-axisymmetric Stellarator at National Institute for Fusion Science

Mitsutaka Isobe<sup>1,2</sup>, Akihiro Shimizu<sup>1,2</sup>, Kunihiro Ogawa<sup>1,2</sup>, Hiromi Takahashi<sup>1,2</sup>,  
Takanori Murase<sup>1</sup>, Hiroyuki Tanoue<sup>1</sup>, Sho Nakagawa<sup>1</sup>, Masaki Osakabe<sup>1,2</sup>,  
and Hiroyuki Yamaguchi<sup>1,2</sup>

<sup>1</sup> *National Institute for Fusion Science, National Institutes of Natural Sciences  
322-6, Oroshi, Toki, 509-5292, Japan  
isobe.mitsutaka@nifs.ac.jp*

<sup>2</sup> *The Graduate University for Advanced Studies, SOKENDAI  
322-6, Oroshi, Toki, 509-5292, Japan*

A stellarator embedded with the magnetic symmetry of tokamak, hereafter quasi-axisymmetric stellarator (QAS), was proposed in the middle of 1990s [1,2], and is now attracting attention again[3-6] since it will be disruption-free and is expected to provide plasma confinement relevant to that of tokamaks while retaining steady-state operation capability.

The National Institute for Fusion Science (NIFS) has been developing QAS, i.e., net-current-free tokamak in both physics and engineering aspects since 1996. The first QAS in NIFS was designed to be post-CHS, and was named CHS-qa. The toroidal period number ( $N$ ) and major radius ( $R$ ) of CHS-qa were 2 and 1.5 m, respectively. The target maximum toroidal magnetic field strength ( $B_t$ ) was 1.5 T. To be closer to aspect ratio ( $A_p$ ) of tokamak, the CHS-qa was designed to be low  $A_p$  of 3.2, following the policy of CHS. A primary purpose of CHS-qa was to explore higher confinement regime of stellarator plasma through embedding axisymmetry to 3-D torus and resulting reduction of non-axisymmetric magnetic field ripple. The CHS-qa was not realized, and the design work was completed in 2004.

After many years, the opportunity to construct QAS came in 2017. NIFS and Southwest Jiaotong University, China decided to implement a joint project together for design and construction of a new stellarator CFQS based upon a quasi-axisymmetry (QA) concept. The CFQS has  $N$  of 2 like CHS-qa and  $R$  of 1 m, and is now under construction [7]. The first plasma of CFQS will be achieved in 2024. To reduce technology challenges coming from strong electromagnetic force, space availability, and manufacturability due to low  $A_p$ , we chose  $A_p$  of 4 and the maximum  $B_t$  of 1 T for the CFQS. The CFQS will be dedicated to proof-of-principle experiment to prove intrinsic advantages of QAS with superior plasma diagnostics [8].

Lately significant progress has been made in QAS development at NIFS. We have found QA configuration of which QA-ness is largely enhanced compared with that of CHS-qa and CFQS. In this paper, progress of physics and engineering design for QAS at NIFS are presented.

[1] J. Nührenberg *et al.*, in Theory of Fusion Plasmas (Proc. Joint Varenna-Lausanne Int. Workshop Varenna, 1994), (Bologna:Editrice Compositori), p3 (1994).

[2] P.R. Garabedian, Phys. Plasmas **3** (1996) 2483.

[3] M. Isobe *et al.*, Plasma Fus. Res. **14** (2019) 3402074.

[4] S.A. Henneberg *et al.*, Nucl. Fusion **59** (2019) 026014.

[5] Z.Y. Lu *et al.*, Nucl. Fusion **61** (2021) 106028.

[6] T. Qian *et al.*, Nucl. Fusion **62** (2022) 084001.

[7] A. Shimizu *et al.*, Nucl. Fusion **62** (2022) 016010.

[8] A. Shimizu *et al.*, JINST **17** (2022) C06004.

## Low-Temperature Sintering of Activated Carbon Using Spark Plasma Sintering

Yuto YANAGIHARA<sup>1</sup>, Sho NAKAGAWA<sup>1</sup>, Takanori MURASE<sup>1</sup>, Kazuki NAGAHARA<sup>1</sup>, Hiroyuki TANOUE<sup>1</sup>, Mitsutaka ISOBE<sup>1,2</sup>, Kunihiro OGAWA<sup>1,2</sup>, Akihiro SHIMIZU<sup>1,2</sup>, Hiroyuki NOTO<sup>1</sup>, Yuki HAYASHI<sup>1,2</sup>, Pham Thi Huong Ngat<sup>3</sup>, Tomohiro SHIOZAKI<sup>3</sup>, Toshiaki SOGABE<sup>3</sup> and Mudtorlep Nisoa<sup>4</sup>

<sup>1</sup> National Institute for Fusion Science, National Institutes of Natural Sciences  
322-6, Oroshicho, Toki, 509-5292, Japan  
[yanagihara.yuto@nifs.ac.jp](mailto:yanagihara.yuto@nifs.ac.jp)

<sup>2</sup> The Graduate University for Advanced Studies, SOKENDAI  
322-6, Oroshicho, Toki, 509-5292, Japan

<sup>3</sup> ANAORI CARBON Co., Ltd.  
6-20, Hatakedacho, Ibaraki, Osaka, 567-0028, Japan

<sup>4</sup> Functional Materials & Nanotechnology Center of Excellence, Walailak University  
Nakhon Si Thammarat, 80160, Thailand

In the plasma experimental device at National Institute for Fusion Science, activated carbon is utilized as an adsorbent within a cryopump to create the ultra-high vacuum environment necessary for generating high-temperature plasma. The extensive porous structure of activated carbon is employed as a substrate in the cryopumps, adsorbing gas molecules, including hydrogen, on its surface at cryogenic temperatures.

In this study, we aim to develop suitable activated carbon for cryopump applications. Solidified activated carbon is necessary to mount it in a cryopump. Usually, activated carbon is solidified by mixing the activated carbon powder with a binder. However, the use of binders obstructs the pores of the activated carbon, leading to a decline in its adsorption performance. Thus, the focus shifts to the Spark Plasma Sintering (SPS) method, a technique involving pressure and pulsed current heating to facilitate the sintering of activated carbon without binders.

Using the SPS technique, commercially available activated carbon powder was sintered at six different temperatures ranging from 650°C to 1600°C. As a result, the activated carbons were successfully sintered at every sintering temperature. Notably, as shown in Fig. 1, the specific surface area of the activated carbon exhibited an increase with lower temperature sintering. Additionally, activated carbon sintered at temperatures below 800°C displayed a greater specific surface area compared to powdered activated carbon prior to sintering. Details will be reported in the presentation.

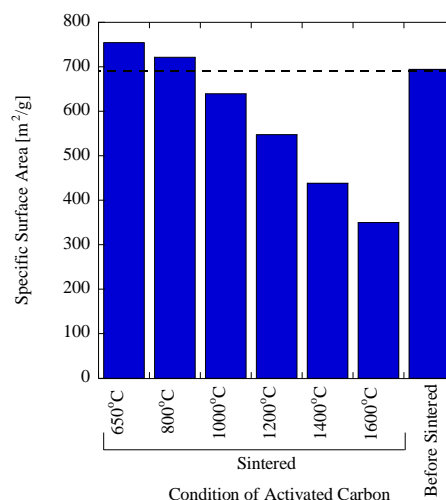


Fig. 1: Specific surface area of activated carbon at each sintering temperature and prior to sintering.

## Enhancement to gas puffing control system in LHD

Kazuki Nagahara, Hiromi Hayashi, Naoyuki Suzuki, Takanori Murase, Kohji Yasui, Yasuyuki Tsuchibushi, Hiromi Kato, Masateru Kawai, Hidenori Takubo, Sho Nakagawa, Hiroki Chimura, Yuto Yanagihara

*National Institute for Fusion Science, National Institutes of Natural Sciences,  
322-6 Oroshi-cho, Toki, Gifu 509-5292, Japan  
[nagahara.kazuki@nifs.ac.jp](mailto:nagahara.kazuki@nifs.ac.jp)*

In the Large Helical Device (LHD), the precise control of electron density is often required according to the plasma experiment scenario. The electron density is controlled by supplying the prescribed amount of fuel gas through the piezo valve. The previous gas puffing control system was based on the feedback control of conventional proportional (P) control and required several shots of plasma discharge to obtain the target electron density. To improve the performance of electron density control, we have developed the feedback control system based on proportional-integral (PI) control.

PI control is expressed by the following equation:

$$V_{ctrl} = K_P e + K_I \int e dt,$$

where  $V_{ctrl}$ ,  $K_P$ ,  $e$ , and  $K_I$  represent the control voltage of the piezo valve, the P gain, the deviation of the current value from the target value of electron density, and the I gain, respectively. P gain and I gain (PI gain) adjustment is essential for the proper PI control. PI gain adjustment was performed during the actual plasma discharge. First, the initial value of the PI gain was determined using the electron density signal simulated for that of far-infrared laser interferometer by use of a function generator as a referential signal. PI control was performed with the initial PI gain value, but the electron density oscillated unfavorably in this case. Next the PI gain was adjusted to obtain the optimum value. As a result of applying the optimal value for the PI gain, the target electron density could be obtained in almost all cases in a single shot. The time evolutions of electron density with the initial value and the optimal value are shown in Fig. 1.

In addition to constant electron density control, other density controls, e.g., ramp-up control, which increases the density at a constant rate of change, and sinusoidal control, which makes the electron density sinusoidal are required. With gain-optimized PI control, these controls could also be easily implemented.

In this presentation, details of the gain adjustment and examples of well controlled various electron density will be presented.

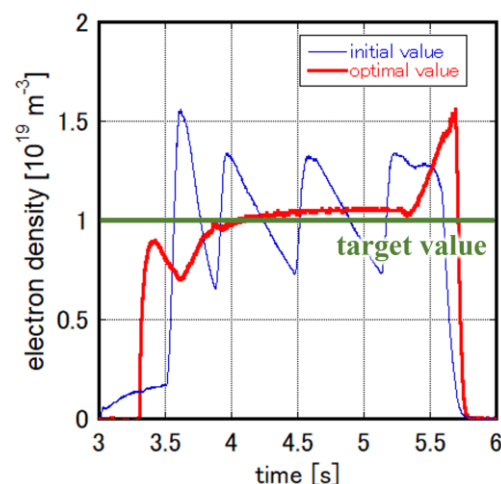


Fig. 1: Time evolution of electron density with PI control with gain as the initial value (shot# 163827) and the optimal value (shot# 182450).

## Surface observation on heat-treated activated carbon derived from unutilized biomass

Sho NAKAGAWA<sup>1</sup>, Yuto YANAGIHARA<sup>1</sup>, Takanori MURASE<sup>1</sup>, Kazuki NAGAHARA<sup>1</sup>,  
Hiroyuki TANOUE<sup>1</sup>, Mitsutaka ISOBE<sup>1,2</sup>, Kunihiro OGAWA<sup>1,2</sup>, Akihiro SHIMIZU<sup>1,2</sup>,  
Hiroyuki NOTO<sup>1</sup>, Yuki HAYASHI<sup>1,2</sup>, Pham Thi Huong Ngat<sup>3</sup>, Tomohiro SHIOZAKI<sup>3</sup>,  
Toshiaki SOGABE<sup>3</sup>, Mudtorlep Nisoa<sup>4</sup>

<sup>1</sup> National Institute for Fusion Science, National Institutes of Natural Sciences  
Toki, Gifu 509-5292, Japan  
[nakagawa.sho@nifs.ac.jp](mailto:nakagawa.sho@nifs.ac.jp)

<sup>2</sup> The Graduate University for Advanced Studies, SOKENDAI  
Toki, Gifu 509-5292, Japan

<sup>3</sup> ANAORI CARBON Co., Ltd  
Ibaraki, Osaka, 567-0028 Japan

<sup>4</sup> Functional Materials & Nanotechnology Center of Excellence, Walailak University,  
Nakhon Si Thammarat, 80160, Thailand

The purpose of this research is to develop a functional activated carbon with outstanding adsorption property using unutilized biomass as raw material. To achieve this goal, various attempts have been made, such as vacuum heating for removing silica and Spark Plasma Sintering (SPS) for binder-less solidification.

Microstructures and adsorption properties of prepared samples have been investigated. In surface analysis with SEM-EDS, needle-like structure of silicon carbide (SiC), known as SiC whisker, was observed on some samples. It is known that SiC whisker has excellent properties such as high strength and high temperature resistance and can be used as reinforcement composite material for metals and ceramics to improve their mechanical property.

Figure 1 shows image of SiC whiskers observed on a surface of biomass carbon, which is sintered by SPS at 1600°C and 30 MPa. Figure 2 shows EDS elemental mapping of carbon and silicon. It indicates a presence of Si on the whiskers in Fig. 1, which suggests that they are made of SiC.

In this presentation, we will focus on SiC whiskers, and report on the differences in their growing states depending on the treatment conditions and their potential application.

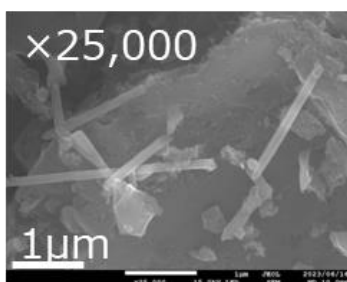


Fig. 1: Image of SiC whiskers observed on biomass carbon

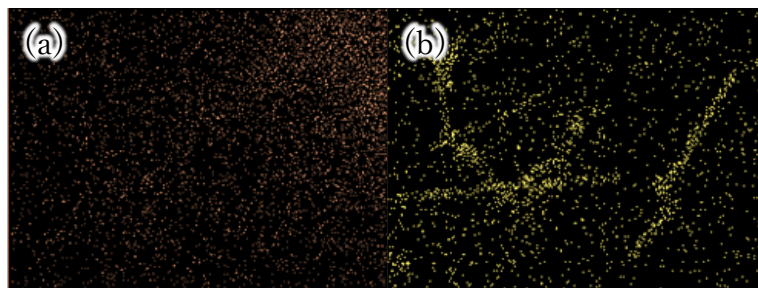


Fig. 2: Images of EDS elemental mapping (a) of Carbon (b) and Silicon

## Ferroptosis induced by plasma-activated Ringer's lactate solution prevents oral cancer progression

Kotaro Sato<sup>1,2,\*</sup>, Ming Yang<sup>1,2</sup>, Kae Nakamura<sup>3</sup>, Hiromasa Tanaka<sup>3</sup>, Masaru Hori<sup>3</sup>, Miki Nishio<sup>4</sup>, Akira Suzuki<sup>4</sup>, Hideharu Hibi<sup>1,3</sup>, Shinya Toyokuni<sup>2,3</sup>

<sup>a1</sup>*Department of Oral and Maxillofacial Surgery, Nagoya University Graduate School of Medicine, 65 Tsurumai-cho, Showa-ku, Nagoya 466-8550, Japan*

<sup>b2</sup>*Department of Pathology and Biological Responses, Nagoya University Graduate School of Medicine, 65 Tsurumai-cho, Showa-ku, Nagoya 466-8550, Japan*

<sup>c3</sup>*Center for Low-Temperature Plasma Sciences, Nagoya University, Furo-cho, Chikusa-ku, Nagoya 464-8603, Japan*

<sup>d4</sup>*Division of Molecular and Cellular Biology, Kobe University Graduate School of Medicine, 7-5-1 Kusunoki-cho, Chuo-ku, Kobe 650-0017, Japan*

**Objective:** This study aimed to investigate the effect of plasma-activated Ringer's lactate solution (PAL) on oral squamous cell carcinoma (OSCC) cells and carcinogenic processes with a particular focus on iron and collagenous matrix formation.

**Materials and Methods:** We used three OSCC cell lines, one keratinocyte cell line and two fibroblast lines, and cell viability assays, immunoblotting, flow cytometry and transmission electron microscopy were performed to evaluate the effect and type of cell death. The effect of PAL treatment on lysyl oxidase (LOX) expression was investigated *in vitro* and *in vivo*. Tamoxifen-inducible *Mob1a/b* double-knockout mice were used for the *in vivo* experiment.

**Results:** PAL killed OSCC cells more effectively than control nontumorous cells and suppressed cell migration and invasion. The type of cell death was ferroptosis, and the protein level of LOX was down-regulated in cancer cells *in vitro* and *in vivo*. Additionally, PAL improved the survival rate of mice and suppressed collagenous matrix formation.

**Conclusions:** We demonstrated that PAL specifically kills OSCC cells and that ferroptosis occurs *in vitro* and *in vivo*. Furthermore, PAL can prevent oral carcinogenesis and improve the survival rate by changing collagenous matrix formation via LOX suppression.

## Plasma-activated solutions invigorate anti-tumor immune response in the intraperitoneal environments of ovarian cancer

Kae Nakamura<sup>1,2</sup>, Nobuhisa Yoshikawa<sup>1</sup>, Hiromasa Tanaka<sup>2,3</sup>, Kenji Ishikawa<sup>2</sup>  
Masaaki Mizuno<sup>3</sup>, Shinya Toyokuni<sup>2,4</sup>, Masaru Hori<sup>2</sup> and Hiroaki Kajiyama<sup>1,2</sup>

<sup>1</sup> Department of Obstetrics and Gynecology, <sup>3</sup> Center for Advanced Medicine and Clinical Research,  
<sup>4</sup> Department of Pathology and Biological Responses, Nagoya University Graduate School of Medicine,  
65 Tsurumai-Cho, Showa-ku, Nagoya, 466-8550, Japan

<sup>2</sup>Center for Low-temperature Plasma Sciences  
Furo, Chikusa, Nagoya 464-8603, Japan  
k-naka@med.nagoya-u.ac.jp

Epithelial ovarian cancer (EOC) is the most lethal gynecologic malignancy. Due to its asymptomatic progression, the majority of EOC patients are initially diagnosed at an advanced stage, accompanied by peritoneal metastasis, and the current treatments yield unfavorable prognoses for these patients. Peritoneal dissemination in EOC is recognized as an emblematic pathological condition of refractoriness and therapeutic resistance. Within the intraperitoneal tumor microenvironment, peritoneal mesothelial cells and other immune system cells transform into cancer-associated cells, forming the foundation for refractory and treatment-resistant characteristics. Therefore, managing intraperitoneal dissemination in EOC represents a crucial therapeutic approach.

As well as direct plasma, plasma-activated solutions have been proposed as a new therapeutic tool for cancer treatment. Numerous studies have demonstrated the direct cytotoxic effects of plasma-activated solutions on various cancer cells [1]. In our research, we showed the effective inhibition of intraperitoneal metastasis in EOC mouse model using plasma-activated medium (PAM) [2]. Further investigations illuminated that PAM evoked an immune response, leading to the infiltration of M1-type macrophages at the dissemination site [3]. In this study, we examined the effects of plasma-activated lactate Ringer's solution (PAL) on immune cells, focusing mainly on the activation of T cells, which play a pivotal role in anti-tumor immunity.

Recent reports have proposed that the intra-abdominal environment of EOC patients is highly immunosuppressed. Initial investigations have confirmed strong suppression of human CD8 positive T cells by EOC patient-derived malignant ascites, implying the induction of immunosuppression. Subsequently, we explored the potential of plasma-activated solutions to cancel this immune suppression. The results indicated that under optimal conditions, PAL could reverse the immune suppression induced by ascites. This might provide the potential of a plasma-activated solution to exhibit efficacy not only on macrophages but also on other immune cell types, suggesting a potential approach for cancer immunotherapy.

This work was partly supported in part by JSPS KAKENHI Grant Numbers 19H05462, 20K09640 and 23K08884 from the Ministry of Education, Culture, Sports, Science and Technology of Japan.

- [1] N. Yoshikawa, K. Nakamura, and H. Kajiyama, *Free Radical Research*, **57**, 69 (2023).
- [2] K. Nakamura, Y. Peng, F. Utsumi, H. Tanaka, M. Mizuno, S. Toyokuni, M. Hori, F. Kikkawa and H. Kajiyama, *Sci. Rep.*, **7**, 6085 (2017).
- [3] K. Nakamura, N. Yoshikawa, Y. Mizuno, M. Ito, H. Tanaka, M. Mizuno, S. Toyokuni, M. Hori, F. Kikkawa, and H. Kajiyama, *Cancers (Basel)*, **13**, (2021).

## Prevalence of antibiotic-resistant *E. coli* in wastewater treatment plant effluent and the southern watershed of Lake Biwa

Chih-Yu Ma<sup>1</sup>

<sup>1</sup> *Louis Pasteur Center for Medical Research*  
103-5 Tanaka Monzencho, Sakyo-ku, Kyoto, 606-8225, Japan  
Takara1419@gmail.com

The overuse and imprudent use of antibiotic agents in agriculture, veterinary, and medical sectors contribute significantly to the global epidemic increase in antimicrobial resistance (AMR). Wastewater treatment plants (WWTPs) are generally considered hotspots for the dissemination of AMR into the aquatic environment because the biological treatment processes applied in WWTPs cannot effectively remove both antibiotic-resistant bacteria (ARBs) and the relevant genes (ARGs).

In this study, we investigated the occurrence of antibiotic-resistant *E. coli* in the southern watershed of Lake Biwa. A two-year monitoring of antibiotic-resistant *E. coli* was conducted in the southern part of Lake Biwa, inflow rivers, and at three WWTPs around the southern part of the lake. Concentrations of *E. coli* resistant to ampicillin (AMP), cefotaxime (CTX), ceftazidime (CAZ), levofloxacin (LVFX), tetracycline (TC), and amikacin (AMK) were measured using the culture method. Among these antibiotic-resistant *E. coli*, AMP-resistant *E. coli* were found to be the most prevalent, followed by LVFX, CTX, CAZ, TC, and AMK-resistant strains, both in the influent and effluent of WWTPs. These resistance patterns in wastewater mirror those seen in clinical samples in Japan. The numbers of antibiotic-resistant *E. coli* decreased by approximately a factor of 1000 during the wastewater treatment processes, but the resistance ratio clearly increased, suggesting that the selection for antibiotic resistance might occur during the wastewater treatment process. AMP-resistant and TC-resistant *E. coli* were also detected in Lake Biwa and inflow rivers, suggesting that antibiotic resistance might originate not only from WWTPs but also from livestock farms and small-scale wastewater treatment facilities located in the river catchment.

Consequently, there is an urgent need to develop an efficient approach for the removal of AMR in aquatic environments. The plasma-assisted advanced oxidation process, capable of generating a large quantity of radicals and active species (including  $\cdot\text{OH}$ ,  $\text{O}_3$ , and  $\text{H}_2\text{O}_2$ ), is garnering increased attention as a novel method for water treatment and the removal of chemical and biological pollutants from water. However, studies related to plasma in addressing the AMR issue are still limited, and further research is necessary to evaluate its feasibility and utility.

## **Production of large volume plasma-activated water(PAW) for food and agricultural applications**

D. Srinoum, S. Kaewpawong, Karaket Wattanasit and M. Nisoa

*Plasmas and electromagnetic wave research laboratory,  
Walailak University: 222 Taiburi, Tasala, Nakhon si thammarat, 80160, Thailand  
mnisoa@gmail.com*

Recently, plasma activated waters (PAW) have been investigated intensively for sustainable agriculture and post-harvest technology. The waters can be used effectively as green fertilizers, decontamination agent and green pesticides, while no harmful by products left over[1-2]. The acidic characteristics of the PAW, resulted from nitrate and hydrogen peroxide, can produce high germination rate of various seeds[1,3]. In this work, PAW produced by RF cold atmospheric plasma in moderated pressure will be presented. The plasma is generated in closed chamber, whereas part of the chamber volume was filled with water. The floating electrode, made of tungsten rod and inserted in the Pyrex glass tube, is powered by RF power supply of 7 – 9 kV and 50 – 800 kHz. The plasmas, generated above the water surface, for production of PAW. Various characteristics of large volume PAW for the setup will be discussed.

1. L. Sivachan Ndiran and A. Khacef, Enhanced seed germination and plant growth by atmospheric pressure cold air plasma: combined effect of seed and water treatment, RSC Adv., 2017, 7, 1822–1832
2. Jin Shen and et.al., Bactericidal Effects against *S. aureus* and Physicochemical Properties of Plasma Activated Water stored at different temperatures, Scientific Reports, 6:28505, DOI: 10.1038/srep28505
3. S. Zhang, A. Rousseau and T. Dufour, Promoting lentil germination and stem growth by plasma activated tap water, demineralized water and liquid fertilizer, RSC Adv., 2017, 7, 31244–31251



## Development of 10 kW helicon plasma source for material-plasma interaction studies

S. Kaewpawong<sup>1</sup>, W. Kongsawat<sup>1</sup>, R. Taleh<sup>1</sup>, D. Srinoum<sup>1</sup>, A. Tamman<sup>2</sup>,  
S. Dangtip<sup>2</sup>, Boonyarit Chatthong<sup>3</sup> and M. Nisoa<sup>1</sup>

<sup>1</sup>*Plasmas and electromagnetic waves research laboratory, Walailak University: 222 Taiburi, Tasala, Nakhon si thammarat, 80160, Thailand*

*mnisoa@gmail.com*

<sup>2</sup>*Center of Excellence in Engineering and Nuclear Technology, Thailand Institute of Nuclear Technology, Nakhon Nayok, 26120 Thailand*

<sup>3</sup>*Division of Physical Science, Faculty of Science, Prince of Songkla University, Songkhla, Thailand*

High-density linear plasma devices can produce plasmas similar to that of the Tokamaks[1,2]. But they are simple and compact than the tokamaks. The linear devices are much more cost-effective than the tokamaks for research on plasma material interactions.

In this research, a linear helicon plasma device with permanent magnets was fabricated. A half-turn helical antenna and 13.56 MHz RF were used to excite helicon wave of  $m = +1$ . The 800 G magnetic field is uniform in the vicinity of the antenna. Ar gas was used for the plasma discharges. The electron temperatures and plasma densities were obtained by using optical emission spectroscopy(OES) and Langmuir probe. When the helicon waves were excited by RF power more than 400 W, high-density plasmas of more than  $10^{13} \text{ cm}^{-3}$  were obtained. The electron temperatures were in the ranges of 1 – 5 eV. The linear helicon plasma device developed in work is excellence for the studies of plasma material interaction (PMI) for development of fusion related materials. The ion fluence, similar to that of the plasma-facing wall in tokamaks, can be investigated.

### Reference

- [1] Caughman et al., *Plasma source development for fusion-relevant material testing*, Journal of Vacuum Science & Technology A: Vacuum, Surfaces, and Films 35, 03E114 (2017)
- [2] R. H Goulding et al., *Progress in the Development of a High Power Helicon Plasma Source for the Materials Plasma Exposure Experiment*, Fusion Science and Technology, (2017)

## **Characteristics of high-power DC thermal plasmas for treatment of medical wastes**

R. Taleh, S. Kaewpawong, W. Kongsawat, D. Srinoum and M. Nisoa

*Plasmas and electromagnetic wave research laboratory,  
Walailak University: 222 Taiburi, Tasala, Nakhon si thammarat, 80160, Thailand  
mnisoa@gmail.com*

The 30 kW DC plasma torch system with the well-type cathode (WTC) has been developed to generate thermal plasma above 1200 0C, which is adding the external magnetic coil on the cathodic part of the torch. The well-type torch is hollow cylindrical copper's 5 mm thickness, whose cathode electrode and anode electrode was 150 mm in each length, the diameter is 22 mm through the center, The gap between both electrodes is 1.5 mm isolated with a swirl gas ring.

Under the experimental conditions at 0.5 - 0.8 MPa compressed air is applied to both sides of the torch, the airflow rate is 60 L/min and 120 L/min from the sides, and above, as followed. the thermal plasma has been generated, their maximum current is 200 A and 160 V, the length is about 30 cm, its diameter about 3 to 5 cm wide, recognized UV emission has been present.

In this work, the 500 G of the magnetic field produced by an external solenoid has been developed, to drive the arc root and reduce the cathode erosion damage. The result shows the necessity of a magnetic field, a rotational arc root inside the cathode surface, and electrode life hours are compared with the case of un magnetic field-driven has been present. Finally, the knowledge of this work to extend electrode life and applied to the system to be suitable for the disposal of infectious wastes.

## Atmospheric pressure hybrid plasma jet for oxygen atom generation

Akihiro Kajino<sup>1</sup>, Keigo Takeda<sup>1</sup> and Mineo Hiramatsu<sup>1</sup>

<sup>1</sup> Meijo University

1-501, Shiogamaguchi, Tempaku, Nagoya 468-8502, Japan  
223427012@ccmailg.meijo-u.ac.jp

Application of non-equilibrium atmospheric pressure plasma (NEAPP) to biological field has attracted because of its ability to produce reactive oxygen species (ROS) with high reactivity at low temperatures. It has been reported that the ROS such as ground state oxygen (O) atoms and ozone (O<sub>3</sub>) generated by the NEAPP inactivate various microorganisms [1]. The O atom which is one of the important ROS is generated by the collisional dissociation of molecular oxygen (O<sub>2</sub>) with relatively high energy electron. On the other hand, the generation of O atom due to the electron collisional dissociation of O<sub>3</sub> occurs at the lower electron energy than the dissociation of O<sub>2</sub> [2]. Therefore, the addition of O<sub>3</sub> to the NEAPP discharge gas is expected to increase the efficiency of O atom generation. In this study, the hybrid atmospheric pressure plasma jet (APPJ) apparatus has been constructed to supply O<sub>3</sub> generated in dielectric barrier discharge (DBD) plasma to an AC-excited APPJ (AC-APPJ) [3] in order to establish the efficient O generation method.

Figure 1 shows a schematic of the hybrid APPJ apparatus constructed in this study. N<sub>2</sub> (5000 sccm) and air (500 sccm) were introduced into the quartz tube as discharge gas. And then, by applying an AC high voltage to DBD electrode and AC-APPJ electrode, a DBD and the AC-APPJ were generated inside the quartz tube and near the exit port of gas jet, respectively. In order to investigate the effect of the O<sub>3</sub> supply timing on the generation of O atom in the AC-APPJ, the distance between the DBD and the AC-APPJ electrodes were set at 46, 56, 66, 76, 86, and 96 mm, and the emission intensity of O atoms in the AC-APPJ was observed at a wavelength of 844 nm.

Figure 2 shows the optical emission intensity ratios of O atom to N atom (observed 746 nm) for the AC-excited APPJ at the distance of 46, 56, 66, 76, 86, and 96 mm between DBD and AC-APPJ electrodes together with that of AC-APPJ without DBD (No DBD). At 86 and 96 mm, the intensity ratio was relatively higher than that at No DBD condition. On the other hand, the intensity ratios at 46, 56, 66, and 76 mm were lower than that of No DBD condition. This indicates that the O atom generation was affected by the supply timing of O<sub>3</sub>. From the result, it is considered the supply of O<sub>3</sub> by the hybrid plasma was effective in its generation.

[1] S. Iseki, et. al, Appl. Phys. Express 4, 116201 (2011).

[2] M. Kuzumoto, et.al, JAPAN TAPPI JOURNAL 51, 2, 345 (1997).

[3] M. Iwasaki, et. al, Appl. Phys. Lett. 92, 081503 (2008).

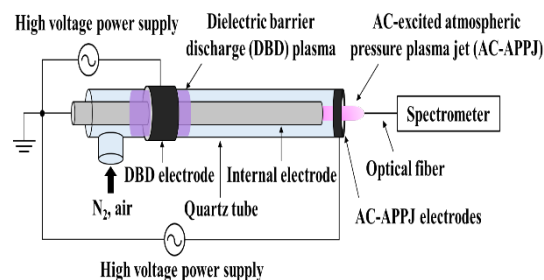


Fig. 1 Schematic of the hybrid APPJ.

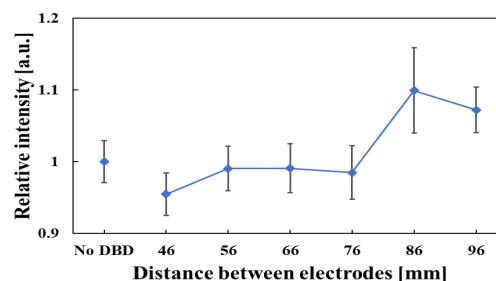


Fig. 2 Optical emission intensity ratio of O (844 nm) to N atoms (746 nm) as a function of the distance between DBD and AC-APPJ electrodes.

## **Analysis of plasma flow velocity in highly collisional plasma jet by using Mach probe for plasma aerosol deposition**

In Je Kang\*, Hyonu Chang, Soo Ouk Jang, Chang Hyun Cho, Ji Hun Kim, Hyun Jae Park, and Yong-Sup Choi

*Institute of Plasma Technology, Korea Institute of Fusion Energy, Gunsan 54004, Republic of Korea  
ijkang@kfe.re.kr*

Experimental studies on plasma flow velocity under highly collisional plasma conditions are insufficient with reliable results although the flow velocity is one of key parameters for the plasma aerosol deposition as the application of ceramic coating with plasma jet. In this presentation, the parallel Mach probe was used to experimentally analyze the normalized plasma flow velocity in a highly collisional plasma formed by a microwave plasma jet [1,2]. The velocity is a dimensionless unit which represents the plasma flow velocity relative to the ion acoustic velocity. To estimate the plasma flow velocity under highly collisional plasma conditions with 1 – 6 Torr, a collisional model of the Mach probe was proposed. Additionally, the turbulent model was used to calculate the neutral gas flow velocity, which was assumed to be the plasma flow velocity. The experimentally estimated results were found to be in good agreement with a difference rate of 10 – 30% when compared to the results of the turbulent model. After the optimization of conditions considering plasma flow velocity with the substrate position, the Y<sub>2</sub>O<sub>3</sub> coatings were deposited on an aluminum substrate. The thickness of the coating layer was ~50 μm, with pore properties <10%.

This research was supported by the R&D Program of “Plasma Convergence and Fundamental Research” (Grant No. EN2321-11) through the Korea Institute of Fusion Energy (KFE) funded by the Government funds, Republic of Korea.

[1] In Je Kang, Hyonu Chang, Yong-Sup Choi, Soo Ouk Jang, Chang Hyun Cho, Ji Hun Kim, Hyun Jae Park, *Curr. Appl. Phys.*, **39**, 45 (2022).

[2] Kyu-Sun Chung, *Plasma Sources Sci. Technol.*, **21**, 063001 (2012).

## **Design on versatile large area PECVD system for the assessment of plasma property**

Hyunyeong Lee\*, Kangil Lee, Young-Gi Kim, Daechul Kim, Jongsik Kim, Miyoung Song,  
and Yongsup Choi

*Korea Institute of Fusion Energy  
37 Dongjangan-ro, Gunsan, Jeollabuk-do 54004, Republic of Korea  
hylee@kfe.re.kr*

Plasma processing including etching and deposition has an essential role for surface treatment in semiconductor and display industry. Plasma processing for surface treatment has an economic ripple effect and it is essential to identify the specifications and the assessment of the plasma property for plasma processing. Therefore, the large area PECVD (Plasma Enhanced Chemical Vapor Deposition) system for 300 mm wafer has been designed for versatile experiments with assessment of plasma property. The CCP (Capacitively Coupled Plasma) type PECVD has been designed for using 3 kW 13.56 MHz RF (Radio Frequency) power and will be extended to 5 kW. In addition, OES (Optical Emission Spectroscopy) utilizing HR6 UV-VIS spectrometer will be installed for diagnosing the processing plasma and experimental condition. The detailed experimental conditions of versatile large area PECVD system will be presented.

## Etch characteristics of ITO using various hydrofluorocarbon gases

Jong Woo Hong<sup>1\*</sup>, Dong Woo Kim<sup>1</sup>, Yu Gwang Jeong<sup>3</sup>, Hyun Min Cho<sup>3</sup>, Da Woon Jung<sup>3</sup>,  
Yun Jong Yeo<sup>3</sup>, Geun Young Yeom<sup>1,2</sup>

<sup>1</sup> School of Advanced Materials Science and Engineering, Sungkyunkwan University  
2066 Seobu-ro, Jangan-gu, Suwon-si, Gyeonggi-do, Republic of Korea  
gyeom@skku.edu

<sup>2</sup> SKKU Advanced Institute of Nanotechnology (SAINT), Sungkyunkwan University  
2066 Seobu-ro, Jangan-gu, Suwon-si, Gyeonggi-do, Republic of Korea

<sup>3</sup> Process Research Team, Samsung Display  
1, Samsung-ro, Giheung-gu, Yongin-si 17113, Gyeonggi-do, Republic of Korea

In this study, the etching characteristics of ITO were investigated using various hydrocarbon gases mixed with Ar and examined the cleaning properties of etch residue with H<sub>2</sub>/Ar. The use of hydrofluorocarbon gases with a higher C/H ratio not only improved the etch rate of ITO but also increased the etch selectivity over PR. This increase in etch selectivity can be attributed to the reduced hydrogen content in the gas mixture, which not only enhances PR etching but also minimizes damage to the PR material. The etching of ITO using various hydro mixed with Ar appeared to involve the formation of compounds such as InC<sub>x</sub>H<sub>y</sub>, SnH<sub>x</sub>, SnC<sub>x</sub>H<sub>y</sub>, and CO<sub>x</sub> on the ITO surface, followed by the sputtering of these compounds by Ar<sup>+</sup> ion bombardment. Among the sputtered compounds, less volatile and adhesive compounds seemed to adhere to the chamber walls, forming a polymer etch residue layer. This polymer layer could be effectively removed using H<sub>2</sub>/Ar plasmas, leading to the formation of more volatile compounds such as In(CH<sub>3</sub>)<sub>x</sub> (x=2,3), SnH<sub>4</sub>, and CH<sub>4</sub>.

[1] J. Lee, D. Kim, D. Yang, S. Hong, K. Yoon, P. Hong, C. Jeong, H. Park, S. Kim, S. Lim, S. S. Kim, K. Son, T. Kim, J. Kwon, and S. Lee, SID Symposium Digest of Technical Papers, **39**, 1 (2008).

[2] D.H. Kang, I. Kang, S.H. Ryu, and J. Jang, IEEE Electron Device Lett., **32**, 10 (2011).

[3] S.W. Tsao, T.C. Chang, S.Y. Huang, M.C. Chen, S.C. Chen, C.T. Tsai, Y.J. Kuo, Y.C. Chen, and W.C. Wu, Solid-State Electron., **54**, 12 (2010).

## Etching characteristics of SiON films with a low global warming potential gas replacing CF<sub>4</sub>

Hyun Woo Tak<sup>1</sup>, Kim Seul Ki<sup>2</sup>, Seong Bae Kim<sup>1</sup>, Chan Hyuk Choi<sup>3</sup>, Dong Woo Kim<sup>1</sup> and Geun Yong Yeom<sup>1,3</sup>

<sup>1</sup> School of Advanced Materials Science and Engineering, Sungkyunkwan University  
2066 Seobu-ro, Jangan-gu, Suwon-si, Gyeonggi-do, Republic of Korea  
gyyeom@skku.edu

<sup>2</sup> Department of Semiconductor Display Engineering Sungkyunkwan University  
2066 Seobu-ro, Jangan-gu, Suwon-si, Gyeonggi-do, Republic of Korea

<sup>3</sup> SKKU Advanced Institute of Nano Technology (SAINT)  
2066 Seobu-ro, Jangan-gu, Suwon-si, Gyeonggi-do, Republic of Korea

To fabricate semiconductor devices, dielectric etching is essential for creating nanoscale devices with high integration circuits. As the integration level of semiconductor devices increases, more etching steps and etching time are required, ultimately leading to the use of large quantities of fluorocarbon and hydrofluorocarbon gases. Commercial etch gases such as CF<sub>4</sub>, CHF<sub>3</sub>, and C<sub>4</sub>F<sub>8</sub> have high global warming potentials of 7380, 14600, and 10200, respectively. This is a critical concern, especially in light of the recent statement from the United Nations in July 2023, warning of "The era of global warming."

Recent studies have actively explored the replacement of CHF<sub>3</sub> and C<sub>4</sub>F<sub>8</sub> with low Global Warming Potential (GWP) gases, while meeting the requirements for improved etching properties in high aspect ratio contact structure etching using high-polymer-forming fluorocarbons and hydrofluorocarbons. However, the replacement of CF<sub>4</sub> has not been widely investigated, as it possesses unique properties, with carbon bonded to four fluorine atoms. It is also produced at a low cost and is chemically stable, making it relatively easy to understand its plasma dissociation properties, which result in intuitive etching behavior.

In this study, we propose a novel fluorocarbon base gas as a replacement for CF<sub>4</sub> in SiON etching, which is one of the essential steps required to form hardmasks, such as amorphous carbon layers commonly used in various semiconductor manufacturing processes. Additionally, we have designed the etching process with CH<sub>2</sub>F<sub>2</sub>, which has a relatively low GWP value of 771 among hydrofluorocarbons. SiON etching also requires hydrogen to form volatile HCN. Based on detailed etching results in SiON with nanoscale hole-patterned photoresist, we can suggest that replacing CF<sub>4</sub> with the novel gas and CH<sub>2</sub>F<sub>2</sub> as an alternative etching process in semiconductor manufacturing can effectively achieve the same (F-H)/(C-O) ratio, offering an environmentally sustainable solution.

[1] H. S. Lee, K. C. Yang, S. G. Kim, Y. J. Shin, D. W. Suh, H. D. Song, N. E. Lee, and G. Y. Yeom, *J. Vac. Sci. Technol. A*, **36**, 061306 (2018).

[2] H. W. Tak, H. J. Lee, L. Wen, B. J. Kang, D. Sung, J. W. Bae, D. W. Kim, W. Lee, S. B. Lee, K. Kim, B. O. Cho, Y. L. Kim, H. D. Song, and G. Y. Yeom, *Appl. Surf. Sci.*, **600**, 154050 (2022).

[3] H. J. Lee, H. W. Tak, S. B. Kim, S. K. Kim, T. H. Park, J. Y. Kim, D. Sung, W. Lee, S. B. Lee, K. Kim, B. O. Cho, Y. L. Kim, K. C. Lee, D. W. Kim, and G. Y. Yeom, *Appl. Surf. Sci.*, **639**, 158190 (2023).

## Dependence of the film qualities on the solied densities of the targets prepared by sputtering deposition with mixture powder targets

H. Kawasaki<sup>1</sup>, T. Satake<sup>1,2</sup>, T. Ohshima<sup>3</sup>, T. Kikuchi<sup>4</sup>, T. Sasaki<sup>4</sup>, A. Sugiura<sup>2</sup>, S. Aoqui<sup>2</sup>

<sup>1</sup>National Institute of Technology, Sasebo College, 1-1 Okishin, Sasebo, Ngasaki 857-1193, Japan

<sup>2</sup>Sojo University, Ikeda, Nishi-ku, Kumamoto, 860-0082, Japan

<sup>3</sup>Nagasaki University, I 1-14 Bunkyo, Nagasaki, Japan 852-8521, Japan

<sup>4</sup>Nagaoka University of Technology, 1603-1, Kamitomioka Nagaoka, Niigata, 940-2188, Japan

ITO (Sn doped  $\text{In}_2\text{O}_3$ ), which has excellent electrical conductivity and transparency, is the current mainstream transparent conductive film. However, indium, the raw material of ITO, is a rare metal and therefore expensive. As an alternative material to ITO, we focused on the fabrication of AZO thin films by doping Al into ZnO, which is abundant in resources and inexpensive. However, it is hard to control metal doping ratio using conventional sputtering deposition method, because high density bulk targets are generally used in the sputtering deposition method. To prepare a thin film with certain element ingredients, we have been developed new sputtering deposition method using powder targets. In this method, several kind of powders were mixed by mixer, and just put on the target holder in the vacuum chamber. And then, thin films were deposited on the substrate which was set to the counter side. Therefore, it is easy to change doping density to control the target powder mixture. In this report, those Al doped ZnO thin films were prepared using several types of Al and ZnO mixture powder targets. We prepared the Al doped ZnO thin films by sputtering deposition using 4 kinds of targets, which are 1) Unprocessed, 2) Heated to 150°C on target holder, 3) Pressurized at 15 MPa, 4) Pressurized at 4.5t. Deposition rate of the film using sputtering deposition as a function of the powder target condition, not shown here. Deposition rate using pressurized target are higher than that of the un pressurized one. Figure 2 shows the XRD pattern of the prepared film using sputtering deposition as a function of the powder target condition. All of the film shows ZnO(002) peaks ( $2\theta=34.4^\circ$ ). Peak intensities of the prepared film using pressurized target are higher than that of the un pressurized one. These results suggest that Al and ZnO mixture powder targets mixture thin films were successfully prepared on the Si and glass substrates surface, and their deposition rate and crystalinity changed by solied density of the targets. This study was supported in part by a Grant-in-Aid for Scientific Research in Priority Areas (A) (No. 18H03848) and (C) (No.23340181 and No. 16K04999), Grant for joint research between National College of Technology and Nagaoka University of Technology, Takahashi Industrial and Economic Research Foundation and Nippon Sheet Glass Foundation for Materials Science and Engineering

- [1] H. Kawasaki, H. Nishiguchi, T. Furutani, T. Ohshima, Y. Yagy, T. Ihara, M. Shinohara, Y. Suda, Jpn. J. Appl. Phys. **57**, 01AB02 (2018)
- [2] H. Nishiguchi, T. Ohshima, H. Kawasaki, T. Fukuda, Jpn. J. Appl. Phys. **55**, 01AF05 (2016).
- [3] H. Kawasaki, Y. Suda, T. Ohshima, Y. Yagy, M. Shinohara, and T. Ihara, Jpn. J. Appl. Phys **58**, SAAD04 (2019).

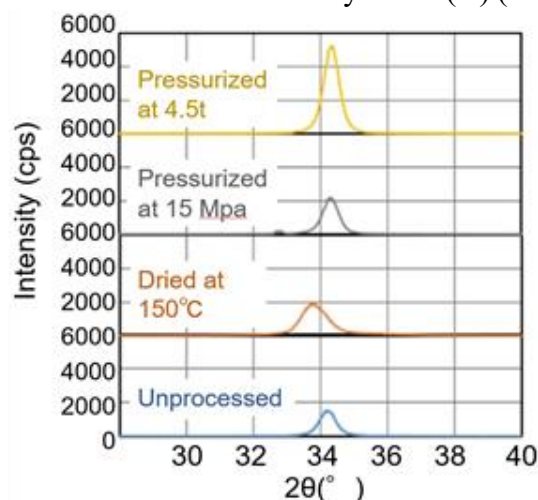


Fig. 1 XRD pattern of the prepared film using sputtering deposition as a function of the powder target condition.



## **Introduction to IAEA coordinated research program (CRP): AI for Fusion (AI4F)**

Masayuki Yokoyama

*National Institute for Fusion Science, Rokkasho Research Center,  
2-166 Obuchi-Omotodate, Rokkasho, Aomori 039-3212, Japan*

The IAEA (International Atomic Energy Agency) organized the Technical Meeting on Artificial Intelligence (AI) for Nuclear Technology and Applications (#AI4Atoms) on 25–29 October 2021, to programmatically discuss to form the roadmap for IAEA role & support in use of AI in nuclear science, technology, and applications. It consisted of 10 working groups (WGs) along with cross-cutting groups (enabling infrastructure, and advanced modelling and simulation methodologies). There is a “Nuclear Fusion” WG (NFWG) in 10 WGs.

Prof. Hideo Nagatomo (Osaka University) and I (Masayuki Yokoyama) joined this NFWG from Japan, to launch continuously discuss to form the Coordinated Research Project (CRP). It resulted in the launch of CRP on AI for Accelerating Fusion R&D (2022–2027) with the objective of accelerating fusion R&D with Machine Learning (ML)/AI, through the creation of a platform and cross-community network for innovation and partnership.

(cf., <https://nucleus.iaea.org/sites/ai4atoms/ai4fusion/SitePages/What-is-AI-for-Fusion-.aspx?web=1>)

This CRP is composed by four Work Packages (WP), as follows.

WP 1: Real-time MFE System Behaviour Prediction, Identification & Optimization Using ML/AI Methods (MFE: Magnetic Fusion Energy)

WP 2: IFE Physics Understanding through Simulation, Theory and Experiment Using ML/AI Methods (IFE: Inertial Fusion Energy)

WP 3: Feasibility of MFE and IFE Image Database

WP 4: Community Engagement & Workforce Development

The objectives, expected activities/output/outcomes for each WP are described on the above-mentioned webpage.

This information was distributed via the mailing list of The Japan Society of Plasma Science and Nuclear Fusion Research in Japan, for calling the proposal from institutions/universities in Japan. Then, Osaka University and NIFS individually applied, and they were approved by the IAEA.

The progress and on-going activities within this CRP framework, with emphasis on the NIFS proposal entitled as Radiation collapse database (no disruptions) from LHD (Large Helical Device), will be reported in the forum.